QUANTUM VACUUM RADIATION IN OPTICAL MEDIA

by

Niclas Kim Lennart Westerberg

1st Supervisor: Prof. Patrik Öhberg

2nd Supervisor: Prof. Daniele Faccio FRSE

Submitted for the Degree of

Doctor of Philosophy

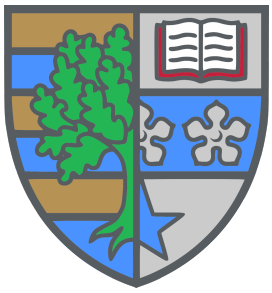

School of Engineering and Physical Sciences

Heriot-Watt University

October, 2019

Abstract

In this thesis we study quantum vacuum radiation. This is the radiation that is emitted due to changes of the electromagnetic vacuum in time. Specifically, we explore the phenomena in optical media at a macroscopic scale by introducing a time-dependent permittivity. We model this by inducing time varying changes to the medium's resonance frequencies.

To start with, we build a perturbative model, from which we learn that the physics of quantum vacuum radiation is well-described in terms of the collective light-matter excitations (polaritons) but that the retarded response of the matter degree of freedom should not be forgotten. In particular, the retarded response of the medium leads to quantum vacuum radiation that can be driven not only by frequencies supported by the spectrum of the modulation, but also local frequencies, such as the beating pattern of two waves. We then apply this model to analyse a fibre optics experiment where photon pair production was measured, and find a good agreement between the measured and predicted spectrum. Interestingly, the measured photon pair production coincide with quantum vacuum radiation driven by the beating pattern formed by a travelling polarisation wave and the spatial modulation of the fibre.

Following this, we use the perturbative model to study a scenario mimicking a rapidly ($\sim$ optical timescales) expanding and contracting spacetime. In this scenario however, the probability to excite quantum vacuum radiation in naturally occurring materials is vanishingly small. Motivated partly by this, we turn to study vacuum radiation in man-made metamaterials, where large changes to the optical properties in time are possible. Specifically, we study an ε-near-zero metamaterial whose time-dependent permittivity has been experimentally measured. In a model that neglects the retarded response of this metamaterial, we find that the quantum vacuum radiation becomes strongly peaked around the point where the real permittivity passes through zero.

In order to extend the perturbative model to also include large changes to the optical properties in time, we finish this thesis by mapping macroscopic quantum electrodynamics to a trapped particle in a magnetic field. Using the intuition gained from this, we study a variety of non-perturbative settings including bichromatic periodic driving and return to ε-near-zero metamaterials. This confirms some of the previous analysis, as well as provides an intuitive explanation for the physics.

To the memory of
Ernst Owe Westerberg
1931-2018

"Från fäder det kommet, till söner skall det gå, så långt som unga hjärtan ännu i Norden slå"*

*From *Skaldestycken* by Erik Gustaf Geijer, 1835. It translates as:
"From fathers it has come, to sons it goes, as long as young hearts yet beat in the North."

Acknowledgements

Scientia scientiae gratia.

Right. This is the part where I give thanks to everyone that has helped me to actually get this far. I must admit that at this point I am rather tired of writing, seeing that for reasons I currently cannot fathom I decided to write this part last. Perhaps more importantly, I feel that I cannot possibly convey my gratitude properly here. That being said, there are certainly people that I should mention here, and I will try my very best.

A good starting point to all this should be to thank my supervisors, Prof. Patrik Öhberg and Prof. Daniele Faccio, without whom this thesis, for somewhat natural reasons, couldn't possibly exist. The list of lessons, and tricks of the trade, that they have taught me would be hard to summarise, though possibly the next 150 or so pages will make an attempt at this (and also discuss some physics). Patrik has been a sage guide throughout this time as a doctoral student, a key advice from whom has been to have fun and enjoy what you do. And also that 'nog' has quite a different meaning in Fenno-Swedish as compared to Scanish. In a friendly but antagonistic manner, Daniele has many times served as a sparring partner, rooting out incorrect physics even when I have stubbornly stuck to what the equations were telling me, and in the process distilled out some physics. As annoyed as I have been sometimes, I am grateful for this. And I should probably also put a special thanks to Daniele for taking me under his wings all those years ago, when as an undergraduate I figured that a good use of my spare time would be to get myself involved in research. I would also like to thank both of them for letting me work on, and guiding me through, such a variety of different topics.

None of this would have been possible without the post-doctoral researchers Dr Angus Prain and Dr Manuel Valiente. Many of the hard skills I learned from you, and the variety of topics pursued truly would not have been possible without your expertise and support. Angus, I am pretty sure I would never have cleared up all my confusion about analogue gravity without you. Manuel, my attempts to simulate few-body physics with light never would have started had it not been for you. Thank you both for guiding me through all this, and thanks for pushing me to do well. Also, I think a comment about attention to detail, and scepticism of misleading and careless work, is suitable here — lessons you don't always think about but are nonetheless vital.

I would also like to give thanks to the rest of both the 'Quantum Optics and Cold Atoms' group and the 'Extreme Light' group, perhaps especially Callum Duncan of the former. Throughout these four years we have shared an office, too many

discussions to count, a fair few publications, as well as our fair share of pints. I can safely say that my PhD would have been a different experience without you there. Oh, and as it has been the staple diet for long days in our office, I should also thank Maoam Pinballs, bags of which I have had far too many. From the groups, members former and present, I also want to give a shout out to Julius Heitz, Mihail Petev, Calum Maitland, Dr Thomas Roger, Dr Kali Wilson, Dr Stefano Vezzoli, Dr Shraddha Rao, Dr Ashley Lyons, Dr David Vocke and Dr Salvatore Butera, with all of whom I have had the pleasure to work directly. The list is long and I am sure I've forgotten someone. And thanks to Prof. Ewan M. Wright of the University of Arizona for all the discussions and good work together.

My thanks also goes out to the people of the Scottish Centre for Doctoral Training in Condensed Matter Physics, especially Debra Thompson, Wendy Clark and Dr Julie Massey. You have given me many opportunities that otherwise would have been missed, from courses to outreach, and not to mention all the conferences and travel that you afforded me. I might have complained a fair share about the former at times, but all in all, sometimes you shouldn't listen to feedback! I think it says it all that I consider my doctoral studies to have been at the CM-CDT, with an office at Heriot-Watt University. That being said, I'd like to thank Loraine Cameron, without whom no physics research would get done at Heriot-Watt University. Here I should also give thanks to the University of Glasgow, for the hospitality they offered me as a visiting postgraduate researcher.

In addition to this, I would like to acknowledge my friends, you know who you are. Thanks for keeping me sane through the years with the lunch walks of ever increasing length, the Highlands hikes and wild camping, the many nights of games, food and drink, and the otherwise good times. And thanks for the (possibly anachronistic) letter correspondence that I would dearly miss. I would especially like to thank Rachael Tobin, Dr John Tobin, Dr Jack Wildman, and Pete Connolly who also helped to proofread this thesis. Thanks for that. And extra gratitude to Rachael as a writing-up buddy, the last few months surely would have been much worse without the shared complaints.

Last but not least, my gratitude goes out to my family. My partner Lisa, without you surely I would be lost. I mean this in both a figurative and literal sense. And as is particularly relevant for this thesis, thanks for reading it, and correcting the countless errors. Especially the plurals. To my sister Michaela goes further thanks and gratitude; for the never-ending encouragements and perhaps mostly for putting up with my silliness over the years. Thanks also to my mother Liselott, without you, your countless advice and never-ending support none of this would have happened. And although you will never read this, I would like to thank my father Owe, to whom I dedicate this thesis. Thanks for everything.

Ur hjärtat gående, tack till er alla.

ACADEMIC REGISTRY

Research Thesis Submission

Please note this form should be bound into the submitted thesis.

Name:	Niclas Kim Lennart Westerberg		
School:	Engineering and Physical Sciences		
Version: *(i.e. First, Resubmission, Final)*		Degree Sought:	PhD Physics

Declaration

In accordance with the appropriate regulations I hereby submit my thesis and I declare that:

1. The thesis embodies the results of my own work and has been composed by myself
2. Where appropriate, I have made acknowledgement of the work of others
3. Where the thesis contains published outputs under Regulation 6 (9.1.2) these are accompanied by a critical review which accurately describes my contribution to the research and, for multi-author outputs, a signed declaration indicating the contribution of each author (complete Inclusion of Published Works Form – see below)
4. The thesis is the correct version for submission and is the same version as any electronic versions submitted*.
5. My thesis for the award referred to, deposited in the Heriot-Watt University Library, should be made available for loan or photocopying and be available via the Institutional Repository, subject to such conditions as the Librarian may require
6. I understand that as a student of the University I am required to abide by the Regulations of the University and to conform to its discipline.
7. Inclusion of published outputs under Regulation 6 (9.1.2) shall not constitute plagiarism.
8. I confirm that the thesis has been verified against plagiarism via an approved plagiarism detection application e.g. Turnitin.

* *Please note that it is the responsibility of the candidate to ensure that the correct version of the thesis is submitted.*

Signature of Candidate:		Date:	

Submission

Submitted By *(name in capitals):*	NICLAS WESTERBERG
Signature of Individual Submitting:	
Date Submitted:	

For Completion in the Student Service Centre (SSC)

Received in the SSC by *(name in capitals):*			
Method of Submission *(Handed in to SSC; posted through internal/external mail):*			
*E-thesis Submitted (**mandatory for final theses**)*			
Signature:		Date:	

ACADEMIC REGISTRY

Inclusion of Published Works

Declaration

This thesis contains one or more multi-author published works. In accordance with Regulation 6 (9.1.2) I hereby declare that the contributions of each author to these publications is as follows:

Citation details	N. Westerberg, A. Prain, D. Faccio, P. Öhberg, *Vacuum radiation and frequency-mixing in linear light-matter systems*, J. Phys. Commun. **3**, 065012 (2019)
N. Westerberg	NW developed the theory.
A. Prain	AP contributed to the theory development, as well as provided critical input.
D. Faccio	DF contributed to conceiving the idea.
P. Öhberg	PÖ supervised the work, and provided valuable discussion.
Signature:	
Date:	

Citation details	S. Vezzoli, A. Mussot, N. Westerberg, A. Kudlinski, H. Dinparasti Saleh, A. Prain, F. Biancalana, E. Lantz, D. Faccio, *Optical Analogue of the Dynamical Casimir Effect in a Dispersion-Oscillating Fiber*, Nat. Comm. Phys. **2**, 84 (2019)
S. Vezzoli	SV developed the experimental setup and collected the data, as well as analyzed the data.
A. Mussot	AM contributed to conceiving the idea, to the development of the experimental setup, as well as to the data collection and analysis.
N. Westerberg	NW developed the theoretical framework, in particular the connection to quantum vacuum radiation in the co-moving frame.
A. Kudlinski	AK designed and fabricated the fibre.
H. Dinparasti Saleh	HDS contributed to the development of the experimental setup, as well as to the data collection.
A. Prain	AP contributed to the development of the theoretical framework.
F. Biancalana	FB contributed to conceiving the idea, as well as to the development of the theoretical framework.
E. Lantz	EL contributed to the data analysis.
D. Faccio	DF contributed to conceiving the idea, as well as to the development of the theoretical framework.
Signature:	
Date:	

ACADEMIC REGISTRY

Citation details	A. Prain, S. Vezzoli, N. Westerberg, T. Roger, D. Faccio, *Spontaneous photon production in time-dependent epsilon-near-zero materials*, Phys. Rev. Lett. **118**, 133904 (2017)
A. Prain	AP developed the theory together with NW, and produced the figures.
S. Vezzoli	SV provided experimental data and input where relevant in the manuscript.
N. Westerberg	NW contributed to the development of the theoretical framework, in particular the development of the model.
T. Roger	TR provided experimental data where relevant in the manuscript.
D. Faccio	DF conveived the idea, as well as supervised the work.
Signature:	
Date:	

List of Publications

Publications on which this thesis is based

1. **N. Westerberg**, A. Prain, D. Faccio, P. Öhberg, *Vacuum radiation and frequency-mixing in linear light-matter systems*, J. Phys. Commun. **3**, 065012 (2019)

2. S. Vezzoli, A. Mussot, **N. Westerberg**, A. Kudlinski, H. Dinparasti Saleh, A. Prain, F. Biancalana, E. Lantz, D. Faccio, *Optical Analogue of the Dynamical Casimir Effect in a Dispersion-Oscillating Fiber*, *Nat. Comm. Phys. **2**, 84 (2019)*

3. A. Prain, S. Vezzoli, **N. Westerberg**, T. Roger, D. Faccio, *Spontaneous photon production in time-dependent epsilon-near-zero materials*, Phys. Rev. Lett. **118**, 133904 (2017).

Directly relevant publications

4. **N. Westerberg**, S. Cacciatori, F. Belgiorno, F. Dalla Piazza, D. Faccio, *Experimental quantum cosmology in time-dependent optical media*, New. J. Phys. **16**, 075003 (2014).

5. M. Petev, **N. Westerberg**, D. Moss, E. Rubino, C. Rimoldi, S.L. Cacciatori, F. Belgiorno, D. Faccio, *Blackbody Emission from Light Interacting with an Effective Moving Dispersive Medium*, Phys. Rev. Lett. **111**, 043902 (2013).

Other publications

6. C. W. Duncan, C. Ross, **N. Westerberg**, M. Valiente, B. J. Schroers, P. Öhberg, *Linked and knotted synthetic magnetic fields*, Phys. Rev. A **99**, 063613 (2019).

7. D. Johnstone, **N. Westerberg**, C. W. Duncan, P. Öhberg, *Staggered Ground States in an Optical Lattice*, arXiv preprint arXiv:1905.00027 (2019).

8. S. Butera, **N. Westerberg**, D. Faccio, P. Öhberg, *Curved spacetime from interacting gauge theories*, Class. Quantum Grav. **36**, 034002 (2019).

9. **N. Westerberg**, K. E. Wilson, C. W. Duncan, D. Faccio, E. M. Wright, P. Öhberg, M. Valiente, *Self-bound droplets of light with orbital angular momentum*, Phys. Rev. A **98**, 053835 (2018).

10. K. E. Wilson, **N. Westerberg**, M. Valiente, C. W. Duncan, E. M. Wright, P. Öhberg, D. Faccio, *Observation of photon droplets and their dynamics*, Phys. Rev. Lett. **121**, 133903 (2018).

11. T. Roger, A. Lyons, **N. Westerberg**, S. Vezzoli, C. Maitland, J. Leach, M. Padgett, D. Faccio, *How fast is a twisted photon?*, Optica **5**, 682-686 (2018).

12. A. Luna, R. Monteiro, I. Nicholson, A. Ochirov, D. O'Connell, **N. Westerberg**, C. D. White, *Perturbative spacetimes from Yang-Mills theory*, J. High Energ. Phys. 2017: 69, (2017).

13. M. Petev, **N. Westerberg**, E. Rubino, D. Moss, A. Couairon, F. Légaré, R. Morandotti, D. Faccio, M. Clerici, *Phase-Insensitive Scattering of Terahertz Radiation*, Photonics **4**(1), 7, (2017).

14. T. Roger, C. Maitland, K. Wilson, **N. Westerberg**, D. Vocke, E. M. Wright, D. Faccio, *Optical analogues of the Newton-Schrodinger equation and boson star evolution*, Nature Communications **7**, 13492 (2016).

15. **N. Westerberg**, C. Maitland, D. Faccio, K. Wilson, P. Öhberg, E. M. Wright, *Synthetic magnetism for photon fluids*, Phys. Rev. A **94**, 023805 (2016).

16. S. M. Rao, J. J. F. Heitz, T. Roger, **N. Westerberg**, D. Faccio, *Coherent control of light interaction with graphene*, Opt. Lett. **39**, 5345 (2014).

17. M. Conforti, **N. Westerberg**, F. Baronio, S. Trillo, D. Faccio, *Negative-frequency dispersive wave generation in quadratic media*, Phys. Rev. A **88**, 013829 (2013).

Contents

Chapter 1

Introduction: Quantum vacuum radiation in some context

"So BAM, he invents light, day one
and then he misses the dark part
so he invents night too"

Cory O'Brien in *Zeus grants stupid wishes*, 2013

There are two ways we can start this discussion, opening either with the first or the second part of the thesis title — 'quantum vacuum radiation' or 'optical media'. Perhaps mainly for the sake of sticking to some order, let us start with the former. A good outset to this is possibly defining exactly what we mean with 'quantum vacuum radiation'. It is radiation, by which we mean travelling electromagnetic waves, or simply 'light' for short [1]. Furthermore, the part in the title about the quantum vacuum refers to the origin of this radiation, namely the electromagnetic vacuum state, defined as the lowest energy configuration [2]. Crudely speaking, quantum vacuum radiation is the radiation that can be emitted when you start changing this lowest energy state with time. This relies on the fact that the ground state, and consequently particle number in general, is only defined for systems with time-translational invariance [3].[1] Therefore, when we say that the ground state is time-dependent what we really refer to is that the ground state becomes ill-defined for a period of time. Generally speaking, after some such period of time-dependence, the system may not return to the ground state, but may find itself in an excited state. The quanta in the excited states are the quantum vacuum radiation.

Now that we have gotten the definition out the way, there are many examples of quantum vacuum radiation, but I will restrict the discussion somewhat. Perhaps the conceptually simplest and most famous example is the so-called dynamical Casimir effect, where radiation is emitted from the vacuum state in a cavity whose mirrors oscillate in time [6]. We see that this fulfils the above definition of quantum vacuum radiation if we note that the vacuum energy of the cavity is proportional to $1/L$ (with L being the length of the cavity) — introducing a time-dependent length $L(t)$

[1] This follows because energy is conserved only in such systems (Noether's theorem) [4, 5].

therefore leads to a time-dependent vacuum state. However, a quick back-of-the-envelope calculation[2] also tells us that the mirror would have to move at relativistic speeds ($\sim c$) in order to observe this radiation. Instead, this was first observed in a superconducting circuit, where an effective length could be introduced for a microwave cavity, and consequently modulated in time [7, 8].

This effect is quite general and can be extended to many different schemes, including circuits and optical systems [9, 10], and may have links to sonoluminescence — the light emitted from a collapsing bubble [11] — although this might have a more complicated origin [12–14]. Indeed, quantum vacuum radiation can furthermore be emitted from a single moving mirror [15–18]. Now, the special case of a uniformly accelerated mirror brings us to the so-called Unruh effect [19, 20], where an accelerated observer measures a thermal vacuum state with temperature $T \propto$ acceleration. By the equivalence principle, the principle that equates gravitational acceleration to its motional counterpart, this has further links to the famous Hawking radiation [21, 22], the thermal radiation emitted from a black hole [23]. Likewise, we can directly link this to cosmological particle creation [15], i.e. the particles excited from the vacuum state by rapidly expanding spacetimes.

Just like the dynamical Casimir effect, the radiation emitted by cosmological expansion, a black hole, or a uniformly accelerated mirror, are experimentally inaccessible in real life scenarios because the radiation is typically very weak. An example of this is that the temperature of most black holes is lower than the cosmic background radiation. An alternative is to study related effects in condensed matter and optical systems [9, 24]. For instance, cosmological particle creation has been studied in cold atomic gases [25–28], ion traps [29, 30] and optical media [31]. Indeed, Steinhauer [32] recently claimed to have observed 'Hawking radiation' [32, 33], and a quantum simulation of the Unruh effect was reported in Ref. [34], both in Bose-Einstein condensates. The classically stimulated variant of the former has also been observed in an optical fibre [35]. This is a topic which we will return to in Chapter 5, but there has of course been a good amount of theoretical study leading up to these observations, a review of which can be found in Ref. [24].

In broad strokes, the link between all these effects is that they rely on quantum field theory on a time-dependent background [15, 36–39]. In general, we can think of this as a physical system with temporally varying natural oscillation frequencies [30]. As hinted towards in the previous paragraph, the quantum radiation that we have discussed so far also has a classical counterpart. Classically, what we describe here are parametric oscillators [40], studied for mechanical motion [41–44], in fluids

[2]Let us assume the frequency of the emitted radiation to be inversely proportional to the mirror displacement timescale T_{oscil}, i.e. $\omega_{\text{rad}} = 2\pi/T_{\text{oscil}}$. In order for this radiation to be detected, it is also reasonable to assume that the radiation should be in the optical regime, since current technology is most efficient there. If we now suppose a modest mirror displacement of $L_{\text{oscil}} \simeq 0.5\ \mu$m, and $T_{\text{oscil}} \simeq L_{\text{oscil}}/v_{\text{oscil}}$, then we must demand that $v_{\text{oscil}} \simeq 0.5c$ in order for $\omega_{\text{rad}} \simeq 2\pi c/1000$ nm. Note that this does not estimate how much energy that is radiated.

[45, 46], electronics [47, 48] and light-matter systems [49], to name but a few. In short, it is the physics of a swing, or multiple swings coupled together with springs in the case of light in optical media. We will return this point later (Chapter 6).

It is also worth noting that in some scenarios the phenomenology of quantum vacuum radiation in optical media overlaps with parametric fluorescence (also called spontaneous parametric down-conversion) [50, 51], where photons are emitted from the vacuum state due to the presence of a pump beam. This is routinely used to generate photon pairs in quantum optics experiments [52]. In particular, the two effects overlap when nonlinear effects are used to generate periodic time-dependent changes in the optical medium. This is the case for some of the scenarios that we will study in this thesis. However, by doing so we bring a different perspective on the physics. This can illuminate previously overlooked physics (for instance physics at frequencies well-separated from the pump frequency), as well as provide a complete model of the dispersion properties (which is commonly treated perturbatively [53] around the pump frequency). Importantly however, the phenomenology *can*, but doesn't *have to* overlap.

Let us return to the second part of the thesis title: optical media. In this context, by dispersion we mean that an optical medium respond differently to different frequencies of light travelling through it. For example, the light coming through your window pane is qualitatively different from the light passing through your cup of coffee. Most commonly we refer to the phase velocity of light v_{ph} that vary for different frequencies ω, as quantified by the refractive index $n(\omega)$ [54] such that $v_{\text{ph}} = c/n(\omega)$.

Likewise, if we are to quantise the electromagnetic vacuum inside a medium, we would expect it to be different from the vacuum in absence of charges. This is naturally well-known and, at the scale of crystals and glasses as opposed to individual atoms, is captured extremely well by the theory of macroscopic electrodynamics [1, 55]. In this we aim to construct an effective model for the medium that ignores the microscopic detail, whilst still yielding the same results at a macroscopic scale. Microscopically, dispersion is caused by the chain of absorption and re-emission events of the medium constituents. Generally, we expect the probability of such an event to occur to depend on the frequency of light, as the constituents are generally some kind of oscillator [1, 56] and oscillators have some natural oscillation frequencies.[3] Here these natural oscillation frequencies correspond to the resonance frequencies of the medium. In macroscopic quantum electrodynamics, we take this into account by posing a phenomenological frequency-dependent permittivity ε.[4]

Whilst this greatly simplifies the mathematics on a classical level, it does introduce some difficulties when quantising the system. First of all, all media are absorbing, a simple consequence of causality as expressed through the Kramers-

[3] A consequence of having a minimum energy.

[4] In most cases linked to the refractive index as $\varepsilon = n^2$.

Kronig relations. These relations relate the real (retarded response) and imaginary (absorption) parts of the permittivity [1]. Even in the case where absorption can be neglected, a frequency dependent permittivity by necessity leads to a temporally non-local equation of motion for the electromagnetic field. Suppose for instance we have a uniform and isotropic medium whose permittivity is given by $\varepsilon(\omega)$, then the electric field $\mathbf{E}$ can be shown to be governed by

$$-\nabla^2\mathbf{E}(t) + \frac{1}{c^2}\frac{\partial^2}{\partial t^2}\left[\mathbf{E}(t) + \int_{-\infty}^{t} ds\, \chi\,(t-s)\,\mathbf{E}(s)\right] = 0, \tag{1.1}$$

where $\chi(t) = \int_{-\infty}^{\infty}\frac{d\omega}{2\pi}e^{-i\omega t}\left[\varepsilon(\omega)-1\right]$ is the medium response function, and c is the speed of light. Quantising this is possible, but conceptually difficult as most quantisation schemes rely on time-locality.[5] In particular, the temporal nonlocality and absorption can make Lagrangians and Hamiltonians of macroscopic electrodynamics ill-defined. As a consequence, a multitude of different models have been developed over the years, which are nicely reviewed in Refs. [57, 58] and the references therein.

The solution to this is to introduce a microscopic matter degree of freedom phenomenologically, that is, chosen such that it reproduces the correct physics on a macroscopic scale. Often this is done by introducing an effective degree of freedom for the polarisability of the medium, as was first done by Hopfield [59] for non-absorbing media, and later extended to include absorption by Huttner and Barnett [60], and Philbin [61]. Usually, the matter degree of freedom is modelled by a simplified version of the actual microscopic detail. For instance, a large enough set of two-level atoms with the same resonance frequency will behave collectively like a harmonic oscillator. Now, as we mentioned earlier, the mere presence of the medium affects the structure of the electromagnetic quantum vacuum, leading to Casimir, and Casimir-Polder, forces, a review of which can be found in Ref. [62].

Our interest is in quantum vacuum radiation, and this leads us directly to optical media with time-dependent properties. This is naturally linked to all excitations in temporally modulated quantum systems [63, 64]. There have been a wide range of studies into time-varying optical media, perhaps starting with the study of Unruh-like acceleration radiation in a rapidly expanding plasma by Yablonovitch [65]. These studies include so-called time-refraction in the limit where dispersion can be neglected [66, 66–69], which is the analogue of spatial refraction (Snell's law [54]) for abrupt changes in time, as well as the study of the emitted radiation in the same limit [70, 71]. Some studies include dispersion, such as Refs. [72–74], but tend to only consider effects that are first order in the refractive index variation. It might thus be worth asking if the dispersion can cause non-trivial changes to the quantum vacuum radiation.

This is further related to the direct study of collective excitations in light-matter

[5] We will discuss this further in Chapter 2.

systems, that is, the study of polaritons. In general, coupled systems offers a variety of phenomena to be explored, such as combined resonances and transport properties, and this is, of course, the case also for polaritons [75, 76]. As such, there have been a large number of studies, of which we will mention here but a few. Cavities offer strong light-matter coupling, and this has commonly been the scenario in which polaritons have been studied. For instance, the cavity quantum electrodynamics of polaritons have been explored in Refs. [77, 78], and this has further been linked to driven-dissipative photon fluids [79, 80] where the polaritons form a fluid-like state similar to a Bose-Einstein condensate. Another interesting aspect of polariton physics is optomechanical systems [81, 82], where the light-matter system is further coupled to mechanical motion, as well as surface-plasmon polaritons [83] for metal-dielectric interfaces.

Quantum vacuum radiation in time-dependent optical media for these systems becomes the study of exciting polaritons by temporally modulating its vacuum state. As with all studies of polaritons, this has a rich history, especially for micro-cavity polaritons and semi-conductor exciton-polaritons [49, 84–93], whereas limited studies have focused on surface-plasmon polaritons [94, 95].

In this thesis, I will, for the most part, focus on polaritons in bulk optical media, such as a piece of glass or an optical fibre. My aim is to build models for quantum vacuum radiation that takes all dispersion fully into account, ideal for the theoretical modelling of experiments such as those reported in Refs. [96] and [97]. I will start by introducing some background methods required for this in Chapter 2. This is followed by a perturbative model for quantum vacuum radiation, based on macroscopic quantum electrodynamics in the spirit of Hopfield, in Chapter 3. We then apply this to the experiment of Ref. [97] in Chapter 4, and show that the radiation observed is consistent with quantum vacuum radiation. The thesis then has a small intermission in Chapter 5, where we further explore the link to the cosmological physics we discussed earlier, as well as motivate the need for building a non-perturbative model of quantum vacuum radiation. We then build such a model in Chapter 6, where we link the physics of light-matter systems to that of a trapped particle in a magnetic field. The thesis then finishes with some concluding remarks in Chapter 7.

Finally, I want to note that I will base this thesis on Items 1-3 (with some commentary from Items 4 and 5) in the List of Publications. The remaining articles (Items 6-17) are on related subjects in the topics of optical and cold atom physics (and a diversion into high-energy physics), but not directly relevant to this thesis. As a practical aside, I should note that, unless otherwise stated, all figures in this thesis is produced using *Mathematica* (versions 10 and 11), specifically as analytical expressions of some variables.

Chapter 2

Background theory and methods

"Take one step at a time, it is in fact the only way forward."

An old proverb

Before we delve into the main work of this thesis it is a good idea to put ourselves on firm theoretical footing. Primarily we will work with quantum field theory (QFT), but in our context it is instructive to think of it as quantum mechanics with fields.[1] The following chapter is heavily influenced by Feynman *et al.* [3], as well as Grosche and Steiner [98], and Altland and Simons [5]. Mainly, we will concern ourselves with Feynman's path integrals, but we will also discuss other approaches to quantum mechanics (and field theory), specifically the Schrödinger equation and canonical quantisation. In other words, we will define the following:

- The path integral

$$\langle \phi_b(x), t_b | \phi_a(x), t_a \rangle = \int_{\phi(x,t_a)=\phi_a(x)}^{\phi(x,t_b)=\phi_b(x)} \mathcal{D}\phi \; e^{iS[\phi]}. \tag{2.1}$$

- The Schrödinger equation

$$i\frac{\partial}{\partial t}\Psi\left[\phi(x), t\right] = \left[\hat{\pi}_\phi^2/2 + V(\hat{\phi}, t)\right] \Psi\left[\phi(x), t\right]. \tag{2.2}$$

- And time-evolution of canonical operators

$$\frac{d\hat{a}_\phi}{dt} = i\left[\hat{H}, \hat{a}_\phi\right]. \tag{2.3}$$

A sketch of the different quantisation schemes can be seen in Fig. 2.1. There are of course many more representations of quantum mechanics and quantum field theory, but we will limit ourselves to the ones used in the thesis. We will also study a

[1] This is sometimes known as second quantisation, as opposed to first quantisation (that is quantum mechanics). Such a notion is mostly relevant when for instance treating the Schrödinger equation as a quantum field, as is commonly done in condensed matter physics, but not for electromagnetism due to its field nature in both a classical and quantum setting. I will return to this point in Section 2.2

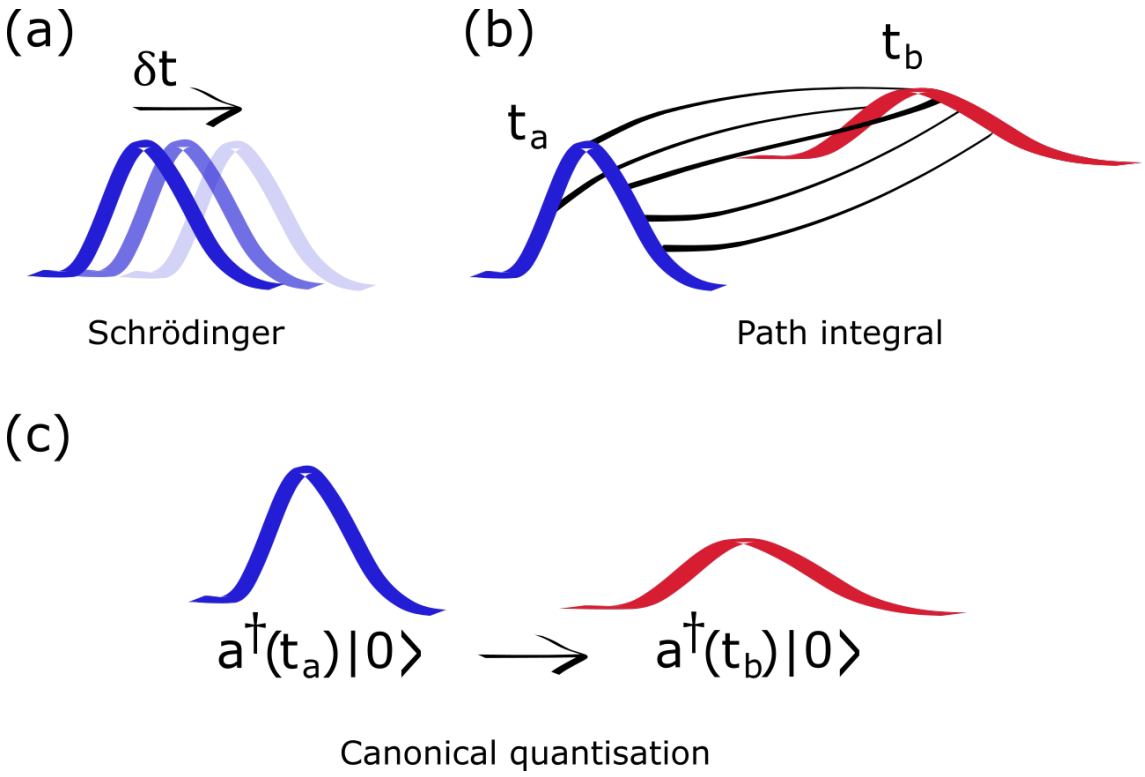

Figure 2.1: Illustrations of the different quantisation techniques used in this thesis. **(a)** In the Schrödinger equation, the wavefunction (here illustrated in position space) is evolved each time-step δt according to a differential equation. **(b)** The path integral, on the other hand, is the sum over all classical paths (represented as black lines) that starts within the wavefunction at time t_a, from which we can find the wavefunction at time t_b. **(c)** Canonical quantisation instead evolves some operator $a^\dagger$ in time, which ultimately contains information about the wavefunction.

simple example using the above versions of quantum mechanics. Whilst some of the topics we will discuss might seem somewhat trivial, and the definitions feel overly complicated, a solid starting point is important for what follows.

2.1 Quantum mechanics - the abridged version

Let us start with a couple of definitions. Here we will be dealing with a single particle in 1-dimensional space x. Generalising to further dimensions, as well as to fields, is fairly straightforward, and where relevant we will discuss this directly in each chapter. For simplicity, in this thesis we will work with units such that $\hbar = 1$, and for our quantum mechanics discussion here set the particle mass m to unity. We will also be using concepts from classical mechanics, in particular the Lagrangian

$$\begin{aligned} L &= \text{kinetic energy} - \text{potential energy} \\ &= \dot{x}^2/2 - V(x,t), \end{aligned} \tag{2.4}$$

as well as the Hamiltonian

$$\begin{aligned} H &= \text{kinetic energy} + \text{potential energy} \\ &= p^2/2 + V(x,t). \end{aligned} \tag{2.5}$$

In general, we can move between the two formulations of classical mechanics by defining the momentum p conjugate to x as

$$p = \frac{\partial L}{\partial \dot{x}}. \tag{2.6}$$

The Hamiltonian is then defined as the Legendre transformation of the Lagrangian

$$H = p\dot{x} - L. \tag{2.7}$$

Furthermore, we will simply assume the following since we do not intend to dwell on the intricacies of how quantum theory is defined:

- We can express any state as $|\psi\rangle$, and the overlap between two states is given by $\langle\phi|\psi\rangle$, which represents the probability amplitude of measuring $|\phi\rangle$ from a state $|\psi\rangle$. It follows then that $|\langle\phi|\psi\rangle|^2$ is the associated probability.

- As long as a representation forms a complete basis, we can resolve the identity by

$$\mathbb{I} = \sum_A |A\rangle \langle A| . \tag{2.8}$$

- We can resolve the state $|\psi\rangle$ in terms of a basis. For instance, $\psi(x)$ is given by

$$\begin{aligned} |\psi\rangle &= \int_{-\infty}^{\infty} dx \ \ |x\rangle \langle x|\psi\rangle \\ &= \int_{-\infty}^{\infty} dx \ \ |x\rangle \psi(x), \end{aligned} \tag{2.9}$$

  where $|x\rangle$ is the position state defined as the eigenstate of the position operator,[2] and we define the overlap $\langle x|\psi\rangle = \psi(x)$. Likewise, we could expand in the energy basis as

$$|\psi\rangle = \sum_n |n\rangle \langle n|\psi\rangle = \sum_n |n\rangle a_n. \tag{2.10}$$

[2] That is, $\hat{x}\,|x\rangle = x\,|x\rangle$.

- We combine two representations of a state through

$$|\psi\rangle = \int_{-\infty}^{\infty} dx \ |x\rangle \langle x|\psi\rangle = \int_{-\infty}^{\infty} dx \sum_n \ |n\rangle \langle n|x\rangle \langle x|\psi\rangle$$
$$= \int dx \sum_n \ |n\rangle \psi_n^*(x)\psi(x) = \sum_n \ a_n |n\rangle \,, \tag{2.11}$$

  where $\psi_n(x)$ is the representation of the energy eigenstate in the position basis, and $a_n = \int_{-\infty}^{\infty} dx \ \psi_n^*(x)\psi(x)$ is the overlap between the state $|\psi\rangle$ and the energy eigenstate $|n\rangle$.

- The position operator $\hat{x}$ and the momentum operator $\hat{p}$ do not commute,[3] and their commutator is given by $[\hat{x}, \hat{p}] = i$.

This will give us a starting point for the discussion.

2.1.1 The Schrödinger equation

As it forms a good starting point, let us quickly introduce the formulation of quantum mechanics that relies on the Schrödinger equation. It is intimately linked to the path integral formulation, but will also come in use in later chapters. Here we are interested in finding a wavefunction $\psi(x,t)$ such that $|\psi(x,t)|^2$ gives us the probability of finding a particle at position x and time t. We suppose that this wavefunction will satisfy

$$i\frac{\partial}{\partial t}\psi(x,t) = \hat{H}\psi(x,t)$$
$$= \left[\frac{1}{2}\hat{p}^2 + V(\hat{x},t)\right]\psi(x,t), \tag{2.12}$$

where p is the momentum of the particle and V is its potential energy. From analytical mechanics we know that we can define the momentum as

$$p = \frac{\partial L}{\partial \dot{x}}. \tag{2.13}$$

Now, we know also that $[\hat{x}, \hat{p}] = i$, and we find the x-representation of this algebra by letting the momentum and position operators take the form

$$\hat{p} = -i\frac{\partial}{\partial x},$$
$$\hat{x} = x, \tag{2.14}$$

[3] We define the commutator as $\left[\hat{a}, \hat{b}\right] = \hat{a}\hat{b} - \hat{b}\hat{a}$.

in the Schrödinger equation of Eq. (2.12). We thus arrive at the familiar

$$i\frac{\partial}{\partial t}\psi(x,t) = \left[-\frac{1}{2}\frac{\partial^2}{\partial x^2} + V(x,t)\right]\psi(x,t). \tag{2.15}$$

2.1.2 The position space path integral

Suppose now that we wish to calculate the probability amplitude of transitioning from some initial state $|i\rangle$ to a final state $|f\rangle$.[4] Such an amplitude is given by $\langle f|i\rangle$. Furthermore, we can at some time t_1 ask ourselves if the particle is at a position x_1, and sum over all possible positions. This is a type of resolution of identity

$$\mathbb{I} = \int dx_1 \ \left|x_1, t_1\right\rangle \left\langle x_1, t_1\right|, \tag{2.16}$$

where we resolve the identity in space. Therefore, we can write our probability amplitude of starting in $|i\rangle$ and finishing in $|f\rangle$ as

$$\begin{aligned}\langle f|i\rangle &= \int dx_1 \ \langle f|x_1,t_1\rangle \langle x_1,t_1|i\rangle \\ &= \int dx_1 ... \int dx_N \langle f|x_N,t_N\rangle ... \langle x_2,t_2|x_1,t_1\rangle \langle x_1,t_1|i\rangle ,\end{aligned} \tag{2.17}$$

where in the second line we have simply repeated this procedure N times.

Now if we want to calculate the probability amplitude of starting at position x_a at time t_a and finishing at position x_b at time t_b, then we set $|i\rangle = |x_a, t_a\rangle$ and $|f\rangle = |x_b, t_b\rangle$. For simplicity, we can choose our times where we resolve the identity as

$$t_n = t_a + n\epsilon \tag{2.18}$$

where

$$\epsilon = \frac{t_b - t_a}{N+1}. \tag{2.19}$$

We then have

$$\langle x_b, t_b|x_a, t_a\rangle = \left(\prod_{n=1}^{N}\int dx_n\right)\left(\prod_{n=1}^{N+1}\langle x_n, t_n|x_{n-1}, t_{n-1}\rangle\right). \tag{2.20}$$

In the limit where $N \to \infty$ we can write this as

$$\langle x_b, t_b|x_a, t_a\rangle = \int_{x(t_a)=x_a}^{x(t_b)=x_b} \mathcal{D}x \ \langle x_b, t_b|x_a, t_a\rangle \big|_{x(t)}. \tag{2.21}$$

This is indeed the path integral for quantum mechanics in position space. The

[4] Here we will follow closely the derivation outlined in Ref. [99].

question now becomes finding an expression for $\langle x_b, t_b | x_a, t_a \rangle \big|_{x(t)}$. To do this, we should define the action

$$S[x] = \int_{t_a}^{t_b} dt\ L(x, \dot{x}, t), \tag{2.22}$$

where L is the Lagrangian as defined in Eq. (2.4)

From classical mechanics, we know that by extremising the action in Eq. (2.22) we find the classical equation of motion, i.e. we want to compute

$$\left.\frac{\delta S}{\delta x}\right|_{x=x_{\mathrm{cl}}} = 0. \tag{2.23}$$

Supposing that such a solution exists then it is easily shown to be given by the Euler-Lagrange equation[5]

$$\frac{d}{dt}\left(\frac{\partial L}{\partial \dot{x}}\right) - \frac{\partial L}{\partial x} = 0, \tag{2.24}$$

which does indeed yield the expected classical equation of motion

$$\ddot{x} + \frac{\partial V}{\partial x} = 0. \tag{2.25}$$

With this in hand, we can assert

$$\langle x_b, t_b | x_a, t_a \rangle \big|_{x(t)} = \exp\left(iS[x]\right), \tag{2.26}$$

where $S[x]$ is the action in Eq. (2.22). This is an assumption, based upon the semi-classical expansion of the Schrödinger equation, that turns out to be correct. Finally we arrive at the usual formula for the position space path integral

$$\langle x_b, t_b | x_a, t_a \rangle = \int_{x(t_a)=x_a}^{x(t_b)=x_b} \mathcal{D}x\ e^{iS[x]}. \tag{2.27}$$

We could also define this as the Green's function of the Schrödinger equation, as it is straightforward (albeit somewhat algebraically intensive) to show that

$$\left[-\frac{1}{2}\frac{\partial^2}{\partial x_b^2} + V(x_b, t) - i\frac{\partial}{\partial t_b}\right] \langle x_b, t_b | x_a, t_a \rangle = -i\delta(t_b - t_a)\delta(x_b - x_a). \tag{2.28}$$

[5]For this we want to compute

$$\begin{aligned}\delta S &= S[x + \delta x] - S[x] \\ &= \left[\frac{\partial L}{\partial \dot{x}}\delta x\right]_{t_a}^{t_b} - \int_{t_a}^{t_b} dt\ \left[\left(\frac{d}{dt}\left(\frac{\partial L}{\partial \dot{x}}\right) - \frac{\partial L}{\partial x}\right)\delta x + \mathcal{O}\left(\delta x^2\right)\right],\end{aligned}$$

where the first term goes to zero as we choose $\delta x(t_b) = \delta x(t_a) = 0$. Such a term is usually referred to as a surface term.

Therefore, we can find the wavefunction at time $t = T$ from the wavefunction at time $t = 0$ by computing

$$\psi(x, T) = \int dx_0 \ \langle x, T|x_0, 0\rangle \, \psi(x_0, 0). \tag{2.29}$$

2.1.3 Canonical quantisation

In this scheme we will concern ourselves with the time-evolution of operators instead of wavefunctions. Specifically, we will turn to the canonical raising (lowering) operators $\hat{a}^\dagger$ ($\hat{a}$) associated with jumps within energy space. Our discussion here is centred around the work by Jacobson [37]. We will (mostly) be working within the so-called Heisenberg representation of quantum mechanics, where the operators have a time-dependence, as opposed to the Schrödinger representation where the states depend on time. Canonical quantisation is in general based on a quantum mechanical version of Hamiltonian mechanics, where the so-called Poisson brackets are promoted to commutators.[6] An operator $\hat{A}$ has the time-dependence

$$\frac{d\hat{A}}{dt} = i\left[\hat{H}, \hat{A}\right] + \frac{\partial \hat{A}}{\partial t} \tag{2.30}$$

in this picture, where the partial derivative becomes important if the operator is explicitly time-dependent. This is of course also true for the position and momentum operators, but what is of more interest here are the operators $\hat{a}$ and $\hat{a}^\dagger$, as they tell us about changes in the systems energy.

Let us start at a classical level. Suppose that the classical equation of motion is given by

$$\ddot{x}(t) + \frac{\partial V(x, t)}{\partial x} = 0. \tag{2.31}$$

This is a second order ordinary differential equation. By the usual theory of differential equations [100] this has two independent solutions, which we will call $f(t)$ and $g(t)$. In particular, we can choose these functions to be orthonormal according to the norm

$$(f, g) = i\Big[f^* \partial_t g - g \partial_t f^*\Big]. \tag{2.32}$$

[6] Say x and p are related by Eq. (2.13) along with the Hamiltonian $H = \dot{x}p - L$, then for any function f we find

$$\begin{aligned}\frac{d}{dt} f\,(p, x, t) &= \frac{\partial f}{\partial x}\frac{dx}{dt} + \frac{\partial f}{\partial p}\frac{dp}{dt} + \frac{\partial f}{\partial t} \\ &= \frac{\partial f}{\partial x}\frac{\partial H}{\partial p} - \frac{\partial f}{\partial p}\frac{\partial H}{\partial x} + \frac{\partial f}{\partial t} = \{f, H\} + \frac{\partial f}{\partial t},\end{aligned}$$

where we used Hamilton's equations in the second line. Here $\{f, g\}$ is the Poisson bracket, which is promoted to a commutator by letting $\{f, g\} \to i[\hat{f}, \hat{g}]$.

Therefore, we can always choose to expand any solution to Eq. (2.31) as

$$x(t) = af(t) + bg(t). \tag{2.33}$$

If we now return to the quantum mechanical problem at hand, where the position operator obeys

$$\frac{d\hat{x}}{dt} = i\left[\hat{H}, \hat{x}\right]. \tag{2.34}$$

We find that we can likewise expand the time-dynamics of the position operator as

$$\hat{x}(t) = f(t)\hat{a} + g(t)\hat{a}^\dagger, \tag{2.35}$$

where we have suggestively chosen $\hat{a}$ and $\hat{a}^\dagger$ as the two independent operators (in the Schrödinger picture), and where f and g satisfy the classical equation of motion. Note here that whilst $\hat{x}$ is Hermitian, $\hat{a}$ and $\hat{a}^\dagger$ are not. Specifically, we choose f to be the independent function with positive norm, i.e. such that $(f, f) = 1$ whereas $(g, g) = -1$. Now, we find that

$$\left[\hat{a}, \hat{a}^\dagger\right] = 1, \tag{2.36}$$

since we have defined f and g to be orthonormal according the norm in Eq. (2.32). In other words, $\hat{a}$ and $\hat{a}^\dagger$ satisfy the canonical commutation relation. We can also define the ladder operators as

$$\begin{aligned} \hat{a} &= (f, \hat{x}) \\ \hat{a}^\dagger &= -(g, \hat{x}), \end{aligned} \tag{2.37}$$

where the sign on the second line follows from $(g, g) = -1$. Another way to approach this is to define the norm such that the canonical commutation relations are satisfied. We can now construct the energy space of the problem, by first finding a ground state that satisfies

$$\hat{a}\left|0\right\rangle = 0. \tag{2.38}$$

This of course assumes that such a ground state exists. We can obtain the Heisenberg representation by defining the time-dependence as

$$\begin{aligned} \hat{a}(t) &\equiv f(t)\hat{a} \\ \hat{a}^\dagger(t) &\equiv g(t)\hat{a}^\dagger. \end{aligned} \tag{2.39}$$

It follows that

$$\frac{d\hat{a}(t)}{dt} = i\left[\hat{H}, \hat{a}(t)\right]. \tag{2.40}$$

2.1.4 An example: the harmonic oscillator

Up to this point this has perhaps been fairly abstract, so let us apply the different methods to the most common example of all: the harmonic oscillator. Our starting point will be the classical equation of motion

$$\ddot{x}(t) + \omega^2 x(t) = 0. \tag{2.41}$$

This can be found from extremising the action

$$S[x] = \int_{t_a}^{t_b} dt\, \frac{1}{2}\left[\dot{x}^2 - \omega^2 x^2\right]. \tag{2.42}$$

We thus have the Lagrangian

$$L = \frac{1}{2}\left[\dot{x}^2 - \omega^2 x^2\right], \tag{2.43}$$

from which we can define the conjugate momentum to x as

$$p \equiv \frac{\partial L}{\partial \dot{x}} = \dot{x}. \tag{2.44}$$

Finally, by the Legendre transform we find the Hamiltonian

$$\begin{aligned} H &= p\dot{x} - L \\ &= \frac{1}{2}\left[p^2 + \omega^2 x^2\right]. \end{aligned} \tag{2.45}$$

This defines the classical physics. Let us now quantise this problem using the above mentioned approaches.

2.1.4.1 Schrödinger equation

We start by promoting the position x to the position operator $\hat{x}$, as well as the momentum p to the momentum operator $\hat{p}$. We can then promote the Poisson bracket[7] of x and p to a commutator that satisfies the commutation relation

$$[\hat{x}, \hat{p}] = i, \tag{2.46}$$

[7] That is, $\{x, p\} = 1$.

which we can satisfy by writing the momentum operator in position space as

$$\hat{p} = -i\frac{\partial}{\partial x}. \tag{2.47}$$

The Schrödinger equation thus becomes

$$i\frac{\partial}{\partial t}\psi(x,t) = \left[-\frac{1}{2}\frac{\partial^2}{\partial x^2} + \frac{\omega^2 x^2}{2}\right]\psi(x,t). \tag{2.48}$$

It is straightforward to confirm that the ground state has energy $E = \omega/2$, and its wavefunction is given by

$$\psi_0(x,t) = \left(\frac{\omega}{\pi}\right) e^{-\omega x^2/2} e^{-i\omega t/2}. \tag{2.49}$$

As usual, this is the first of the infinite set of energy states of a harmonic oscillator found, up to a normalisation constant, by computing $(\hat{a}^\dagger)^n \psi_0$.[8]

2.1.4.2 Position space path integral

In the path integral the relevant quantity is the action

$$S[x] = \int_{t_a}^{t_b} dt\, \frac{1}{2}\left[\dot{x}^2 - \omega^2 x^2\right], \tag{2.50}$$

and as such this will be our starting point. We now wish to compute

$$\langle x_b, t_b | x_a, t_a \rangle = \int_{x(t_a)=x_a}^{x(t_b)=x_b} \mathcal{D}x\; e^{iS[x]}. \tag{2.51}$$

Whilst this can be done by discretising time, as is done in its definition, there are several more straightforward methods. Let us first focus on the action $S[x]$. Suppose that we split x into its classical dynamics and quantum fluctuations. Specifically $x = x_{\rm cl} + \eta$ where $x_{\rm cl}(t_a) = x_a$ and $x_{\rm cl}(t_b) = x_b$ whereas $\eta(t_a) = \eta(t_b) = 0$. Now $x_{\rm cl}$ obeys

$$\ddot{x}_{\rm cl} + \omega^2 x_{\rm cl} = 0 \tag{2.52}$$

with the above boundary conditions. If we substitute this into the action in Eq. (2.50) we find that

$$\begin{aligned} S[x_{\rm cl} + \eta] &= \int_{t_a}^{t_b} dt\, \frac{1}{2}\left[(\dot{x}_{\rm cl} + \dot{\eta})^2 - \omega^2 (x_{\rm cl} + \eta)^2\right] \\ &= S[x_{\rm cl}] + S[\eta], \end{aligned} \tag{2.53}$$

[8] The definition of $\hat{a}^\dagger$ can be found in Section 2.1.4.3.

where we used the boundary conditions of η as well as the classical equation of motion in order to obtain the second line. In other words, it separates into the classical and quantum action. This is a feature of all quadratic actions. We can change the basis of the path integral, and integrate over η instead of x. This yields

$$\begin{aligned}\langle x_b, t_b | x_a, t_a \rangle &= e^{iS[x_{\rm cl}]} \int_{\eta(t_a)=0}^{\eta(t_b)=0} \mathcal{D}\eta \, \exp\left(-\frac{i}{2} \int_{t_a}^{t_b} dt \, \eta(t) \left[-\frac{d^2}{dt^2} - \omega^2 \right] \eta(t) \right) \\ &= \sqrt{\frac{1}{\pi i \det\left[-\frac{d^2}{dt^2} - \omega^2 \right]}} e^{iS[x_{\rm cl}]} \equiv \mathbb{D}_\omega(T) e^{iS[x_{\rm cl}]}, \end{aligned} \tag{2.54}$$

where we have defined the functional determinant

$$\det\left[-\frac{d^2}{dt^2} - \omega^2 \right] \tag{2.55}$$

in analogy with the usual Gaussian integral. Eq. (2.54) is the probability amplitude for finding the particle at position x_b at time t_b if it starts at position x_a at time t_a. We will return to this shortly, but let us first calculate the classical action.

In order to compute the classical action, we must first find the solution to the classical equation of motion in Eq. (2.52) with the boundary conditions $x_{\rm cl}(t_a) = x_a$ and $x_{\rm cl}(t_b) = x_b$. It is straightforward to verify that this is given by

$$x_{\rm cl}(t) = \frac{1}{\sin \omega T} \left[x_b \sin \omega(t - t_a) + x_a \sin \omega(t_b - t) \right], \tag{2.56}$$

where $T = t_b - t_a$ is the total time. Furthermore,

$$\begin{aligned} S\left[x_{\rm cl}\right] &= \int_{t_a}^{t_b} dt \, \frac{1}{2} \left[\dot{x_{\rm cl}}^2 - \omega^2 x_{\rm cl}^2 \right] \\ &= \frac{1}{2} \left[x_{\rm cl} \dot{x}_{\rm cl} \right]_{t_a}^{t_b} - \int_{t_a}^{t_b} dt \, x_{\rm cl} \left[\ddot{x}_{\rm cl} + \omega^2 x_{\rm cl} \right] = \frac{1}{2} \left[x_{\rm cl} \dot{x}_{\rm cl} \right]_{t_a}^{t_b}, \end{aligned} \tag{2.57}$$

where we made use of the classical equation of motion in the last step. Thus we find the standard result

$$S_{\rm cl} = S\left[x_{\rm cl}\right] = \frac{\omega}{2 \sin \omega T} \left[\left(x_b^2 + x_a^2 \right) \cos \omega T - 2 x_b x_a \right]. \tag{2.58}$$

What is left to find is the transition amplitude in Eq. (2.51) for which we need to compute the functional determinant in Eq. (2.55).

Functional determinants and Morette-Van Hove Perhaps the most straightforward, but very specialised, way of computing this functional determinant is to recognise that due to time-translational invariance it can only depend on the total

time T. We can then use a resolution of identity to compute

$$\begin{aligned}\mathbb{D}_\omega(T) = \langle 0,T|0,0\rangle &= \int_{-\infty}^{\infty} dx\ \langle 0,T|x,t\rangle\langle x,t|0,0\rangle \\ &= \mathbb{D}_\omega(T-t)\mathbb{D}_\omega(t)\int_{-\infty}^{\infty} dx \exp\left(\frac{i\omega\cos\omega\,(T-t)}{2\sin\omega\,(T-t)}x^2\right)\exp\left(\frac{i\omega\cos\omega t}{2\sin\omega t}x^2\right) \\ &= \mathbb{D}_\omega(T-t)\mathbb{D}_\omega(t)\sqrt{\frac{2\pi i\sin\omega\,(T-t)\sin\omega t}{\omega\sin\omega T}}. \end{aligned} \tag{2.59}$$

From this we can obtain

$$\mathbb{D}_\omega(T) = \sqrt{\frac{\omega}{2\pi i\sin\omega T}} \tag{2.60}$$

by expanding for $T \gg t$. It is also worth noting that in the $\omega \to 0$ limit, we are left with a free particle, whose pre-factor is

$$\mathbb{D}_0(T) = \sqrt{\frac{1}{2\pi i T}}. \tag{2.61}$$

From this we find the solution to the functional determinants

$$\begin{aligned}\det\left[-\frac{d^2}{dt^2}-\omega^2\right] &= \frac{2\sin\omega T}{\omega}, \\ \det\left[-\frac{d^2}{dt^2}\right] &= 2T. \end{aligned} \tag{2.62}$$

This doesn't however generalise very well, as indeed not all problems are time-translational invariant. In fact, the problems that we want to study are not. To resolve this, and develop a more general method of evaluating functional determinants, we can start with defining it in analogy with a matrix determinant as [98]

$$\det\left[\hat{O}\right] = \prod_n \mu_n, \tag{2.63}$$

where $\hat{O}$ is some operator and μ_n are its eigenvalues on the interval $t \in [t_a, t_b]$. In particular, we define the eigenvalues through

$$\hat{O}f(t) = \lambda f(t), \quad f(t_a) = f(t_b) = 0. \tag{2.64}$$

For instance, if we apply this to the free particle, i.e. $\hat{O} = -d^2/dt^2$, then we find the eigenvalues $\lambda_n = (n\pi/T)^2$ for $n \in \mathbb{Z}^+$. We therefore want to compute the product

$$\det\left[-\frac{d^2}{dt^2}\right] = \prod_n \left(\frac{n\pi}{T}\right)^2. \tag{2.65}$$

However, computing functional determinants as an infinite product is not straightforward, and usually divergent. These divergences commonly arise due to a lack of

a reference point. For instance, the electric potential energy of an infinite line of charges is infinite, but the electric field, which measures the difference in electric potential between neighbouring points, is finite and calculable [101]. We can remedy this by regularisation, which is a procedure designed to remove the problematic infinities and leave only the terms contributing to the physical observable (such as the electric field). A way to regularise functional determinants is to define them through [98]

$$\det \hat{O} = \exp\left[-\zeta'_{\hat{O}}(0)\right], \tag{2.66}$$

where $\zeta_{\hat{O}}(s)$ is the zeta function associated with $\hat{O}$, defined through the spectrum of $\hat{O}$ as

$$\zeta_{\hat{O}}(s) \equiv \mathrm{Tr}\, \hat{O}^{-s} = \sum_{n=1}^{\infty} \lambda_n^{-s}. \tag{2.67}$$

This takes care of the regularisation. In particular, we find that

$$\zeta_{-d^2/dt^2}(s) = \left(\frac{T}{\pi}\right)^{2s} \zeta(2s), \tag{2.68}$$

where $\zeta(2s)$ is the usual Riemann-Zeta function defined by $\zeta(s) = \sum_{n=1}^{\infty} n^{-s}$. We can thus compute the zeta regularised functional determinant of $-d^2/dt^2$ as

$$\det\left[-\frac{d^2}{dt^2}\right] = 2T, \tag{2.69}$$

using the fact that $\zeta(0) = -1/2$ and $\zeta'(0) = -\ln(2\pi)/2$. This is in agreement with above. We can similarly obtain the functional determinant for the harmonic oscillator, after some algebra,

$$\begin{aligned} \zeta_{-d^2/dt^2-\omega^2}(s) &= \left(\frac{T}{\pi}\right)^{2s} \sum_{n=1}^{\infty} \frac{1}{\left[n^2 - (\omega T/\pi)^2\right]^s} \\ \Rightarrow \det\left[-\frac{d^2}{dt^2} - \omega^2\right] &= \exp\left[\zeta'_{-d^2/dt^2-\omega^2}(0)\right] = 2\sin(\omega T)/\omega. \end{aligned} \tag{2.70}$$

This is indeed the same result as Eq. (2.62).

This doesn't however lend itself very easily to computations. Commonly, it is

far simpler to compute the functional determinants as ratios, such as

$$\begin{aligned}\det\left[-\frac{d^2}{dt^2}-\omega^2\right] &= \det\left[-\frac{d^2}{dt^2}\right]\frac{\det\left[-\frac{d^2}{dt^2}-\omega^2\right]}{\det\left[-\frac{d^2}{dt^2}\right]}\\ &= \det\left[-\frac{d^2}{dt^2}\right]\prod_{n=1}^{\infty}\left(1-\frac{\omega^2T^2}{\pi^2n^2}\right)\\ &= 2T\frac{\sin\omega T}{\omega T} = \frac{2\sin\omega T}{\omega},\end{aligned} \tag{2.71}$$

where in the last step we used the definition of the sinc-function as an infinite product. This is because the determinant in the denominator provides a reference point and regularises the problem. In particular, this allows us also to use the so-called Gel'fand-Yaglom formalism [102, 103], where we can compute a ratio of functional determinants by first calculating

$$\begin{aligned}\hat{O}F(t) = 0, \quad F(t_a) = 0,\ F'(t_a) = 1,\\ \hat{A}G(t) = 0, \quad G(t_a) = 0,\ G'(t_a) = 1.\end{aligned} \tag{2.72}$$

The ratio of functional determinants of $\hat{O}$ and $\hat{A}$ on the interval $t \in [t_a, t_b]$ is then given by

$$\det\left[\hat{O}\right] / \det\left[\hat{A}\right] = F(t_b)/G(t_b). \tag{2.73}$$

In our case, it is easy to show that

$$\begin{aligned}\left[-\frac{d^2}{dt^2}-\omega^2\right]F(t) = 0, \quad F(t_a) = 0,\ F'(t_a) = 1,\\ \left[-\frac{d^2}{dt^2}\right]G(t) = 0, \quad G(t_a) = 0,\ G'(t_a) = 1,\end{aligned} \tag{2.74}$$

has solutions $F(t_b) = \sin(\omega T)/\omega$ and $G(t_b) = T$. Thus we find

$$\frac{\det\left[-\frac{d^2}{dt^2}-\omega^2\right]}{\det\left[-\frac{d^2}{dt^2}\right]} = \frac{\sin\omega T}{\omega T}. \tag{2.75}$$

The proof of Eq. (2.73) can be found in Appendix A of Ref. [104].[9] Finally, let us turn to the Morette-van Hove determinant [98, 103, 105]. The Morette-van Hove determinant is an especially useful way to compute the pre-factor of the path integral

[9] This proof goes as follows. Note this is intended as a brief overview only and I refer the reader to Ref. [104] for further details. Suppose we have an eigenvalue equation of the form

$$-\frac{d^2}{dt^2}\psi^{(1)}(t) + V^{(1)}(t)\psi(t) = \lambda\psi^{(1)}(t),$$

on the interval $t \in [0, T]$. We can let $\psi_\lambda^{(1)}$ be the solution with initial conditions $\psi_\lambda^{(1)}(0) = 0$ and $\dot{\psi}_\lambda^{(1)}(0) = 1$. Now the operator $-\frac{d^2}{dt^2} + V^{(1)}(t)$ acting on the same interval has an eigenvalue $\lambda_n^{(1)}$

where we find, given an action that is at most quadratic in the coordinates,

$$\mathbb{D}(T) = \frac{1}{\sqrt{2\pi i}^N} \left(\det \left[-\frac{\partial^2 S_{\rm cl}}{\partial x_b^i \partial x_a^j} \right] \right)^{-1/2} . \tag{2.76}$$

Here N is the dimension of your space such that $\mathbf{x} = \left(x^1, x^2, ..., x^N\right)$, and 'det' is in this case the usual matrix determinant.[10] If the action is not quadratic, then this determinant forms the semi-classical expansion [98, 105, 106]. In the case of the harmonic oscillator, it is easy to confirm that the Morette-van Hove determinant yields

$$-\frac{\partial^2 S_{\rm cl}}{\partial x_b \partial x_a} = \frac{\sin \omega T}{\omega}, \tag{2.77}$$

and thus Eq. (2.76) is in agreement with Eq. (2.60) for the harmonic oscillator.

---

if and only if

$$\psi^{(1)}_{\lambda^{(1)}_n}(T) = 0.$$

This is similarly true for some other operator $-\frac{d^2}{dt^2} + V^{(2)}(t)$. Both the left hand side and right hand side of the following

$$\frac{\det\left[-\frac{d^2}{dt^2} + V^{(1)}(t) - \lambda\right]}{\det\left[-\frac{d^2}{dt^2} + V^{(2)}(t) - \lambda\right]} = \frac{\psi^{(1)}_\lambda(T)}{\psi^{(2)}_\lambda(T)}$$

are meromorphic functions of λ with simple zeros at $\lambda^{(1)}_n$ and simple poles at $\lambda^{(2)}_n$. Furthermore, by Fredholm theory we see that the left hand side goes to unity as λ approaches infinity in any direction but the real axis (determinant is dominated by λ). Also, the right hand side behaves identically as λ approaches infinity (differential equation dominated by λ). The two sides are thus the same, and when $\lambda = 0$ we recover the result stated in the text.

[10] To prove this, let us return to $N = 1$. Suppose we study classical particle dynamics given by the equation of motion

$$\ddot{x} - \Omega(t)x = 0.$$

Suppose now that $F_a(t)$ and $F_b(t)$ are the solutions to this equation with boundary conditions $F_a(t_a) = 0$, $\dot{F}_a(t_a) = 1$ and $F_b(t_b) = 0$, $\dot{F}_b(t_b) = -1$ respectively. Given an initial position x_a and velocity $\dot{x}_a$ we can then express any solution as

$$x(x_a, \dot{x}_a, t) = \frac{1}{F_b(t_a)} \left[F_b(t) - F_a(t)\dot{D}_b(t_a) \right] - D_a(t)\dot{x}_a.$$

Thus we have

$$\begin{aligned} F_a(t_b) = \frac{\partial x_b}{\partial \dot{x}_a} &= \left(\frac{\partial \dot{x}_a}{\partial x_b} \right)^{-1} \\ &= \left(\frac{\partial}{\partial x_b} \left[-\frac{\partial S_{\rm cl}}{\partial x_a} \right] \right)^{-1} = \left(-\frac{\partial S_{\rm cl}}{\partial x_b \partial x_a} \right)^{-1}, \end{aligned}$$

where the second line follows from a small variation to the initial position and time to the classical action. Since $F_a(t_b)$ satisfies the conditions for the Gel'fand-Yaglom theorem after suitable normalisation, we find the Morette-van Hove determinant.

Solution to the path integral After a few detours on useful ways to compute the functional determinants, we arrive at the transition amplitude for the harmonic oscillator as

$$\begin{aligned}\langle x_b, t_b | x_a, t_a \rangle &= \int_{x(t_a)=x_a}^{x(t_b)=x_b} \mathcal{D}x \; e^{iS[x]} \\ &= \sqrt{\frac{\omega}{2\pi i \sin \omega T}} \exp\left[\frac{i\omega}{2\sin\omega T}\left[\left(x_b^2 + x_a^2\right)\cos\omega T - 2x_b x_a\right]\right]. \end{aligned} \tag{2.78}$$

As mentioned earlier, this is the probability amplitude of measuring the particle at position x_b at time t_b given that it was at position x_a at time t_a. Importantly, Eq. (2.78) can be used to compute the time evolution of any wavepacket in a harmonic potential, if we recall Eq. (2.29). The phase terms in Eq. (2.78) tells us the varying phases acquired by different parts of the wavefunction, whereas the pre-factor is related to the amplitude.

2.1.4.3 Canonical quantisation

In the Heisenberg picture, we have the equations of motion

$$\begin{aligned}\frac{d\hat{x}}{dt} &= i\left[\hat{H}, \hat{x}\right] = \hat{p} \\ \frac{d\hat{p}}{dt} &= i\left[\hat{H}, \hat{p}\right] = -\omega^2 \hat{x}. \end{aligned} \tag{2.79}$$

Substituting the first line into the second yields

$$\left[\frac{d^2}{dt^2} + \omega^2\right]\hat{x} = 0. \tag{2.80}$$

We can now expand

$$\hat{x} = f(t)\hat{a} + g(t)\hat{a}^\dagger, \tag{2.81}$$

where f and g satisfy the above equation of motion for $\hat{x}$. It is easy to see that

$$\begin{aligned} f(t) &= \frac{e^{-i\omega t}}{\sqrt{2\omega}} \\ g(t) &= \frac{e^{i\omega t}}{\sqrt{2\omega}} \end{aligned} \tag{2.82}$$

satisfy Eq. (2.80) and are orthonormal according to the norm in Eq. (2.32). In other words, we have chosen the normalisation such that $(f, f) = 1$ and $(g, g) = -1$.

Assuming that we can find a ground state satisfying[11]

$$\hat{a}\,|0\rangle = 0. \tag{2.83}$$

Using this we can for instance calculate the vacuum expectation value of the position operator $\langle\hat{x}(t)\rangle$ as

$$\langle\hat{x}(t)\rangle = \frac{1}{\sqrt{2\omega}}\langle 0|\left(e^{-i\omega t}\hat{a} + e^{i\omega t}\hat{a}^\dagger\right)|0\rangle = 0, \tag{2.84}$$

whereas

$$\langle\hat{x}(t)\hat{x}(t')\rangle = \frac{1}{2\omega}\langle 0|\left(e^{-i\omega t}\hat{a} + e^{i\omega t}\hat{a}^\dagger\right)\left(e^{-i\omega t'}\hat{a} + e^{i\omega t'}\hat{a}^\dagger\right)|0\rangle = e^{-i\omega(t-t')}/2\omega. \tag{2.85}$$

Furthermore, we can obtain $\hat{p}$ from Eq. (2.79) as

$$\hat{p}(t) = \frac{d\hat{x}}{dt} = \frac{-i\omega}{\sqrt{2\omega}}\left(e^{-i\omega t}\hat{a} - e^{i\omega t}\hat{a}^\dagger\right). \tag{2.86}$$

Using this we find the somewhat more usual expression of the ladder operators as

$$\begin{aligned}\hat{a} &= \sqrt{\frac{\omega}{2}}\left(\hat{x} + \frac{i}{\omega}\hat{p}\right),\\ \hat{a}^\dagger &= \sqrt{\frac{\omega}{2}}\left(\hat{x} - \frac{i}{\omega}\hat{p}\right),\end{aligned} \tag{2.87}$$

where we set $t = 0$ so that the Heisenberg picture and Schrödinger picture coincide. The above methodology might seem overly complicated at the moment, but it is crucial for more complicated scenarios.

2.1.5 Two-time potentials

It might seem that the position space path integral does not offer many advantages as compared to the other methods. That is indeed the case for a harmonic oscillator, but the path integral offers a structured approach to perturbations, especially when dealing with time-nonlocal quantum mechanics (which is indeed something we will consider in this thesis). To demonstrate this, let us consider an action of the form

$$S[x] = \int_{t_a}^{t_b} dt\,\frac{1}{2}\left[\dot{x}^2 - \int_{t_a}^{t_b} ds\; x(t)K(t,s)x(s)\right]. \tag{2.88}$$

[11] This is formally derived by expressing $\hat{H}$ in terms of $\hat{a}$ and $\hat{a}^\dagger$ [$\hat{H} = \omega\left(\hat{a}^\dagger\hat{a} + 1/2\right)$], using which we can define the number operator $\hat{n} = \hat{a}^\dagger\hat{a}$. The number operator defines the number states $|n\rangle$ such that $\hat{n}\,|n\rangle = n\,|n\rangle$, and using this we find $\hat{a}\,|n\rangle = \sqrt{n}\,|n-1\rangle$. This recursion series terminates when $n = 0$, defining the ground state.

Commonly $K(t,s)$ is a Green's function after integrating out some other degree of freedom. As such, it satisfies some equation of the form

$$\mathcal{L}\left[\frac{d}{dt}\right]K(t,s)=\delta(t-s). \tag{2.89}$$

Schematically, we can write this as $K(t,s)=\mathcal{L}^{-1}\delta(t-s)$, which can in turn be expanded as

$$K(t,s)=\sum_n a_n\frac{d^n}{dt^n}\delta(t-s). \tag{2.90}$$

This is indeed a common approach in fibre optics theory [107]. When we substitute this back into the action, we find

$$S\left[x\right]=\int_{t_a}^{t_b}dt\;\frac{1}{2}\left[\dot{x}^2-x(t)\left(\sum_n\left(-1\right)^n a_n\frac{d^n}{dt^n}x(t)\right)\right]. \tag{2.91}$$

In this way we can apply the usual quantisation procedures. However, in the Schrödinger and canonical quantisation language we must define an infinite set of conjugate momenta such that

$$\begin{aligned}
p_{n-1}&\equiv\frac{\partial L}{\partial x^{(n)}},\\
p_{n-2}&\equiv\frac{\partial L}{\partial x^{(n-1)}}-\dot{p}_{n-1},\\
&\vdots\\
p_0&\equiv\frac{\partial L}{\partial\dot{x}}-\dot{p}_1,
\end{aligned} \tag{2.92}$$

where $x^{(n)}$ denotes the n^{th} time-derivative. Perhaps understandably, this makes computations algebraically cumbersome. A good discussion of this can be found in Ref. [108].

In the path integral language we can instead work directly with the Lagrangian. This does not require the Legendre transform to the Hamiltonian representation. We can then simply define the path integral as usual, where its evaluation requires us to find the classical action. Whilst this is well-defined, it can nonetheless be non-trivial. For instance, we first need to solve the classical equation of motion

$$\ddot{x}+\frac{1}{2}\int_{t_a}^{t_b}ds\left[K(t,s)+K(s,t)\right]x(s)=0 \tag{2.93}$$

with boundary conditions $x(t_a)=x_a$ and $x(t_b)=x_b$.

2.1.5.1 Defining nonlocal perturbation theory

Luckily, we can solve this perturbatively, and the path integral offers a structured approach. For this, let us start with a time-local perturbation $V(x,t)$. We are first going to solve the driven problem, and then replace $x(t)$ in the perturbation by functional derivatives with respect to the driving force $J(t)$. In order to do this, we must first introduce such a driving force to the Lagrangian. This is done by letting

$$L \to L + \int_{t_a}^{t_b} dt\; x(t)J(t).$$

Hence we have the total Lagrangian

$$L = \int_{t_a}^{t_b} dt\; \frac{1}{2}\left[\dot{x}^2 + V(x,t)\right] \to \int_{t_a}^{t_b} dt\; \frac{1}{2}\left[\dot{x}^2 + V(x,t)\right] + xJ.$$

Our goal is now to let

$$V(x,t) \to V\left(\frac{\delta}{i\delta J(t)}, t\right). \tag{2.94}$$

Since the driving term J couples linearly to the coordinate x, it is easy to show that it does not change the pre-factor in the path integral.[12] It does however affect the classical action, because the classical equation of motion is now given by $\ddot{x}+\partial_x V = J$. In general, we thus have

$$\begin{aligned}
\langle x_b, t_b | x_a, t_a\rangle &= \int_{x(t_a)=x_a}^{x(t_b)=x_b} \mathcal{D}x\; \exp\left(i\int_{t_a}^{t_b} dt\; \frac{1}{2}\left[\dot{x}^2 - V(x,t)\right]\right) \\
&= \int_{x(t_a)=x_a}^{x(t_b)=x_b} \mathcal{D}x\; \exp\left[-\frac{i}{2}\int_{t_a}^{t_b} dt\; V\left(\frac{\delta}{i\delta J(t)}, t\right)\right] e^{i\int_{t_a}^{t_b} dt\; \frac{1}{2}\left[\dot{x}^2\right] + J(t)x(t)}\Bigg|_{J=0} \\
&= \exp\left[-\frac{i}{2}\int_{t_a}^{t_b} dt\; V\left(\frac{\delta}{i\delta J(t)}, t\right)\right] \langle x_b, t_b | x_a, t_a\rangle_J \Bigg|_{J=0},
\end{aligned} \tag{2.95}$$

where $\langle x_b, t_b | x_a, t_a\rangle_J$ is the driven transition amplitude, and where $J=0$ should be interpreted as setting the driving function to zero for all time after the functional derivatives are performed. Similarly, in the time-nonlocal case we have

$$\begin{aligned}
\langle x_b, t_b | x_a, t_a\rangle^{\mathrm{K}} &= \int_{x(t_a)=x_a}^{x(t_b)=x_b} \mathcal{D}x\; \exp\left(i\int_{t_a}^{t_b} dt\; \frac{1}{2}\left[\dot{x}^2 - \int_{t_a}^{t_b} ds\; x(t)K(t,s)x(s)\right]\right) \\
&= \exp\left[-\frac{i}{2}\int_{t_a}^{t_b} dt \int_{t_a}^{t_b} ds\; K(t,s)\frac{\delta}{i\delta J(t)}\frac{\delta}{i\delta J(s)}\right] \langle x_b, t_b | x_a, t_a\rangle_J^{\mathrm{free}} \Bigg|_{J=0},
\end{aligned} \tag{2.96}$$

where we should note that the ordering of the derivatives does not matter in this case, since we are dealing with a single variable. In our example, the free driven

[12] This is done in an identical manner as to Eq. (2.53).

transition amplitude is given by

$$\begin{aligned}\langle x_b, t_b | x_a, t_a \rangle_J^{\text{free}} =& \sqrt{\frac{1}{2\pi i T}} \exp\left[i \left(x_b - x_a\right)^2 / 2T\right] \\ & \times \exp\left[i x_b \int_{t_a}^{t_b} dt \, \left(\frac{t}{T}\right) J(t)\right] \exp\left[i x_a \int_{t_a}^{t_b} ds \, \left(\frac{T-s}{T}\right) J(s)\right] \\ & \times \exp\left[-i \int_{t_a}^{t_b} dt \int_{t_a}^{t} ds \, J(t) \left(\frac{s\,(T-t)}{T}\right) J(s)\right], \end{aligned} \tag{2.97}$$

from which the nonlocal transition amplitude can be computed.

2.2 Quantum field theory - minimal version

We can define quantum field theory analogously to what we did for quantum mechanics, but where the position x is replaced by a field variable $\phi(\mathbf{x}, t)$. In other words, in the above we let

$$x(t) \to \phi(\mathbf{x}, t). \tag{2.98}$$

In analogy with the position state $|x\rangle$ for quantum mechanics, which is defined as the eigenstate of the position operator $\hat{x}$, we can introduce the field state $|\phi\rangle$ as the eigenstate of the field operator $\hat{\phi}(\mathbf{x})$. We can also introduce the classical field momentum

$$\pi(x) \equiv \frac{\partial L}{\partial \dot{\phi}(\mathbf{x}, t)}$$

in an analogous way as the classical momentum p [Eq. (2.13)]. The momentum can then be promoted to a field momentum operator $\hat{\pi}(\mathbf{x}, t)$, and together the field and momentum operators satisfy the equal-time commutator

$$[\hat{\phi}(\mathbf{x}, t), \hat{\pi}(\mathbf{x}, t)] = i\delta(\mathbf{x} - \mathbf{y}). \tag{2.99}$$

Along with these definitions and the resolution of identity defined as [109]

$$\int \mathcal{D}\phi(\mathbf{x}) \, |\phi\rangle \, \langle\phi| = \mathbb{I}, \tag{2.100}$$

we can go through the same procedure as was done in Section 2.1. We should also note that we can switch between Heisenberg representation where the time-dependence is in the operators [e.g. $\hat{\phi}(\mathbf{x}, t)$] and Schrödinger representation where the time-dependence is in the states [e.g. $|\phi, t\rangle$], just like in quantum mechanics.

2.2.1 Introducing spatial modes

It is however often beneficial to expand the field in a set of spatial modes $u_{\mathbf{k}}(\mathbf{x})$ such that

$$\phi(\mathbf{x}, t) = \sum_{\mathbf{k}} u_{\mathbf{k}}(\mathbf{x}) \phi_{\mathbf{k}}(t). \tag{2.101}$$

These spatial modes $u_{\mathbf{k}}(\mathbf{x})$ are generally the set of solutions that satisfy the spatial part of the classical equation of motion for the field. This also serves to define a *dispersion relation*, i.e. an equation that relates ω and $\mathbf{k}$. For instance, suppose we

consider a free field whose classical equation of motion is given by

$$\ddot{\phi} - \nabla^2 \phi = 0.$$

We can now expand ϕ using Eq. (2.101), and this allows us to separate the temporal and spatial degrees of freedom, yielding the equations of motion

$$\nabla^2 u_{\mathbf{k}}(\mathbf{x}) + \lambda_{\mathbf{k}} u_{\mathbf{k}} = 0, \tag{2.102}$$

$$\ddot{\phi}_{\mathbf{k}} + \lambda_{\mathbf{k}} \phi_{\mathbf{k}} = 0. \tag{2.103}$$

The first line defines $\lambda_{\mathbf{k}}$, and depends on the spatial boundary conditions. In the simplest case of an infinite space (with period boundary conditions), we can set $u_{\mathbf{k}} \propto \exp(i\mathbf{k} \cdot \mathbf{x})$ where the normalisation is determined by

$$\int d^N x \; u^*_{\mathbf{k}}(\mathbf{x}) u_{\mathbf{p}}(\mathbf{x}) = \delta_{\mathbf{k},\mathbf{p}} \tag{2.104}$$

with N being the dimension of $\mathbf{x}$-space. Now Eq. (2.102) implies that $\lambda_{\mathbf{k}} = |\mathbf{k}|^2$. Furthermore, Eq. (2.103) becomes

$$\ddot{\phi}_{\mathbf{k}} + |\mathbf{k}|^2 \phi_{\mathbf{k}} = 0,$$

which can be quantised using the methods discussed in Section 2.1. In other words, given that the spatial modes form a complete set of solutions for the spatial degrees of freedom, we can do quantum mechanics for each spatial mode amplitude $\phi_{\mathbf{k}}$, almost exactly as in the previous section.

Put differently, we can treat each spatial mode independently. Suppose we start in a state $|\phi(\mathbf{x}), t\rangle$. This state can then be expanded in its corresponding spatial modes, such that

$$|\phi(\mathbf{x}), t\rangle = |\phi_{\mathbf{k}_1}, t\rangle \, |\phi_{\mathbf{k}_2}, t\rangle \, |\phi_{\mathbf{k}_3}, t\rangle \, ... = |\{\phi_{\mathbf{k}}, t\}\rangle \, , \tag{2.105}$$

where we use the notation $|\{a_{\mathbf{k}}\}\rangle$ as shorthand for the tensor product between all states with label $\mathbf{k}$, as is commonly done in quantum optics [2]. Note that the number of modes depend on the physical situation, but in the example of a free field as used above there is a continuum of modes. If we want to calculate the expectation value of some operator, say for instance $\hat{\phi}(\mathbf{x})$, then we find

$$\begin{aligned}
\phi(\mathbf{x}, t) &= \langle \phi(\mathbf{x}), t | \, \hat{\phi}(\mathbf{x}) \, | \phi(\mathbf{x}), t \rangle = \langle \phi(\mathbf{x}), t | \sum_{\mathbf{k}} u_{\mathbf{k}}(\mathbf{x}) \hat{\phi}_{\mathbf{k}} \, | \phi(\mathbf{x}), t \rangle \\
&= \langle \phi(\mathbf{x}), t | \sum_{\mathbf{k}} u_{\mathbf{k}}(\mathbf{x}) \hat{\phi}_{\mathbf{k}} \, | \{\phi_{\mathbf{p}}, t\} \rangle = \langle \phi(\mathbf{x}), t | \sum_{\mathbf{k}} u_{\mathbf{k}}(\mathbf{x}) \phi_{\mathbf{k}}(t) \, | \{\phi_{\mathbf{p}}, t\} \rangle \\
&= \sum_{\mathbf{k}} u_{\mathbf{k}}(\mathbf{x}) \phi_{\mathbf{k}}(t),
\end{aligned} \tag{2.106}$$

where $\phi(\mathbf{x}, t)$ is the configuration of the field at time t, and where in the third line we used that $\hat{\phi}_{\mathbf{k}} |\phi_{\mathbf{p}}, t\rangle = \phi_{\mathbf{k}}$ if and only if $\mathbf{k} = \mathbf{p}$, otherwise zero. Furthermore, we can expand each amplitude state $|\phi_{\mathbf{k}}, t\rangle$ in terms of the number state basis $|n_{\mathbf{k}}\rangle$, such that

$$|\phi_{\mathbf{k}}, t\rangle = \sum_{n_{\mathbf{k}}} a_n^{\mathbf{k}}(t) \, |n_{\mathbf{k}}\rangle \, ,$$

from which it follows that

$$|\phi(\mathbf{x}), t\rangle = |\{\phi_{\mathbf{k}}, t\}\rangle = \sum_{n_{\mathbf{k}}} a_n^{\mathbf{k}}(t) \, |\{n_{\mathbf{k}}\}\rangle \, . \tag{2.107}$$

2.2.2 Wavefunctionals and wavefunctions

It is at this point instructive to introduce the wavefunctional representation of the field. In general, just like the position x in quantum mechanics is only known up to some uncertainty,[13] the field $\phi(\mathbf{x}, t)$ is only known up to some uncertainty. In quantum mechanics, the position uncertainty can be embodied by the wavefunction $\psi(x)$, and it follows that we can define the wavefunctional $\Psi[\phi(\mathbf{x}, t)]$ for quantum field theory. A general state is therefore best denoted $|\Psi, t\rangle$, and we can expand this in the wavefunctional basis by

$$|\Psi, t\rangle = \int \mathcal{D}\phi(\mathbf{x}) \, |\phi\rangle \, \langle\phi|\Psi, t\rangle = \int \mathcal{D}\phi(\mathbf{x}) \;\; |\phi\rangle \, \Psi[\phi(\mathbf{x}), t] \tag{2.108}$$

using the resolution of identity in Eq. (2.100), and where we define the wavefunctional as the overlap $\Psi[\phi(\mathbf{x}), t] \equiv \langle\phi|\Psi, t\rangle$. Using the spatial modes discussed in Section 2.2.1, we can then further resolve the state $|\Psi, t\rangle$ by expanding the field state in terms of the normal modes [Eq. (2.105)], yielding

$$\begin{aligned} |\Psi, t\rangle &= \int \mathcal{D}\phi(\mathbf{x}) \, |\phi\rangle \, \langle\phi|\Psi, t\rangle \\ &= \left[\prod_{\mathbf{k}} \int d\phi_{\mathbf{k}}\right] |\{\phi_{\mathbf{k}}\}\rangle \, \langle\{\phi_{\mathbf{k}}\}|\Psi, t\rangle \\ &= \left[\prod_{\mathbf{k}} \int d\phi_{\mathbf{k}} \; \psi_{\mathbf{k}}(\phi_{\mathbf{k}}, t)\right] |\{\phi_{\mathbf{k}}\}\rangle \, , \end{aligned} \tag{2.109}$$

where $\psi_{\mathbf{k}}(\phi_{\mathbf{k}}, t) \equiv \langle\phi_{\mathbf{k}}|\Psi, t\rangle$ is the overlap between the general state $|\Psi, t\rangle$ and each spatial mode state $|\phi_{\mathbf{k}}\rangle$. Note that $\psi_{\mathbf{k}}(\phi_{\mathbf{k}}, t)$ is a wavefunction, as opposed to the wavefunctional $\Psi[\phi(\mathbf{x}), t]$. If we compare Eq. (2.108) and Eq. (2.109), we find that $\Psi[\phi(\mathbf{x}), t] = \prod_{\mathbf{k}} \psi_{\mathbf{k}}(\phi_{\mathbf{k}}, t)$.

[13] Basically Heisenberg's uncertainty principle.

2.2.3 On treating each spatial mode independently

In this thesis, we will often be interested in the probability of measuring a change in some specific spatial mode $u_{\mathbf{p}}(\mathbf{x})$, in a system described by the state $|\Psi, t\rangle$. Let us call such a probability amplitude $\mathcal{A}_{\mathbf{p}}$, whose probability is given by $|\mathcal{A}_{\mathbf{p}}|^2$. For instance, say we want to find the probability of measuring the 1^{st} excited state in the spatial mode $\mathbf{p}$. We would then calculate the overlap between the state $|\Psi, t\rangle$ and an almost identical state $|\Psi_{\not\mathbf{p}}, 1_{\mathbf{p}}, t\rangle$ that has the same amplitude in all spatial modes apart from $\mathbf{p}$, denoted here with the $\not\mathbf{p}$-subscript. Such a state $|\Psi_{\not\mathbf{p}}, 1_{\mathbf{p}}, t\rangle$ can written as

$$|\Psi_{\not\mathbf{p}}, 1_{\mathbf{p}}, t\rangle = \left(\prod_{\mathbf{k}\neq\mathbf{p}} \int d\phi_{\mathbf{k}}\ \psi_{\mathbf{k}}(\phi_{\mathbf{k}}, t)\right) \left[\int d\phi_{\mathbf{p}}\ \varphi_1(\phi_{\mathbf{p}})\right] |\{\phi_{\mathbf{k}}\}\rangle\,, \tag{2.110}$$

which we will denote by $|1_{\mathbf{p}}\rangle$ as a shorthand. Here $\varphi_1(\phi)$ is the wavefunction of the 1^{st}-excited state, whereas $\psi_{\mathbf{k}}(\phi)$ is the wavefunction for each spatial mode $\mathbf{k} \neq \mathbf{p}$ as introduced in Eq. (2.109). It now follows that the amplitude $\mathcal{A}$ can be computed as

$$\begin{aligned}\mathcal{A}_{\mathbf{p}} = \langle 1_{\mathbf{p}}|\Psi, t\rangle &= \left(\prod_{\mathbf{k}\neq\mathbf{p}} \int d\phi_{\mathbf{k}}\, |\psi_{\mathbf{k}}(\phi_{\mathbf{k}}, t)|^2\right) \left[\int d\phi_{\mathbf{p}}\ \varphi_1^*(\phi_{\mathbf{p}})\psi_{\mathbf{p}}(\phi_{\mathbf{p}}, t)\right] \\ &= \int d\phi_{\mathbf{p}}\ \varphi_1^*(\phi_{\mathbf{p}})\psi_{\mathbf{p}}(\phi_{\mathbf{p}}, t),\end{aligned} \tag{2.111}$$

where second line follows from the first since each state is normalised to unity.

As can be seen in Eq. (2.111), the resulting amplitude and probability depends only on the wavefunction of the single mode $\mathbf{p}$, the rest being superfluous. This follows because the set of spatial modes forms a complete set. Therefore, within this formalism we might as well have treated each spatial mode independently, and discussed only the properties of the part of the state associated with spatial mode $u_{\mathbf{p}}(\mathbf{x})$. In the remainder of the thesis, we will do exactly this, whilst the reader is advised that this is only shorthand, and the wavefunctional $|\Psi, t\rangle$ is a tensor product over all spatial modes. Especially of interest in this thesis is the ground state of the field, which would be described by a wavefunctional. However, in light of the above discussion, it suffices to discuss the ground state of each spatial mode independently.

Note also that the spatial modes might couple for potentials that depend on space $V(\phi(\mathbf{x}), \mathbf{x}, t)$. First of all, the potential defines a new set of spatial modes, as each set of spatial modes is tied to a certain potential. Commonly however, we can treat this perturbatively using spatial modes that are defined in the absence of the potential, given that the spatial variation is small compared to other factors in the dynamics. This then yields a coupling between the spatial modes, and consequently transitions between spatial modes are allowed. Nonetheless, in this scenario, the dynamics is computed independently for each spatial mode at zeroth order in the perturbation series. All the following orders will however contain sums over all

spatial modes, taking the transitions into account.

2.2.4 Connecting discrete modes to continuum modes

Finally, we should note that we have so far implicitly assumed that the spatial modes form a discrete set. In this treatment, we have been using sums and Kronecker δ-functions, such as $\sum_{\mathbf{k}}$ and $\delta_{\mathbf{k},\mathbf{p}}$. For instance in the orthonormality condition in Eq. (2.104), we assumed that $\mathbf{x}$ is a continuum, whereas $\mathbf{k}$ forms a discrete set. If we treat a physical situation where a continuum of spatial modes $u_{\mathbf{k}}(\mathbf{x})$ is more appropriate, then we should replace Eq. (2.104) with

$$\int d^N x \; u^*_{\mathbf{k}}(\mathbf{x}) u_{\mathbf{p}}(\mathbf{x}) = (2\pi)^N \delta(\mathbf{k}-\mathbf{p}). \tag{2.112}$$

As can be seen, this changes the dimensionality of the problem, since the Dirac δ-function carries the dimension of $1/\mathcal{V}$, where $\mathcal{V}$ is the volume of $\mathbf{x}$-space. This is to ensure that

$$\int \frac{d^N k}{(2\pi)^N} \int d^N x \; u^*_{\mathbf{k}}(\mathbf{x}) u_{\mathbf{p}}(\mathbf{x}) = \int \frac{d^N k}{(2\pi)^N} (2\pi)^N \delta(\mathbf{k}-\mathbf{p}) = 1, \tag{2.113}$$

as compared to

$$\sum_{\mathbf{k}} \int d^N x \; u^*_{\mathbf{k}}(\mathbf{x}) u_{\mathbf{p}}(\mathbf{x}) = \sum_{\mathbf{k}} \delta_{\mathbf{k},\mathbf{p}} = 1 \tag{2.114}$$

for the discrete modes. In fact, in the case of fields in the bulk, where the boundary conditions can be allowed to be periodic, we can view Eq. (2.113) as the limit of Eq. (2.114), as the volume $\mathcal{V}$ approaches infinity.[14] As long as we are consistent with this, we can keep working with discrete modes, and thus use sums $\sum$ and Kronecker δ-functions, until the need to specify arises. If we need to transition to continuum modes, we will use the following replacements throughout this thesis:

$$\sum_{\mathbf{k}} \to \mathcal{V} \int \frac{d^N k}{(2\pi)^N}, \tag{2.115}$$

where N is the dimension of $\mathbf{x}$-space, and $\mathcal{V}$ is the volume, and

$$\delta_{\mathbf{k},\mathbf{p}} \to \delta(\mathbf{k}-\mathbf{p})/\mathcal{V}. \tag{2.116}$$

As a last comment, we note that this convention also applies to commutators. In particular, the discrete mode commutator can be connected to the continuum mode

[14] Some care must be taken when considering structured volumes, as the boundary conditions can make a difference.

commutator as

$$\left[\hat{\phi}_{\mathbf{k}}, \hat{\pi}_{\mathbf{p}}\right] = i\delta_{\mathbf{k},\mathbf{p}} \leftrightarrow \left[\hat{\phi}_{\mathbf{k}}, \hat{\pi}_{\mathbf{p}}\right] = i\delta(\mathbf{k}-\mathbf{p}), \tag{2.117}$$

where the nature of the mode amplitudes $\hat{\phi}_{\mathbf{k}}$ and $\hat{\pi}_{\mathbf{p}}$ must be inferred from the context, and where $\hat{\pi}_{\mathbf{k}}$ is defined through $\hat{\pi}(\mathbf{x}) = \sum_{\mathbf{k}} u_{\mathbf{k}}(\mathbf{x})\hat{\pi}_{\mathbf{k}}$ (for discrete modes). Finally, we can keep only the $\mathbf{k} = \mathbf{p}$ term in Eq. (2.117), if there is no spatial dependence in the problem that can cause transitions between spatial modes.

2.2.5 QFT in summary

In summary, since we can treat each spatial mode independently, we find:

- The path integral

$$\langle \phi_{\mathbf{k},b}\ t_b | \phi_{\mathbf{k},a}\ t_a \rangle = \int \mathcal{D}\phi_{\mathbf{k}}\ e^{iS[\phi_{\mathbf{k}}]}, \tag{2.118}$$

  from which we can construct $\langle \phi_b(x), t_b | \phi_a(x), t_a \rangle = \langle \{\phi_{\mathbf{k},b}\ t_b\} | \{\phi_{\mathbf{k},a}\ t_a\} \rangle$.

- The Schrödinger equation

$$i\frac{\partial}{\partial t}\psi_{\mathbf{k}}(\phi_{\mathbf{k}}, t) = \left[\hat{\pi}_{\mathbf{k}}^2/2 + V(\hat{\phi}_{\mathbf{k}}, t)\right] \psi_{\mathbf{k}}(\phi_{\mathbf{k}}, t), \tag{2.119}$$

  where the momentum operator $\hat{\pi}_{\mathbf{k}}$ is defined through $\hat{\pi}(\mathbf{x}) = \sum_{\mathbf{k}} u_{\mathbf{k}}(\mathbf{x})\hat{\pi}_{\mathbf{k}}$. Also, we find the full wavefunctional as $\Psi\left[\phi(x), t\right] = \prod_{\mathbf{k}} \psi_{\mathbf{k}}(\phi_{\mathbf{k}}, t)$.

- Time-evolution of canonical operators

$$\frac{d\hat{a}_{\mathbf{k}}}{dt} = i\left[\hat{H}, \hat{a}_{\mathbf{k}}\right]. \tag{2.120}$$

Whilst the first and third representation is common for fields, the Schrödinger language is somewhat unusual, but we nonetheless find it useful. We will address the details of this procedure as we proceed in the thesis.

Chapter 3

Vacuum radiation from small variations to the optical properties

"It doesn't prove anything very much except that the awesome splendour of the universe is much easier to deal with if you think of it as a series of small chunks."

Terry Pratchett in *Mort*, 1987

Let now start to explore quantum vacuum radiation in optical media. In particular, this chapter is based on Item 1 in the List of Publications, and is a perturbative treatment suitable to small changes in the optical properties.

If we recap a little of what we discussed in the introduction, quantum vacuum radiation, although it sounds like an oxymoron, is a term for radiation that is emitted from the vacuum state when, colloquially speaking, the mode density of the vacuum is changed in time. Physically, the notion of a particle becomes ill-defined as the mode density changes [15], allowing for the final state to have a non-zero occupation number. The term encompasses phenomena from many fields of study in physics, astrophysical scenarios (Hawking radiation/cosmological particle creation) and optical settings (dynamical Casimir effect/time-dependent media) alike. Our focus here is the study of vacuum radiation in temporally varying optical media, which is introduced by making some parameter in the model depend on time. However, optical media are dispersive, that is, the response of the medium depends on the frequency of light with which it interacts. In the time-domain, this leads to a delayed response. The interplay between this delayed temporal response and the time-dependent optical parameters is at the heart of this chapter.

In order to study this, it is convenient to turn to macroscopic quantum electrodynamics — the study of light-matter systems on a scale at which the microscopic details of the medium can be taken into account by an effective model. That being said, nature allows for many approaches to treating quantum electrodynamics at a macroscopic scale. This is hardly surprising, given that it is an effective model. The model in question here, indeed the one we will use throughout, was proposed by Hopfield [59] and introduces the optical medium as a phenomenological matter degree of freedom coupled to light through a simple dipole coupling. Such a model is

valid in frequency-ranges away from a medium resonance, as it neglects absorption. Whilst it should be noted that the vacuum state includes all frequencies (see discussion in Section 2.2), we will see later in this chapter that only some small frequency range, which is determined by the time-dependence of the optical properties, contributes to any given vacuum radiation process. This allows us to effectively ignore the regions around the medium's resonance frequencies.

In this chapter, we will aim to form an effective action by 'integrating out' the matter degree of freedom, allowing us to describe the problem in terms of the relevant quasiparticles of the system: polaritons. The action will however, by necessity, be nonlocal in time, that is (in part) dependent on past events. This will complicate the quantisation, as time plays a special role in quantum theory. By and large, we will devote a large portion of this chapter to the procedure used to manage this complication, discussed in Section 3.1, 3.2 and 3.3. The introduction of the time-dependent media will be treated in Section 3.4, and the resulting quantum vacuum radiation will then be discussed in Section 3.5.

3.1 Model

We wish to study optical media that can be described by a refractive index n of so-called Sellmeier's form. Such models for the refractive index encompass the linear response of many bulk crystals and glasses, as discussed in for instance Ref. [54](p. 85). These are media that has N resonances at frequencies Ω_i, with a coupling to light characterised by a coupling strength g_i respectively, as well as negligible absorption. We can characterise Sellmeier's type media by a refractive index of the form

$$n^2(\omega) = 1 - \sum_{i=1}^{N} \frac{g_i^2}{\omega^2 - \Omega_i^2}. \tag{3.1}$$

Note that g_i is the effective plasma frequency of the i^{th} resonance. Introducing a time-varying refractive index can now be done simply by introducing time-dependencies in the resonance (Ω_i) or the plasma (g_i) frequencies. Here we will focus on the former. From a physical perspective, such a time-dependency of the resonance frequency can be produced through the quadratic Stark shift [110], where the resonance shifts under the influence of a strong electric field E_{pump} as $\Omega_i(\mathbf{x}, t) \equiv \Omega_i + \alpha E^2_{\text{pump}}(\mathbf{x}, t)$.[1] Naturally, it would be incorrect to write $n(\omega, t)$ since ω (frequency) and t (time) are conjugate variables. Instead, we must introduce a phenomenological matter degree of freedom, such that the effective equation of

[1] Acousto-optic modulation would rather change the density of the media in time, but nonetheless introduce a time-dependent refractive index.

motion for the electromagnetic field has a dispersion relation given by

$$-|\mathbf{k}|^2 + \omega^2 n^2(\omega) = 0, \tag{3.2}$$

with $n(\omega)$ given by Eq. (3.1). Consequently, we will consider a quasi-microscopic action for the electromagnetic field, $\mathbf{E}$ and $\mathbf{B}$, coupled to a set of harmonic oscillators $\mathbf{R}_i$ through a dipole term. Also, we should note that we will work in units $c = 1$, $\hbar = 1$ and $\varepsilon_0 = 1$ for notational simplicity.

To establish such a quasi-microscopic model for macroscopic electromagnetism, let us start with Maxwell's equations in a (dielectric and non-magnetic) macroscopic medium with no free charges [1, 111],

$$\begin{aligned} \boldsymbol{\nabla} \cdot \mathbf{B} &= 0, \qquad & \boldsymbol{\nabla} \times \mathbf{E} &= -\dot{\mathbf{B}} \\ \boldsymbol{\nabla} \cdot \mathbf{D} &= 0, \qquad & \boldsymbol{\nabla} \times \mathbf{B} &= \dot{\mathbf{D}}, \end{aligned} \tag{3.3}$$

where $\mathbf{D} = \mathbf{E} + \mathbf{P}$ is the electric displacement field, and $\mathbf{P}$ is the polarisation field. Eq. (3.3) establishes the relevant setting for this thesis. From it, we find an equation of motion for the electric field $\mathbf{E}$ of the form

$$\boldsymbol{\nabla} \times \boldsymbol{\nabla} \times \mathbf{E} + \partial_t^2 \left[\mathbf{E} + \mathbf{P}\right] = 0. \tag{3.4}$$

If we now further suppose that the polarisation $\mathbf{P}$ varies sufficiently slowly in space,[2] then $\boldsymbol{\nabla} \cdot \mathbf{P} \simeq 0$ and from the first equation on the second line of Eq. (3.3) we find that $\boldsymbol{\nabla} \cdot \mathbf{E} = 0$. This implicitly assumes that the physics we study is in the bulk of the medium, or that any spatial variation is slow as compared to the wavelength. Nonetheless, within these assumptions, Eq. (3.4) reduces to the more familiar wave equation

$$-\nabla^2 \mathbf{E} + \partial_t^2 \left[\mathbf{E} + \mathbf{P}\right] = 0, \tag{3.5}$$

which can be readily compared to Eq. (1.1).

The question then becomes: how do we construct $\mathbf{P}$ such that we attain a dispersion relation of the form seen in Eq. (3.2)? Suppose for now that the material properties are constant in time, then the Fourier transform of Eq. (3.5) is given by

$$\left(|\mathbf{k}|^2 - \omega^2\right) \mathbf{E}_{\mathbf{k}}(\omega) - \omega^2 \mathbf{P}_{\mathbf{k}}(\omega) = 0, \tag{3.6}$$

where we define

$$f_{\mathbf{k}}(\omega) = \mathcal{F}\left[f(t, \mathbf{x})\right] = \int d^3x \; e^{-i\mathbf{k}\cdot\mathbf{x}} \int dt \; e^{i\omega t} f(t, \mathbf{x}).$$

[2] Intuitively, the relevant length scale to which comparison is made here is the wavelength of light. This will become important later in the chapter.

Let us now split the polarisation into N contributions, as in $\mathbf{P} = \sum_i^N \mathbf{P}_i$, and then further let

$$\mathbf{P}_i = \int dt' \; \chi_i(t - t')\mathbf{E}(t'), \tag{3.7}$$

with $\chi_i(t - t')$ being the medium response function for each resonance. Moreover, suppose that the equation of motion for $\mathbf{R}_i$ is given by

$$\left[\ddot{\mathbf{R}}_i + \Omega_i^2 \mathbf{R}_i\right] = q_i \mathbf{E}, \tag{3.8}$$

where q_i is the dipole moment for each resonance frequency Ω_i. We can then connect the medium response function χ_i to the component-wise propagator for $\mathbf{R}_i$ [denoted $\Delta_i(t, t')$] through

$$\left[\partial_t^2 + \Omega_i^2\right] \Delta_i(t, t') = -\delta(t - t') \quad \Rightarrow \quad \chi_i(t - t') = \rho q_i^2 \Delta_i(t, t'),$$

where ρ is the density of the oscillators. This also specifies the polarisation $\mathbf{P}_i$ in terms of the oscillator $\mathbf{R}_i$ through

$$\mathbf{P}_i = \rho q_i \mathbf{R}_i. \tag{3.9}$$

The dispersion relation in Eq. (3.2) follows if we now finally identify the plasma frequency of each resonance as $g_i = \sqrt{\rho} q_i$.

This sets-up the problem at hand. Now, as mention in Chapter 2, in order to quantise this, we will need an action and a Lagrangian. Any action from which Maxwell's equations [Eq. (3.3)] along with the correct equation of motion for the oscillators $\mathbf{R}_i$ [Eq. (3.8)] will serve this purpose. Before we do so however, let us specify gauge. As always, both the electric and magnetic field can be represented as a gauge potential [1], given by $\mathbf{E} = -(\partial_t \mathbf{A} + \boldsymbol{\nabla}\varphi)$ and $\mathbf{B} = \boldsymbol{\nabla} \times \mathbf{A}$, where $\mathbf{A}$ and φ are the vector and scalar potentials respectively. For this thesis, we will work in Coulomb gauge, given by the constraint

$$\boldsymbol{\nabla} \cdot \mathbf{A} = 0. \tag{3.10}$$

Now, we previously assumed that spatial variations in the polarisation field $\mathbf{P}$ is sufficiently small so that $\boldsymbol{\nabla} \cdot \mathbf{P} \simeq 0$. In terms of our oscillators $\mathbf{R}_i$, this then implies that

$$\boldsymbol{\nabla} \cdot \mathbf{R}_i \simeq 0. \tag{3.11}$$

Subsequently, the bottom left Maxwell's equation in Eq. (3.3) now reads

$$\boldsymbol{\nabla} \cdot \mathbf{D} = 0 \Rightarrow \nabla^2 \phi = 0,$$

using Eq. (3.11). ϕ decouples from everything else, and we might as well set $\phi = 0$. This further implies that the electric field is now given by $\mathbf{E} = -\partial_t \mathbf{A}$. Finally, from the bottom right of Eq. (3.3) we find

$$\ddot{\mathbf{A}} - \nabla^2 \mathbf{A} = \dot{\mathbf{P}} \quad \Leftrightarrow \quad \ddot{\mathbf{A}} - \nabla^2 \mathbf{A} = \sum_i^N \rho q_i \dot{\mathbf{R}}_i,$$

where we used the vector identity $\boldsymbol{\nabla} \times \boldsymbol{\nabla} \times \mathbf{A} = \boldsymbol{\nabla}(\boldsymbol{\nabla} \cdot \mathbf{A}) - \nabla^2 \mathbf{A}$, along with Coulomb gauge condition in Eq. (3.10).

Now all the gauge freedom has been removed, and we can write down the action for this system in Coulomb gauge. This is given by

$$\begin{aligned} S_\gamma &= \int_{t_i}^{t_f} dt \int d^3x \, \frac{1}{2} \left[\mathbf{E}^2 - \mathbf{B}^2 \right], \\ S_R &= \sum_i \int_{t_i}^{t_f} dt \int d^3x \, \frac{\rho}{2} \left[\dot{\mathbf{R}}_i^2 - \Omega_i^2(\mathbf{x}, t) \mathbf{R}_i^2 \right], \\ S_{\text{int}} &= \sum_i \int_{t_i}^{t_f} dt \int d^3x \; (\rho q_i) \; \mathbf{E} \cdot \mathbf{R}_i, \end{aligned} \tag{3.12}$$

where ρ is the density of oscillators, and q_i are the respective dipole moments. Note that in this action, only the coupling term S_{int} requires us to specify gauge. Written in terms of the vector potential (in Coulomb gauge), we therefore have

$$\begin{aligned} S_\gamma &= \int_{t_i}^{t_f} dt \int d^3x \, \frac{1}{2} \left[\dot{\mathbf{A}}^2 - (\boldsymbol{\nabla} \times \mathbf{A})^2 \right] \\ S_R &= \sum_i \int_{t_i}^{t_f} dt \int d^3x \, \frac{\rho}{2} \left[\dot{\mathbf{R}}_i^2 - \Omega_i^2(\mathbf{x}, t) \mathbf{R}_i^2 \right] \\ S_{\text{int}} &= \sum_i \int_{t_i}^{t_f} dt \int d^3x \; (-\rho q_i) \; \dot{\mathbf{A}} \cdot \mathbf{R}_i, \end{aligned} \tag{3.13}$$

where, as a reminder, the electric field is given by $\mathbf{E} = -\partial_t \mathbf{A}$ along with the magnetic field $\mathbf{B} = \boldsymbol{\nabla} \times \mathbf{A}$. We should note that the electric field $\mathbf{E}$, the vector potential $\mathbf{A}$, as well as the oscillators $\mathbf{R}_i$ (by assumption) are all completely transverse.

Here we have also introduced a space- and time-dependent medium by letting the natural oscillation frequencies $\Omega_i^2(\mathbf{x}, t)$ be space- and time-dependent. As for the space-dependence, we can allow for spatial variations that are sufficiently slow

as compared to the wavelength of light, specifically such that

$$\left|\frac{\boldsymbol{\nabla}\Omega_i^2(\mathbf{x},t)}{\Omega_i^2(\mathbf{x},t)}\right| \ll |\mathbf{k}|, \tag{3.14}$$

where $|\mathbf{k}| = 2\pi/\lambda$ is the wavenumber of light, with λ its wavelength. We require this condition so that we can still work in Coulomb gauge.[3] Eq. (3.14) follows from Eq. (3.8). Specifically if we take the divergence $[\boldsymbol{\nabla}\cdot]$ of Eq. (3.8) with the electric field written in Coulomb gauge $\mathbf{E} = -\partial_t\mathbf{A}$, we arrive at the consistency relation

$$\left[\partial_t^2 + \Omega_i^2(\mathbf{x},t)\right]\boldsymbol{\nabla}\cdot\mathbf{R}_i + \boldsymbol{\nabla}\Omega_i^2(\mathbf{x},t)\cdot\mathbf{R}_i = 0,$$

since $\boldsymbol{\nabla}\cdot\mathbf{A} = 0$. Suppose now that $\mathbf{R}_i = \mathbf{c}\exp(i\mathbf{k}\cdot\mathbf{x} - i\omega t)$ for some constant vector $\mathbf{c}$, where $\mathbf{k}$ is the wave vector of the electric field $\mathbf{E}$ driving the oscillator [Eq. (3.8)]. The above consistency relation then reduces to

$$i\mathbf{c}\cdot\mathbf{k} + \frac{\mathbf{c}\cdot\boldsymbol{\nabla}\Omega_i^2(\mathbf{x},t)}{-\omega^2 + \Omega_i^2(\mathbf{x},t)} = 0,$$

which can be approximated as

$$i\mathbf{c}\cdot\mathbf{k} \simeq 0 \Leftarrow \boldsymbol{\nabla}\cdot\mathbf{R}_i \simeq 0,$$

given Eq. (3.14).[4] Therefore, this formulation is self-consistent given that the spatial variations in the resonance frequencies Ω_i are sufficiently slow to satisfy Eq. (3.14).

We should also note that we will, in this thesis, mostly concern ourselves with bulk media, or the bulk response in structured media. In these cases, we consider spatially uniform resonance frequencies. We do however consider slow spatial variation in Chapter 4, and this is therefore important to keep in mind. The action in Eq. (3.13) is inspired by the Hopfield models employed in Refs. [59, 60, 73, 110, 112]. In the case of constant $\Omega_i(\mathbf{x},t) \equiv \Omega_i$, we find that Eq. (3.13) leads to a dispersion relation for the electric field in the familiar Sellmeier form [see Eq. (3.1)]. In other words, the action in Eq. (3.13) is a suitable starting point for modelling any dielectric where absorption is negligible.

3.2 Effective action and spatial mode expansion

As of yet, we have simply defined the classical dynamics of the fields $\mathbf{A}$ and $\mathbf{R}_i$, whose equations of motion are found by minimising the action in Eq. (3.13). We now want to describe the dynamics using only $\mathbf{A}$. Let us however first consider the oscillator field, whose dynamics we will be integrating out in order to form an

[3] Remember, this is because Coulomb gauge here relies on $\boldsymbol{\nabla}\cdot\mathbf{R} \simeq 0$.

[4] Or alternatively, $\left|\boldsymbol{\nabla}\Omega_i^2(\mathbf{x},t)/\omega^2\right| \ll |\mathbf{k}|$ for $\omega \gg \Omega_i^2$.

effective action for the photons $S_{\text{eff}}[\mathbf{A}]$. This is done schematically by computing the path integrals over $\mathbf{R}_i$, as in

$$\exp iS_{\text{eff}}[\mathbf{A}] = \mathcal{N}\int \mathcal{D}\mathbf{R}_i \; e^{i(S_\gamma[\mathbf{A}]+S_R[\mathbf{R}_i]+S_{\text{int}}[\mathbf{A},\mathbf{R}_i])}, \tag{3.15}$$

where we will be using the boundary conditions $\mathbf{R}_i(\mathbf{x},t_i) = \mathbf{R}_i(\mathbf{x},t_f) = 0$, since the dynamics of $\mathbf{R}_i$ are not a concern here. Importantly, the coupling between the vector potential $\mathbf{A}$ and the oscillator $\mathbf{R}_i$ in the action $S_{\text{int}}[\mathbf{A},\mathbf{R}_i]$ is linear in each field. Consequently, the full action $S_{\gamma+R+\text{int}}$ is quadratic in the fields, using which it is easy to show that the quantum fluctuation of $\mathbf{R}_i$ does not affect $\mathbf{A}$ directly. We should nonetheless note that setting these boundary conditions constitute an approximation, where we assume that the oscillator dynamics has but a small contribution to the overall dynamics of the system. This is well justified in regimes in which the electromagnetic field dominates, which is indeed the case in the optical regime where our interest lies. We will relax this approximation in Chapter 6. Within this approximation, we can therefore contain all quantum fluctuations in the matter degree of freedom in the normalisation constant $\mathcal{N}$ (which we will from here on set to unity) [3].

Because the action is quadratic in the fields, we can perform the path integrals in Eq. (3.15) simply by finding the classical action for the oscillators, driven by $-q_i\dot{\mathbf{A}}$ and with boundary conditions $\mathbf{R}_i(\mathbf{x},t_i) = \mathbf{R}_i(\mathbf{x},t_f) = 0$ [98]. In other words, we wish to solve

$$\ddot{\mathbf{R}}_i + \Omega_i^2(\mathbf{x},t)\mathbf{R}_i = -q_i\dot{\mathbf{A}}, \tag{3.16}$$

with boundary conditions as stated above, the solution of which we substitute into the action S_R. This is most conveniently done by first calculating the Green's functions

$$\left[\partial_t^2 + \Omega_i^2(\mathbf{x},t)\right]\Delta_i = -\delta(t-t'), \tag{3.17}$$

with boundary conditions $\Delta_i(\mathbf{x},t_f,t') = \Delta_i(\mathbf{x},t_i,t') = 0$. We can get the effective action for photons by substituting

$$\mathbf{R}_i(\mathbf{x},t) \to \frac{q_i}{2}\int_{t_i}^{t_f} dt'\Delta_i(\mathbf{x},t,t')\dot{\mathbf{A}}(\mathbf{x},t')$$

into $S_{\text{int}}[\mathbf{A},\mathbf{R}]$, where the factor $1/2$ comes from a contribution in S_R. Furthermore, the Coulomb gauge condition in Eq. (3.10) allows us to expand the vector potential in the polarisation vectors $\mathbf{A} = \sum_{\lambda=1,2}\mathbf{e}_\lambda A_\lambda$, where $\mathbf{e}_\lambda\cdot\mathbf{e}_{\lambda'} = \delta_{\lambda,\lambda'}$ is defined with respect to some reference vector $\mathbf{p}$ such that $\mathbf{e}_\lambda\cdot\mathbf{p} = 0$. Also, we can expand the oscillators $\mathbf{R}_i$ into the same polarisation modes, since we previously assumed that

the oscillators approximately satisfy the Coulomb 'gauge' condition $\boldsymbol{\nabla}\cdot\mathbf{R}_i \simeq 0$ (i.e. their spatial variation is slow as compared to the wavelength of light). Finally, this yields the effective and time-nonlocal action

$$S_{\text{eff}}[\mathbf{A}] = \sum_\lambda \frac{1}{2}\Bigg(\int_{t_i}^{t_f} dt \int d^3x \left[\dot{A}_\lambda{}^2 - (\boldsymbol{\nabla} A_\lambda)^2 \right. \\ \left. - \sum_i g_i^2 \int_{t_i}^{t_f} dt'\; \dot{A}_\lambda(\mathbf{x},t)\Delta_i(\mathbf{x},t,t')\dot{A}_\lambda(\mathbf{x},t') \right] \Bigg), \tag{3.18}$$

where Δ_i is the oscillator propagator given in Eq. (3.17), and $g_i = \sqrt{\rho} q_i$ are the effective plasma frequencies for each resonance. As can be seen, this action has the time-local free propagation on the first line, followed by the time-nonlocal self-energy acquired through the interaction with the matter degree of freedom on the second line. We can also note that the two polarisations de-couple and so from this point, we will for notational simplicity work with the scalar quantity $A(\mathbf{x},t)$ by dropping the λ-subscript.

Until this point the treatment is completely general, and we have not specified any space or time-dependence of Ω_i^2. We will next discuss how to expand $A(\mathbf{x},t)$ into suitable spatial modes for various spatial configurations. First we will focus on a spatially homogeneous situation (as in bulk media), and subsequently introduce space-dependencies to Ω_i^2, although we should note that we need to be careful to still satisfy $\boldsymbol{\nabla}\cdot\mathbf{R}_i \simeq 0$. As mentioned earlier, this translates into requiring that the variation satisfies Eq. (3.14). By introducing spatial variations, we will complicate the dispersion relation in Eq. (3.2), as this is strictly speaking only valid for plane waves. As discussed in Section 2.2, this will also let us treat this quantum field theory problem in an essentially quantum mechanical fashion, by treating each spatial mode independently.

3.2.1 Dispersion relation and expansion into spatial modes

Let us expand the vector potential into a set of orthonormal spatial modes $u_{\mathbf{k}}(\mathbf{x})$ such that

$$A(\mathbf{x},t) = \sum_{\mathbf{k}} u_{\mathbf{k}}(\mathbf{x}) A_{\mathbf{k}}(t),$$

which we will normalise by $\int d^3x\; u^*_{\mathbf{k}}(\mathbf{x}) u_{\mathbf{l}}(\mathbf{x}) = \delta_{\mathbf{kl}}$. In order to find a suitable set of such orthonormal modes, it is useful to first find the classical equation of motion for the vector potential, as given by minimising the action in Eq. (3.18). This yields

$$\left(\partial_t^2 - \nabla^2\right) A(\mathbf{x},t) + \sum_i \int_{t_i}^{t_f} dt' \dot{\Delta}_i(\mathbf{x},t,t')\dot{A}(\mathbf{x},t') = 0, \tag{3.19}$$

where the spatial boundary conditions would depend on the geometry investigated, i.e. the values of $A(\partial S, t)$ for some surface ∂S. If we furthermore assume that the oscillator frequency is time-independent, then we can expand the vector potential as

$$A(\mathbf{x}, t) = \sum_{\mathbf{k}} u_{\mathbf{k}}(\mathbf{x}) \int \frac{d\omega}{2\pi} A_{\mathbf{k}}(\omega) e^{-i\omega t},$$

which after substituting into Eq. (3.19) yields

$$\left[\nabla^2 + \omega^2 \left(1 - \sum_i \frac{g_i^2}{\omega^2 - \Omega_i^2(\mathbf{x})}\right)\right] u_{\mathbf{k}}(\mathbf{x}) = 0,$$

or more succinctly

$$\left[\nabla^2 + \omega^2 n^2(\omega, \mathbf{x})\right] u_{\mathbf{k}}(\mathbf{x}) = 0, \tag{3.20}$$

with appropriate spatial boundary conditions. In its simplest case when $n(\omega, \mathbf{x}) \equiv n(\omega)$, this is simply the Helmholtz equation. The set of solutions to this equation is what we will use as spatial modes. As is outlined below, such a set of solutions include the usual plane waves and paraxial waves, but also fibre-like scenarios. We will however mostly concern ourselves with plane waves.

3.2.1.1 Bulk media

Modelling bulk media, such as a bulk crystal or glass, now becomes straightforward if we assume that the refractive index of the medium is constant in space, which here maps to a spatially constant Ω_i. In this case, we define the spatial modes as appropriately normalised solutions to the Helmholtz equation

$$\left[\nabla^2 + \omega^2 n^2(\omega)\right] u_{\mathbf{k}}(\mathbf{x}) = 0. \tag{3.21}$$

Plane waves In the absence of any boundaries, the most natural modes are the plane waves

$$u_{\mathbf{k}}(\mathbf{x}) = e^{i\mathbf{k}\cdot\mathbf{x}}/\mathcal{V}, \tag{3.22}$$

where we have assumed an overall volume $\mathcal{V}$ (which will later be used as a quantisation box [2]). This leads to the dispersion relation

$$-|\mathbf{k}|^2 + \omega^2 n^2(\omega) = 0. \tag{3.23}$$

Paraxial waves In many experiments however, plane waves are not a good description of the spatial modes, in which case they are replaced by structured parax-

ial beams. In this case, we construct a complete set of spatial modes if we expand $u_{\mathbf{k}}(\mathbf{x}) \propto u_k(\boldsymbol{\rho}, z)e^{ikz}$ with $q^2/2k^2 \ll 1$, where k is the momentum in the z-direction (chosen arbitrarily) and $\mathbf{q}$ is the momentum in the transverse direction conjugate to the transverse coordinate $\boldsymbol{\rho}$. In doing this, we can reduce Eq. (3.21) to the paraxial wave equation

$$\left(\nabla_\perp^2 + 2ik\partial_z\right) u_k(\boldsymbol{\rho}) = 0, \tag{3.24}$$

where $\nabla_\perp^2$ is the transverse Laplacian. In this case, the dispersion relation relates only to k, as in

$$-k^2 + \omega^2 n^2(\omega) = 0. \tag{3.25}$$

Solutions to the paraxial wave equation in Eq. (3.24) include the familiar Laguerre-Gaussian modes and Hermite-Gaussian modes [113]. Using these in a quantisation procedure was previously done in Ref. [114].

3.2.1.2 Structured media

We can similarly expand in some spatial modes also when the medium has some sort of spatial structure. As an example, let us here suppose that we wish to model a parabolic fibre, such that the refractive index $n^2(\omega, \boldsymbol{\rho}) \simeq n_0^2(\omega) + \nu(\omega)(1 - r^2)$ for some small r, with r being the transverse radial coordinate, and $\nu(\omega) \geq 0$. This can be modelled in two separate ways, either by introducing a spatial dependence to the density $\rho \to \rho\left[1 + \delta_\rho(\mathbf{x})\right]$, or to the resonance frequencies $\Omega_i^2 \to \Omega_i^2\left[1 - \delta_\Omega(\mathbf{x})\right]$. As a reminder, here the density enters the refractive index through the plasma frequency $g_i^2 = \rho q_i^2$. For the purpose of modelling a refractive index, these two approaches are equivalent. This yields a refractive index of the form

$$\begin{aligned} n^2(\omega) &= \left(1 - \sum_i \frac{q_i^2 \rho}{\omega^2 - \Omega_i^2}\right) - \left(\sum_i \frac{q_i^2 \rho}{\omega^2 - \Omega_i^2}\right) \delta_\rho(\mathbf{x}) \\ &= n_0^2(\omega) + \left(\sum_i \frac{g_i^2}{\omega^2 - \Omega_i^2}\right) \delta_\rho(\mathbf{x}) \end{aligned}$$

and

$$\begin{aligned} n^2(\omega) &= \left(1 - \sum_i \frac{g_i^2}{\omega^2 - \Omega_i^2\left[1 - \delta_\Omega(\mathbf{x})\right]}\right) \\ &\simeq n_0^2(\omega) + \left(\sum_i \frac{g_i^2 \Omega_i^2}{\left(\omega^2 - \Omega_i^2\right)^2}\right) \delta_\Omega(\mathbf{x}) \end{aligned}$$

respectively, where in the latter case we have expanded to first order for $\delta_\Omega \ll 1$, for which we assume that ω is far away from Ω_i. In either case, it takes the form of

$n_0^2(\omega) + \nu(\omega)\delta(\mathbf{x})$.

Let us return to the parabolic fibre, by assuming that $\delta(\mathbf{x}) = (1 - r^2)$ within some small interval for r. If we further suppose that $u_{\mathbf{k}}(\mathbf{x}) = u_{k_z}(\boldsymbol{\rho})e^{ik_z z}$, then we find a spatial mode equation of the form

$$\left[\nabla_\perp^2 + \nu(\omega)\omega^2(1 - r^2)\right] u_{k_z}(\boldsymbol{\rho}) = \left[k_z^2 - \omega^2 n_0^2(\omega)\right] u_{k_z}(\boldsymbol{\rho}),$$

or written more suggestively

$$\left[-\frac{1}{2}\nabla_\perp^2 + \left(\frac{\nu(\omega)\omega^2}{2}\right) r^2\right] u_{k_z}(\boldsymbol{\rho}) = \frac{1}{2}\left[\omega^2\left\{n_0^2(\omega) + \nu(\omega)\right\} - k_z^2\right] u_{k_z}(\boldsymbol{\rho}).$$

This is simply the equation for a 2-dimensional harmonic oscillator with 'energy'

$$\mathcal{E} = \frac{1}{2}\left[\omega^2\left\{n_0^2(\omega) + \nu(\omega)\right\} - k_z^2\right],$$

from which the solutions can be extracted [3]. After re-arranging the energy condition $\mathcal{E} = \omega^2\nu(\omega)\left[n + m + 1\right]$ for $n, m \in \mathbb{N}$, we find the dispersion relation

$$\omega^2\left(n_0^2(\omega) - \nu(\omega)\right) = k_z^2 + 2\nu(\omega)\omega^2\left[n + m\right].$$

Note that in reality, only the lower lying 'energy' eigenstates (small n and m) can be used from this treatment, since it is only valid for small r.

In the following, we will be considering bulk media but as can be seen from this discussion, we are able to generalise it to also include structured media in certain circumstances.

3.3 Quantisation

Let us return to the effective action for the vector potential in Eq. (3.18). We now wish to expand this in terms of the spatial modes discussed in the previous section, but in order to proceed, let us first transform to frequency space, using the convention

$$A(\mathbf{x}, t) = \int \frac{d\omega}{2\pi} A(\mathbf{x}, \omega)e^{-i\omega t}.$$

This yields

$$S_{\text{eff}} = \frac{1}{2}\int \frac{d\omega}{2\pi}\int d^3x\; A^*(\mathbf{x}, \omega)\left[\nabla^2 + \;\omega^2 n^2(\omega, \mathbf{x})\right] A(\mathbf{x}, \omega),$$

where we note that $A^*(\mathbf{x}, \omega) = A(\mathbf{x}, -\omega)$ since $A(\mathbf{x}, t)$ is a real number. Here $\Delta_i(\mathbf{x}, t, t')$ is given by Eq. (3.17), and we have used that it is diagonal in the frequency domain when Ω_i is time-independent, as well as integrated by parts on the $\boldsymbol{\nabla}$-term.

At this point, we can further expand in the spatial modes which was discussed in Section 3.2, that is

$$A(\mathbf{x},\omega) = \sum_{\mathbf{k}} A_{\mathbf{k}}(\omega)\; u_{\mathbf{k}}(\mathbf{x}).$$

After this we find the effective action

$$S_{\text{eff}} = \frac{1}{2}\sum_{\mathbf{k}} \int \frac{d\omega}{2\pi}\; A^*_{\mathbf{k}}(\omega) D(\mathbf{k},\omega) A_{\mathbf{k}}(\omega), \tag{3.26}$$

where again $A^*_{\mathbf{k}}(\omega) = A_{-\mathbf{k}}(-\omega)$, and where we have used that the spatial modes are by definition orthonormal (i.e. $\int d^3x\; u^*_{\mathbf{k}}(\mathbf{x}) u_{\mathbf{l}}(\mathbf{x}) = \delta_{\mathbf{kl}}$). Here we have used $D(\mathbf{k},\omega)$ to denote a general dispersion relation which depends on the particular spatial modes. For instance, for bulk media the dispersion relation is given by

$$\begin{aligned} D(\mathbf{k},\omega) &\equiv -|\mathbf{k}|^2 + \omega^2 n^2(\omega) \\ &= -|\mathbf{k}|^2 + \omega^2 \left(1 - \sum_i \frac{g_i^2}{\omega^2 - \Omega_i^2}\right). \end{aligned} \tag{3.27}$$

Commonly, it is noted in textbooks (such as Refs [2–4]) that the quantisation of a quantum field is done by considering an infinite set of quantum mechanical problems, usually harmonic oscillators, for each position or momentum (in this context spatial mode $\mathbf{k}$). This is especially evident in a canonical quantisation scheme, which is the most common blueprint used in quantum optics [2]. In particular, the canonical operators and commutation relations are somewhat straightforwardly duplicated for each spatial mode, *ad infinitum*. However, in a path integral setting, such a construct is mostly used anecdotally in order to aid understanding [4]. Whilst this has been considered briefly in Refs. [3, 115], it is not common to use this for actual computations. As we shall see in this section however, this turns out to be particularly suitable for addressing the quantisation of macroscopic electrodynamics.

Nonetheless, a brief glance at the effective action in Eq. (3.26) tells us that this problem is nonlocal in time. This is the nature of optical dispersion and cannot be avoided. Temporal nonlocalities do however interrupt the usual quantisation schemes, as time does play a special role in quantum theory (and field theory). Quantisation of nonlocal field theories can nevertheless be done, which is a concept that often crops up when constructing effective field theories where one or more fields are integrated out: the most famous example being the Euler-Heisenberg Lagrangian of quantum electrodynamics [116], where the electron field has been integrated out by assuming that the electromagnetic field is essentially static as compared to the electron field.[5] Effective field theories [117, 118] can be found by integrating out fields (as in Refs. [116, 119]), which is what we will be doing here,

[5]This is a low-energy approximation.

or simply proposed *ad hoc*. They are not always nonlocal, although one should note that higher order derivatives masquerade as nonlocalities, as in the Lee-Wick model [120]. Interestingly, and connected to this, it is common to expand $D(\mathbf{k},\omega)$ as a series in ω around some frequency ν in the context of quantum optics [107], truncating at some $\mathcal{O}(\omega^n)$. One can then return to temporal space by replacing $\omega^n \to (-i\partial_t)^n$. For instance, by truncating this expansion at $\mathcal{O}(\omega^4)$, we can take into account group velocity dispersion. This does however treat the dispersion in a perturbative manner and does not capture the whole picture. We will avoid these complications by using the fact that we are free to rescale the field variables, something which will only introduce a constant in the path integral, although we note that this also involves approximations, but of a different nature.

The specific rescaling that we intend to do will trade the temporal nonlocality for a spatial nonlocality in the new coordinates, which is easier to treat in quantum theory. Let us first consider the solution to the classical equations of motion for each spatial mode. Schematically, we can write this equation as

$$D(\mathbf{k},\omega)A_{\mathbf{k}}(\omega) = 0,$$

which has the solutions $A_{\mathbf{k}} \propto \exp(\pm i\omega_\alpha t)$, where $\omega_\alpha(\mathbf{k})$ is given by the zeros of $D(\mathbf{k},\omega)$. In this way we can define the relevant quasiparticles of the system by solving $D(\mathbf{k},\omega) = 0$ for ω^2 as a function of spatial mode label $\mathbf{k}$. In doing so, we find $N+1$ quasiparticle branches (where N is the number of resonances of the medium) for bulk media, and possibly more for structured media depending on the exact frequency dependence of the dispersion relation $D(\mathbf{k},\omega)$. As discussed in Chapter 1, we refer to the quasiparticles in light-matter systems as *polaritons*. The polariton branches will here be labelled by the subscript α. For a single-resonance medium where $n^2(\omega) = 1 - g^2/(\omega^2 - \Omega^2)$, which is a good model for diamond, the polariton modes are the solutions of $\omega^2 n^2(\omega) - |\mathbf{k}|^2 = 0$ for ω as a function of $\mathbf{k}$. These are given by

$$\omega_\pm^2(\mathbf{k}) = \frac{1}{2}\left(|\mathbf{k}|^2 + g^2 + \Omega^2 \pm \sqrt{\left(|\mathbf{k}|^2 + g^2 + \Omega^2\right)^2 - 4|\mathbf{k}|^2\Omega}\right).$$

In a more complicated example, such as fused silica, the mathematical expressions for the polariton modes become too lengthy to write down here, but can in principle be found in the same manner. Fused silica is the medium which we will use as an example here, due to its common usage in optical experimental set-ups, and as such, we can see the branches in Fig. 3.1(a). In particular, fused silica is here modelled

using the following resonance frequencies Ω_i and plasma frequencies g_i:

$$\begin{aligned}\Omega_1 &= 1.90342 \times 10^{14}\ \mathrm{s}^{-1},\\ \Omega_2 &= 1.62047 \times 10^{16}\ \mathrm{s}^{-1},\\ \Omega_3 &= 2.7537 \times 10^{16}\ \mathrm{s}^{-1},\end{aligned} \tag{3.28}$$

and

$$\begin{aligned}g_1 &= 1.803 \times 10^{14}\ \mathrm{s}^{-1},\\ g_2 &= 1.035 \times 10^{16}\ \mathrm{s}^{-1},\\ g_3 &= 2.298 \times 10^{16}\ \mathrm{s}^{-1}.\end{aligned} \tag{3.29}$$

Using these polariton branches, inspired by Ref. [112], we can now do the following field transformation

$$\begin{aligned}A_{\mathbf{k}}(\omega) &= \sqrt{\frac{\omega^2-\omega_\alpha^2(\mathbf{k})}{D(\mathbf{k},\omega)}}A_{\mathbf{k}\alpha}(\omega) = \sqrt{\frac{\omega^2-\omega_\alpha^2(\mathbf{k})}{\omega^2 n^2(\omega)-|\mathbf{k}|^2}}A_{\mathbf{k}\alpha}(\omega)\\ &= \mathcal{P}_{\mathbf{k}\alpha}(\omega)A_{\mathbf{k}\alpha}(\omega).\end{aligned} \tag{3.30}$$

This defines what we will refer to as a polariton coordinates. Importantly, this transformation might appear ill-defined but is truly finite since the poles of $1/D(\mathbf{k},\omega)$ coincide with the roots of $\omega^2-\omega_\alpha^2(\mathbf{k})$. Indeed, if we carefully take the limit of $\mathcal{C}_{\mathbf{k}\alpha} \equiv \mathcal{P}^2_{\mathbf{k}\alpha}(\omega\to\omega_\alpha)$, we see that

$$\mathcal{C}_{\mathbf{k}\alpha} = \lim_{\omega\to\omega_\alpha}\left[\frac{\omega^2-\omega_\alpha^2}{D(\mathbf{k},\omega)}\right] = \frac{\prod_i(\omega_\alpha^2-\Omega_i^2)}{\prod_{\gamma\neq\alpha}\left(\omega_\alpha^2-\omega_\gamma^2\right)}.$$

Here we have used the fact that the dispersion relation can be factorised as

$$D(\mathbf{k},\omega)\prod_i\left(\omega^2-\Omega_i^2\right) = \prod_\gamma\left(\omega^2-\omega_\gamma^2\right).$$

This coefficient $\mathcal{P}_{\mathbf{k}\alpha}$ is the projection of the photon field onto a polariton field. It will appear in any physical result, commonly squared and it is thus convenient to work with $\mathcal{C}_{\mathbf{k}\alpha}$. It can be absorbed into the measure in the path integral, so we can ignore it there. In other words, we normalise our probabilities such that the $\mathcal{P}_{\mathbf{k}\alpha}$-coefficients do not contribute, which is a well-defined procedure also for a frequency-dependent coefficient such as this. This coefficient signifies the degree to which any polariton branch α is photon-like for a specific $\mathbf{k}$, and can be seen as a generalisation of the Hopfield coefficients [59]. As such, it follows that $0 \leq \mathcal{C}_{\mathbf{k}\alpha} \leq 1$, and that this constant will be close to unity when the polariton branch dispersion relation $\omega_\alpha(\mathbf{k})$ is similar to a free photon, and vice-versa. We can see an example of this in Fig. 3.1(b) for fused silica.

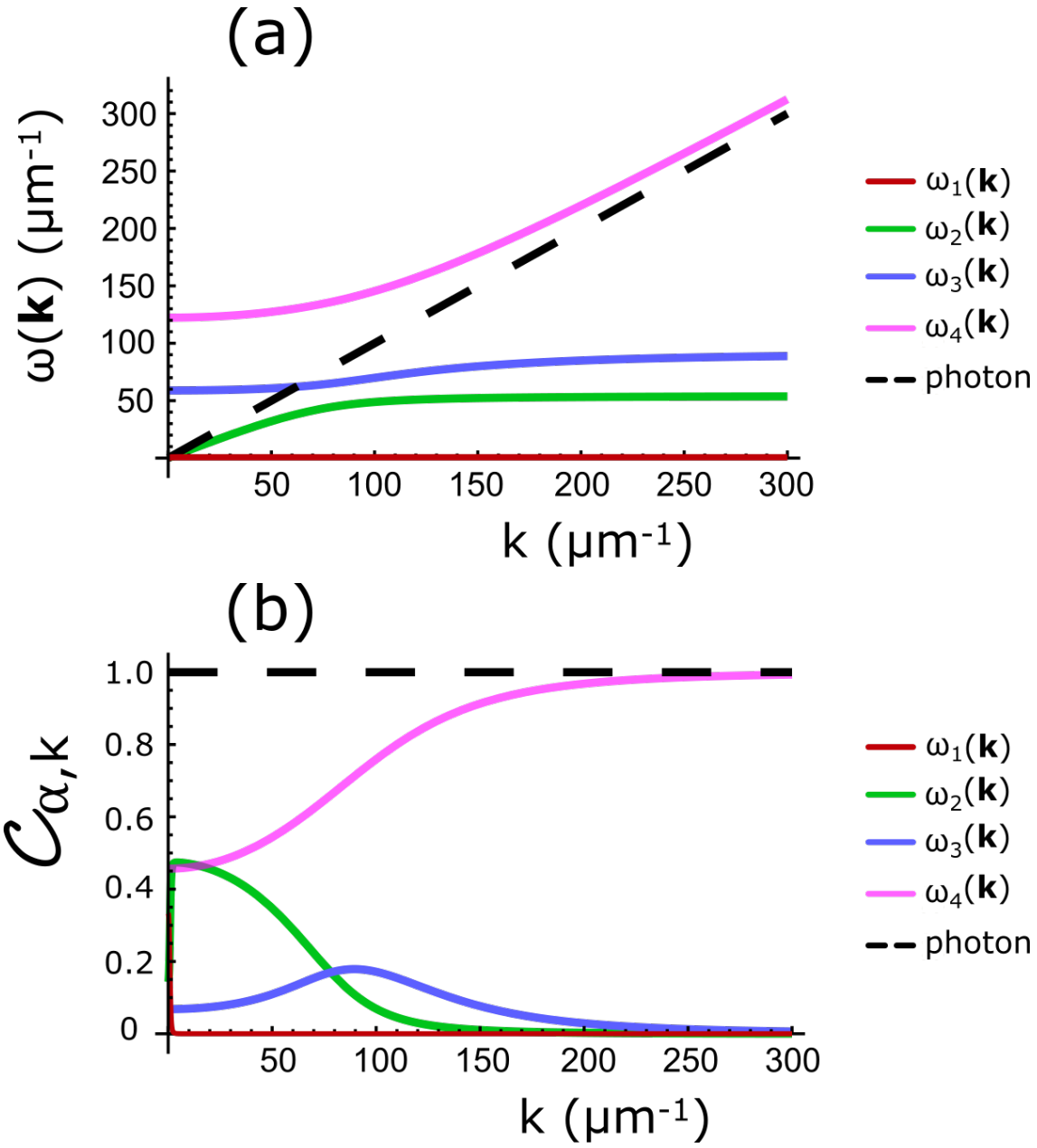

Figure 3.1: **(a)** The dispersion relation for the fused silica polariton branches (solid) in units of $c = 1$, and free photon dispersion relation (dashed). In these units, the optical regime lies between $3 - 20\ \mu\text{m}^{-1}$. **(b)** Generalised Hopfield coefficients $\mathcal{C}_{\mathbf{k}\alpha}$ for the different branches. Compare to (a), and note that this coefficient is close to unity when a branch can be characterised as 'photon-like'.

As we will see, the main benefit is that the action (and corresponding equation of motion) becomes local in time when written in polariton fields, as opposed to the time-nonlocal action seen in Eq. (3.18). Thus, we incorporate the temporally delayed response directly in the definition of the polariton field and their dependence on the spatial mode $\mathbf{k}$. We have here traded the temporal nonlocality for a spatial nonlocality, which means that the polariton branch frequency $\omega(\mathbf{k})$ contains higher order terms than $\mathcal{O}(\mathbf{k})$. This simplifies the quantisation procedure. As mentioned earlier, it is possible to treat temporally nonlocal field theories, but this commonly involves either truncating to some 'order of nonlocality' or it comes at a computational cost as one must define an infinite set of conjugate momenta (see for instance Refs [121, 122]). A spatial nonlocality is, on the other hand, straightforward to implement, as we can treat each spatial mode independently. We should note that this process relies on knowledge of all the polariton modes.

By design the temporally nonlocal action in Eq. (3.26) now reduces to the action of a set of complex harmonic oscillators when written in field-coordinates A_α. Specifically, we find after transforming back into temporal space the effective action

$$S_{\text{eff}} = \sum_{\mathbf{k},\alpha} \int_{t_i}^{t_f} dt\, \frac{1}{2} \left(|\dot{A}_{\mathbf{k}\alpha}(t)|^2 - \omega_\alpha^2 |A_{\mathbf{k}\alpha}(t)|^2 \right). \tag{3.31}$$

The discussion in this chapter is centred around this action, and since we will mostly consider a single spatial mode $\mathbf{k}$ in branch α, we will drop the sum over $\mathbf{k}$ and α and simply refer to them implicitly.

As we have mentioned previously (Section 2.2), macroscopic quantum electrodynamics is indeed a field theory, but can be treated as a quantum mechanical problem in this context. We will return to issue of the infinite set of spatial modes $\mathbf{k}$ later in the chapter (Section 3.6), including the accompanying problem of regularisation. Here, we will use a quantum-mechanical-style path integral, but it is instructive to also consider a Schrödinger equation for the purpose of building intuition. The latter will be discussed in Section 3.3.2.

We can now proceed as usual in quantum mechanics through single-particle path integrals. First, we want to add a driving term $J_{\mathbf{k}\alpha}(t)$ to the problem. From the perspective of macroscopic quantum electrodynamics, this represents the additional dynamics of free charges in the medium. We will briefly discuss the radiation from a uniformly moving charge in a medium in Section 3.4.1, but we will mainly use these extra driving terms as a means for computations.

Thus, after some simple algebra, and after simplifying the notation slightly, we arrive at the following action:

$$S_{\text{eff}}[J, J^*] = \int_{t_i}^{t_f} dt\, \frac{1}{2} \left(|\dot{A}|^2 - \omega_\alpha^2 |A|^2 + J^* A + J A^* \right). \tag{3.32}$$

This is what we intend to quantise, that is, calculate the probability amplitude of a polariton in branch α, mode $\mathbf{k}$ and polarisation λ having amplitude A_i at the initial time t_i and finishing with the final amplitude A_f at time t_f. Schematically, this is given by the integral

$$\langle A_f, t_f | A_i, t_i \rangle_J = \int \mathcal{D}A\mathcal{D}A^* \ \exp\left(iS_{\text{eff}}\left[J, J^*\right]\right),$$

where we have the boundary condition $A(t_i) = A_i$ and $A(t_f) = A_f$. This is in complete analogy with the quantum mechanical amplitudes considered in Ref. [3], albeit with some extra indices of which we need to take care.

Because this problem is quadratic in the fields, it is easy to show that the classical and quantum dynamics completely decouple, such that

$$\begin{aligned}\langle A_f, t_f | A_i, t_i \rangle &= e^{iS_{\text{cl}}} \int_{\eta(t_i)=0}^{\eta(t_f)=0} \mathcal{D}\eta\mathcal{D}\eta^* \ \exp\left(iS_{\text{eff}}[0,0]\right) \\ &= \mathcal{F}(T) e^{iS_{\text{cl}}}.\end{aligned}$$

This is done by substituting $A(t) \to A_{\text{cl}}(t) + \eta(t)$ into the action, where we assume that $\eta(t_i) = \eta(t_f) = 0$. Consequently, we find that the transition amplitude factorises as $\mathcal{F}(T)\exp\left[iS_{\text{cl}}\right]$, where the pre-factor $\mathcal{F}(T)$ is determined by the quantum fluctuations and $S_{\text{cl}} = S_{\text{eff}}\left[A_{\text{cl}}\right]$ is the classical action.

Let us first consider the classical dynamics, which we can find after minimising the action in Eq. (3.32). This yields the (approximate) polariton equation

$$\ddot{A}_{\text{cl}}(t) + \omega_\alpha^2 A_{\text{cl}}(t) = J(t)$$

with the boundary conditions $A_{\text{cl}}(t_f) = A_f$ and $A_{\text{cl}}(t_i) = A_i$. The equation of motion for A_{cl}^* is identical. This further separates into two terms, the free homogeneous term A_{H} and the driven inhomogeneous term A_{I}, where for the latter we require $A_{\text{I}}(t_f) = A_{\text{I}}(t_i) = 0$. This has the solution

$$\begin{aligned}A_{\text{H}}(t) &= \frac{1}{\sin\omega_\alpha T}\left[A_f \sin\omega_\alpha(t - t_i) + A_i \sin\omega_\alpha(t_f - t)\right] \\ A_{\text{I}}(t) &= -\Bigg[\frac{\sin\omega_\alpha(t_f - t)}{\omega_\alpha \sin\omega_\alpha T}\int_{t_i}^{t} dt' \ \sin\omega_\alpha(t' - t_i)J(t') \\ &\qquad + \quad \frac{\sin\omega_\alpha(t - t_i)}{\omega_\alpha \sin\omega_\alpha T}\int_{t}^{t_f} dt' \ \sin\omega_\alpha(t_f - t')J(t')\Bigg].\end{aligned} \tag{3.33}$$

We can now either directly substitute this into the action in Eq. (3.32), or with considerably less algebra, integrate the kinetic term by parts and use the classical

equations of motion to find

$$S_{\rm cl}[J,J^*] = \frac{1}{2}\left[A^*_{\rm H}\dot{A}_{\rm H}\right]_{t_i}^{t_f} + \frac{1}{2}\left[A^*_{\rm H}\dot{A}_{\rm I}\right]_{t_i}^{t_f} + \frac{1}{2}\int_{t_i}^{t_f} dt\; J^*(t)\left[A_{\rm H}(t) + A_{\rm I}(t)\right]. \tag{3.34}$$

If we now substitute the classical solutions from Eq. (3.33) we find, after some tedious but straightforward algebra,

$$\begin{aligned} S_{\rm cl}[J,J^*] = \;& \frac{\omega_\alpha}{2\sin\omega_\alpha T}\left[\left(|A_f|^2 + |A_i|^2\right)\cos\omega_\alpha T - \left(A^*_f A_i + c.c.\right)\right] \\ & + \frac{1}{2\sin\omega_\alpha T}\Bigg[\int_{t_i}^{t_f} dt\,\Big(A_f \sin\omega_\alpha\left(t-t_i\right) J^*(t) \\ & \qquad + A_i \sin\omega_\alpha\left(t_f - t\right) J^*(t)\Big) + \text{c.c.}\Bigg] \\ & - \frac{1}{2\omega_\alpha \sin\omega_\alpha T}\Bigg[\int_{t_i}^{t_f} dt \int_{t_i}^{t_f} dt'\; J^*(t)\sin\omega_\alpha\left(t_f - t\right) \\ & \qquad \times \sin\omega_\alpha\left(t' - t_i\right) J(t') + \text{c.c.}\Bigg], \end{aligned} \tag{3.35}$$

where c.c. denotes the complex conjugate. Finally, we wish to compute the pre-factor

$$\mathcal{F}(T) = \int_{\eta(t_i)=0}^{\eta(t_f)=0} \mathcal{D}\eta\mathcal{D}\eta^*\; e^{\frac{i}{2}\int_{t_i}^{t_f} dt\,\left(|\dot{\eta}|^2 - \omega_\alpha^2|\eta|^2\right)}.$$

The simplest approach to this is to use the time-translational invariance of the problem. Since this normalisation factor depends only on the total time T, it follows that

$$\mathcal{F}(T) = \langle 0, T|0,0\rangle = \left(\frac{\omega_\alpha}{4\pi i \sin\omega_\alpha T}\right).$$

In the end, we find that the transition amplitude is given by

$$\langle A_f, t_f|A_i, t_i\rangle_J = \left(\frac{\omega_\alpha}{4\pi i\sin\omega_\alpha T}\right) e^{iS_{\rm cl}[J,J^*]}, \tag{3.36}$$

where $T = t_f - t_i$ and the classical action $S_{\rm cl}[J,J^*]$ is that of a complex driven simple harmonic oscillator. Physically, Eq. (3.36) is the probability amplitude for the polariton field in branch α in spatial mode $\mathbf{k}$ and amplitude A_i at time t_i to transition to amplitude A_f at time t_f. Note that since the polaritons are the normal modes of the system, and because the spatial modes form a complete basis, this transition amplitude involves only dynamics within its own branch α and spatial mode $\mathbf{k}$. Also, it is the propagator for the wavefunction of a polariton in branch α and spatial mode $\mathbf{k}$, and we can use this to calculate the time-propagation of some initial state $\psi(A_i, t_i)$. This expression contains a fair amount of information about the system; extracting it can however require a fair bit of algebra. For instance, we

will present the Fock space (excitation number) wavefunctions in the Section 3.3.1.

Interestingly, if we were, at this point, to sum over all spatial modes $\mathbf{k}$ we would find a divergent transition amplitude. This is well-known, and requires regularisation [4, 115]. As we shall see in Section 3.4, we can avoid this issue by calculating differences in number state population. We should, as a final aside, note that as $T \to n\pi/\omega_\alpha$ for $n \in \mathbb{Z}$, the propagator in Eq. (3.36) reduces to

$$\langle A_f, t_f | A_i, t_i \rangle_J = \delta(A_f - (-1)^n A_i),$$

which is as expected for a harmonic oscillator since this signifies that the field returns to its previous value after a full period of $2\pi/\omega_\alpha$.

3.3.1 Polariton wavefunctions

As a first example of information that we can extract from the transition amplitude in Eq. (3.36), let us calculate the Fock space wavefunctions. These wavefunctions are the usual probability amplitudes Ψ_{mn} associated with each energy state, and they are written as mn-states where m and n denote the number of $-\mathbf{k}$ and $\mathbf{k}$ polaritons respectively (whose classical amplitude is given by A^* and its complex conjugate A respectively), with a total number of polaritons given by $m + n$.

Whilst it is possible to find these wavefunctions through a direct expansion of Eq. (3.36) in orders of $\exp(-i\omega_\alpha T)$, it is more convenient to first calculate the transition amplitude of starting in a state displaced from the centre by a, and finishing in a state displaced by b. The initial state is given by

$$\phi_a(A) = \sqrt{\frac{\omega_\alpha}{2\pi}} e^{-\omega_\alpha |A-a|^2/2},$$

where the normalisation is such that

$$\int d^2A \ |\phi_a(A)|^2 = 1,$$

where $d^2A = dA dA^*$ is the complex differential area element. Here the subscript a denotes the distance that the field variable A is displaced from the origin. The final state is in this notation given by $\phi_b(A)$. In other words, we want to calculate

$$F(b,a) = \int d^2A_f d^2A_i \ \phi_b^*(A_f) \langle A_f, t_f | A_i, t_i \rangle \big|_{J=0} \phi_a(A_i). \tag{3.37}$$

Note that this transition amplitude is closely related to the coherent state transition amplitude, as indeed $\phi_a(A)$ forms the real part of a coherent state of amplitude a.[6] It is however *not* a coherent state, and we will therefore from now on refer to

[6] It is missing a 'momentum' kick given to the wavefunction by the imaginary part of the coherent state.

such states as 'displaced states' rather than 'coherent states'. Also, Eq. (3.37) is a generalisation of the quantum mechanical calculation in Ref. [3]. As these are simply Gaussian integrals which can readily be computed, we find

$$F(b,a) = \gamma e^{-\omega_\alpha\left(|b|^2+|a|^2\right)/4} \exp\left[\frac{\gamma\omega_\alpha}{4}(ba^* + b^*a)\right], \tag{3.38}$$

where $\gamma = \exp(-i\omega_\alpha T)$. It is now much simpler to expand in orders of γ.

In order to find the Fock space wavefunctions $\Psi_{mn}(a)$, let us now expand the displaced state $\phi_a(A)$ in terms of these wavefunctions, with some coefficient $\psi_{mn}(a)$, i.e.

$$\phi_a(A) = \sum_{mn} \psi_{mn}(a)\Psi_{mn}(A),$$

where we have to sum over both m and n because $-\mathbf{k}$ and $\mathbf{k}$-polaritons acts independently. By virtue that the amplitudes $\psi_{mn}(a)$ must only depend on a and not A, we find

$$\psi_{mn}(a) = e^{-\frac{\omega_\alpha}{4}|a|^2}\left(\frac{\omega}{4}\right)^{\frac{m+n}{2}} \frac{(a^*)^m\, a^n}{\sqrt{m!n!}}. \tag{3.39}$$

We can now also expand the displaced state transition amplitude in Eq. (3.37) in terms of Fock space wavefunctions, yielding

$$\begin{aligned} F(b,a) &= \int d^2A_f d^2A_i\ \phi_b^*(A_f)\,\langle A_f, t_f|A_i, t_i\rangle\,\big|_{J=0}\phi_a(A_i) \\ &= \sum_{mnpq} \psi_{mn}^*(b)\psi_{pq}(a) \int d^2A_f d^2A_i\ \Psi_{mn}^*(A_f)\,\langle A_f, t_f|A_i, t_i\rangle_{J=0}\,\Psi_{pq}(A_i) \\ &= \sum_{mn} \psi_{mn}^*(b)\psi_{mn}(a)\gamma^{m+n+1}. \end{aligned} \tag{3.40}$$

At this point, let us expand both Eq. (3.38) and Eq. (3.40) in orders of γ. Finally with the use of Eq. (3.39), we can extract the Fock space wavefunctions $\Psi_{mn}(A)$. For notational simplicity, let us introduce the complex Hermite polynomials $H_{mn}(x^*, x)$

$$H_{mn}(x^*,x) = \sum_{k=0}^{\min(m,n)} (-1)^k k! \binom{m}{k}\binom{n}{k} (x^*)^{m-k}\, x^{n-k}, \tag{3.41}$$

as discussed in Refs. [123–125]. Finally, we find a compact notation for the Fock space wavefunctions as

$$\Psi_{mn}(A,t) = \sqrt{\frac{\omega_\alpha}{2\pi}} \frac{e^{-\omega_\alpha|A|^2/2}}{\sqrt{m!n!}} H_{mn}(\sqrt{\omega_\alpha}A^*, \sqrt{\omega_\alpha}A) e^{-i(m+n+1)\omega_\alpha t}. \tag{3.42}$$

As expected, they are the generalisation of the quantum harmonic oscillator wavefunctions for complex coordinates. For the sake of clarity, the 0-, 1- and 2-polariton

states are given by

$$\Psi_{00}(A_{\mathbf{k}\alpha},t) = \sqrt{\frac{\omega_\alpha}{2\pi}} e^{-\frac{\omega_\alpha}{2}|A_{\mathbf{k}\alpha}|^2} e^{-i\omega_\alpha t}$$

$$\Psi_{01\vee 10}(A_{\mathbf{k}\alpha},t) = \sqrt{\frac{\omega_\alpha}{2\pi}} \left[\left\{ \sqrt{\omega_\alpha} A_{\mathbf{k}\alpha} \right\} \vee \left\{ \sqrt{\omega_\alpha} A^*_{\mathbf{k}\alpha} \right\} \right] e^{-\frac{\omega_\alpha}{2}|A_{\mathbf{k}\alpha}|^2} e^{-2i\omega_\alpha t}$$

$$\Psi_{02\vee 20\vee 11}(A_{\mathbf{k}\alpha},t) = \sqrt{\frac{\omega_\alpha}{2\pi}} \left[\left\{ \frac{\omega_\alpha}{\sqrt{2}} (A_{\mathbf{k}\alpha})^2 \right\} \vee \left\{ \frac{\omega_\alpha}{\sqrt{2}} (A^*_{\mathbf{k}\alpha})^2 \right\} \vee \left\{ \left(\omega_\alpha |A_{\mathbf{k}\alpha}|^2 - 1\right) \right\} \right] \times e^{-\frac{\omega_\alpha}{2}|A_{\mathbf{k}\alpha}|^2} e^{-3i\omega_\alpha t},$$

with $\vee$ (i.e. 'or') denoting what combination of $\mathbf{k}$ and $-\mathbf{k}$ modes are excited, and where the phase factor is given by $\exp\left[-i(m+n+1)\omega_\alpha t\right]$ as expected.

3.3.2 Schrödinger equation

Let us instead see what happens if we quantise the action in Eq. (3.31) in an alternative fashion, such that we obtain a Schrödinger equation. We will have to use complex coordinates, but this does not change the viability of the method. For instance, Ref. [126] considered a complex quantum mechanical harmonic oscillator. First of all, let us define the canonical momenta as

$$\pi_{\mathbf{k}\alpha} = \frac{\delta \mathcal{L}_{\text{eff}}}{\delta \dot{A}_{\mathbf{k}\alpha}} = \frac{1}{2}\dot{A}^*_{\mathbf{k}\alpha}, \quad \pi^*_{\mathbf{k}\alpha} = \frac{\delta \mathcal{L}_{\text{eff}}}{\delta \dot{A}^*_{\mathbf{k}\alpha}} = \frac{1}{2}\dot{A}_{\mathbf{k}\alpha},$$

where, as usual, the Lagrangian is defined from the action as

$$S_{\text{eff}} = \int_{t_i}^{t_f} dt\ \mathcal{L}_{\text{eff}}.$$

Using this we can calculate the Hamiltonian

$$\hat{H}_{\mathbf{k}\alpha} = 2\hat{\pi}^*_{\mathbf{k}\alpha}\hat{\pi}_{\mathbf{k}\alpha} + \frac{1}{2}\omega^2_\alpha(\mathbf{k})\hat{A}^*_{\mathbf{k}\alpha}\hat{A}_{\mathbf{k}\alpha}.$$

In order to quantise this, we must now enforce the following canonical commutation relations

$$\left[\hat{A}_{\mathbf{k}\alpha}, \hat{\pi}_{\mathbf{k}\alpha}\right] = \left[\hat{A}^*_{\mathbf{k}\alpha}, \hat{\pi}^*_{\mathbf{k}\alpha}\right] = i,$$

where we use discrete spatial modes $\mathbf{k}$ (so that the relevant δ-function is a Kronecker δ-function), and where we can focus on a single spatial mode $\mathbf{k}$ because there is no potential present that can induce transitions.[7] This yields the canonical represen-

[7] Note also the discussion in Section 2.2.3 on this topic.

tation

$$\hat{\pi}_{\mathbf{k}\alpha} = \frac{\partial}{i\partial A_{\mathbf{k}\alpha}}, \quad \hat{\pi}^*_{\mathbf{k}\alpha} = \frac{\partial}{i\partial A^*_{\mathbf{k}\alpha}},$$

which is nothing but a complex harmonic oscillator. The Schrödinger equation of each α mode now reads directly as

$$i\partial_t \Psi(A_{\mathbf{k}\alpha}, t) = \left[-2\frac{\partial^2}{\partial A_{\mathbf{k}\alpha}\partial A^*_{\mathbf{k}\alpha}} + \frac{1}{2}\omega^2_\alpha(\mathbf{k})|A_{\mathbf{k}\alpha}|^2 \right] \Psi(A_{\mathbf{k}\alpha}, t),$$

where we can use partial derivatives (∂_A) rather than functional ones ($\delta/\delta A$) since here we treat each mode quantum mechanically. It is important to note that the probability amplitude product over all spatial modes $\mathbf{k}$, polariton branches α, and polarisations λ will yield a functional Schrödinger equation. Here however, we can treat each mode independently and work as if $A_{\mathbf{k}\alpha}$ is simply a complex number.

Using this, it is easy to verify that the ground state wavefunction is given by

$$\Psi(A_{\mathbf{k}\alpha}, t) = \sqrt{\frac{\omega_\alpha(\mathbf{k})}{2\pi}} \exp\left(-\omega_\alpha(\mathbf{k})\left|A_{\mathbf{k}\alpha}\right|^2/2\right) e^{-i\omega_\alpha(\mathbf{k})t}.$$

This is in agreement with Section 3.3.1, Ref. [126] for the quantum mechanical complex harmonic oscillator, and for the ground state of the field theories discussed in Refs [3, 4].

3.4 Transitions between number states

We have now quantised the coupled light and oscillator system in terms of polaritons. In other words, the dynamics of the system can be described by some set number of polariton quanta. In this section, we will discuss changes in the number of quanta in time. Generally, changes to the number of quanta are associated with the introduction of some time-dependent drive or potential. Introducing a temporally varying medium will induce the latter, an effective time-dependent potential. As we will see, this will excite quanta from the vacuum state, i.e. quantum vacuum radiation. The fact that some quanta is indeed excited should not come as a surprise, as light in a time-dependent optical medium is very closely linked to quantum fields on time-dependent backgrounds [15]. Interestingly, and usually ignored because of its relative insignificance,[8] the vacuum state can also be made to absorb quanta in a similar but time-reversed process.

In the language we use here, the excitation (or absorption) of quanta is easily interpreted as transitions between the Fock space number states we discussed in Section 3.3.1. Any such process has some probability amplitude associated with it,

[8]The probability of transition depends on the density of states of the initial state, which in the case of an excited state will be negligible as compared to the vacuum.

which we will denote as

$$G^{\mathbf{k}\alpha}_{mn\leftarrow pq}(t_f,t_i)=\int d^2A_f d^2A_i\ \Psi^*_{mn}(A_f)\,\langle A_f,t_f|A_i,t_i\rangle\,\Psi_{pq}(A_i).$$

Here we start in a state with $p+q$ polaritons at time t_i, and finish in a state with $m+n$ polaritons some time later at time t_f. As we have done throughout most of this chapter, we will drop the subscripts that identify the spatial mode $\mathbf{k}$ and polariton branch α, unless necessary. The spatial modes in question will be the plane waves living in volume $\mathcal{V}$ discussed in Section 3.2, that is

$$u_{\mathbf{k}}(\mathbf{x})=e^{i\mathbf{k}\cdot\mathbf{x}}/\sqrt{\mathcal{V}}.$$

As such, it is natural to refer to $\mathbf{k}$ as the momentum, and we will do so from here on. In order to treat a time-dependent medium, we will (as alluded to earlier) start with a driven system, discussing the effect of free currents $J(t)$ on the amount of polaritons.

3.4.1 Direct driving of the system

We first introduced free currents $J(t)$, i.e. the motion of free charges, into the action in Eq. (3.32). We will now use the resulting transition amplitude [Eq. (3.36)] to calculate the probability amplitudes associated with transitions between number states. This we can later use as generating functionals for constructing the corresponding transition amplitudes for a potential in a perturbative manner, given that the initial and final vacua are equivalent (with some period in-between where the vacuum is ill-defined).

As it will be the building block for what follows, let us first calculate the vacuum persistence amplitude. That is the probability amplitude for starting in the vacuum state and finishing in the vacuum state $G^J_{00\leftarrow 00}(t_f,t_i)$ (which we will denote $G^J_{00}(t_f,t_i)$ for notational simplicity). This is computed as

$$G^J_{00}(t_f,t_i)=\int d^2A_f d^2A_i\ \Psi^*_{00}(A_f)\,\langle A_f,t_f|A_i,t_i\rangle_J\,\Psi_{00}(A_i),$$

where we now make use of the ground state wavefunction $\Psi_{00}(A)$ found in Section 3.3.1 (albeit a time-independent version). As before, A is a complex variable and thus the integral can be computed, yielding

$$G^J_{00}(t_f,t_i)=\exp\left[-\frac{1}{4\omega_\alpha}\int dt\int dt'\,J(t)\cos\omega_\alpha(t-t')J^*(t')\right]e^{-i\omega_\alpha T}. \tag{3.43}$$

Perhaps unsurprisingly, this is once again the natural extension to complex variables of the vacuum persistence amplitude for real variables, discussed in Ref. [3].[9]

[9]Differently to the real variable case, we do not need to keep track of the order of integration

In principle, we can compute the analogous integrals for more general number state transitions. Unfortunately, this quickly becomes untenable simply due to the sheer amount of algebra required. We will therefore once again compute the associated displaced-state transition amplitude between wavefunctions starting at displacement a [i.e. $\phi_a(A)$] and finishing at displacement b [i.e. $\phi_b(A)$], where as a reminder a displace state is given by

$$\phi_a(A) = \sqrt{\frac{\omega_\alpha}{2\pi}} e^{-\omega_\alpha |A-a|^2/2}.$$

Also note that physically these states $\phi_a(A)$ signify a quantum state with average field amplitude a. This means that we instead want to calculate the transition amplitude

$$F(b,a)_J = \int d^2A_f d^2A_i \; \phi_b^*(A_f) \left\langle A_f, t_f | A_i, t_i \right\rangle_J \phi_a(A_i), \tag{3.44}$$

which we will once again use purely for computational purposes. Just as we did in Section 3.3.1, by expanding ϕ_a and ϕ_b in terms of the Fock wavefunctions Ψ_{mn}, we find

$$\begin{aligned} F(b,a)_J &= \sum_{mnpq} \psi_{mn}^*(b)\psi_{pq}(a) \int d^2A_f d^2A_i \; \Psi_{mn}^*(A_f) \left\langle A_f, t_f | A_i, t_i \right\rangle_J \Psi_{pq}(A_i) \\ &= \sum_{mnpq} \psi_{mn}^*(b)\psi_{pq}(a) G^J_{mn\leftarrow pq}(t_f, t_i). \end{aligned}$$

The integral in Eq. (3.44), on the other hand, yields

$$\begin{aligned} F(b,a)_J = \gamma G_{00}^J e^{-\frac{\omega_\alpha}{4}\left(|b|^2+|a|^2\right)} \exp\left[\frac{\gamma\omega_\alpha}{4}(ba^* + b^*a)\right] \\ \times \quad \exp\left[i\gamma\sqrt{\frac{\omega_\alpha}{4}}\left(b\beta_+^* + b^*\beta_+\right)\right] \\ \times \quad \exp\left[i\sqrt{\frac{\omega_\alpha}{4}}\left(a\beta_-^* + a^*\beta_-\right)\right] \end{aligned} \tag{3.45}$$

where $\gamma = \exp(-i\omega_\alpha T)$, and

$$\begin{aligned} \beta_\pm &= \frac{1}{\sqrt{4\omega_\alpha}} \int_{t_i}^{t_f} dt \; e^{\pm i\omega_\alpha(t-t_i)} J(t) \\ \beta_\pm^* &= \frac{1}{\sqrt{4\omega_\alpha}} \int_{t_i}^{t_f} dt \; e^{\pm i\omega_\alpha(t-t_i)} J^*(t). \end{aligned} \tag{3.46}$$

From the displaced-state transition amplitude in Eq. (3.45), we can then obtain the

here and can safely extend the integral over both t and t' to the full interval between $[t_i, t_f]$. This follows because the integrand is symmetric under exchange of $t \leftrightarrow t'$. Had this not been the case, then we would have to use $t \in [t_i, t_f]$ and $t' \in [t_i, t]$, and multiply the integrand by a factor of two.

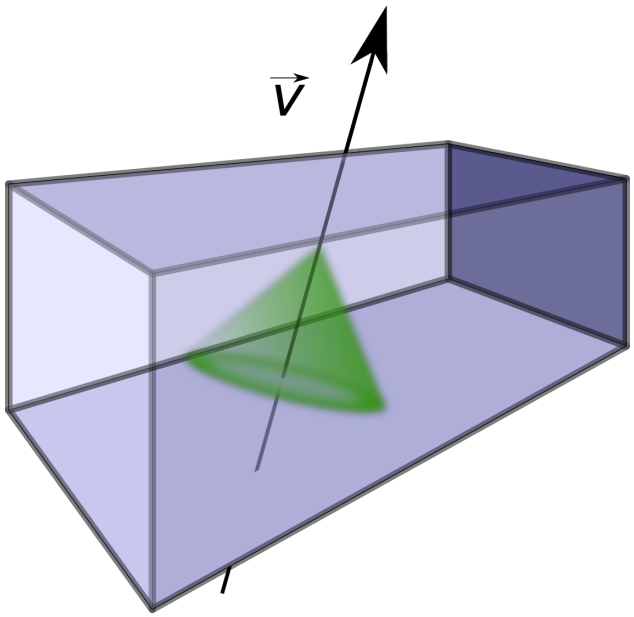

Figure 3.2: Schematic of a charge moving at a constant velocity through a medium, and the radiation excited in its wake.

number state transition amplitudes by expanding in order of γ. This yields

$$G^J_{mn\leftarrow pq}(t_f,t_i) = G^\alpha_{00}\frac{(-1)^{m+q}e^{-iE_{mn}T}}{\sqrt{m!n!p!q!}}H_{nq}(i\beta_+,-i\beta_-^*)H_{pm}(i\beta_-,-i\beta_+^*)$$

with $E_{mn} = (m+n)\omega_\alpha$, and H_{mn} being the complex Hermite polynomials given in Eq. (3.41). Thus we have found the transition amplitudes associated with all processes involving number states that are possible.

As an example, which we will also use later, we find that the probability amplitude of exciting two polaritons back-to-back from the vacuum state into mode $\mathbf{k}$ in branch α is given by

$$G^J_{11\leftarrow 00} = \left(\frac{1}{4\omega_\alpha}\right)\int dt\int dt'\ J(t)e^{i\omega_\alpha t}e^{i\omega_\alpha t'}J^*(t')e^{-\frac{1}{4\omega_\alpha}\int dt\int dt' J(t)\cos\omega_\alpha(t-t')J^*(t')}, \tag{3.47}$$

where global phases $\propto \exp(\pm i\omega_\alpha t_i)$ have been ignored.

3.4.1.1 Quantum Cherenkov Radiation

An example of a free current is that of a point charge moving through the medium. This is a physically rather artificial example, since the emission of radiation will damp the motion, but it is nonetheless instructive. Let us here work out the probability of exciting photons in its wake. A schematic of this can be seen in Fig. 3.2. This we will show to be the quantum emission of Cherenkov radiation [127], also studied recently in Ref. [128]. The interaction action of a point charge moving at a

constant velocity is

$$S_Q = \int_{t_i}^{t_f} \int d^3x\, \gamma(\mathbf{v}) Q \delta\left(\mathbf{x} - \mathbf{v}t\right) \mathbf{v} \cdot \mathbf{A}(\mathbf{x}, t),$$

where $\gamma(\mathbf{v}) = 1/\sqrt{1-v^2}$ is the usual relativistic γ-factor. This we can then expand in the polarisation modes discussed in Section 3.1, with v_λ denoting the projection of the velocity into the polarisation direction $\mathbf{e}_\lambda$. We can, as before, treat both polarisation modes independently but we will keep the λ-subscript in the following as a reference. Now, in the Fourier domain, the above action reads

$$S_Q = \frac{1}{2} \sum_{\mathbf{k}} \int \frac{d\omega}{2\pi}\, Q v_\lambda \gamma(\mathbf{v}) \mathcal{P}_{\mathbf{k}\alpha}(\omega) \mathcal{V}^{-1/2} \delta(\omega - \mathbf{v}\cdot\mathbf{k}) \left[A_{\mathbf{k}\alpha}(\omega) + A^*_{\mathbf{k}\alpha}(\omega)\right],$$

where we have projected into the polariton degree of freedom using $\mathcal{P}_{\mathbf{k}\alpha}(\omega)$. The first part of this we will interpret as the polariton projected driving force defined as

$$J_{\mathbf{k}\alpha}(t) = \frac{1}{\sqrt{\mathcal{V}}} \int \frac{d\omega}{2\pi} e^{-i\omega t}\, Q v_\lambda \gamma(\mathbf{v}) \mathcal{P}_{\mathbf{k}\alpha}(\omega) \delta(\omega - \mathbf{v}\cdot\mathbf{k}),$$

where $J_{\mathbf{k}\alpha} = J^*_{\mathbf{k}\alpha}$ since $P_{\mathbf{k}\alpha}$ is even in ω for the dispersion relations of interest here. The action now has the form of Eq. (3.32), and we can use the results obtained thus far.

Let us consider an initial state at $t_i = -T/2$ and a final state at $t_f = T/2$. Then we find that the transition amplitude of exciting two polaritons back-to-back is

$$G^{\alpha}_{11\leftarrow 00} \simeq \left(\frac{T^2}{4\omega_\alpha \mathcal{V}}\right) Q^2 v_\lambda^2 \gamma^2 \mathcal{C}_{\mathbf{k}\alpha}\, \mathrm{sinc}^2\left([\omega_\alpha - \mathbf{v}\cdot\mathbf{k}]T/2\right) e^{-\frac{Q v_\lambda^2 \gamma^2}{2\omega_\alpha \mathcal{V}} \mathcal{C}_{\mathbf{k}\alpha} \pi^2 \delta^2(\omega_\alpha - \omega_*)},$$

where $\mathrm{sinc}(x) = \sin(x)/x$, and where $\omega_*(\mathbf{k})$ is the frequency that satisfies $\omega_\alpha = \mathbf{k}\cdot\mathbf{v}$. In the exponential, we assumed that $T \gg 1/\omega_\alpha$ so that we could approximate the integration over t and t' to the interval $(-\infty, \infty)$, as this result would be the dominating contribution. The most likely emission is thus when $\omega_\alpha = \mathbf{k}\cdot\mathbf{v}$, or written in the more familiar form for Cherenkov radiation

$$v_{\mathrm{ph}} = v\cos\theta, \tag{3.48}$$

where we have defined the phase velocity $v_{\mathrm{ph}} = \omega_\alpha/k$, and θ is the emission angle (the angle between the velocity $\mathbf{v}$ and wavevector $\mathbf{k}$). The frequency of emission ω_* is set by $n^{-1}(\omega_*) = v\cos\theta$, and the probability of emission is

$$P_{11\leftarrow 00} = \mathcal{C}^2_{\mathbf{k}_*\alpha} \left(\frac{T^4}{16\mathcal{V}^2 k_*^2 v^2 \cos^2\theta}\right) Q^4 v_\lambda^4 \gamma^4 e^{-\frac{T^2}{\omega_\alpha \mathcal{V}}\left[\mathcal{C}_{\mathbf{k}\alpha}\pi^2 Q v_\lambda^2 \gamma^2\right]},$$

where $\delta(0) = T$ is the total time the charge is in the medium, $\mathcal{V}$ can be interpreted as the total volume of the medium, and $\cos\theta$ is determined by Eq. (3.48). Here

k_* is the wavenumber such that Eq. (3.48) is satisfied. Lastly, with our choice of polarisation vectors $\lambda = \{1, 2\}$, then $v_1 = v \sin\theta \cos\phi$ and $v_2 = v \sin\theta \sin\phi$.

3.4.2 Time-dependent media

Albeit the radiation produced by moving free charges is interesting in its own right, our main interest is in the radiation produced by time-dependent changes to the properties of optical media. Let us thus re-introduce the space- and time-dependent oscillator frequency discussed in Section 3.1. Specifically, we will here treat small changes to the resonance frequency such that

$$\Omega_i^2(\mathbf{x}, t) \equiv \Omega_i^2 \left[1 + f_i(\mathbf{x}, t)\right] \tag{3.49}$$

where $|f_i| \ll 1$ for all time. Now, we can use the results from the direct driving discussed in Section 3.4.1. In essence, the small changes to the oscillator frequency will act as sources in some sense.

Let us start with perturbatively constructing the propagator for the oscillators. If we return to Eq. (3.17) and substitute in Eq. (3.49), we find

$$\left[\partial_t^2 + \Omega_i^2 \left\{1 + f_i(\mathbf{x}, t)\right\}\right] \Delta_i(\mathbf{x}, t, t') = -\delta(t - t'). \tag{3.50}$$

This we can solve perturbatively, by assuming that the perturbative propagators contribute at appropriate orders of $|f_i|$, such that

$$\Delta_i(\mathbf{x}, t, t') = \Delta_i^0(\mathbf{x}, t, t') + \Delta_i^1(\mathbf{x}, t, t') + \Delta_i^2(\mathbf{x}, t, t') + \mathcal{O}(|f_i|^3),$$

where we truncate at 2^{nd} order as it to contains sufficient complexity. Let us now transform Eq. (3.50) into frequency space,[10] from which we can obtain

$$\begin{aligned}
\Delta_i^0(\mathbf{x}, \omega, \omega') &= \frac{2\pi\delta(\omega + \omega')}{\omega^2 - \Omega_i^2} \\
\Delta_i^1(\mathbf{x}, \omega, \omega') &= \Omega_i^2 \frac{\tilde{f}_i(\mathbf{x}, \omega + \omega')}{(\omega^2 - \Omega_i^2)\,(\omega'^2 - \Omega_i^2)} \\
\Delta_i^2(\mathbf{x}, \omega, \omega') &= \Omega_i^4 \int \frac{d\omega''}{2\pi} \frac{\tilde{f}_i(\mathbf{x}, \omega'')}{[(\omega - \omega'')^2 - \Omega_i^2]} \frac{\tilde{f}_i(\mathbf{x}, \omega + \omega' - \omega'')}{[\omega^2 - \Omega_i^2]\,[\omega'^2 - \Omega_i^2]},
\end{aligned} \tag{3.51}$$

where we denote the Fourier transform of f_i as $\tilde{f}_i$, specifically such that

$$\tilde{f}_i(\mathbf{x}, \omega) = \int \frac{d\omega}{2\pi} e^{-i\omega t} f(\mathbf{x}, t).$$

Here we can note a few things. To 0^{th} order in $|f_i|$, we obtain the usual propagator for

[10] These are exact when $T \to \infty$, but generally useful when $T \gg 1/\omega_\alpha$, as the Fourier transform is generally between t_i and t_f.

the oscillator, which will be taken into account through the polariton transformation of Eq. (3.30). Also, since $\tilde{f}$ is not a δ-function, we cannot do a similar trick to take these extra parts of the propagator into account. Rather, the second and third line of Eq. (3.51) will show up as temporally nonlocal potentials, which we will treat perturbatively. This is simply because $\omega' \neq -\omega$ in these terms, which would be required for the action to be diagonal in the frequency domain. For the rest of this section, it will be useful to denote the characteristic amplitude of $|f_i|$ as ϵ_i, which is defined such that

$$f_i(\mathbf{x}, t) = \epsilon_i \mathfrak{f}_i(\mathbf{x}, t),$$

for some function $\mathfrak{f}_i(\mathbf{x}, t)$ with unit maximum amplitude. Finally, it is useful to note that the refractive index perturbation is to first order given by

$$\begin{aligned} n(\omega, \epsilon) &= \sqrt{1 - \sum_i \frac{g_i^2}{\omega^2 - \Omega_i^2(1+\epsilon_i)}} \\ &\simeq n(\omega) + \delta n(\omega) \end{aligned} \tag{3.52}$$

where we have defined

$$\delta n(\omega) = \sum_i \delta n_i(\omega) = -\frac{1}{2n(\omega)} \sum_i \frac{g_i^2 \Omega_i^2}{\left(\omega^2 - \Omega_i^2\right)^2} \epsilon_i. \tag{3.53}$$

Let us now proceed with some care, and return to the action before any transformation into polariton field coordinates, that is, Eq. (3.26). If we now substitute the oscillator propagator that we found perturbatively in Eq. (3.51) into this action, we find

$$\begin{aligned} S_{\text{eff}} =& \frac{1}{2} \sum_{\mathbf{k}} \int \frac{d\omega}{2\pi}\, A_{\mathbf{k}}(\omega) D(\mathbf{k}, \omega) A^*_{\mathbf{k}}(\omega) \\ &- \frac{1}{2} \sum_{\mathbf{k},\mathbf{k}'} \int \frac{d\omega}{2\pi} \frac{d\omega'}{2\pi}\, A_{\mathbf{k}}(\omega) \sigma_{\mathbf{k}'-\mathbf{k}}(-\omega, \omega') A^*_{\mathbf{k}'}(\omega'), \end{aligned}$$

At this point, we have defined the auxiliary propagator

$$\sigma_{\mathbf{k}}(\omega, \omega') = \frac{1}{\mathcal{V}} \sum_i g_i^2\, \omega\omega' \left[\Delta_i^1(\mathbf{k}, \omega, \omega') + \Delta_i^2(\mathbf{k}, \omega, \omega')\right], \tag{3.54}$$

out of the perturbative parts of the propagator in Eq. (3.51). We can now proceed as before and apply the polariton transformation from Eq. (3.30). From this we find

$$\begin{aligned} S_{\text{eff}} =& \int_{t_i}^{t_f} dt\, \frac{1}{2} \left(|\dot{A}_{\mathbf{k}\alpha}(t)|^2 - \omega_\alpha^2 |A_{\mathbf{k}\alpha}(t)|^2 \right) \\ &- \frac{1}{2} \sum_{\mathbf{k}'\alpha'} \int_{t_i}^{t_f} dt \int_{t_i}^{t_f} dt'\, A_{\mathbf{k}\alpha}(t) \sigma^{\alpha\alpha'}_{\mathbf{k}\mathbf{k}'}(t, t') A^*_{\mathbf{k}'\alpha'}(t'), \end{aligned} \tag{3.55}$$

after some simple algebra. Note that we sum over auxiliary momenta $\mathbf{k}'$ and polariton branches α'. In addition to this, we have also defined the polariton projected auxiliary propagator $\sigma^{\alpha\alpha'}_{\mathbf{k}\mathbf{k}'}(t,t')$ through

$$\sigma^{\alpha\alpha'}_{\mathbf{k}\mathbf{k}'}(t,t') = \int \frac{d\omega}{2\pi}\frac{d\omega'}{2\pi} e^{-i\omega t} e^{-i\omega' t'} \mathcal{P}_{\mathbf{k}\alpha}(\omega)\sigma_{\mathbf{k}'-\mathbf{k}}(\omega,\omega')\mathcal{P}_{\mathbf{k}'\alpha'}(\omega'), \tag{3.56}$$

where $\mathcal{P}_{\mathbf{k}\alpha}(\omega)$ is given in the polariton projection defined in Eq. (3.30). As expected, we find a complex harmonic oscillator that is perturbed by a *delayed response* harmonic potential of the form

$$V\left(A(t), A^*(t')\right) = \sum_{\mathbf{k}'\alpha'} A_{\mathbf{k}\alpha}(t)\sigma^{\alpha\alpha'}_{\mathbf{k},\mathbf{k}'}(t,t')A^*_{\mathbf{k}'\alpha'}(t'). \tag{3.57}$$

This potential enables transitions between polaritons with momentum $\mathbf{k}$ and branch α and those with momentum $\mathbf{k}'$ in branch α'.

As discussed, we will treat this temporally nonlocal potential of Eq. (3.57) in a perturbative manner. Following the prescription from Section 2.1.5 of Chapter 2, we can compute the probability amplitude of transitions from a (p,q)-state to a (m,n)-state as induced by this potential. This involves computing

$$G^V_{mn\leftarrow pq} = \exp\left(-\frac{i}{2}\sum_{\mathbf{k}'\alpha'}\int_{t_i}^{t_f} dt \int_{t_i}^{t_f} dt'\ \sigma^{\alpha\alpha'}_{\mathbf{k},\mathbf{k}'}(t,t')\frac{\delta}{i\delta J^*_{\mathbf{k}\alpha}(t)}\frac{\delta}{i\delta J_{\mathbf{k}'\alpha'}(t')}\right) G^J_{mn\leftarrow pq}\Big|_{J=0}. \tag{3.58}$$

As can be seen, the radiation emitted from time-dependent changes to the medium separates into two sectors. The emitted polaritons can either be excited into the same polariton branch, or into two different ones. Whilst the mathematics is fairly similar, we will discuss each separately, both for clarity and because the physics is somewhat different. We will refer to these as intrabranch and interbranch vacuum radiation respectively, depending on whether it involves the same branch (intra-) or two different (inter-) branches. In either case, we will focus on the probability amplitude of starting from the vacuum state at time $t_i = -\infty$, and finding two polaritons emitted back-to-back at time $t_f = \infty$, as is illustrated in Fig. 3.3. Put differently, we will focus on quantum vacuum radiation.[11]

3.4.2.1 Intrabranch vacuum radiation

Suppose now that $\alpha' = \alpha$ in the perturbative transition amplitude in Eq. (3.58). We want to study the probability amplitude of emitting two polaritons back-to-back,

[11] Specifically, quantum vacuum radiation of the parametric excitation kind.

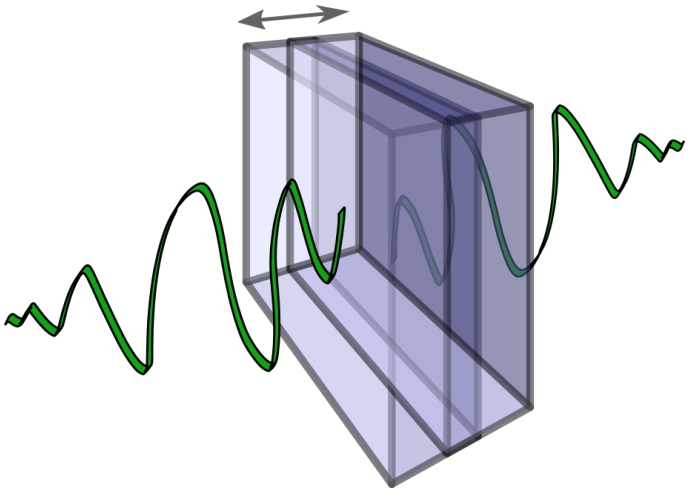

Figure 3.3: Schematic representation of two polaritons generated back-to-back from the time-modulation of an optical medium. Instantaneous refractive index is represented by the size of the box.

and so the appropriate driven transition amplitude is

$$G^{J}_{11\leftarrow 00} = \left(\frac{1}{4\omega_\alpha}\right)\int dt \int dt'\; J(t)e^{i\omega_\alpha t}e^{i\omega_\alpha t'}\,J^*(t')e^{-\frac{1}{4\omega_\alpha}\int dt\int dt' J(t)\cos\omega_\alpha(t-t')J^*(t')}, \tag{3.59}$$

Let us now we expand the exponential in Eq. (3.58) containing the functional derivatives with respect to the current J to 2^{nd}-order, so that we are consistent with the perturbative order. This yields

$$\begin{aligned} G^{\text{intra}}_{11\leftarrow 00} = \frac{i}{8\omega_\alpha}\sigma^{\alpha\alpha}_{\mathbf{kk}}(\omega_\alpha,\omega_\alpha) - \frac{1}{64\omega_\alpha^2}\Big[&\sigma^{\alpha\alpha}_{\mathbf{kk}}(\omega_\alpha,\omega_\alpha)\sigma^{\alpha\alpha}_{\mathbf{kk}}(\omega_\alpha,-\omega_\alpha) \\ &+\; \sigma^{\alpha\alpha}_{\mathbf{kk}}(\omega_\alpha,\omega_\alpha)\sigma^{\alpha\alpha}_{\mathbf{kk}}(-\omega_\alpha,\omega_\alpha)\Big] \\ &+ \mathcal{O}(\sigma^3), \end{aligned} \tag{3.60}$$

after performing the derivatives, setting J to zero, and performing the integrals in t and t'. In this, we have ignored global phases [$\propto \exp(-i\omega_\alpha t_i)$] as they do not contribute to anything physically. If we now substitute into this the definition of the nonlocal potential in term of auxiliary propagators, as defined in Eq. (3.54), we

find

$$G^{\text{intra}}_{11\leftarrow 00} = i\mathcal{C}_{\mathbf{k}\alpha}\mathcal{V}^{-1}\sum_i \frac{g_i^2\Omega_i^2}{8\left(\omega_\alpha^2-\Omega_i^2\right)^2}\Bigg[\omega_\alpha \tilde{f}_i\left(\mathbf{0},2\omega_\alpha\right) + \int\frac{d\omega'}{2\pi}\frac{d^3k'}{(2\pi)^3}\frac{\omega_\alpha\Omega_i^2}{\left(\omega_\alpha-\omega'\right)^2-\Omega_i^2}\tilde{f}_i\left(\mathbf{k}',\omega'\right)\tilde{f}_i\left(-\mathbf{k}',2\omega_\alpha-\omega'\right)\Bigg] + \mathcal{C}_{\mathbf{k}\alpha}^2\mathcal{V}^{-2}\sum_{ij}\frac{g_i^2g_j^2\Omega_i^2\Omega_j^2}{64\left(\omega_\alpha^2-\Omega_i^2\right)^2\left(\omega_\alpha^2-\Omega_j^2\right)^2}\left[\omega_\alpha^2\tilde{f}_i\left(\mathbf{0},2\omega_\alpha\right)\tilde{f}_j\left(\mathbf{0},0\right)\right] + \mathcal{O}(f^3), \tag{3.61}$$

where we can interpret $\delta(\mathbf{0}) = \mathcal{V}$ as the volume of the medium that is temporally modulated, which is important when moving between discrete and continuous momentum modes. From this amplitude there are several items to note. First of all, since we are discussing back-to-back emission of polaritons, momentum is naturally conserved and we will sample the homogeneous part of the medium modulation ($\tilde{f}_i(\mathbf{0},\nu)$ for some frequency ν). Secondly, most types of temporal modulation have a negligible response at zero frequency, as this would involve a perturbation with no characteristic time-scale. This is certainly true for the dynamical Casimir-like emission from periodic modulation which we will consider in Section 3.5. Therefore, we can safely neglect the final term in Eq. (3.61), since it is proportional to the zero-frequency part of the modulation. Finally, we should note that there are two different mechanisms for vacuum radiation at play here. On the first line of Eq. (3.61), we see that the amplitude of vacuum radiation is directly proportional to the spectrum of the modulation. On the second line however, we find a term that depends explicitly on past events (due to the integral over auxiliary frequency ω'). Such a term allows for vacuum radiation to be emitted also outside the spectrum of the modulation, specifically by allowing mixing of drive frequencies.

3.4.2.2 Interbranch vacuum radiation

In the case of interbranch vacuum radiation, i.e. when $\alpha \neq \alpha'$ in Eq. (3.58), we consider transitions that connect two different branches. Because of the distinguishably of the polaritons (as they are at different frequencies), we should consider a slightly different driven transition amplitude. Therefore, instead of Eq. (3.47), we will use the product of the amplitude of exciting one polariton into each branch.[12]

[12]This is not an approximation, given that the unperturbed branches and spatial modes are independent.

This yields

$$G^{J}_{11\leftarrow 00} = G^{J,\alpha}_{10\leftarrow 00} G^{J,\alpha'}_{01\leftarrow 00} \tag{3.62}$$

$$\begin{aligned} &= \left(\frac{1}{4\sqrt{\omega_\alpha \omega_{\alpha'}}}\right) \int dt\ J^*_\alpha(t) e^{i\omega_\alpha t} \int dt'\ J(t') e^{i\omega_{\alpha'} t'} \\ &\quad \times\ \exp\left[-\frac{1}{4\omega_\alpha}\int dt \int dt' J_\alpha(t) \cos\omega_\alpha (t-t') J^*_\alpha(t')\right] \\ &\quad \times\ \exp\left[-\frac{1}{4\omega_{\alpha'}}\int dt \int dt' J_{\alpha'}(t) \cos\omega_{\alpha'} (t-t') J^*_{\alpha'}(t')\right], \end{aligned} \tag{3.63}$$

where we have re-introduced the subscripts for the different branches α and α' to aid clarity. As we consider back-to-back emission, this amplitude involves one $\mathbf{k}$ and one $-\mathbf{k}$ polariton. Just as for the intrabranch vacuum radiation, we can substitute this into Eq. (3.58) to find the corresponding amplitude for a modulated medium (where we now assume $\alpha \neq \alpha'$). This yields a similar amplitude of the form

$$G^{\text{inter}}_{11\leftarrow 00} = \frac{i}{8\sqrt{\omega_\alpha \omega_{\alpha'}}} \sigma^{\alpha\alpha'}_{\mathbf{kk}}(\omega_\alpha, \omega_{\alpha'}) - \frac{1}{128\sqrt{\omega^3_\alpha \omega_{\alpha'}}} \sigma^{\alpha\alpha'}_{\mathbf{kk}}(-\omega_\alpha, \omega_{\alpha'}) \sigma^{\alpha\alpha}_{\mathbf{kk}}(\omega_\alpha, \omega_\alpha). \tag{3.64}$$

For the same reason as for the intrabranch radiation, we have neglected terms that involve $\tilde{f}_i(\mathbf{0}, 0)$. If we now substitute the definition of the two-time potential in terms of auxiliary propagators, we find the transition amplitude

$$\begin{aligned} G^{\text{inter}}_{11\leftarrow 00} = i\sqrt{\mathcal{C}_{\mathbf{k}\alpha}\mathcal{C}_{\mathbf{k}\alpha'}}\mathcal{V}^{-1} \sum_i \frac{g_i^2 \Omega_i^2}{8\left(\omega_\alpha^2 - \Omega_i^2\right)\left(\omega_{\alpha'}^2 - \Omega_i^2\right)} \Bigg[&\sqrt{\omega_\alpha \omega_{\alpha'}}\, \tilde{f}_i\left(\mathbf{0}, \omega_\alpha + \omega_{\alpha'}\right) \\ + \int \frac{d\omega'}{2\pi} \frac{d^3k'}{(2\pi)^3} &\frac{\sqrt{\omega_\alpha \omega_{\alpha'}}\Omega_i^2}{\left(\omega_\alpha - \omega'\right)^2 - \Omega_i^2} \tilde{f}_i\left(\mathbf{k}', \omega'\right) \tilde{f}_i\left(-\mathbf{k}', \omega_\alpha + \omega_{\alpha'} - \omega'\right) \Bigg] \\ + \mathcal{C}_{\mathbf{k}\alpha}\mathcal{C}_{\mathbf{k}\alpha'}\mathcal{V}^{-2} \sum_{ij} &\frac{g_i^2 g_j^2 \Omega_i^2 \Omega_j^2 \sqrt{\omega_\alpha^3 \omega_{\alpha'}}}{128\left(\omega_\alpha^2 - \Omega_i^2\right)\left(\omega_{\alpha'}^2 - \Omega_i^2\right)\left(\omega_\alpha^2 - \Omega_j\right)^2} \\ &\times \left[\tilde{f}_i\left(\mathbf{0}, \omega_{\alpha'} - \omega_\alpha\right) \tilde{f}_j\left(\mathbf{0}, 2\omega_\alpha\right)\right] \\ + \mathcal{O}(f^3). \end{aligned} \tag{3.65}$$

Similarly to the intrabranch transition amplitude in Eq. (3.61), we can note that the second line opens up emission at frequencies outside the spectrum of the modulation. However, since ω_α and $\omega_{\alpha'}$ are at different frequencies, the first line of Eq (3.65) also involve a type of frequency mixing. In addition to this, we can neglect the final line, because it is unlikely that $\tilde{f}_i(\mathbf{0}, 2\omega_\alpha)$ and $\tilde{f}_i(\mathbf{0}, \omega_{\alpha'} - \omega_\alpha)$ are large simultaneously and can therefore be assumed to be negligible.

3.4.2.3 Correlators

In this framework, we can also study the correlations between the emitted polaritons, given a process. In order to do this, before we set the amount of free currents J

in the system to zero when computing the transition amplitude in Eq. (3.58), we apply an appropriate amount of further functional derivatives with respect to J. The number depends on the situation. For example, we can compute the field-field time correlator for back-to-back emission of polaritons through

$$\langle 1_{\mathbf{k}}, 1^*_{\mathbf{k}}|A_{\mathbf{k}\alpha}(t)A^*_{\mathbf{q}\alpha'}(\tau)|\Psi\rangle = \frac{\delta}{i\delta J^*_{\mathbf{k}\alpha}(t)}\frac{\delta}{i\delta J_{\mathbf{q}\alpha'}(\tau)}\left(e^{-iS_1\left[\frac{\delta}{i\delta J^*_{\mathbf{k}\alpha}},\frac{\delta}{i\delta J_{\mathbf{k}\alpha'}}\right]}G^J_{mn\leftarrow pq}(t_f,t_i)\right)_{J=0},$$

where we with $|\Psi\rangle$ denote the ground state $|0\rangle$ which has been propagated with the time-modulated version of the kernel in Eq. (3.36). In this, we have defined the S_1 as the perturbative action in the exponential of Eq. (3.58), that is

$$S_1\left[\frac{\delta}{i\delta J^*_{\mathbf{k}\alpha}},\frac{\delta}{i\delta J_{\mathbf{k}\alpha'}}\right] = \frac{1}{2}\sum_{\mathbf{k}'\alpha'}\int_{t_i}^{t_f}dt\int_{t_i}^{t_f}dt'\;\sigma^{\alpha\alpha'}_{\mathbf{k},\mathbf{k}'}(t,t')\frac{\delta}{i\delta J^*_{\mathbf{k}\alpha}(t)}\frac{\delta}{i\delta J_{\mathbf{k}'\alpha'}(t')}.$$

When considering periodic modulation, rather than studying the physics of scattering states that originate at $t_i = -\infty$ and finish at $t_f = \infty$, it is more interesting to use $t_i = -T/2$ to $t_f = T/2$ and track correlations as $T = t - \tau$ increases. A quick calculation will tell you that if you measure only at $-\infty$ and ∞ you cannot distinguish whether the two polaritons are emitted simultaneously or are separated by any integer number of the modulation period.

3.5 Quantum vacuum radiation

We are now in a position to return to the actual topic under consideration in this chapter and study quantum vacuum radiation in some detail. In other words, we will explore the physics of the probability amplitudes for exciting two polaritons back-to-back from time-dependent media, as seen in Eqns. (3.61) and (3.65). As we are interested in second order effects, let us suppose that the medium is modulated periodically in time with two frequencies ν_1 and ν_2 for some long time τ. This is captured by a modulation function

$$f_i(\mathbf{x},t) = \epsilon_i\left(\cos\nu_1 t + \cos\nu_2 t\right)e^{-t^2/2\tau^2}, \tag{3.66}$$

whose Fourier transform is given by

$$\tilde{f}_i(\mathbf{k},\omega) = \epsilon_i\tau\mathcal{V}\sqrt{\frac{\pi}{2}}\left[e^{-\frac{1}{2}\tau^2(\omega-\nu_1)^2} + e^{-\frac{1}{2}\tau^2(\omega+\nu_1)^2} + e^{-\frac{1}{2}\tau^2(\omega-\nu_2)^2} + e^{-\frac{1}{2}\tau^2(\omega+\nu_2)^2}\right]. \tag{3.67}$$

As can be seen, the spectrum of the modulation contains the four Gaussians with central frequencies $\pm\nu_{1,2}$. Now, before we substitute this into the probability amplitudes given in the previous section, let us evaluate the retarded response integral

from line two of both the intrabranch [Eq. (3.65)] and interbranch [Eq. (3.61)] sectors. This is an integral over some auxiliary frequency ω', which we will denote $I^{\alpha\alpha'}_{\text{mixing}}$. Since we have assumed that we modulate for a long time as compared to both modulation frequency and mode frequency (i.e. $\tau \gg \max[1/\omega_\alpha, 1/\nu_{1,2}]$), it is straightforward to evaluate this integral for the modulation in Eq. (3.67). If we further assume that the width of each peak is roughly $1/\tau$, such that $d\omega'/(2\pi) \simeq 1/\tau$, then we find

$$\begin{aligned} I^{\alpha\alpha'}_{\text{mixing}} &= \int \frac{d\omega'}{2\pi}\frac{d^3k'}{(2\pi)^3}\frac{\Omega_i^2}{\left(\omega_\alpha-\omega'\right)^2-\Omega_i^2}\sqrt{\omega_\alpha\omega_{\alpha'}}\,\tilde{f}_i\left(\mathbf{k}',\omega'\right)\tilde{f}_i\left(-\mathbf{k}',\omega_\alpha+\omega_{\alpha'}-\omega'\right) \\ &\simeq \frac{\pi}{2}\epsilon_i^2\mathcal{V}\left(\sqrt{\omega_\alpha\omega_{\alpha'}}\tau\right)\sum_{ab}\frac{\Omega_i^2}{\left(\omega_\alpha-\nu_a\right)^2-\Omega_i^2}e^{-\frac{1}{2}\tau^2\left(\omega_\alpha+\omega_{\alpha'}-\nu_a-\nu_b\right)^2}, \end{aligned} \tag{3.68}$$

where the indices a, b denote each frequency possible in the set $\{\pm\nu_1, \pm\nu_2\}$. As is evident, this integral implies that vacuum radiation can be emitted at a plethora of mixed frequencies, involving both a mixing of branches and a mixing of drive frequencies.

For the sake of simplicity, suppose now that we modulate only the q^{th}-resonance of the medium ($\epsilon_i = \epsilon\delta_{iq}$). Furthermore, we can tidy up notation if we recall Eq. (3.53), which relates the change in the refractive index δn to the amplitude of the modulation ϵ. In this case, Eq. (3.53) reduces to

$$\delta n(\omega) = -\frac{1}{2n(\omega)}\frac{g_q^2\Omega_q^2}{\left(\omega^2-\Omega_q^2\right)^2}\epsilon_q. \tag{3.69}$$

Whilst working with δn is physically intuitative, it is more convenient to consider changes to the permittivity $\varepsilon = n^2$. We will denote this $\delta\varepsilon$, and we can relate the change in the refractive index δn to the change in permittivity $\delta\varepsilon$ through

$$\delta\varepsilon(\omega) = -2n(\omega)\delta n(\omega).$$

In our case, this reduces to

$$\delta\varepsilon(\omega) = \sum_i \frac{g_i^2\Omega_i^2}{\left(\omega^2-\Omega_i^2\right)^2}\epsilon_i = \frac{g_q^2\Omega_q^2}{\left(\omega^2-\Omega_q^2\right)^2}\epsilon. \tag{3.70}$$

Let us substitute all of this into the intrabranch transition amplitude of Eq. (3.61). After some algebra, we find

$$\begin{aligned} G^{\text{intra}}_{11\leftarrow 00} = i\sqrt{\frac{\pi}{128}}\mathcal{C}_{\mathbf{k}\alpha}\delta\varepsilon_{\omega_\alpha}\omega_\alpha\tau\sum_a\Bigg[&e^{-\frac{\tau^2}{2}\left(2\omega_\alpha-\nu_a\right)^2} \\ &+\sqrt{\frac{\pi}{2}}\sum_b\delta\varepsilon_{\omega_\alpha}\frac{\left(\omega_\alpha^2-\Omega_q^2\right)^2}{g_q^2\left(\left(\omega_\alpha-\nu_a\right)^2-\Omega_q^2\right)}e^{-\frac{\tau^2}{2}\left(2\omega_\alpha-\nu_a-\nu_b\right)^2}\Bigg], \end{aligned} \tag{3.71}$$

where we have used the notation $\delta\varepsilon_{\omega_\alpha} = \delta\varepsilon(\omega_\alpha)$. In the same manner, we also find that the interbranch transition amplitude yields

$$G^{\text{inter}}_{11\leftarrow 00} = i\sqrt{\frac{\pi}{128}}\sqrt{\mathcal{C}_{\mathbf{k}\alpha}\mathcal{C}_{\mathbf{k}\alpha'}}\sqrt{\delta\varepsilon_{\omega_\alpha}\delta\varepsilon_{\omega_{\alpha'}}}\sqrt{\omega_\alpha\omega_{\alpha'}}\tau\sum_a\Bigg[e^{-\frac{\tau^2}{2}(\omega_\alpha+\omega_{\alpha'}-\nu_a)^2} + \sqrt{\frac{\pi}{2}}\sum_b\sqrt{\delta\varepsilon_{\omega_\alpha}\delta\varepsilon_{\omega_{\alpha'}}}\frac{\left(\omega_\alpha^2-\Omega_q^2\right)\left(\omega_{\alpha'}^2-\Omega_q^2\right)}{g_q^2\left(\left(\omega_\alpha-\nu_a\right)^2-\Omega_q^2\right)}e^{-\frac{\tau^2}{2}(\omega_\alpha+\omega_{\alpha'}-\nu_a-\nu_b)^2} - i\sqrt{\frac{\pi}{512}}\sum_b\mathcal{C}_{\mathbf{k}\alpha}\delta\varepsilon_{\omega_\alpha}\omega_\alpha\tau e^{-\frac{\tau^2}{2}(\omega_{\alpha'}-\omega_\alpha-\nu_a)^2}e^{-\frac{\tau^2}{2}(2\omega_\alpha-\nu_b)^2}\Bigg]. \quad (3.72)$$

Note that in most cases the interbranch transitions are suppressed, as they require that $\mathcal{C}_{\mathbf{k}\alpha}\mathcal{C}_{\mathbf{k}\alpha'} \not\simeq 0$. Physically, this implies that both the α and the α' branch must be photon-like simultaneously, which is unlikely to occur away from a resonance Ω_i. However, this model should not be used close to any of the resonances, because we, by assumption, neglect absorption. The transitions given by Eq. (3.72) are nonetheless non-zero also away from a resonance, which is the reason for their inclusion. They are nevertheless greatly suppressed (since $\mathcal{C}_{\mathbf{k}\alpha}\mathcal{C}_{\mathbf{k}\alpha'}$ is still very small), and we can safely neglect the last two lines of Eq. (3.72) as they then furthermore contribute at the next order of perturbation theory.

Let us now specify the medium as fused silica. This has the branches seen in Fig. 3.1(a) and the coefficients $\mathcal{C}_{\mathbf{k}\alpha}$ seen in Fig. 3.1(b) [p. 46]. Furthermore, as we are mostly interested in the optical regime, suppose we modulate the first ultraviolet resonance, which we will label as Ω_2 (i.e. $q = 2$ in the above). We choose $\nu_1 = \Omega_2/5$ and $\nu_2 = \Omega_2/6$, and suppose that the amplitude of the modulation ϵ is such that $\delta n \simeq 10^{-3}$. This is small, but is a common value of δn for fused silica [107]. Thus, using the above expressions of Eqns. (3.71) and (3.72), we can now calculate the total excitation probability, given by $\left|G^{\text{intra}}_{11\leftarrow 00} + G^{\text{inter}}_{11\leftarrow 00}\right|^2$, as a function of the momentum $\mathbf{k}$, which we will refer to as the excitation spectrum. For the parameters chosen as above, this spectrum can be seen in Fig. 3.4(a), where transparent and solid shading denotes intra- and interbranch processes respectively. In Fig. 3.4(b), we can see the polariton branches into which there is a non-zero probability of emitting quantum vacuum radiation. Also in this we have labelled the modulation terms that are relevant for each process.

We can draw a couple of conclusions from the spectrum in Fig. 3.4. First of all, the temporal modulation of the medium provides energy to the system in packets proportional to $\nu_{1,2}$, and any vacuum radiation emitted will be emitted into branches that are at a similar energy scale. In this case it is the ω_1 and ω_2 polariton branches. Now, the temporal modulation bridges the gap between a polariton branch and some antipolariton branch (which is at negative energy), and thus we see vacuum radiation at points when the modulation energy matches $2\omega_2$ (intrabranch) or $\omega_2 + \omega_1$ (interbranch). Vacuum radiation that connects polariton branch

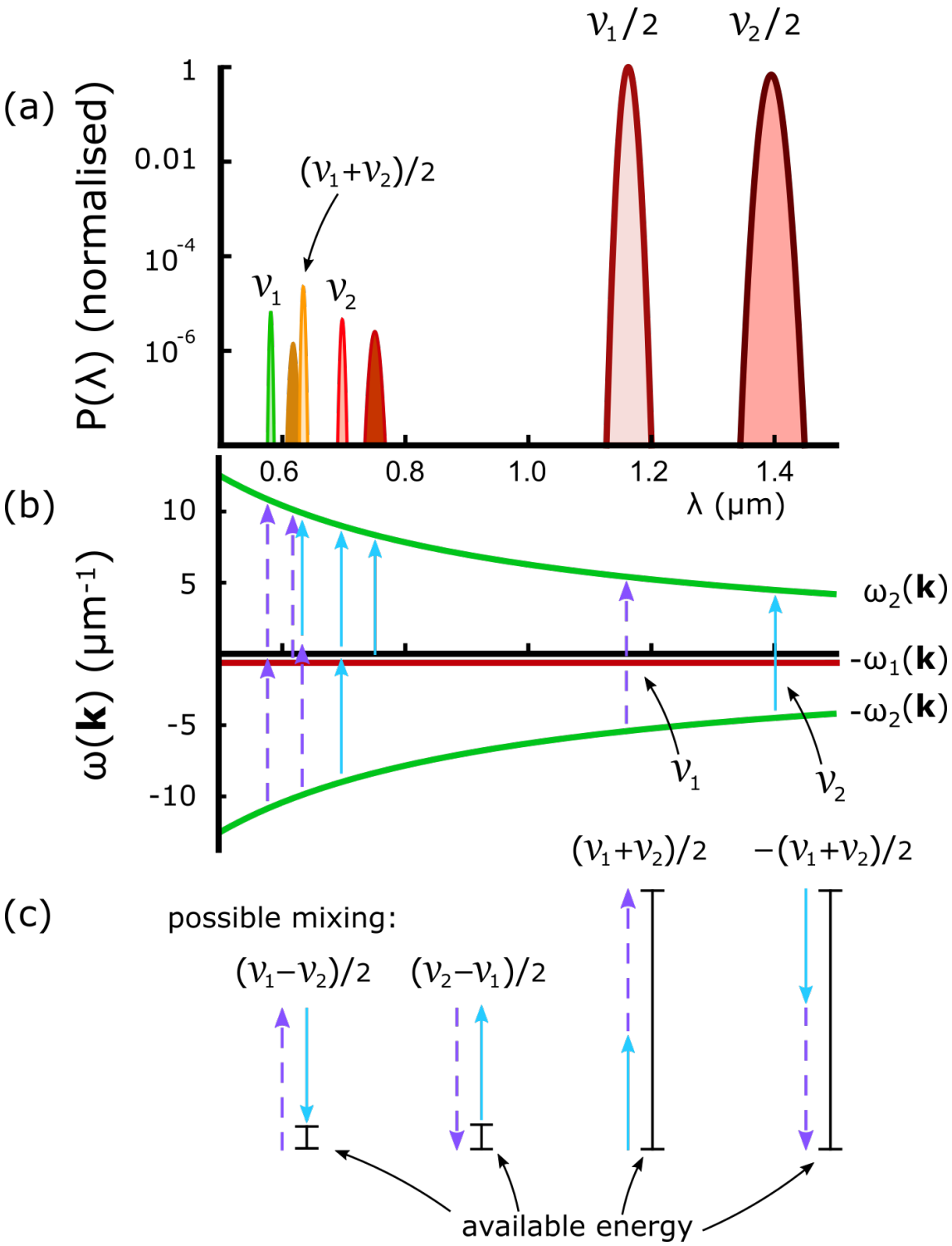

Figure 3.4: **(a)** Probability of emitting quantum vacuum radiation as a function of vacuum wavelength, in the form of two back-to-back polaritons by a time-modulation of the Ω_2-resonance of fused silica. This has been normalised to the maximum probability 4.4×10^{-6}. Shaded (solid) filling denotes the intrabranch (interbranch) processes. Parameters were chosen such that $\delta n \simeq 10^{-3}$, modulated at frequencies $\nu_1 = \Omega_2/5$ and $\nu_2 = \Omega_2/6$ for $\tau \simeq 42$ fs (100 fs full width at half maximum). These numbers where chosen for illustrative purposes, although 100 fs is a common full width at half maximum in experiments. **(b)** The polariton branches involved as function of vacuum wavelength. Temporal modulation connects a polariton (positive frequency) branch and an antipolariton (negative frequency) branch, represented as coloured arrows. **(c)** Possible mixing of drive frequencies.

to polariton branch, such that the difference in energy is $\omega_2 - \omega_1$ requires breaking the symmetry of the light-matter coupling, as discussed in Ref. [129]. Nonetheless, allowing for transitions between different branches opens up for the possibility of frequency-mixed vacuum radiation, in this case a mixing of system frequencies. It is however, worth noting that the polaritons will oscillate at the same frequency as they exit the medium,[13] given by the inverse of their vacuum wavelength. Hence any experimentally measured spectrum will appear as seen in Fig. 3.4(a).

Let us discuss each process separately, starting with the intrabranch resonances. We can see the expected emission at frequencies $\omega_2 = \nu_{1,2}/2$ originating from the two polaritons emitted at the same frequency, when we modulate at the frequency $\nu_{1,2}$. However, we also see emission of two polaritons when $\omega_2 = \nu_{1,2}$, and a mixing of the drive frequencies in the case of $\omega_2 = (\nu_1 + \nu_2)/2$. There is also a difference frequency peak at $\omega_2 = |\nu_1 - \nu_2|/2$, but we will ignore it here since this is in the far infrared. Moving on to the interbranch resonances, we see that two polaritons emitted from the vacuum state, this time at two different frequencies, when $\omega_2 + \omega_1 = \nu_1$ and $\omega_2 + \omega_1 = \nu_2$, which we have chosen to denote by solid shading with yellow and red solid line, respectively, in Fig. 3.4.

All this shares many characteristics with nonlinear processes, a field in which sum and difference frequency generation is well-studied [53, 107]. In this study however, we have explicitly assumed that the system is linear. We can nonetheless find a close connection of these phenomena to the physics of classical parametric oscillators, that is oscillators that are driven in the form

$$\ddot{x}(t) + \left[\Omega^2 + \delta \cos \nu\right] x(t) = 0. \tag{3.73}$$

A single parametric oscillator will increase in amplitude if you modulate at twice the natural oscillator frequency, i.e. when $\Omega = \nu/2$ in Eq. (3.73). This is usually referred to as a *primary* resonance in literature [40]. Less known but nonetheless present is the case that such a system also has resonances when $\Omega = n\nu/2$ for $n \in \mathbb{N}$, referred to as *sub-harmonic*, which are significantly weaker. In addition to this, coupled parametric oscillators have further resonances that combine multiple modes of oscillation, which are called *combination* resonances [41, 42, 129]. As we have modelled changes to the refractive index as shifts to the resonance frequency of a harmonic oscillator, it hardly comes as a surprise that we find these resonances also for the quantum vacuum radiation. As such the quantum vacuum radiation observed here at $2\omega_2 = \nu_{1,2}$ and $\omega_2 = \nu_{1,2}$ is simply the quantum version of the above primary and first sub-harmonic parametric resonance respectively, whereas the radiation at $\omega_2 + \omega_1 = \nu_{1,2}$ is an example of a combination resonance.

Nevertheless, this does not adequately explain the resonances of the form $\omega_\alpha + \omega_{\alpha'} = |\nu_1 \pm \nu_2|$. These resonances, of which only $2\omega_\alpha = \nu_1 + \nu_2$ is visible in the

[13] Exiting the medium is a classical process, and it doesn't concern us here.

spectrum in Fig. 3.4, are of a different type. Not only do they mix the driving frequencies, but in doing so they also allow for emission outside the support of the spectrum of the modulation.[14] This is related to the 'superoscillations' discussed in Ref. [130]. The origin in this case is nonetheless familiar. When we study the drive $f \propto \cos\nu_1 t + \cos\nu_2 t$ we notice a beating between the waves, specifically at frequencies $|\nu_1 \pm \nu_2|/2$. It is from this beating pattern that the vacuum state absorbs energy. This is a virtual two-stage process in which a quanta of energy from the first modulation wave is absorbed into the system (say ν_1). The second modulation wave then either contributes with another quanta (ν_2) or an antiquanta ($-\nu_2$). The total energy ($|\nu_1 \pm \nu_2|$) is then emitted into some polariton branch. This requires the system to store energy for some time, which correlates well with the fact that the origin of these peaks in the vacuum radiation spectrum is the temporally nonlocal integral of Eq. (3.68). As such, this effect requires the retarded response of the medium.

3.6 Regularisation and probabilities

The issue of regularisation has been left untreated so far. As this is a field theory, we would expect the need to regularise. Indeed, the propagator in Eq. (3.36) is formally divergent (as is well-known [115]). However, we avoid regularisation by directly computing observables, i.e., the transition probabilities. For a transition probability, or amplitude, we measure only the difference in occupation between two states, and we need not worry about the actual occupation of each (which would be infinite for the ground state and zero for any excited state).

Also, we should note that the probabilities calculated in the previous section are indeed probabilities and not probability densities. For instance in Section 3.4, we calculate the probability for the vacuum state to transition into a 2-polariton state in spatial mode $\mathbf{k}$ in branch α. The total probability density for the process is found by summing over all modes $\mathbf{k}$ and branches α and dividing by the volume (as is commonly done, see for instance Ref. [37]),

$$\frac{dP}{d\mathcal{V}} = \frac{1}{\mathcal{V}} \sum_{\mathbf{p}\alpha'} P_{\mathbf{p}\alpha'} = \sum_{\alpha'} \int \frac{d^3p}{(2\pi)^3} |G^{\mathbf{p}\alpha'}_{11\leftarrow 00}|^2,$$

with the last step being exact for continuum states only. As discussed in Section 2.2.4, we can transition between continuum and discrete states, given that we are consistent in the treatment of each.

[14] The support of the spectrum is the frequency ranges of the spectrum that are non-zero.

3.7 Conclusions from a perturbative setting

In this chapter, we focused on quantum vacuum radiation emitted due to small time-dependent variations to the properties of optical media. In this, we had bulk media or simple structured media such as fibres in mind,[15] and used fused silica as an example. In particular, we studied the effect of changing the resonance frequencies in time, and examined how the time-delayed response of the medium affected the spectrum of emitted photons. We found that two frequency mixing mechanisms emerge in the system, both of which are of linear origin. The spectrum of quantum vacuum radiation nonetheless takes on a 'nonlinear' character, with photons emitted from the vacuum state due to both sum and difference frequency processes.

In particular, the photons are emitted when the sum of two polariton branch frequencies equal a combination of modulation frequencies. Since we focused on a medium whose resonance is modulated at two frequencies, ν_1 and ν_2, we found that polaritons are emitted when

$$\begin{aligned}
\omega_\alpha + \omega_{\alpha'} &= \nu_{1,2}, \\
\omega_\alpha + \omega_{\alpha'} &= 2\nu_{1,2}, \\
\omega_\alpha + \omega_{\alpha'} &= \nu_1 \pm \nu_2, \\
\omega_\alpha + \omega_{\alpha'} &= \nu_2 \pm \nu_1,
\end{aligned} \tag{3.74}$$

where α and α' can denote the same branch, or two different branches. This encompasses the expected emission at frequencies $\nu_1/2$ and $\nu_2/2$, as well as emission at $|\nu_1 \pm \nu_2|/2$. The latter is the aforementioned sum and difference frequency emission. The system is at all times linear however, not nonlinear. We found that mixing of frequencies can still occur in a linear system by two different mechanisms, involving either *energy emission* or *energy absorption*. Note that here we refer to a different kind of absorption than the one related to dissipation. Rather, in this context 'absorption' refers to the systems ability to gather energy.

Let us first consider the mixing process associated with emission. This is quantum vacuum radiation that involves two different branches, i.e. when $\alpha \neq \alpha'$ in Eq. (3.74). The physics behind this relates to the nature of coupled systems, which has multiple modes of oscillation, here the polariton branches. For instance, in the simple case of a medium with only one resonance Ω, there are two mode frequencies given by

$$\omega_\pm = \left| \sqrt{\frac{1}{2}\left((k^2 + \Omega^2 + g^2) \pm \sqrt{(k^2 + \Omega^2 + g^2)^2 - 4k^2\Omega^2} \right)} \right|. \tag{3.75}$$

[15] In particular, media where the bulk excitations can be treated independently, with some spatial degree of freedom fixed by the structure.

At a quantum level, it follows that excitations of the system (of which the quantum vacuum radiation is an example) will consist of some superposition of ω_+–polaritons and ω_-–polaritons. In fused silica there are four branches whose algebraic form is much more complicated (depicted in Fig. 3.1) but the physics is nonetheless the same. Hence, as it is in general possible to create an excitation that consists of a superposition of two different polariton branches, it follows that quantum vacuum radiation will also mix the branches. Notwithstanding, the likelihood for the excitation of polaritons in the same branch is higher, because the modulation couples more strongly to 'photon-like' branches and throughout most of the spectrum only one branch is 'photon-like' at any one time.

Now, quantum vacuum radiation that contains the sum and difference of drive frequencies however, i.e. the terms in Eq. (3.74) that involve $|\nu_1 \pm \nu_2|$, has its origin not in the emission process (where two polaritons are emitted) but in the absorption process. This is a consequence of the time-delayed response of the medium to variations in its resonance frequencies. It requires the optical medium to absorb energy in a two-step process, allowing it to be driven by the beating pattern of the drive. The modulation which we used here $[f(t) \propto \cos\nu_1 t + \cos\nu_2 t]$ beats at the frequencies $|\nu_1 \pm \nu_2|/2$, frequencies which are absent from its spectrum $\widetilde{f}(\omega)$. In order for this to be absorbed, the medium first absorbs one (anti)quanta of energy $(-)\nu_1$, which is stored until a second (anti)quanta of energy $(-)\nu_2$ is absorbed. The energy stored, $|\nu_1 \pm \nu_2|$, is then emitted in terms of polaritons, and energy conservation demands that $\omega_\alpha + \omega_{\alpha'} = |\nu_1 \pm \nu_2|$. The origin of this absorption process is the time-delayed response, as captured in the model by the mixing-integral of Eq. (3.68).

We should also note that the probabilities seen in Fig. 3.4 are low, but the number of polaritons emitted in an experimentally feasible scenario can still be significant. We can estimate this by assuming a fused silica slab of roughly 100 μm thickness, and a transverse area that is considerably larger than a pump laser spot size of A_{spot}. The number of photon pairs emitted per unit angle $d\theta$ is then

$$\begin{aligned}\frac{dP}{d\theta} &= \int_0^\infty dk\; k \left|G^{\text{intra}}_{11\leftarrow 00} + G^{\text{inter}}_{11\leftarrow 00}\right|^2 \\ &\simeq A_{\text{spot}} \left(\frac{2\pi}{\tau}\right)\left(\frac{2\pi}{\lambda_{\text{mix}}}\right)\left|G^{\text{intra}}_{11\leftarrow 00} + G^{\text{inter}}_{11\leftarrow 00}\right|^2 (\lambda_{\text{mix}}) \simeq 3\times 10^{-6}, \end{aligned} \tag{3.76}$$

where we assumed that $A_{\text{spot}} = 250\ \mu\text{m}^2$ and approximated $dk \simeq 2\pi/\tau$. We have focused on the vacuum radiation whose origin is the beating pattern in the modulation, specifically the $(\nu_1 + \nu_2)/2$-resonance seen in Fig. 3.4 whose vacuum wavelength is given by $\lambda_{\text{mix}} \simeq 0.65\ \mu$m. The polaritons excited from the vacuum state would propagate in the orthogonal direction to the pump beam (i.e. the transverse plane). This estimate is the probability of emission per pulse with a full-width-at-half-maximum of 100 fs. If we furthermore assume a repetition rate of 1 MHz we find that roughly three photon pairs per second are emitted. Given that the

polaritons can be out-coupled from the transverse plane, this is feasible to measure with current technology [131]. An important point is that these frequency-mixed polaritons are background free, and would therefore be unlikely to be affected by any filtering.

Finally, we should also mention that in this chapter we studied specifically quantum vacuum radiation originating from small changes to the resonance frequencies. This model is readily applicable to experiments in bulk media, where the resonance frequency is shifted through the quadratic Stark shift, as mentioned in Section 3.1. Indeed, in Chapter 4 we will apply the results discussed here to the the fibre experiment in Ref. [97]. Whilst the quadratic Stark shift introduces a nonlinear light-matter coupling, we expect the quantum vacuum fluctuations to be too small to impact the results discussed here. It is important to note that the results are completely general with regards to how the resonance frequency is modulated in time, and thus does not require the modulation to be nonlinear in origin. It is also related to polaritons in microcavities, such as those discussed in Refs. [84–88], although in such a scenario the light-matter coupling is modulated (the Rabi frequency) rather than the resonance frequency.

We can also gain some insight into what we might expect from an experiment such as the one described in Ref. [71], where the time-delayed response of dispersion was neglected. In the proposed experiment, building on experiments performed in Refs. [96, 132], an ε-near-zero metamaterial is illuminated by a pulse of light from a strong pump. This changes both the refractive index and the absorption rapidly in time a process akin to the quadratic Stark shift.[16] We can still expect some of the intuition gained here to apply in this situation, although we cannot apply the results directly as absorption plays an important role, and as the changes to the refractive index are non-perturbative. We will discuss this in later chapters, where we treat non-perturbrative changes to the medium properties.

[16]Note that the exact physical process is not currently known.

Chapter 4

Perturbative quantum vacuum radiation in experiments

"Theories come and go, but good measurements endure."
— "And as often it is the other way around."

Dr Kurt Hansen, random conversation, Lund, Dec. 2018
— addendum by Prof. Claudia Eberlein

Whilst it is interesting to study quantum vacuum radiation in a purely theoretical setting, it is always healthy to have a grounding in experiments. In this chapter, we will analyse the experimental situation of Item 2 from the List of Publications using the formalism built in Chapter 3. The actual experiment was primarily performed by Dr Stefano Vezzoli. We expect the theory to be readily applicable, as the experiment deals with small changes to the optical properties in a near-absorptionless optical medium. In particular, the experiment concerns an optical fibre with a modulated dispersion parameter in space. The time-dependence is then introduced by a travelling high-intensity pump pulse. It is this time-dependence that will be responsible for exciting quantum vacuum radiation, and we can link this to dynamical Casimir-like physics in the co-moving frame of the pump pulse.

4.1 The experiment, brief introduction to fibre optics and building a model

Let us start with describing the experiment in some more detail, although we should note that the finer details are not relevant. As can be seen in Fig. 4.1(a), the fibre cladding diameter is periodically stretched during fabrication. This results in effective changes to the optical parameters of the fibre in space. Specifically, we are here discussing a dispersion modulated photonic crystal fibre. However, let us first give a small introduction to fibre optics, whilst a lengthier discussion can be found in Ref. [107].

As mentioned briefly in Section 3.2.1.2 in Chapter 3, a fibre is a waveguide where the light is guided by a small spatial variation to the refractive index in

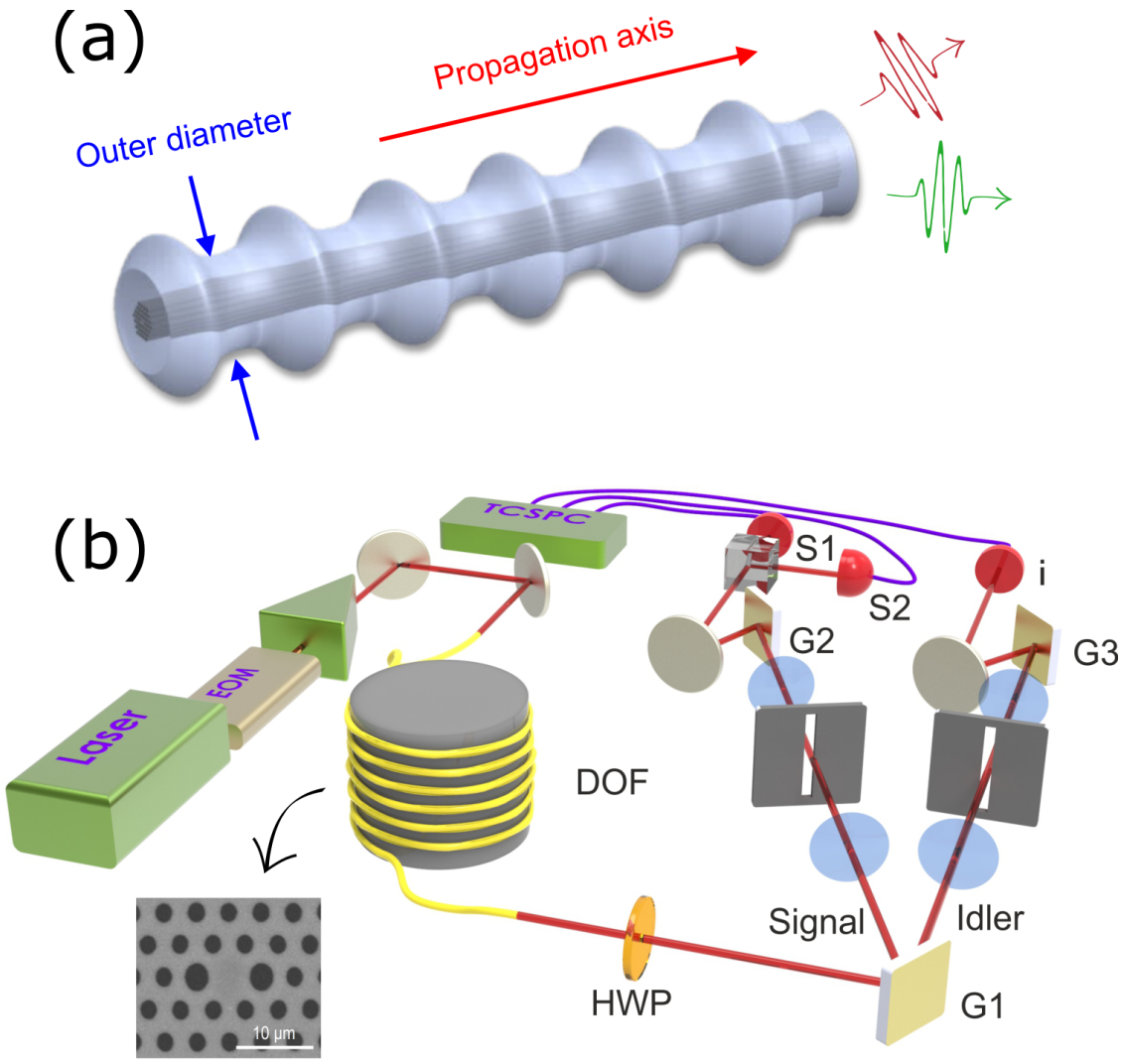

Figure 4.1: **(a)** Schematic of the fibre, where the modulation along with the travelling pump pulse leads to the emission of quantum vacuum radiation. **(b)** Experimental set-up. Here DOF is the dispersion-oscillating fibre, the transverse plane of which can be seen in the inset. HWP is a half-wave plate responsible for rotating the output polarisation, whereas G1, G2 and G3 are gratings used for filtering. Note the position of the idler detector *i*, as well as the signal detectors *S1* and *S2*. All detectors are single photon avalanche detectors (SPADs). Figure adapted from Ref. [97].

the transverse plane (with respect to the propagation direction). We can usually assume the dynamics of the transverse plane $[(x, y)]$ to be fixed, (set by the structure of the fibre, which acts like a potential), and consider only the dynamics along the propagation direction $[z]$. Therefore, it is appropriate to expand in some polarisation λ, as well as some transverse mode $F_{\mathbf{n}}(x, y)$, such that the electric field is given by

$$\mathbf{E}(\mathbf{x}, t) = \sum_{\lambda} F_{\mathbf{n}}(x, y)\mathbf{e}_{\lambda}\, E_{\lambda\mathbf{n}}(z, t). \tag{4.1}$$

Fibre optics is the study of $E_{\lambda\mathbf{n}}(z, t)$. We will however drop the subscript as we will only consider a single transverse mode at a time, along with one polarisation.

Suppose now that we have a plane wave travelling down the fibre. This would be characterised by a frequency dependent wavenumber $k_0 = k(\omega_0)$ [107] such that the electric field

$$E(z, t) \propto \exp(-i\left[\omega_0 t - k(\omega_0)z\right], \tag{4.2}$$

where we have chosen z to be the direction of the fibre. If this wave is no longer a plane wave but a Gaussian wavepacket with a central frequency ω_0, then we can characterise its propagation as

$$E(z, t) \propto \int d\omega\; e^{-i\omega t} e^{-(\omega-\omega_0)^2/2\sigma^2} \exp\left(ik(\omega)z\right)$$

where

$$\begin{aligned} k(\omega) &\simeq k_0 + \frac{\partial k}{\partial \omega}\left(\omega - \omega_0\right) + \frac{1}{2}\frac{\partial k^2}{\partial \omega^2}\left(\omega - \omega_0\right)^2 + ... \\ &\equiv k_0 + \beta_1\left(\omega - \omega_0\right) + \frac{1}{2}\beta_2\left(\omega - \omega_0\right)^2 + ... \end{aligned} \tag{4.3}$$

In fibre optics, it is customary to characterise dispersion by the dispersion parameters β_i governing the i^{th}-order dispersion. For instance β_1 relates to the group velocity, whereas β_2 characterises the change in the group velocity during propagation. Hence β_2 is called the group velocity dispersion.

The photonic crystal fibre used in this experiment is spatially varied in such a way that the group-velocity dispersion parameter β_2 becomes space-dependent, i.e. $\beta_2 \to \beta_2(z)$. In particular, as can be seen in Fig. 4.2, the modulation in the fibre takes the form

$$\begin{aligned} \beta_2(z) &\simeq \beta_2^0 + \delta_\beta \sum_{n=0}^{L/\Lambda} \exp\left[-\left(z - \Lambda n\right)^2 / 2\sigma_\beta^2\right] \\ &= \beta_2^0 + \Delta_\beta(z), \end{aligned} \tag{4.4}$$

where Λ is the period of the modulation, which in the experiment is 5 m, and where

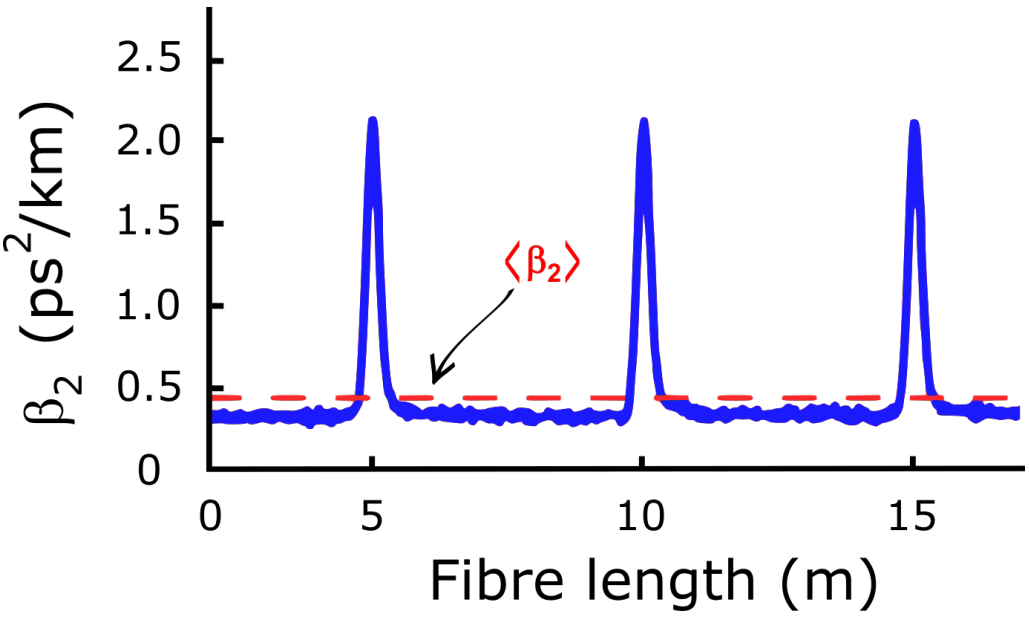

Figure 4.2: Experimental group velocity dispersion parameter β_2 as a function of distance along the fibre. Note the Gaussian-like modulation with period $\Lambda = 5$ m. Figure adapted from Ref. [97].

L is the length of the fibre. To model this in the context of Chapter 3, we can return to the dispersion relation in Eq. 3.2 in the case of a time- and space-independent optical medium. We can rewrite this as

$$\begin{aligned} k(\omega) &= \omega n(\omega) \\ &= \omega \sqrt{1 - \sum_i \frac{g_i^2}{\omega^2 - \Omega_i^2}}. \end{aligned} \tag{4.5}$$

If we expand this around some central frequency ω_0 in orders of $\omega - \omega_0$, we find

$$\begin{aligned} k(\omega) \simeq\ & n(\omega_0)\omega_0 + \left[n(\omega_0) + \omega_0 n'(\omega_0)\right](\omega - \omega_0) \\ & + \frac{1}{2}\left[2n'(\omega_0) + \omega_0 n''(\omega_0)\right](\omega - \omega_0)^2 + \ldots \end{aligned} \tag{4.6}$$

Thus we can identify

$$\begin{aligned} \beta_2 &\equiv 2n'(\omega_0) + \omega_0 n''(\omega_0) \\ &= \sum_i \frac{1}{n_0}\left[\frac{3g_i^2\omega_0}{\left(\omega_0^2 - \Omega_i^2\right)^2} - \frac{4g_i^2\omega_0^3}{\left(\omega_0^2 - \Omega_i^2\right)^3} - \sum_j \frac{g_i^2 g_j^2 \omega_0^3}{\left(\omega_0^2 - \Omega_i^2\right)^2\left(\omega_0^2 - \Omega_j^2\right)^2 n_0^2}\right], \end{aligned} \tag{4.7}$$

where we let $n_0 = n(\omega_0)$. In the context of Chapter 3, the simplest option to create a space-dependent β_2 is to introduce a space-dependent change in the resonance

frequencies $\Omega_i^2 \to \Omega_i^2 (1 + \Delta_i^z)$, such that

$$\Delta_i^z(z) = -\eta_i \sum_{n=0}^{L/\Lambda} \exp\left[-(z - \Lambda n)^2 / 2\sigma_\beta^2\right], \tag{4.8}$$

where η_i is the amplitude of the modulation and Λ is as before the periodicity. We can assume that the optical characteristics (such as resonance and plasma frequencies) are similar to fused silica, as it is the main component of the fibre [133]. Using this as a starting point, it is straightforward to obtain β_2 and β_4 as reported in Ref. [97] by slightly shifting the infrared plasma frequency of fused silica (here g_1) — this is well justified physically as the fibre is stretched during fabrication, changing in oscillator density. Importantly all the physics we are concerned with takes place close to the pump frequency of $\omega_p \simeq 2\pi c/1050$ nm, meaning that we can separate this from the physics close to the infrared resonance frequency.[1] In particular, we use the background resonance frequencies of fused silica

$$\begin{aligned} \Omega_1 &= 1.90342 \times 10^{14}\ \mathrm{s}^{-1} \\ \Omega_2 &= 1.62047 \times 10^{16}\ \mathrm{s}^{-1} \\ \Omega_3 &= 2.7537 \times 10^{16}\ \mathrm{s}^{-1}, \end{aligned} \tag{4.9}$$

as well as slightly modified plasma frequencies

$$\begin{aligned} g_1 &= \kappa\ 1.803 \times 10^{14}\ \mathrm{s}^{-1} \\ g_2 &= 1.035 \times 10^{16}\ \mathrm{s}^{-1} \\ g_3 &= 2.298 \times 10^{16}\ \mathrm{s}^{-1}, \end{aligned} \tag{4.10}$$

with $\kappa = 1.48$ is a phenomenological scale factor used to match the reported dispersion parameters at the pump frequency. Finally, we can reproduce β_2 from Fig. 4.2 by choosing $\Lambda = 5$ m and $\eta_i = 0.042\delta_{i,2}$ so that we only spatially modulate the near-visible ultaviolet resonance Ω_2. Interestingly, the change in dispersion parameters β_i for these values is in the order of $\sim 0.5 - 1\%$ *except* for the the group velocity dispersion β_2 where the relative shift is $\sim 600\%$. This is a consequence of the higher derivatives involved when calculating the group velocity dispersion. Clearly the physics as modelled here will be dominated by the physics of a modulated group velocity dispersion, as in the experiment.

In addition to the periodic modulation in space, the medium is changed in time by a strong pump pulse E_{pump}. As discussed in Chapter 3, we can understand this through the quadratic Stark shift to the resonance frequencies of the medium $\Omega_i \to \Omega_i + \alpha_{\mathrm{nonlin}} E_{\mathrm{pump}}^2$, where α_{nonlin} is the nonlinear polarisability. In particular,

[1] Note that this is naturally an approximation.

we will choose our parameters such that $\Omega_i^2 \to \Omega_i^2\,(1+\Delta_i^t)$ with

$$\Delta_i^t(z,t) = \alpha_K \left|E_{\rm pump}(z,t)\right|^2 + \alpha_P E_{\rm pump}^2(z,t), \tag{4.11}$$

where we have separated the response into the so-called Kerr response, proportional to intensity $|E_{\rm pump}|^2$, and the polarisation wave $\propto E_{\rm pump}^2$ [53]. Here α_K and α_P are the nonlinear polarisabilities for the respective effects. For a pump pulse travelling down the fibre we have

$$\begin{aligned} E_{\rm pump}^2 &= I_0 e^{-(z-v_g t)/2\tau^2}\cos\left(2\omega_p t - 2k_p z\right) \\ \left|E_{\rm pump}\right|^2 &= I_0 e^{-(z-v_g t)/2\tau^2}. \end{aligned} \tag{4.12}$$

Thus we arrive at a model for the dispersion modulated photonic crystal fibre that can be analysed in the context of Chapter 3, where in total we have a modulation to Ω_2 as

$$\begin{aligned} \Omega_2^2(z,t) &= \Omega_2^2\left[1+\Delta_2^z(z)+\Delta_2^t(z,t)\right] \\ &= \Omega_2^2\Bigg(1-\eta\sum_{n=0}^{L/\Lambda} e^{-(z-\Lambda n)^2/2\sigma_\beta^2} \\ &\qquad + \; I_0 e^{-(z-v_g t)/2\tau^2}\Big[\alpha_K+\alpha_P\cos\left(2\omega_p t-2k_p z\right)\Big]\Bigg), \end{aligned} \tag{4.13}$$

where η is the relative amplitude of the spatial modulation in Ω_2. Finally, we can define

$$f(z,t) = -\eta\left[\sum_{n=0}^{L/\Lambda} e^{-(z-\Lambda n)^2/2\sigma_\beta^2}\right] + I_0 e^{-(z-v_g t)/2\tau^2}\Big[\alpha_K+\alpha_P\cos\left(2\omega_p t-2k_p z\right)\Big], \tag{4.14}$$

to bring the notation in line with Chapter 3, in particular Eq. (3.49). Eq. (4.14) is the total space and time modulation in the Ω_2-resonance of the medium.

4.2 Modulation leads to vacuum radiation

Let us now analyse the quantum vacuum radiation emitted in the fibre from this type of mixed spatial and temporal modulation. Apart from the straightforward restriction from 3-dimensional space to 1-dimension, we can directly apply the formalism developed in Chapter 3. However, because of the spatial modulation, we can no longer assume that back-to-back emission of polaritons will be the most significant process. In fact, this is likely no longer the case. It follows that the polaritons are no longer identical even in the intrabranch vacuum radiation processes. Also,

we should note that this removes the mathematical differences between intrabranch and interbranch processes. In general, we will label the polariton pair as composed of a *signal* polariton along with an *idler* polariton of frequencies ω_s and ω_i, respectively. These polaritons are also characterised by differing wavenumbers, k_s and k_i respectively.

For notational simplicity, let us first rewrite f from Eq. (4.14) as

$$\begin{aligned} f(z,t) &= \eta\Bigg(-\left[\sum_{n=0}^{L/\Lambda} e^{-(z-\Lambda n)^2/2\sigma_\beta^2}\right] \\ &\qquad + \left[\frac{\alpha_K I_0}{\eta} + \frac{\alpha_P I_0}{\eta}\cos\left(2\omega_p t - 2k_p z\right)\right] e^{-(z-v_g t)/2\tau^2}\Bigg) \\ &= \eta\left(-\left[\sum_{n=0}^{L/\Lambda} e^{-(z-\Lambda n)^2/2\sigma_\beta^2}\right] + \left[\delta_K + \delta_P\cos\left(2\omega_p t - 2k_p z\right)\right] e^{-(z-v_g t)/2\tau^2}\right), \end{aligned} \tag{4.15}$$

as we expect η to be the dominating contribution to the shift in the resonance frequency.[2] This follows from the experimental setting in Ref. [97], because in the experiment the intensity of the pump pulse is very weak and yielding only small changes in the optical parameters as compared to the spatial dispersion variation. Only in this limit is quantum correlations observed. Here we defined the dimensionless parameters $\delta_{K,P}$ as the shifts from the Kerr effect and polarisation wave respectively.

It now follows from Chapter 3 that the probability amplitude for the emission of quantum vacuum radiation is

$$\begin{aligned} G_{11\leftarrow 00} = i\sqrt{\mathcal{C}_s\mathcal{C}_i}L^{-1}\frac{\sqrt{\delta\varepsilon_{\omega_s}\delta\varepsilon_{\omega_i}}}{8\eta}\Bigg[&\sqrt{\omega_s\omega_i}\tilde{f}(k_s-k_i,\omega_s+\omega_i) + I^{si}_{\text{mixing}} \\ &- i\sqrt{\mathcal{C}_s\mathcal{C}_i}L^{-1}\frac{\delta\varepsilon_{\omega_s}}{8\eta}\sqrt{\omega_s^3\omega_i}\tilde{f}(k_s-k_i,\omega_s+\omega_i)\tilde{f}(0,0) \\ &- i\sqrt{\mathcal{C}_s\mathcal{C}_i}L^{-1}\frac{\delta\varepsilon_{\omega_s}}{16\eta}\sqrt{\omega_s^3\omega_i}\tilde{f}(k_s-k_i,\omega_i-\omega_s)\tilde{f}(0,2\omega_s)\Bigg], \end{aligned} \tag{4.16}$$

where $\mathcal{C}_s = \mathcal{C}_{k_s\alpha}$, and where we have suppressed the index α for notational simplicity. Here we have defined the mixing integral as

$$\begin{aligned} I^{si}_{\text{mixing}} &= \int\frac{d\omega'}{2\pi}\frac{dk'}{2\pi}\frac{\Omega_2^2}{(\omega_s-\omega')^2-\Omega_2^2}\sqrt{\omega_s\omega_i}\tilde{f}\left(k_s+k',\omega'\right)\tilde{f}\left(-k_i-k',\omega_s+\omega_i-\omega'\right) \\ &= \int\frac{d\nu}{2\pi}\frac{dk'}{2\pi}\frac{\Omega_2^2}{\nu^2-\Omega_2^2}\sqrt{\omega_s\omega_i}\tilde{f}\left(k_s+k',\omega_s+\nu\right)\tilde{f}\left(-k_i-k',\omega_i-\nu\right), \end{aligned} \tag{4.17}$$

where in the second line we have defined $\nu = \omega' - \omega_s$ in order to bring the integral

[2] For a theoretical perspective, this is rather like dealing with a perturbation to the perturbation.

into a more symmetric form. Note that we evaluate $\tilde{f}$ at $k_s - k_i$ rather than the more conventional $k_s + k_i$ because we have defined the signal and idler polariton to travel at opposite directions in Chapter 3. In other words, if $k_s = k_i$ then the emission is back-to-back.[3]

To evaluate this probability amplitude we first need to compute the mixing integral I^{si}_{mixing}. And in order to do this, it is convenient to define

$$\begin{aligned}\tilde{g}_z[k,\omega] &\equiv \sqrt{2\pi}\sigma_\beta\,[2\pi\delta(\omega)]\sum_{n=0}^{L/\Lambda} e^{-\sigma_\beta^2 k^2/2 - in\Lambda k} \\ &\simeq [2\pi\delta(\omega)]\left[\sqrt{2\pi}\sigma_\beta\mathcal{K}\sum_{n=0}^{L/\Lambda}\delta\left(k-n\mathcal{K}\right)\right], \end{aligned} \tag{4.18}$$

where the last step is valid when $\sigma_\beta \ll \Lambda \ll L$.[4] This is indeed the case for the experimental scenario analysed here. Here, we defined the spatial modulation wavenumber as $\mathcal{K} = 2\pi/\Lambda$. Also, it is convenient to define

$$\tilde{g}_t[k,\omega,K,\Omega] \equiv \sqrt{2\pi}\tau e^{-\tau^2(k-K)^2/2}\left[\pi\delta\left(\omega-\Omega-v_g[k-K]\right)\right] \tag{4.19}$$

such that we find the Fourier transform of the modulation as

$$\tilde{f}(k,\omega) = \eta\Big[-\tilde{g}_z[k,\omega] + 2\delta_K\tilde{g}_t[k,\omega,0,0] + \delta_P\tilde{g}_t[k,\omega,\pm 2k_p,\pm 2\omega_p]\Big]. \tag{4.20}$$

Let us now evaluate some of the terms involved in the mixing integral. There are four terms in total, and we will call these terms T_1 to T_4, respectively. Specifically, we have terms of the form

$$\begin{aligned} T_1 &= \int \frac{d\omega'}{2\pi}\frac{dk'}{2\pi}\frac{\Omega_2^2}{\nu^2-\Omega_2^2}\sqrt{\omega_s\omega_i}\,g_z[k_s+k',\omega_s+\nu]g_z[-k_i-k',\omega_i-\nu] \\ &= \frac{\Omega_2^2}{\omega_s^2-\Omega_2^2}\sqrt{\omega_s\omega_i}\left[2\pi\sigma_\beta^2\delta\left(\omega_i+\omega_s\right)\mathcal{K}^2\sum_{n,m=0}^{L/\Lambda}\delta\left(k_i-k_s+[m-n]\mathcal{K}\right)\right] \\ &= 0, \end{aligned} \tag{4.21}$$

where the last line follows because ω_s and ω_i are both positive quantities. This is expected as it arises from purely spatial modulation. Also, we have the contributions

[3] This is a convenient definition when treating back-to-back emission, but leads to this unconventional sign here.

[4] In the experiment, $\Lambda = 5$ m whereas the fibre length $L = 80$ m.

that mix the spatial and temporal modulation

$$\begin{aligned} T_2[K,\Omega] &= \int \frac{d\omega'}{2\pi}\frac{dk'}{2\pi}\frac{\Omega_2^2}{\nu^2-\Omega_2^2}\sqrt{\omega_s\omega_i}g_z[k_s+k',\omega_s+\nu]g_t[-k_i-k',\omega_i-\nu,K,\Omega] \\ &= \frac{\Omega_2^2}{\omega_s^2-\Omega_2^2}\sqrt{\omega_s\omega_i}\Bigg[\pi\sigma_\beta\tau\mathcal{K}\sum_{n=0}^{L/\Lambda}\delta\left(\omega_s+\omega_i-\Omega-v_g\left[k_s-k_i-K-n\mathcal{K}\right]\right) \\ &\qquad\qquad \times\exp\left(-\tau^2\left(k_s-k_i-K-n\mathcal{K}\right)^2/2\right)\Bigg] \end{aligned} \tag{4.22}$$

as well as

$$\begin{aligned} T_3[K,\Omega] &= \int \frac{d\omega'}{2\pi}\frac{dk'}{2\pi}\frac{\Omega_2^2}{\nu^2-\Omega_2^2}\sqrt{\omega_s\omega_i}g_t[k_s+k',\omega_s+\nu,K,\Omega]g_z[-k_i-k',\omega_i-\nu] \\ &= \frac{\Omega_2^2}{\omega_s^2-\Omega_2^2}\sqrt{\omega_s\omega_i}\Bigg[\pi\sigma_\beta\tau\mathcal{K}\sum_{n=0}^{L/\Lambda}\delta\left(\Omega-\omega_s-\omega_i+v_g\left[k_s-k_i-K-n\mathcal{K}\right]\right) \\ &\qquad\qquad \times\exp\left(-\tau^2\left(k_s-k_i-K-n\mathcal{K}\right)^2/2\right)\Bigg] \\ &= T_2[K,\Omega]. \end{aligned} \tag{4.23}$$

Finally, there is the mixing involving only the temporal modulation

$$\begin{aligned} T_4[K,\Omega,K',\Omega'] &= \int \frac{d\omega'}{2\pi}\frac{dk'}{2\pi}\frac{\Omega_2^2}{\nu^2-\Omega_2^2}\sqrt{\omega_s\omega_i}g_t[k_s+k',\omega_s+\nu,K,\Omega] \\ &\qquad\qquad \times g_t[-k_i-k',\omega_i-\nu,K',\Omega'] \\ &\simeq \frac{\Omega_2^2\sqrt{\omega_s\omega_i}}{\left(\Omega^2-\omega_s\right)^2-\Omega_2^2}\Bigg[2\pi\delta\left(\omega_s+\omega_i-\Omega-\Omega'-v_g\left[k_s-k_i-K-K'\right]\right) \\ &\qquad\qquad \times\frac{\sqrt{\pi}\tau}{2}\exp\left(-\frac{\tau^2}{4}\left(k_s-k_i-K-K'\right)^2\right)\Bigg], \end{aligned} \tag{4.24}$$

where we assumed that $1/\tau \gg K-k_s$ in order to perform the last integral. Now the mixing integral becomes

$$\begin{aligned} I^{si}_{\text{mixing}} = \eta^2\Big(&-4\delta_K T_2[0,0]-2\delta_P T_2[2k_p,2\omega_p]-2\delta_P T_2[-2k_p,-2\omega_p] \\ &+2\delta_P^2 T_4[2k_p,2\omega_p,-2k_p,-2\omega_p]+\delta_P^2 T_4[2k_p,2\omega_p,2k_p,2\omega_p] \\ &+4\delta_K^2 T_4[0,0,0,0]+\delta_P^2 T_4[-2k_p,-2\omega_p,-2k_p,-2\omega_p]\Big). \end{aligned} \tag{4.25}$$

Finally, this yields the probability amplitude of emitting a polariton pair

$$
\begin{aligned}
G_{11\leftarrow 00} =& i\sqrt{\mathcal{C}_s\mathcal{C}_i}\frac{\sqrt{\delta\varepsilon_{\omega_s}\delta\varepsilon_{\omega_i}}}{8}\Bigg[\\
&+ 2\delta_K\Bigg(\sqrt{2\pi}\sqrt{\omega_s\omega_i}\tau\left[1+i(2\pi)^{5/2}\sqrt{\mathcal{C}_s\mathcal{C}_i}\left[\delta\varepsilon_{\omega_s}/8\right]\omega_s\sigma_\beta L/\Lambda\right]e^{-\tau^2(k_s-k_i)^2/2} \\
&\qquad\qquad\times\frac{\pi}{L}\delta\left(\omega_s+\omega_i-v_g[k_s-k_i]\right) \\
&\quad-2\eta\left(\frac{\Omega_2^2}{\omega_s^2-\Omega_2^2}\right)\left(\sqrt{\omega_s\omega_i}\sigma_\beta\tau\mathcal{K}\right)\sum_{n=0}^{L/\Lambda}e^{-\tau^2(k_s-k_i-n\mathcal{K})^2/2} \\
&\qquad\qquad\times\frac{\pi}{L}\delta\left(\omega_s+\omega_i-v_g\left[k_s-k_i-n\mathcal{K}\right]\right)\Bigg) \\
&+\delta_P\Bigg(\sqrt{2\pi}\sqrt{\omega_s\omega_i}\tau\left[1+i(2\pi)^{5/2}\sqrt{\mathcal{C}_s\mathcal{C}_i}\left[\delta\varepsilon_{\omega_s}/8\right]\omega_s\sigma_\beta L/\Lambda\right]e^{-\tau^2(k_s-k_i\pm 2k_p)^2/2} \\
&\qquad\qquad\times\frac{\pi}{L}\delta\left(\omega_s+\omega_i\pm 2\omega_p-v_g[k_s-k_i\pm 2k_p]\right) \\
&\quad-2\eta\left(\frac{\Omega_2^2}{\omega_s^2-\Omega_2^2}\right)\left(\sqrt{\omega_s\omega_i}\sigma_\beta\tau\mathcal{K}\right)\sum_{n=0}^{L/\Lambda}e^{-\tau^2(k_s-k_i\pm 2k_p-n\mathcal{K})^2/2} \\
&\qquad\qquad\times\frac{\pi}{L}\delta\left(\omega_s+\omega_i\pm 2\omega_p-v_g\left[k_s-k_i\pm 2k_p-n\mathcal{K}\right]\right)\Bigg) \\
&+\left[\text{terms of } \mathcal{O}\left(\delta_K^2,\delta_P^2\right) \text{ and thus of limited relevance}\right], \qquad (4.26)
\end{aligned}
$$

where we interpret $\delta(0) = L$. It suffices to limit the discussion to leading order in $\delta_{K,P}$ in Eq. (4.16), as we expect these parameters to be small in the experimental setting. We have also neglected exponentially suppressed terms.[5] Clearly, there is nonetheless a plethora of quantum vacuum radiation with different origin. Interestingly, the vacuum radiation may occupy widely different parts of the spectrum, related to the multitude of time-scales present in the problem.

4.3 Experimentally relevant vacuum radiation

Let us now focus on the one type of quantum vacuum radiation that is measured, namely the mixing term $\propto T_2[2k_p, 2\omega_p]$ found in the last line of Eq. (4.26). Also, let us re-define the direction of the idler, such that $k_i \to -k_i$. In this notation, $k_i = -k_s$ implies back-to-back emission. Now, this mixing term in the amplitude Eq. (4.26)

[5] Terms that originate from $\tilde{f}(k_s-k_i,\omega_i-\omega_s)\tilde{f}(0,2\omega_s)$ are either zero by the δ-function constraint, as in the $\tilde{g}_z$ and $\tilde{g}_t[0,2\omega_s,0,0]$, or exponentially suppressed, as in $\tilde{g}_t[0,2\omega_s,\pm 2k_p,\pm 2\omega_p]$.

has the probability amplitude

$$G_{11\leftarrow 00} = -i\frac{\eta\delta_P}{4}\sqrt{\mathcal{C}_s\mathcal{C}_i}\sqrt{\delta\varepsilon_{\omega_s}\delta\varepsilon_{\omega_i}}\left(\frac{\Omega_2^2}{\omega_s^2-\Omega_2^2}\right)(\sqrt{\omega_s\omega_i}\sigma_\beta\tau\mathcal{K}) \times\sum_{n=0}^{L/\Lambda}e^{-\tau^2(k_s+k_i-2k_p-n\mathcal{K})^2/2}\frac{\pi}{L}\delta\left(\omega_s+\omega_i-2\omega_p-v_g\left[k_s+k_i-2k_p-n\mathcal{K}\right]\right) \tag{4.27}$$

The above amplitude only becomes significant when

$$\omega_s+\omega_i-2\omega_p-v_g\left[k_s+k_i-2k_p-n\mathcal{K}\right]=0. \tag{4.28}$$

This might look rather curious and complicated, mixing both frequency and momentum degrees of freedom. However, considering that we are working with a perturbation to the resonance frequency that is moving at a constant speed v_g, it is natural to shift into the reference frame of this pulse. We will refer to this as the co-moving coordinates, and denote it by primed coordinates. A simple Lorentz boost tells that

$$\omega' = \gamma\left(\omega - v_g k\right), \tag{4.29}$$

where $\gamma = 1/\sqrt{1-v_g^2}$ is the Lorentz factor. We can now re-write the relation in Eq. (4.28) as

$$\omega_s'+\omega_i' = n\theta'+2\omega_p', \tag{4.30}$$

where $\theta' = -\gamma v_g\mathcal{K}$ is the co-moving frequency of the spatial modulation. This puts the results in a new light, where the relevant physics takes place in the co-moving frame. In this frame, the quantum vacuum experiences temporal modulation from the (laboratory frame) spatial modulation, as well as from the polarisation wave. The beating between these two types of modulation results in the energy conservation relation in Eq. (4.30). In essence, this becomes the problem analysed in Section 3.5 of Chapter 3.

Furthermore, let us now assume that we are dealing with intrabranch vacuum radiation, specifically of the most photon-like polariton mode (since the pump will couple most strongly to this). If we then suppose that $\omega_s = \omega_p + \Delta\omega$ and $\omega_i = \omega_p - \Delta\omega$, i.e. a small off-shift around the pump frequency, we can expand

$$\begin{aligned} k_s = k(\omega_s) &\simeq k_p + \langle\beta_1\rangle\Delta\omega + \frac{1}{2}\langle\beta_2\rangle\Delta\omega^2 + \frac{1}{3!}\langle\beta_3\rangle\Delta\omega^3 + \frac{1}{4!}\langle\beta_4\rangle\Delta\omega^4, \\ k_i = k(\omega_s) &\simeq k_p - \langle\beta_1\rangle\Delta\omega + \frac{1}{2}\langle\beta_2\rangle\Delta\omega^2 - \frac{1}{3!}\langle\beta_3\rangle\Delta\omega^3 + \frac{1}{4!}\langle\beta_4\rangle\Delta\omega^4. \end{aligned} \tag{4.31}$$

We should note that the assumption that $\omega_{s,i} = \omega_p \pm \Delta\omega$ implies that we are

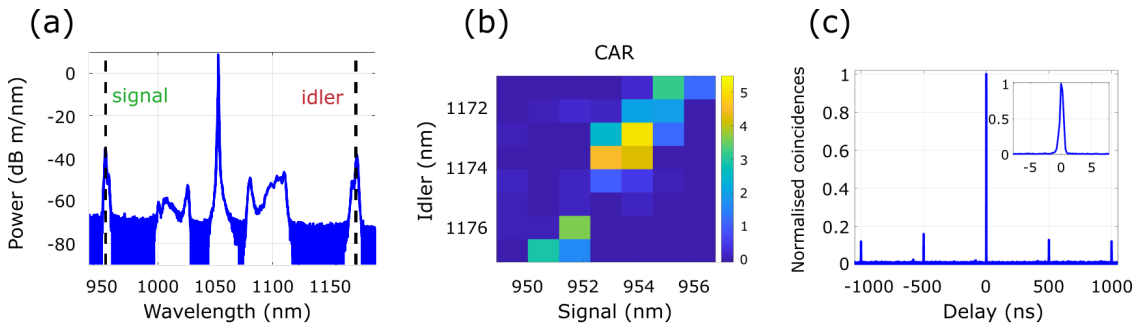

Figure 4.3: **(a)** High power [$P = 12$ W] experimental spectrum as measured at the output of the fibre. Note the position of the signal and idler. This is not the quantum emission, but classically stimulated. **(b)** Low power [$P = 0.03$ W] coincidence-to-accidental ratio with a coincidence window of $\Delta t = 1.7$ ns. As can be seen, the signal and idler have a ratio greater than unity indicating that the photon pair has non-classical correlations. **(c)** Normalised coincidence-to-accidental ratio as a function of the delay. Figure adapted from Ref. [97].

discarding possible vacuum radiation resonances well separated from the pump. Nonetheless, the experiment was performed close to the pump frequency, and it is therefore the relevant frequency region here. Also, we have chosen to truncate the expansion in Eq. (4.31) at 4^{th}-order here, as further orders only leads to very small corrections to the predicted frequencies of the signal and idler. Here it is also appropriate to use the space averaged dispersion parameters to account for the modulation in the dispersion parameters.[6] This is simply because k and z are conjugate variables. Such construction is valid in the limit of $k_{s,i} \gg 2\pi/\Lambda$, which is indeed the case here. Substituting this into Eq. (4.28), we find that

$$\langle\beta_2\rangle\Delta\omega^2 + \frac{1}{12}\langle\beta_4\rangle\Delta\omega_4 = n\mathcal{K}. \tag{4.32}$$

This has solutions

$$\Delta\omega = \pm\sqrt{-\frac{2\sqrt{3}}{\langle\beta_4\rangle}}\sqrt{\sqrt{3}\langle\beta_2\rangle \pm \sqrt{3\langle\beta_2\rangle^2 + \langle\beta_4\rangle n\mathcal{K}}}. \tag{4.33}$$

Note that this has real solutions when $n \leq 3$ for the parameters used in the experiment (β_4 is negative).[7] Specifically, if we focus on the $n = 3$ emission, we see that this predicts that sidebands of quantum vacuum radiation is emitted at

$$\lambda_{s,1} = 954.3 \text{ nm} \tag{4.34}$$

$$\lambda_{i,1} = 1173.1 \text{ nm} \tag{4.35}$$

[6] We define this average as $\langle\beta_i\rangle = \frac{1}{\Lambda}\int_{z_0}^{z_0+\Lambda} dz\ \beta_i(z)$.

[7] The $n = 4$ solution is at the very limit of yielding a real solution here, and will be disregarded.

as well as

$$\lambda_{s,2} = 993.9 \text{ nm}$$
$$\lambda_{i,2} = 1118.4 \text{ nm}. \tag{4.36}$$

Indeed, if we compare this prediction to the experimental data in Fig. 4.3(a), we see that the first set [Eq. (4.34)] are the sidebands observed in the experiment [97]. The second set is also supported by the spectrum, but harder to measure in isolation. We should also note here that we can obtain the same sidebands by a classical nonlinear optics treatment, where $k_s + k_i - 2k_p - n\mathcal{K} = 0$ is known as the phase-matching condition [53]. This was also done in Ref. [97]. Such a treatment is however classical, and perturbatively expands the dispersion relation around the pump frequency.

To delve a little further into the experimental detail, the low-power emission seen in Fig. 4.3(b) shows a coincidence-to-accidental ratio (CAR) greater than unity, implying non-classical correlations between the signal and idler [2]. Here we define the coincidence-to-accidental ratio as

$$\text{CAR} = \frac{N_{s,i}(0) - N_{s,i}(\tau)}{N_{s,i}(\tau)}, \tag{4.37}$$

where $N_{s,i}(0)$ is the total number of detected photon pair coincidences at zero delay within a coincidence time window of Δt and $N_{s,i}(\tau)$ is the average for non-zero delay. A normalised example of photon pair coincidences can be seen in Fig. 4.3(c). Note that coincidence-to-accidental ratio in Eq. (4.37) is implicitly pump intensity dependent, as a high CAR is only likely to occur for quantum correlated photons, which in turn requires a low intensity pump. To further show that the emission did indeed have a quantum origin, we can calculate the second degree of correlation $g^{(2)}$ as

$$g^{(2)}(0) = \frac{N_{s1,s2,i} N_i}{N_{s1,i} N_{s2,i}}, \tag{4.38}$$

where $N_{x,y}$ is the measured coincidence rate between beamsplitter ports x and idler y and $N_{s1,s2,i}$ is the corresponding coincidences between all three. See Fig. 4.1(b) for locations of ports $s1$ and $s2$. Importantly, a $g^{(2)}(0) < 1$ implies that the emission is indeed non-classical [134]. The measurement of this can be seen in Fig. 4.4(b), where $g^{(2)}(0)$ drops far below unity. We can therefore expect that the signal and idler photons are indeed the quantum vacuum radiation, as predicted here.

Indeed, let us we return to discussing the model for this experiment built in this chapter. We see $|G_{11\leftarrow 00}|^2$ for Eq. (4.27) in Fig. 4.5, where $n = 3$ is denoted by solid blue, and the sum of $n = \{0, 1, 2, 3\}$ is denoted by dashed green.[8] Note that

[8]Here we approximated $\delta(...)/L$ as $\exp\left[-(...)^2/2\epsilon^2\right]$ for a small ϵ. In addition to this, we modified the dispersion relation to reproduce the averaged $\langle\beta_2\rangle$ and $\langle\beta_4\rangle$ by letting $\kappa \to 1.51468$ and $\Omega_1 \to 0.5\Omega_1$. We should thus view this as an effective model for the medium. Lastly, we used

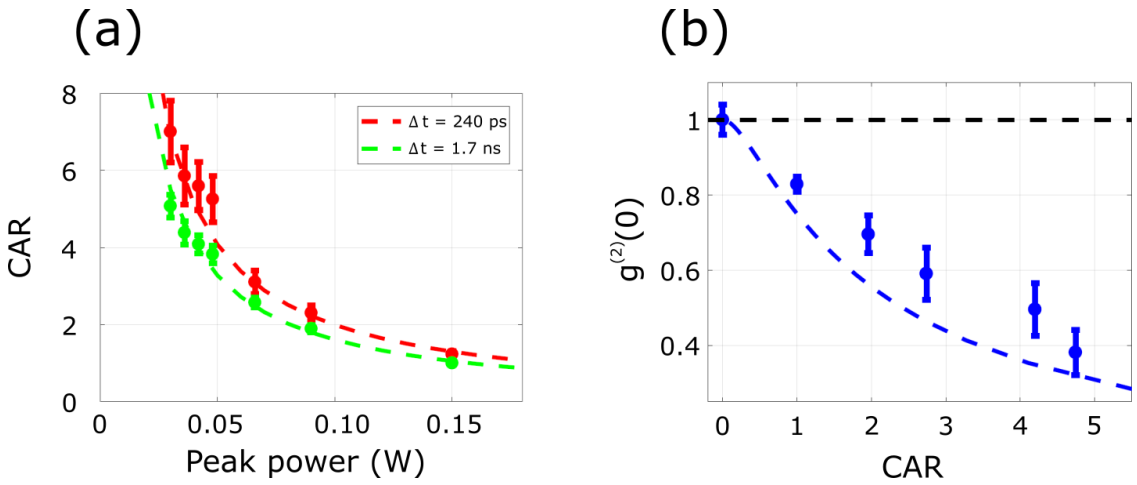

Figure 4.4: **(a)** Coincidence-to-accidental ratio as a function of peak power of the pump beam. Note that it increases rapidly for low peak power. **(b)** Second degree of coherence $g^{(2)}(0)$ at zero time-delay. It quickly decreases below unity for high coincidence-to-accidental ratio, heralding quantum correlations between the signal and idler. Figure adapted from Ref. [97].

we evaluated $|G_{11\leftarrow 00}|^2$ using *Mathematica*. We thus predict exactly the sidebands as measured in the experiment. However, we also predict several other sidebands of similar amplitude for $n = 0, 1, 2$. All these peaks do nonetheless fall within a small window of frequencies and it is possible that further experimental complications, not taken into account by the simple model produced here, act to reduce the amplitude of these, especially since we modelled the photonic crystal fibre at a fairly coarse level. Further inquest into this would be interesting.

4.3.1 What about the other vacuum radiation resonances?

Interestingly, the quantum vacuum radiation amplitude in Eq. (4.26) also contains further resonances, that are independent of the pump wavenumber k_p and frequency ω_p. These are resonances that would often be missed in a fibre setting, as it is commonplace to assume that all physics transpires in a frequency window around the pump [107]. In particular, we also predict vacuum radiation when

$$\omega_s + \omega_i - v_g \left[k_s + k_i - n\mathcal{K}\right] = 0. \tag{4.39}$$

This would, in the co-moving frame, correspond to

$$\omega_s' + \omega_i' = n\theta' \tag{4.40}$$

and we see that this is the first-order effect of the spatial modulation (which becomes temporal in the co-moving frame), without the mixing due to the time-nonlocal response of the medium. This radiation is however, completely independent of the

$\eta = 0.042$, and $\delta_P = 0.001$.

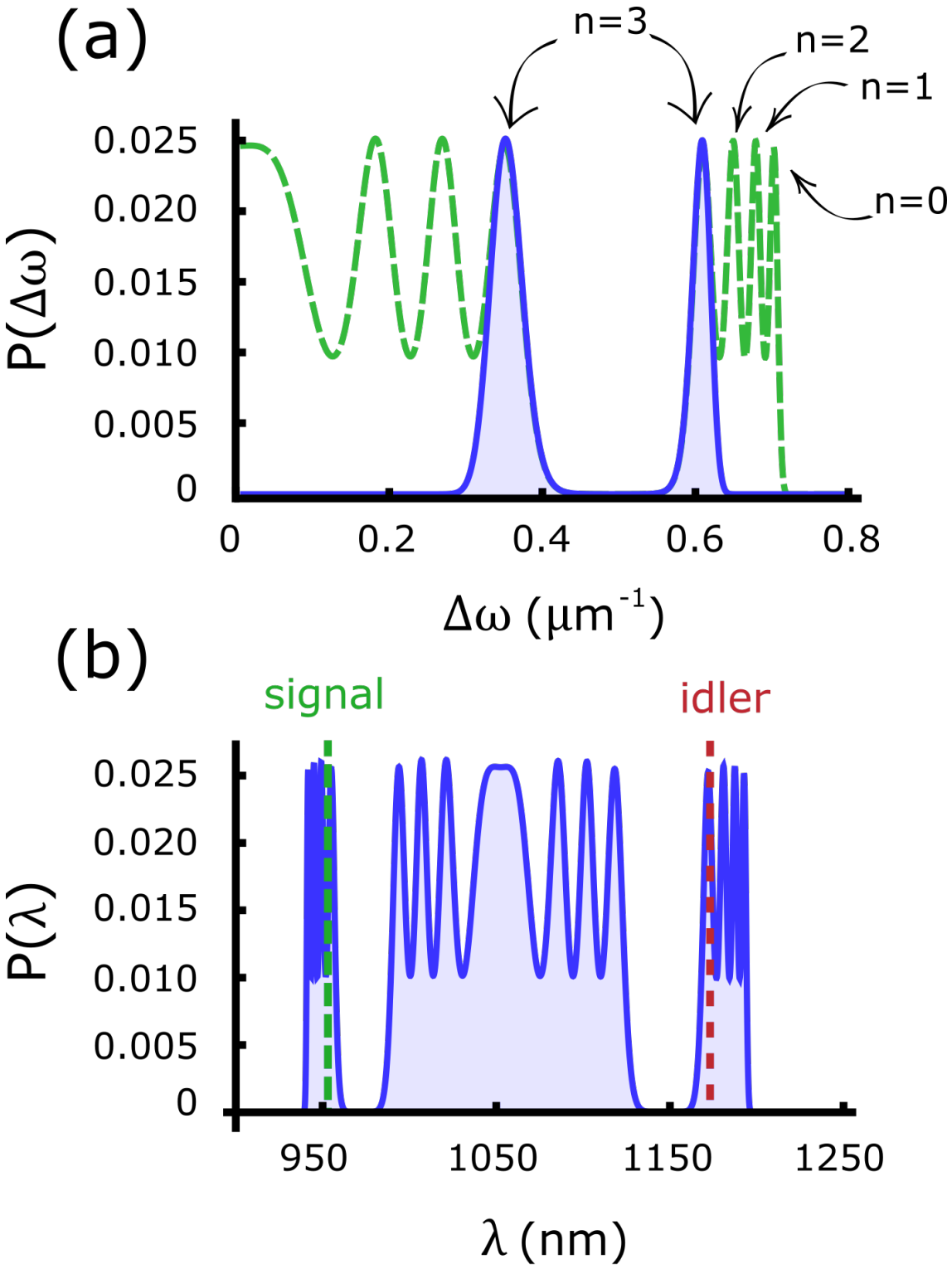

Figure 4.5: **(a)** Probability per unit frequency per unit length of emitting quantum vacuum radiation as a function of the shift from the pump frequency $\Delta\omega$. The experimentally measured $n = 3$ peaks can be seen in solid blue, whereas the sum of $n < 4$ is denoted by dashed green. Note that a shift of $\Delta\omega \sim \pm 0.6$ μm^{-1} corresponds to $\lambda_s = 954$ nm and $\lambda_i = 1173$ nm respectively ($+ \rightarrow$ signal and vice-versa). **(b)** Spectrum of vacuum radiation as a function of measured wavelength. Note the relative similarity to Fig. 4.3(a).

pump frequency, and we expect the resonance to be at low frequencies. Nonetheless, it offers a different avenue of approach to vacuum radiation in a spectral regime offset from the pump.

Even more striking perhaps, the amplitude in Eq. (4.26) also contains

$$\omega_s + \omega_i - v_g \left[k_s + k_i - n\mathcal{K}\right] = 0, \tag{4.41}$$

which in the co-moving frame corresponds to

$$\omega_s' + \omega_i' = 0. \tag{4.42}$$

Importantly, depending on your choice of parameters, the co-moving frequencies *can* be negative, and this condition can be fulfilled. This emission is directly linked to the analogue Hawking-like radiation studied in Refs. [135] whose classical analogue was experimentally verified in Ref. [35].[9]

4.4 Conclusions from analysing an experiment

In this chapter we analysed the experiment performed in Ref. [97] (Item 2 from the List of Publications) in the context of the quantum vacuum radiation. Specifically, we modelled the variations in the fibre group velocity dispersion β_2 as a variation in the resonance frequency in space. Interestingly, from the start this appeared to be a fair model, seeing that the dispersion coefficients β_i were hardly affected, apart from the group velocity dispersion, as intended. In addition to this, we introduced a travelling temporal variation of the resonance frequency through the quadratic Stark shift of the resonance frequency. Through this we could account for the Kerr effect of the 'strong' pump laser pulse used in the experiment, as well as the polarisation wave excited by the pump. As all physics of the experiment could be accounted for through shifts to the resonance frequency, we could apply the framework of Chapter 3.

Through this, we predicted quantum vacuum radiation in agreement with the experimental results, namely sidebands around the pump (which was at 1054.22 nm) at

$$\lambda_{s,1} = 954.3 \text{ nm} \tag{4.43}$$

$$\lambda_{i,1} = 1173.1 \text{ nm}. \tag{4.44}$$

Curiously, the precise form of the energy conservation relation in the probability amplitude of Eq. (4.27) suggests that the physics has a straightforward explanation in the co-moving frame of the pump pulse. Indeed, in the co-moving frame, moving

[9] We will further comment on this in Chapter 5.

with the pump pulse at the group velocity v_g, these sidebands are a result of the frequency mixing due to the time-delayed response of the medium as discussed in Chapter 3. Thus we can immediately write down the energy conservation

$$\omega_s' + \omega_i' = n\theta' + 2\omega_p', \tag{4.45}$$

where θ' is the co-moving frequency of the spatial fibre modulation, as in this frame the fibre appears to be modulated in time. We can compare this to Eq. (3.74) of Chapter 3.

Nevertheless, the theory presented here predicts several other resonances for quantum vacuum radiation. Especially intriguing are those that are disconnected from the pump frequency [Eqns. (4.40) and (4.42)]. Such resonances would be neglected by models that assume all frequencies to be centred around the pump, which is commonplace when discussing fibre optics [107]. Whilst these resonances usually are at low frequency, it nonetheless offers an interesting new avenue to pursue experimentally.

Chapter 5

Intermission: Analogue gravity & photon production in ENZ materials

> *"Strange department, this. Their motto was, 'The comprehension of Infinity requires infinite time.' I didn't argue with that, but then they derived an unexpected conclusion from it: 'Therefore work or not, it's all the same.' In the interests of not increasing the entropy of the universe, they did not work."*
>
> Arkadi and Boris Strugatsky in *Monday begins on Saturday*, 1966

Before we continue it can be instructive to bring in a different perspective of the results obtained so far. The aim of this chapter is to analyse scenarios beyond periodic modulation and perturbation theory, as well as to put the thesis in some further context beyond that already discussed in Chapter 1. We will primarily discuss the results of Chapter 3, but also use work from the previous studies Item 3 (work done in conjunction with Dr Angus Prain) and in Item 4 (work done prior to doctoral studies) from the List of Publications.

5.1 Analogue gravity

Whilst the study of quantum vacuum radiation is fascinating in its own right, our interest originates analogue gravity. Analogue gravity is the study of the quantum fields on a background that simulates the effect of curved spacetime. Importantly, the background here is not a spacetime in any strict sense, and is not required to satisfy Einstein's field equations. Nonetheless, many aspects associated with quantum field theories on curved spacetime are inaccessible experimentally [24], and analogue gravity offers a window through which we can gleam insights. Especially interesting is if the effective spacetime created by the background in analogue gravity can be made to mimic that of a real gravitational system.

As mentioned in Chapter 1, perhaps the two most prominent examples of exotic quantum-field-theoretic effects on curved spacetime are that of photons emitted

from a black hole (Hawking radiation [21, 22]) and particle pair production from an expanding spacetime (cosmological pair production [15]). The former is also closely linked to the Unruh effect [20] by the equivalence principle, where the accelerated observer in flat spacetime measures a thermal vacuum whose temperature is proportional to the acceleration. Analogue gravity was indeed first introduced to study these effects. Specifically, Unruh [19] found that phase fluctuations on a flowing fluid behave analogously to a scalar field on curved spacetime, forming a so-called acoustic metric with line-element

$$ds^2 = \frac{\rho}{c_s}\left[-\left(c_s^2 - v^2\right)dt^2 + \left(d\mathbf{x} - \mathbf{v}dt\right)^2\right], \tag{5.1}$$

where ρ is the density of the fluid, c_s is the local speed of sound and $\mathbf{v}$ is the flow velocity. In this way, Unruh introduced what is usually referred to as a 'dump hole' [24], where the phase fluctuations experience an event-horizon-like point when the fluid flow speed exceeds the local speed of sound. This has recently been observed experimentally for quantum phase fluctuations in a Bose-Einstein condensate [32, 33], as well as studied extensively theoretically [24]. As we are not directly interested in analogue gravity using the acoustic metric, we will simply refer to the comprehensive review found in Ref. [24] for further details.

Also recently, Hawking-like photon pair production in an optical fibre was found experimentally [35] in the case when the emission was seeded not by the quantum vacuum but by a separate beam of light. This is where we will find the link to the work contained in this thesis, as indeed some theoretical work directly related to the recent observation was performed in Ref. [135] (List of Publications, Item 5). The connection between an optical fibre and a black hole is however qualitatively different from the acoustic metric for phase fluctuations on a fluid. Instead, it builds upon the Gordon metric for light in a dispersion-less medium [136]. For a static observer in flat spacetime, this line element takes the form

$$ds^2 = \left(\frac{c}{n(\mathbf{x},t)}\right)^2 dt^2 - d\mathbf{x}^2, \tag{5.2}$$

where n is the refractive index of the medium and c is the speed of light in vacuum. In the case of a time-independent refractive index, this metric links nicely to geometric optics and Fermat's principle, the principle that light will tend to minimize the path traversed between two points $\mathbf{a}$ and $\mathbf{b}$ [54]. The null geodesics of Eq. (5.2), determined by $ds = 0$, is given by

$$\frac{d\mathbf{x}}{dt} = \left(\frac{c}{n(\mathbf{x})}\right). \tag{5.3}$$

This is the equation of motion for a ray of light. Suppose now that we want to

calculate the total time T of propagation, given by

$$\begin{aligned} T &= \int_0^T dt = \int_0^T dt \, \sqrt{\left(\frac{c}{n}\right)^2} \frac{n}{c} = \int_0^T dt \, \sqrt{\frac{d\mathbf{x}}{dt} \cdot \frac{d\mathbf{x}}{dt}} \frac{n}{c} \\ &= \frac{1}{c} \int_{\mathbf{a}}^{\mathbf{b}} ds_{\mathrm{E}} \, n(\mathbf{x}), \end{aligned} \tag{5.4}$$

where the last line is the usual formulation of Fermat's principle and $ds_E = \sqrt{d\mathbf{x} \cdot d\mathbf{x}}$ is the usual Euclidean line element. Interestingly, had we started with a metric of the form

$$ds^2 = c^2 dt^2 - n^2(\mathbf{x}, t) d\mathbf{x}^2, \tag{5.5}$$

we would have arrived at the same answer for null geodesics. This is a common feature of the mapping between refractive index (or more generally permittivity and permeability) and an effective spacetime metric: it is not one-to-one, and there are multiple equally well-defined versions of an optical metric [24]. Note that this is also discussed in the framework of transformation optics [137], where a refractive index profile is chosen to emulate some coordinate transformation. The latter form of the optical metric [Eq. (5.5)] is the metric of interest here. To simplify notation, let us from now on work with units where $c = 1$, $\varepsilon_0 = 1$ and $\hbar = 1$, in accordance with the rest of the thesis.

Importantly, this metric emerges for slowly-varying (low-energy) electromagnetic excitation in Hopfield models for macroscopic quantum electrodynamics, which are the type of models with which we work. Suppose we study a medium where the field is constrained in one spatial dimension, leaving the other two effectively free: the dynamics of the transverse plane of a thin-film medium, where the extent in the z-dimension is much smaller than a wavelength, would be an example of this. As was shown recently by Linder *et al.* [110], if we further consider the limit where the resonance frequency[1] of the medium Ω is much greater than the frequency of light, then the combined light-matter excitations can be described by a scalar field on the metric with line element

$$ds^2 = dt^2 - \left(1 + \frac{g^2}{\Omega^2(t)}\right) \left[dx^2 + dy^2\right]. \tag{5.6}$$

Interestingly, had the dynamics been unconstrained in all three spatial dimensions, then the light-matter excitations would behave as a scalar field in the metric

$$ds^2 = \frac{dt^2}{\sqrt{\left(1 + \frac{g^2}{\Omega^2(t)}\right)}} - \sqrt{\left(1 + \frac{g^2}{\Omega^2(t)}\right)} d\mathbf{x}^2. \tag{5.7}$$

[1] In general, we allow for a time-dependent Ω

Again, this goes to show that the optical mapping in analogue gravity is not one-to-one. In order to show this, let us start at the Hopfield action introduced in Chapter 3. To sum up, this action is given by

$$\begin{aligned} S_\gamma &= \int dt \int d^3x \, \frac{1}{2}\left[\dot{A}_\lambda^2 - (\boldsymbol{\nabla} A_\lambda)^2\right] \\ S_R &= \int dt \int d^3x \, \frac{1}{2}\left[\dot{R}^2 - \Omega^2(t) R^2\right] \\ S_{\text{int}} &= \int dt \int d^3x \, \left(-g \, \dot{A}_\lambda R\right), \end{aligned} \tag{5.8}$$

which is a reduced version of Eq. (3.13) to a single oscillator R, and where we have expanded into polarisation modes $\mathbf{e}_\lambda$ such that $\mathbf{A} = \sum_\lambda A_\lambda \mathbf{e}_\lambda$ and $\mathbf{e}_\lambda \cdot \mathbf{e}_{\lambda'} = \delta_{\lambda,\lambda'}$. We discussed and motivated this in Chapter 3 but in short it describes electromagnetism coupled to an optical medium with resonance frequency Ω. Note that for a time-independent Ω, the refractive index is given by

$$n^2(\omega) = 1 - \frac{g^2}{\omega^2 - \Omega^2},$$

and g is the effective plasma frequency of the medium. The corresponding equations of motion are

$$\begin{aligned} \ddot{A}_\lambda - \nabla^2 A_\lambda &= g\dot{R} \\ \ddot{R} + \Omega^2(t) R &= -g\dot{A}_\lambda. \end{aligned} \tag{5.9}$$

If we suppose that the excitation frequency $\omega \ll \Omega(t)$ so that we can neglect $\ddot{R}$, then the solution to the matter degree of freedom R is simply

$$R \simeq -g\dot{A}_\lambda / \Omega^2(t).$$

Furthermore, if we substitute this solution back into the action in Eq. (5.8) and neglect the surface terms of R by setting $R(t_i) = R(t_f) = 0$,[2] we find

$$S_{\gamma+R+\text{int}} = \int dt \int d^3x \, \frac{1}{2}\left[\left(1 + \frac{g^2}{\Omega^2(t)}\right)\dot{A}_\lambda^2 - (\boldsymbol{\nabla} A_\lambda)^2\right]. \tag{5.10}$$

[2] As we mentioned in Chapter 3, we can simply ignore the free action S_R and substitute this into the interaction action S_{int} along with the factor 1/2. Formally, we can rewrite

$$\begin{aligned} S_R &= \int dt \int d^3x \, \frac{1}{2}\left[\dot{R}^2 - \Omega^2(t) R^2\right] = \int d^3x \left(\frac{1}{2}\left[R\dot{R}\right]_{t_i}^{t_f} - \frac{1}{2}\int dt \, \left[\ddot{R} + \Omega^2 R\right] R\right) \\ &\simeq \frac{1}{2}\int dt \int d^3x \, \left(g\dot{A}_\lambda R\right), \end{aligned}$$

where in the second line we set $R(t_i) = R(t_f) = 0$ (an approximation) and use the classical equations of motion (exact). In total we thus find $S_{R+\text{int}} \simeq \frac{1}{2}\int dt \int d^3x \, \left(-g \, \dot{A}_\lambda R\right)$, and in the low-energy limit we have $S_{R+\text{int}} \simeq \int dt \int d^3x \, \left[g^2/2\Omega^2(t)\right] \dot{A}_\lambda^2$. Eq. (5.10) follows from this.

By comparison with the action of a scalar field ϕ in some metric $\mathfrak{g}_{\mu\nu}$, whose action is

$$S_\phi = \int dt \int d^3x \, \sqrt{-\mathfrak{g}}\mathfrak{g}^{\mu\nu}\partial_\mu\phi\partial_\nu\phi, \tag{5.11}$$

we find the low-energy optical metrics of Eqns. (5.6) and (5.7).[3] Here we define the metric $\mathfrak{g}_{\mu\nu}$, such that the line element is given by $ds^2 = \mathfrak{g}_{\mu\nu}dx^\mu dx^\nu$ [dx^μ is the differential element of the μ^{th} component of the 4-vector $x = (t, \mathbf{x})$], $\mathfrak{g}$ is the metric determinant and $\mathfrak{g}^{\mu\nu}$ is the metric inverse. It is worth mentioning that the slowly-varying limit is exactly the limit where geometric optics is valid.

If we return to the gravity-side of this discussion, we should immediately notice that the metrics (or line elements) of Eqns. (5.5) and (5.6) coincide with the metric of an expanding universe, that is, the Friedmann–Lemaître–Robertson–Walker metric [23]:

$$ds^2 = dt^2 - a^2(t)d\mathbf{x}^2, \tag{5.12}$$

if we identify a purely time-dependent refractive index $n(t)$ with the so-called scale factor $a(t)$. The metric is here written in the coordinates of a stationary observer. In this $a(t)$ is the scale factor, related to the Hubble constant through $H = \dot{a}/a$ [24]. This striking resemblance was the basis of the work in Item 4 from the List of Publications. Indeed, in that work, we studied this analogy in a dispersive medium in the case when the change in refractive index is very small.

We will get to the details of that work shortly, but it is interesting to first note a couple of things regarding particle pair production from cosmological expansion. As was neatly summarised by Wittemer *et al.* [30] in the supplementary materials, cosmological expansion affects different types of quantum fields in a qualitatively different manner. As is commonly done, let us first switch to so-called conformal time η, defined as

$$\eta = \int_0^t \frac{dt'}{a(t')}.$$

The metric for the expanding universe then takes the form

$$ds^2 = a(\eta)^2 \left[d\eta^2 - d\mathbf{x}^2\right].$$

This does not alter the physics but simplifies the algebra. Of special interest to us, they noted that the cosmological expansion couples directly to a scalar field $\phi(\eta, \mathbf{x})$ by changing its mode frequency in time, whereas for a vector field $A^\mu(\eta, \mathbf{x})$ it couples only through the mass term. In particular they found that in a real gravitation field,

[3] For the former, we naturally integrate not over d^3x but d^2x.

the scalar field equation[4] $(\nabla_\mu \nabla^\mu - m^2)\,\Phi = 0$ can be reduced to

$$\ddot{\phi}_{\mathbf{k}} + \left[a^2 m^2 + |\mathbf{k}|^2 - \frac{\ddot{a}}{a}\right] \phi_{\mathbf{k}} = 0 \tag{5.13}$$

for each momentum mode $\mathbf{k}$, where $\dot{f} \equiv df/d\eta$ and $\phi = a^{3/2}\Phi$. As can be seen, even in the massless case the cosmological expansion would change the mode frequency in time, which in turn can lead to particle pair creation for the associated quantum field. On the other hand, the equation of motion for a Proca-style massive photon[5] can be reduced to

$$\ddot{A}_{\mathbf{k},\lambda} + \left[a^2 m^2 + |\mathbf{k}|^2\right] A_{\mathbf{k},\lambda} = 0 \tag{5.14}$$

for some polarisation λ and momentum mode $\mathbf{k}$. Since photons are massless, we would therefore not expect cosmological expansion to excite photon pairs from the vacuum state. This then brings up the question of why we would expect photon pairs to be emitted from an optical medium where the refractive index changes rapidly in time, mimicking cosmological expansion. The reason for this is dispersion. In fact, the metrics established in Eqns. (5.5) and (5.6) are only valid in the limit of geometric optics, where the fields are assumed to be slowly varying. If we instead consider the high energy excitations, i.e. when $\omega \gg \Omega$ with Ω being the resonance frequency of the medium. In this case, we can neglect the Ω^2 term in Eq. (5.9) and the solution to the matter degree of freedom is

$$\dot{R} = -g A_\lambda.$$

The corresponding action is then

$$S_{\gamma+R+\mathrm{int}} = \int dt \int d^3x\, \frac{1}{2}\left[\dot{A}_\lambda^2 - (\boldsymbol{\nabla} A_\lambda)^2 - g^2 A_\lambda^2\right], \tag{5.15}$$

which can be compared with Eq. (5.10). As can be seen, the coupling acts as a mass term! It is noteworthy that this is also the equation of motion for a non-interacting plasma, which does not have a resonance frequency.[6]

Whilst dispersion is a complicated phenomenon, which in general is taken into account by a temporally nonlocal self-interaction (as discussed in Chapter 3), we see from Eqns. (5.10) and (5.15) that in certain limits we can understand the dynamics much more simply. In particular, depending on the frequency of the combined light-matter interaction, the field behaves either as a field on curved spacetime, as in

[4]Here $\nabla_\mu A^\alpha = \partial_\mu A^\alpha + \Gamma^\alpha_{\mu\beta} A^\beta$ is the usual covariant derivative of A^α [15], with $\Gamma^\alpha_{\mu,\beta}$ being the Christoffel symbols associated with the metric $\mathfrak{g}_{\mu\nu}$.

[5]Equation of motion $\nabla_\mu \nabla^\mu A^\alpha - \nabla_\mu \nabla^\alpha A^\mu = m^2 A^\alpha$.

[6]As an interesting aside, we can note that in this offers a natural interpretation of non-propagating electromagnetic modes in a plasma below the plasma frequency: The mode simply does not have enough energy for one 'mass unit' g.

Eq. (5.10), or a free massive field, as in Eq. (5.15). It thus stands to reason that the dispersion will interpolate between these situations. In either case, when introducing a time-dependent refractive index in a manner where dispersion is taken into account, we expect quantum vacuum radiation to be emitted, as indeed the mode frequency changes in time. We can however link it to other scenarios such as cosmological expansion or time-dependent mass terms in certain limits.

Nevertheless, we do wish to advice some caution when attempting to gleam insights into the dynamics of quantum fields on expanding spacetime from the dynamics of electromagnetic excitations in an optical medium with time-dependent parameters. The two situations might share similarities in certain limits, but they are by no means the same. Nonetheless, this is the approach we took in Item 4, of which Chapter 3 can be seen as an extension in some sense. In Item 4, we were motivated by the similarity between the the Gordon-type optical metric of Eq. (5.5) and the metric of cosmological expansion in Eq. (5.12), particularly in the case of a spatially homogeneous refractive index in two spatial dimensions. There we employed a Hopfield model similar to the one used in Chapter 3, albeit truncated at first order and ignoring some of the subtleties involving multiple polariton modes. The medium in question was a thin-film, or slab, where the dynamics of one spatial direction can be ignored. We then modelled 'cosmological expansion' as a change to the refractive index of the form

$$\delta n(t) = \delta n_0 \tanh\left(t/\sigma\right), \tag{5.16}$$

where σ is some time-scale and δn_0 is its amplitude, using a diamond-like medium with a single resonance frequency as a background medium. We would expect the optical metric to be valid in this limit.

In the context of Chapter 3 and the rest of this thesis, this would be the equivalent of a time-dependent resonance frequency of the form

$$\Omega^2(t) = \Omega_0^2\left[1 + \epsilon \tanh\left(t/\sigma\right)\right], \tag{5.17}$$

where ϵ is some amplitude chosen such that it would reproduce δn_0 using Eq. (3.53). We would note that this is not accessible using perturbation theory as

$$\Omega(-\infty) \neq \Omega(\infty), \tag{5.18}$$

and we will replace this with

$$\Omega^2(t) = \Omega_0^2\left[1 + \epsilon\, \mathrm{sech}\left(t/\sigma\right)\right], \tag{5.19}$$

which can be thought of as two successive tanh-profiles. In other words, here $f(t) = \epsilon\, \mathrm{sech}\left(t/\sigma\right)$. We can now apply the model developed in Chapter 3 to this

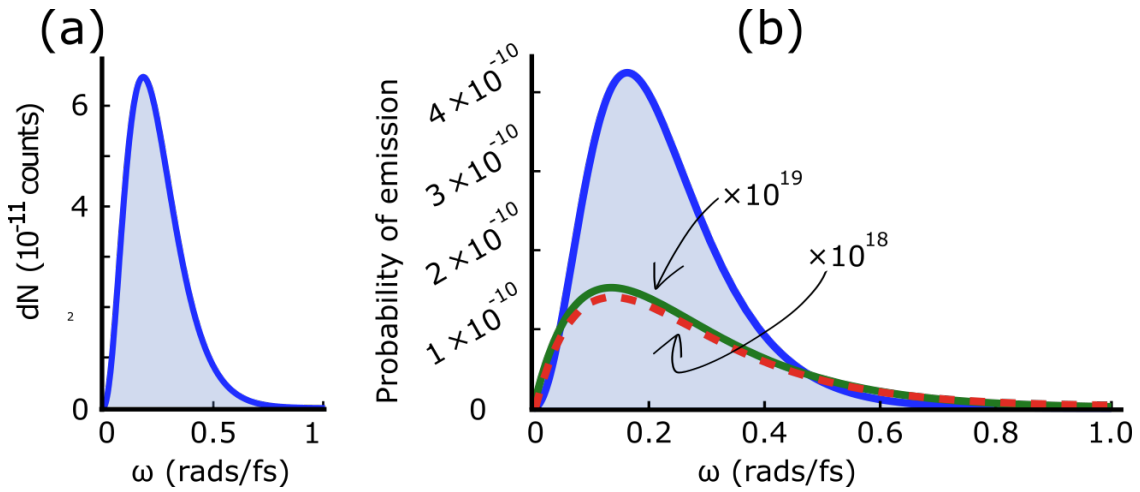

Figure 5.1: **(a)** Spectrum of excited photon pairs for a refractive index variation of $\delta n_0 = 10^{-2}$ within the time-scale of $\sigma = 1.25$ fs. Figure adapted from Ref. [138]. **(b)** Same physical scenario as (a) (regularised as mentioned in the main text), with ϵ chosen such that $\delta n \simeq 10^{-2}$ and with $\sigma = 1.25$ fs. As can be seen, the main intrabranch process of pair production is in agreement between the models (blue shaded). However, the earlier work neglected the interbranch processes (solid green, dashed red).

'cosmological expansion'-like change to the resonance frequency.

Similarly to the previous work, let us assume a diamond-like medium with a single resonance pole at a vacuum wavelength of around 200 nm. The important quantity is as before the Fourier transform of the modulation f:

$$\tilde{f}(\mathbf{k},\omega) = \epsilon\pi\sigma\mathcal{V}\,\mathrm{sech}\left(\frac{\pi\sigma}{2}\omega\right). \tag{5.20}$$

We must however also evaluate the mixing integral from Eq (3.68) in order to find the probability of exciting polariton pairs. Here we find

$$\begin{aligned} I^{\alpha\alpha'}_{\text{mixing}} &= \int \frac{d\omega'}{2\pi}\frac{d^3k'}{(2\pi)^3}\frac{\Omega^2}{(\omega_\alpha-\omega')^2-\Omega_i^2}\sqrt{\omega_\alpha\omega_{\alpha'}}\,\tilde{f}\left(\mathbf{k}',\omega'\right)\tilde{f}\left(-\mathbf{k}',\omega_\alpha+\omega_{\alpha'}-\omega'\right) \\ &= \sqrt{\omega_\alpha\omega_{\alpha'}}\int \frac{d\omega''}{2\pi}\frac{d^3k'}{(2\pi)^3}\frac{\Omega^2}{(\omega'')^2-\Omega^2}\tilde{f}\left(\mathbf{k}',\omega''+\omega_\alpha\right)\tilde{f}\left(-\mathbf{k}',\omega_{\alpha'}-\omega''\right) \\ &= \epsilon^2\mathcal{V}\left[\sigma^2\sqrt{\omega_\alpha\omega_{\alpha'}}\right]\frac{\pi}{2}\int d\omega''\frac{\Omega^2}{(\omega'')^2-\Omega^2}\,\mathrm{sech}\left(\frac{\pi\sigma}{2}\left[\omega''+\omega_\alpha\right]\right) \\ &\qquad\qquad \times\,\mathrm{sech}\left(\frac{\pi\sigma}{2}\left[\omega_{\alpha'}-\omega'\right]\right) \\ &\simeq 0, \end{aligned} \tag{5.21}$$

where in the second line we defined $\omega'' = \omega' - \omega_\alpha$. The last line follows because for the integrand to be significant, ω'' would have to be equal to both $-\omega_\alpha$ as well as $\omega_{\alpha'}$ simultaneously.

Keeping in mind that we now wish to keep also terms that contain $\tilde{f}(\mathbf{0},0)$, we

can express the intrabranch and interbranch amplitudes from Chapter 3 as

$$G^{\text{intra}}_{11\leftarrow 00} = i\mathcal{C}_{\mathbf{k}\alpha}\mathcal{V}^{-1}\frac{\delta\varepsilon_{\omega_\alpha}}{8\epsilon}\left[\omega_\alpha\tilde{f}(\mathbf{0},2\omega_\alpha) + I^{\alpha\alpha}_{\text{mixing}} - i\mathcal{C}_{\mathbf{k}\alpha}\mathcal{V}^{-1}\frac{\delta\varepsilon_{\omega_\alpha}}{8\epsilon}\omega_\alpha^2\tilde{f}(\mathbf{0},2\omega_\alpha)\tilde{f}(\mathbf{0},0)\right] \tag{5.22}$$

and

$$\begin{aligned} G^{\text{inter}}_{11\leftarrow 00} = i\sqrt{\mathcal{C}_{\mathbf{k}\alpha}\mathcal{C}_{\mathbf{k}\alpha'}}\mathcal{V}^{-1}\frac{\sqrt{\delta\varepsilon_{\omega_\alpha}\delta\varepsilon_{\omega_{\alpha'}}}}{8\epsilon}\Bigg[&\sqrt{\omega_\alpha\omega_{\alpha'}}\tilde{f}(\mathbf{0},\omega_\alpha+\omega_{\alpha'}) + I^{\alpha\alpha'}_{\text{mixing}} \\ &- i\sqrt{\mathcal{C}_{\mathbf{k}\alpha}\mathcal{C}_{\mathbf{k}\alpha'}}\mathcal{V}^{-1}\frac{\delta\varepsilon_{\omega_\alpha}}{8\epsilon}\sqrt{\omega_\alpha^3\omega_{\alpha'}}\tilde{f}(\mathbf{0},\omega_\alpha+\omega_{\alpha'})\tilde{f}(\mathbf{0},0) \\ &- i\sqrt{\mathcal{C}_{\mathbf{k}\alpha}\mathcal{C}_{\mathbf{k}\alpha'}}\mathcal{V}^{-1}\frac{\delta\varepsilon_{\omega_\alpha}}{16\epsilon}\sqrt{\omega_\alpha^3\omega_{\alpha'}}\tilde{f}(\mathbf{0},\omega_{\alpha'}-\omega_\alpha)\tilde{f}(\mathbf{0},2\omega_\alpha)\Bigg] \end{aligned} \tag{5.23}$$

respectively. Also note that in this case the polariton modes are those in Eq. (3.75), i.e. $\omega_\alpha \equiv \omega_\pm$. If we then substitute the expressions for the modulation and mixing established in Eqns. (5.20) and (5.21), we find the probability amplitude of exciting a polariton pair in a back-to-back configuration

$$G^{\text{intra}}_{11\leftarrow 00} = i\mathcal{C}_{\mathbf{k}\alpha}(\delta\varepsilon_{\omega_\alpha}/8)\Big[\left[\pi\sigma\omega_\alpha\right]\text{sech}\left(\pi\sigma\omega_\alpha\right) - i\mathcal{C}_{\mathbf{k}\alpha}(\delta\varepsilon_{\omega_\alpha}/8)\left[\pi^2\sigma^2\omega_\alpha^2\right]\text{sech}\left(\pi\sigma\omega_\alpha\right)\Big] \tag{5.24}$$

and

$$\begin{aligned} G^{\text{inter}}_{11\leftarrow 00} = i\sqrt{\mathcal{C}_{\mathbf{k}\alpha}\mathcal{C}_{\mathbf{k}\alpha'}}\frac{\sqrt{\delta\varepsilon_{\omega_\alpha}\delta\varepsilon_{\omega_{\alpha'}}}}{8}\Bigg[&\left[\pi\sigma\sqrt{\omega_\alpha\omega_{\alpha'}}\right]\text{sech}\left(\frac{\pi\sigma}{2}\left[\omega_\alpha+\omega_{\alpha'}\right]\right) \\ -\ &i\sqrt{\mathcal{C}_{\mathbf{k}\alpha}\mathcal{C}_{\mathbf{k}\alpha'}}\frac{\delta\varepsilon_{\omega_\alpha}}{8}\left[\pi^2\sigma^2\sqrt{\omega_\alpha^3\omega_{\alpha'}}\right]\text{sech}\left(\frac{\pi\sigma}{2}\left[\omega_\alpha+\omega_{\alpha'}\right]\right) \\ -\ &i\sqrt{\mathcal{C}_{\mathbf{k}\alpha}\mathcal{C}_{\mathbf{k}\alpha'}}\frac{\delta\varepsilon_{\omega_\alpha}}{16}\left[\pi^2\sigma^2\sqrt{\omega_\alpha^3\omega_{\alpha'}}\right]\text{sech}\left(\frac{\pi\sigma}{2}\left[\omega_{\alpha'}-\omega_\alpha\right]\right)\text{sech}\left(\pi\sigma\omega_\alpha\right)\Bigg] \end{aligned} \tag{5.25}$$

We can see the probability amplitude of emission in Fig. 5.1, but already from the expression in Eq. (5.24) we deduce that the intrabranch emission probability peaks when

$$\omega_\alpha \simeq 0.38/\sigma \tag{5.26}$$

to first order, whereas the second order emission has a contribution at the same frequency. Interestingly, since $I^{\alpha\alpha'}$ is approximately zero, the time-delayed response does not contribute significantly in this situation. The interbranch processes are somewhat more complicated, but follow a similar qualitative picture. Unsurprisingly, the emission is centred around $\sim 1/\sigma$, as σ is the only time-scale in the modulation.

As can be seen when comparing Fig. 5.1(a) and Fig. 5.1(b), the transitions between different polariton modes were neglected in the study in Ref. [138], as the two interbranch probabilities (solid green, dashed red) are missing in (a). Nonetheless, the two spectra are qualitatively similar to first order. Importantly, the new additions obtained using the theory developed in Chapter 3 are the existence of multiple polariton modes.

Let us return to the connection to analogue gravity. We first note that the applicable comparison is in two spatial dimensions, since the material discussed in the above section is of a thin-film, or slab, nature.[7] This doesn't affect the results in Eqns. (5.24) and (5.25), but allows us to easily link the dynamics to that of an expanding universe. In fact, this is exactly the type of scenario we considered in Ref. [138]. Now, a massless scalar field in an expanding (2D) universe and the $\omega \ll \Omega$ limit of light in a time-dependent optical medium [Eq. (5.10)] coincide if we identify

$$a^2(t) = 1 + \frac{g^2}{\Omega^2(t)}. \tag{5.27}$$

We should stress here that this is only true when all oscillation frequencies in the light-matter system are much smaller than the resonance frequency. It follows that we can completely neglect the ω_+-polariton branch from the above consideration. Admittedly, a universe with a scale factor given by Eq. (5.27) is a bit odd, especially with Ω as determined by Eq. (5.19). Such a universe would first contract a little, followed by a small expansion back to its original scale. Nonetheless, light in such a medium still acts as a quantum field on curved spacetime, and we can gain insight about the mechanism in which particles are created. However, particle creation in a particular cosmology remains inaccessible in this scenario.

5.2 ε-near-zero metamaterials

Whether or not we can connect the phenomenology of electromagnetism in time-dependent optical media to the scalar fields in an expanding universe, the probability of exciting photon pairs in this scenario is vanishingly small. The reason for this is two-fold. As can be seen in Fig. 5.1, the quicker the change in refractive index, the more polaritons are excited from the light-matter vacuum. Perhaps more importantly however, in most materials the maximum change in the refractive index obtainable is in the order of 10^{-3}, compared to a background refractive index of order unity. Indeed, in most materials the changes to the refractive index in time is so small [139] that quantum effects of time-dependent backgrounds become inaccessible. Up until recently, this has made some of the physics discussed in this thesis hard to

[7] This heavily restricts the dynamics in one direction.

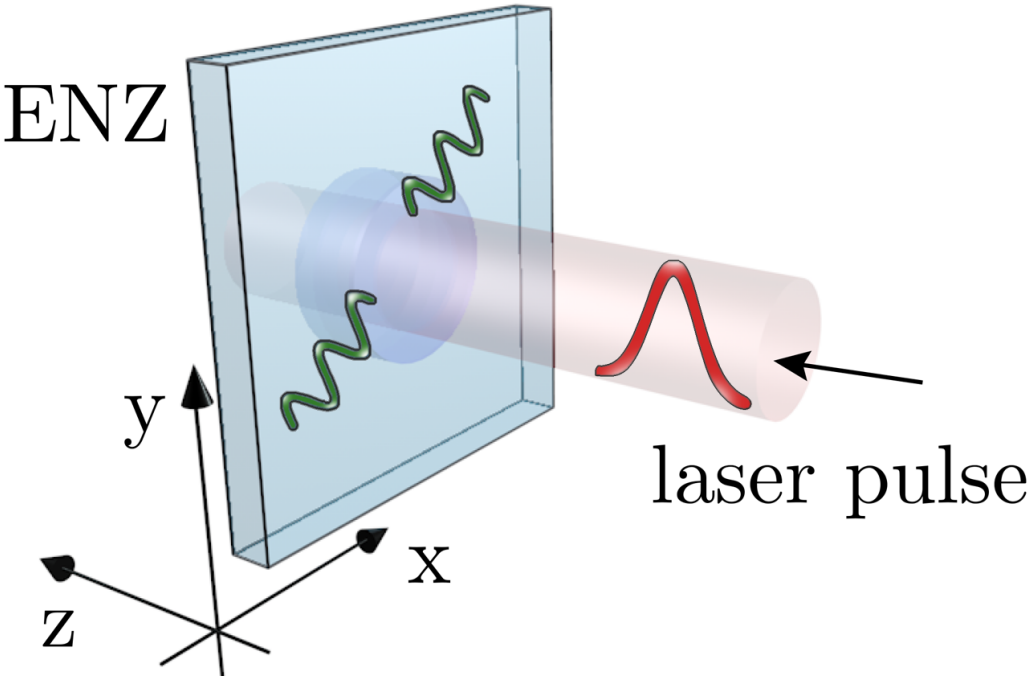

Figure 5.2: Schematic of set-up, where the permittivity of the ENZ metamaterial is changed in time by a strong laser pulse, and quantum vacuum radiation is consequently emitted inside the material. Figure adapted from Ref. [71].

access experimentally, at least in bulk media.[8] Recent years have however, brought the advent of so-called ε-near-zero metamaterials whose background refractive index passes close to zero [140–142] at some wavelength. Around this wavelength, the nonlinear response is also strongly enhanced, leading to a time-dependent refractive index that change from ~ 0.1 to ~ 1 within optical timescales [96, 132]. These materials have thus opened up interest into quantum vacuum radiation beyond first order in perturbation theory, which we studied in Chapter 3. However, absorption cannot be completely neglected in these materials, in fact, absorption also becomes time-dependent.

We explored this in Ref. [71] (Item 3 in the List of Publications), focusing on the physics of quantum vacuum radiation in these materials rather than the connection to analogue gravity. As mentioned earlier, the theoretical work here was done together with Dr Angus Prain. The combination of dispersion, absorption and large changes to the optical properties introduces some theoretical challenges however, and to make the calculations tractable we focused on tackling the large changes, and its spectral dependence, into account. Indeed, the following chapter (Ch. 6) will be focused on putting this work on firmer theoretical footing. As such, what we will discuss here should be seen as valid in a qualitative sense. In particular, we assumed that the time-delayed response of the medium does not qualitatively affect

[8] Similar physics has however been addressed in optical microcavities, such as those investigated in Refs. [84–88]. In those studies, the cavity enabled a strong light-matter coupling regime whose coupling strength the Rabi frequency (here the plasma frequency) was modulated in time.

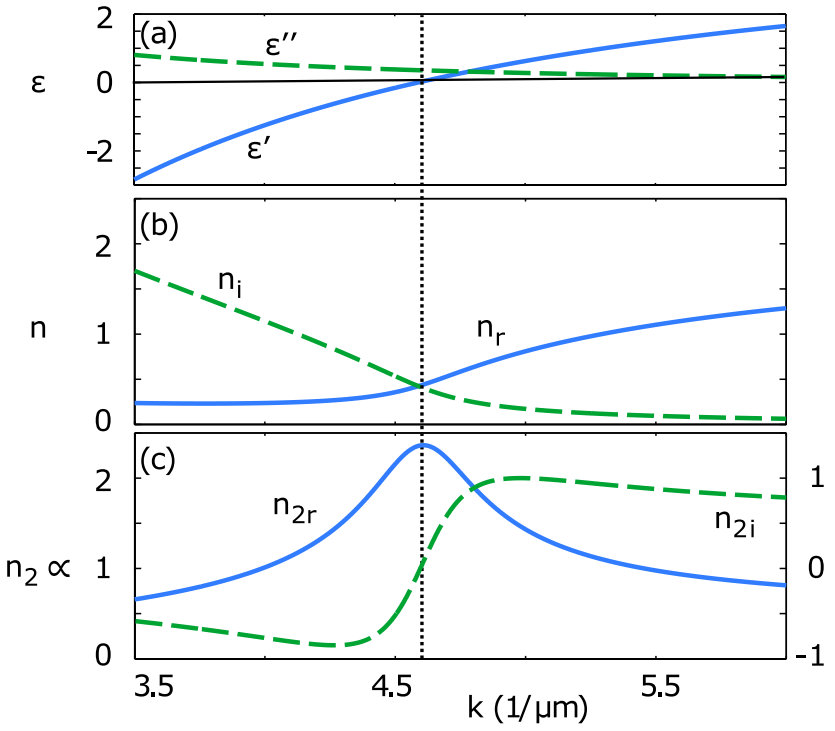

Figure 5.3: **(a)** Permittivity of the metamaterial in question, ITO, as a function of vacuum wavenumber. Note that the real permittivity passes through zero at around 4.56 μm^{-1}. **(b)** Corresponding real and imaginary part of the refractive index as a function of vacuum wavenumber. **(c)** The change in refractive index by the strong laser pulse. Note that the real part peaks at ω_{ENZ}. Figure adapted from Ref. [71].

the spectrum, and that absorption simply introduces an overall loss of the photon pair yield.

As has become a staple of this thesis, we will focus on a scenario such as the one seen in Fig. 5.2 where a strong laser pulse changes the medium properties in time, and we study the polaritons excited back-to-back inside the optical medium.[9] We focused on a particular ENZ metamaterial in this study, ITO, whose optical response can be described using a Drude-Lorentz model

$$\varepsilon' + i\varepsilon'' = \varepsilon_\infty - \frac{\omega_p^2}{\omega^2 + i\omega\Gamma}, \tag{5.28}$$

where ω_p is the by-now familiar plasma frequency, and we have introduced the damping rate Γ. Ref. [143] reported $\varepsilon_\infty \simeq 4.082$, $\omega_p^2 \simeq 7.643 \times 10^{30}$ s^{-2} and $\Gamma \simeq 1.239 \times 10^{14}$ s^{-1}, which we will use here. From this we can define a real and imaginary refractive index through

$$n_{0r} + i n_{0i} = \sqrt{\varepsilon' + i\varepsilon''}. \tag{5.29}$$

This is the background index of the material, which is then made to change in time

[9] As an interesting aside we can note that the 2-dimensional character of these materials does help with the connection to analogue gravity, as discussed in the previous section.

through interaction with a strong laser pulse. Thus we can define the total refractive index as $n_r(t) = n_{0r} + n_{2r}I(t)$, and similarly for the imaginary part. Importantly, the nonlinear response [$\propto I(t)$] has been shown [96] to be proportional to the linear refractive index as

$$n_{2r} \propto \left(\frac{n_{0r} + n_{0i}}{n_{0r}^2 + n_{0i}^2}\right),$$
$$n_{2i} \propto \left(\frac{n_{0r} - n_{0i}}{n_{0r}^2 + n_{0i}^2}\right). \tag{5.30}$$

The dispersion relation for ITO can be seen in Fig. 5.3(a) and (b), whereas the nonlinear response can be seen in (c) for the intensity used in Ref. [96].

There are, as mentioned, two important optical properties in ENZ metamaterials for the excitation of photons from the light-matter vacuum state. Firstly, we can note that the real permittivity crosses zero at some wavelength, at approximately

$$\omega_{\rm ENZ} \simeq \sqrt{\frac{\omega_p^2 - \Gamma^2}{\varepsilon_\infty}}, \tag{5.31}$$

which in this material occurs at 1377 nm. This is marked in Fig. 5.3, by the vertical dotted line. Note that Ref. [71] has a minor error in this expression.

To model this, and extract the number of photons emitted from the quantum vacuum in realistic scenarios, we turn directly to the electric field wave equation in macroscopic quantum electrodynamics. Specifically, let us once again expand in some suitable polarisation vectors $\mathbf{e}_\lambda$ such that $\mathbf{E}(t,\mathbf{x}) = \sum_\lambda E_\lambda(t,\mathbf{x})\mathbf{e}_\lambda$. We can then treat the electric field in each mode polarisation E_λ independently. Furthermore, since the medium in question is uniform and isotropic, the dynamics of each polarisation will be identical and we can for notational simplicity ignore the λ-subscript. Also let us for now assume that the refractive index is constant in time. This yields

$$-\nabla^2 E(t,\mathbf{x}) + \frac{1}{c^2}\partial_t^2\left(E(t,\mathbf{x}) + \int_{-\infty}^{t} ds\ \chi(t-s)E(s,\mathbf{x})\right) = 0 \tag{5.32}$$

where $\chi(t)$ is the optical susceptibility, which takes into account the dispersive effects. Now, in this case

$$\chi(\omega) = (\varepsilon_\infty - 1) - \frac{\omega_p^2}{\omega^2 + i\Gamma\omega}. \tag{5.33}$$

This is complex, and we note this is outside the scope of the version of macroscopic quantum electrodynamics studied in Chapter 3. We will return to this issue shortly, and for now simply proceed at a classical level. In frequency space, which we will here for notational simplicity denote using $f_\omega = \int dt\ e^{i\omega t} f(t)$, the equation of motion

for the electric field in Eq. (5.32) is given by

$$\nabla^2 E_\omega + \frac{\omega^2}{c^2}\left(\varepsilon_\infty - \frac{\omega_p^2}{\omega^2 + i\Gamma\omega}\right) E_\omega = 0. \tag{5.34}$$

In momentum space, this yields the dispersion relation

$$-\left|\mathbf{K}\right|^2 + \frac{\omega^2}{c^2}\left(\varepsilon_\infty - \frac{\omega_p^2}{\omega^2 + i\Gamma\omega}\right) = 0, \tag{5.35}$$

where we have defined the in-material wavevector $\mathbf{K}$ to differentiate it from the vacuum wavevector $|\mathbf{k}| = \omega/c$. The reason for this will be clear shortly. From this we can define

$$|\mathbf{K}(\omega)| = \frac{\omega}{c}\left[n_r(\omega) + i n_i(\omega)\right], \tag{5.36}$$

as is usual in optics literature [54]. Now, the above dispersion relation will also define the mode frequencies $\omega(\mathbf{K})$ of the system (the polariton modes). The full form of these are not important for the following but in general they are different from the vacuum frequencies. In order to simplify the problem, let us now assume that the electric field will oscillate close to its vacuum frequency also inside the material such that $|(\omega(\mathbf{K}) - c\,|\mathbf{k}|)| \simeq 0$. We can thus let

$$\omega \to \omega - c\,|\mathbf{k}|$$

and expand to zeroth order in this difference. This constitutes replacing ω inside the susceptibility χ by $c\,|\mathbf{k}|$, or in other words

$$\chi(\omega) \to \chi(c\,|\mathbf{k}|).$$

This allows us to re-write the dispersion relation from Eq. (5.35) as

$$-\omega^2 + \frac{c^2\left|\mathbf{K}\right|^2}{\varepsilon_\infty - \frac{\omega_p^2}{c^2|\mathbf{k}|^2 + i\Gamma c|\mathbf{k}|}} = 0, \tag{5.37}$$

from which we find the equation of motion

$$\partial_t^2 E_{\mathbf{k}} + \frac{c^2\left|\mathbf{K}\right|^2}{\left[n_r(c\,|\mathbf{k}|) + i n_i(c\,|\mathbf{k}|)\right]^2} E_{\mathbf{k}} = 0. \tag{5.38}$$

In essence, the physical difference between Eq. (5.32) and Eq. (5.38) is that the latter keeps the time-delayed response of the medium only to 0^{th}-order. At this

point, let us re-introduce the time-dependent refractive index as given by

$$\begin{aligned} n_r &= n_{0r} + n_{2r} I(t), \\ n_i &= n_{0i} + n_{2i} I(t). \end{aligned} \tag{5.39}$$

It should be noted that this is an approximation, the nature of which we will discuss shortly. This yields an equation of motion of the form

$$\partial_t^2 E_{\mathbf{k}} + \frac{c^2 |\mathbf{K}|^2}{\left[n_r(t) + i n_i(t)\right]^2} E_{\mathbf{k}} = 0. \tag{5.40}$$

Now, for an observer outside the optical medium the in-medium wavevector is related to the vacuum wavevector as

$$|\mathbf{K}| = |\mathbf{k}| \left[n_{0r}(c\,|\mathbf{k}|) + i n_{0i}(c\,|\mathbf{k}|)\right],$$

and we find

$$\partial_t^2 E_{\mathbf{k}} + c^2 |\mathbf{k}|^2 \left(\frac{\left[n_{0r} + i n_{0i}\right]^2}{\left[n_{0r} + n_{2r} I(t) + i \left\{n_{0i} + n_{2i} I(t)\right\}\right]^2} \right) E_{\mathbf{k}} = 0, \tag{5.41}$$

where we should note that n_{0r}, n_{0i}, n_{2r}, and n_{2i} are all evaluated at the vacuum frequency $c\,|\mathbf{k}|$. Importantly, this equation of motion reduces to that of a free plane wave when $I(t) = 0$. We can furthermore define a natural oscillation frequency as

$$\omega_{\mathbf{k}}^2(t) = c^2 |\mathbf{k}|^2 \left(\frac{\left[n_{0r} + i n_{0i}\right]^2}{\left[n_{0r} + n_{2r} I(t) + i \left\{n_{0i} + n_{2i} I(t)\right\}\right]^2} \right), \tag{5.42}$$

using which we arrive at the equation of motion for a harmonic oscillator

$$\partial_t^2 E_{\mathbf{k}} + \omega_{\mathbf{k}}^2(t) E_{\mathbf{k}} = 0. \tag{5.43}$$

This will be our starting point when analysing the spectrum of emitted photon pairs. We should note here that after the completion of Ref. [71], it was pointed out that when re-introducing the time-dependencies through Eq. (5.39), we neglect terms that depend on the derivatives of the permittivity in time, that is $\dot{\varepsilon}(t)$ and $\ddot{\varepsilon}(t)$ where $\varepsilon\left(c|\mathbf{k}|, t\right) = \left[n_{0r} + n_{2r} I(t) + i \left\{n_{0i} + n_{2i} I(t)\right\}\right]^2$.[10] This is indeed the case, and in particular a term of the form $\ddot{\varepsilon}/\varepsilon$ does contribute to the natural oscillation frequency in Eq. (5.42) $[\omega_{\mathbf{k}}^2(t) \to \omega_{\mathbf{k}}^2(t) + \ddot{\varepsilon}/\varepsilon]$. However, the effect of this is quantitative and could be taken into account by choosing a different form of $I(t)$.[11] Importantly, it does not alter the qualitative picture analysed here. This is in line of the approximations made so far. That being said, the addition of these terms

[10] We thank Prof. Claudia Eberlein for this remark.

[11] In fact, we should expect yet more emitted photon pairs.

would make for an interesting future study.

In the following, we will interpret the real part of $\omega_{\mathbf{k}}$ as being responsible for the pair production, whereas the damping is largely ignored here, leading simply to a reduction of the final yield. The latter is of course an obvious approximation. We have thus made a few approximations here, this, along with neglecting the time-delayed response of the ENZ metamaterial. The latter we did when we assumed that $\omega_{\mathbf{K}} - c\,|\mathbf{k}| \simeq 0$. Nevertheless, in light of the discussion in the previous section of this chapter, it is reasonable to assume that the effects of the time-delayed response are negligible for simple time-dependences.

Within these assumptions, let us now explore the spectrum of emitted photon pairs as detected by an observer in the laboratory. In order to do this, let us first quantise Eq. (5.43). Before this we neglect the imaginary part of $\omega_{\mathbf{k}}(t)$ which, as mentioned earlier, we will assume does not contribute to defining quantum vacuum. The method used here relies on this. We can then quantise Eq. (5.43) by replacing the classical amplitude $E_{\mathbf{k}}$ by the operator $\hat{E}_{\mathbf{k}}$, yielding

$$\partial_t^2 \hat{E}_{\mathbf{k}} + \omega_{\mathbf{k}}^2(t)\hat{E}_{\mathbf{k}} = 0. \tag{5.44}$$

As is outlined in, for instance, Refs. [15, 37], we can find the spectrum of quantum vacuum radiation by calculating the so-called Bogoliubov coefficients, the concept of which we will also describe here. Before we proceed however, it should be noted that since we will here consider bulk excitations in a spatially uniform medium, we can simplify the mathematics somewhat by treating the problem quantum mechanically, as opposed to using quantum field theory. This amounts to ignoring the sums over spatial modes, since the uniformity of the problem implies that only back-to-back emission which naturally conserves momentum are possible. We will continue step-by-step, but this should be seen as a review of the method rather than novel results. Nevertheless, as explained in Chapter 2, we can always decompose the electric field operator $\hat{E}_{\mathbf{k}}$ as

$$\hat{E}_{\mathbf{k}} = f_{\mathbf{k}}(t)\hat{a}_{\mathbf{k}} + f_{\mathbf{k}}^*(t)\hat{a}_{\mathbf{k}}^\dagger, \tag{5.45}$$

where $f_{\mathbf{k}}$ satisfies

$$\ddot{f}_{\mathbf{k}} + \omega_{\mathbf{k}}^2(t) f_{\mathbf{k}} = 0. \tag{5.46}$$

Now, these $f_{\mathbf{k}}$ mode functions are normalised using the norm

$$(f, g) = i\Big[f^*\partial_t g - g\partial_t f^*\Big] \tag{5.47}$$

such that $(f_{\mathbf{k}}, f_{\mathbf{k}}) = 1$.[12] Importantly, $f_{\mathbf{k}}$ is chosen with positive norm $(f_{\mathbf{k}}, f_{\mathbf{k}}) > 0$

[12]Note that this is the quantum mechanical version, as we are dealing with the physics of each

in order to preserve the canonical commutation relations for the ladder operators $\hat{a}_{\mathbf{k}}$ and $\hat{a}^\dagger_{\mathbf{k}}$, i.e. $\left[\hat{a}_{\mathbf{k}}, \hat{a}^\dagger_{\mathbf{k}}\right] = 1$. Also, it follows from this that we can define the ladder operators by

$$\begin{aligned}\hat{a}_{\mathbf{k}} &= \left(f_{\mathbf{k}}, \hat{E}_{\mathbf{k}}\right) \\ \hat{a}^\dagger_{\mathbf{k}} &= -\left(f^*_{\mathbf{k}}, \hat{E}_{\mathbf{k}}\right).\end{aligned} \tag{5.48}$$

Finally, suppose that $\omega_{\mathbf{k}}(t)$ is constant in the limits $t \to \pm\infty$ such that

$$\begin{aligned}\lim_{t\to-\infty} \omega_{\mathbf{k}}(t) &= \omega^{\text{in}}_{\mathbf{k}} \\ \lim_{t\to\infty} \omega_{\mathbf{k}}(t) &= \omega^{\text{out}}_{\mathbf{k}}.\end{aligned}$$

We can always decompose the electric field operator $\hat{E}_{\mathbf{k}}$ in any set of ladder operators. In this case, it is natural to define two sets of mode functions, $f_{\mathbf{k}}$ and $g_{\mathbf{k}}$, related to decomposing the electric field operator $E_{\mathbf{k}}$ in terms of the initial and final state operators respectively. In this case, these are

$$\begin{aligned}f_{\mathbf{k}} &= \frac{1}{\sqrt{2\omega^{\text{in}}_{\mathbf{k}}}} e^{-i\omega^{\text{in}}_{\mathbf{k}} t} \\ g_{\mathbf{k}} &= \frac{1}{\sqrt{2\omega^{\text{out}}_{\mathbf{k}}}} e^{-i\omega^{\text{out}}_{\mathbf{k}} t}.\end{aligned} \tag{5.49}$$

We then arrive at the general decomposition for a quantum electric field $\hat{E}_{\mathbf{k}}$:

$$\begin{aligned}\hat{E}_{\mathbf{k}} &= f_{\mathbf{k}}(t)\hat{a}_{\mathbf{k}} + f^*_{\mathbf{k}}(t)\hat{a}^\dagger_{\mathbf{k}} \\ &= g_{\mathbf{k}}(t)\hat{b}_{\mathbf{k}} + g^*_{\mathbf{k}}(t)\hat{b}^\dagger_{\mathbf{k}}.\end{aligned} \tag{5.50}$$

We can now define the initial vacuum state by $\hat{a}_{\mathbf{k}} \left|0\right\rangle_{\text{in}} = 0$. As we are interested in quantum vacuum radiation, we want the initial electric field at time $t \to -\infty$ to be given by ground state

$$\hat{E}^{\text{in}}_{\mathbf{k}} = \frac{e^{-i\omega^{\text{in}}_{\mathbf{k}} t}}{\sqrt{2\omega^{\text{in}}_{\mathbf{k}}}} \hat{a}_{\mathbf{k}}.$$

This mode function $e^{-i\omega^{\text{in}}_{\mathbf{k}}}/\sqrt{2\omega^{\text{in}}_{\mathbf{k}}}$ will then propagate in time according to Eq. (5.46), which has a region where the mode frequency $\omega_{\mathbf{k}}(t)$ depends on time. After the time-dependency has ended, at $t \to \infty$, we must always be able to decompose the mode function into some combination of $g_{\mathbf{k}}$ and $g^*_{\mathbf{k}}$. The process can thus be described

momentum mode $\mathbf{k}$. It straightforwardly generalises to a field by introducing an integral over $d^N x$ in the definition of the norm, along with subsequent dependencies on $\mathbf{x}$. For each momentum mode such a definition reduces to the version used here, which follows from the problem being spatially uniform. As discussed in Section 2.2.4, the spatial uniformity also allows us to use discrete modes $\mathbf{k}$ rather than continuum modes.

schematically as

$$\frac{e^{-i\omega_{\mathbf{k}}^{\text{in}}t}}{\sqrt{2\omega_{\mathbf{k}}^{\text{in}}}} \xleftarrow{t\to-\infty} f_{\mathbf{k}}(t) \xrightarrow{t\to\infty} \alpha_{\mathbf{k}}\frac{e^{-i\omega_{\mathbf{k}}^{\text{out}}t}}{\sqrt{2\omega_{\mathbf{k}}^{\text{out}}}} + \beta_{\mathbf{k}}\frac{e^{+i\omega_{\mathbf{k}}^{\text{out}}t}}{\sqrt{2\omega_{\mathbf{k}}^{\text{out}}}}$$

Therefore we must have

$$f_{\mathbf{k}} = \alpha_{\mathbf{k}} g_{\mathbf{k}} + \beta_{\mathbf{k}} g_{\mathbf{k}}^*, \tag{5.51}$$

where $\alpha_{\mathbf{k}}$ and $\beta_{\mathbf{k}}$ are known as Bogoliubov coefficients. By substituting this into Eq. (5.50), we find

$$\hat{b}_{\mathbf{k}} = \alpha_{\mathbf{k}}\hat{a}_{\mathbf{k}} + \beta_{\mathbf{k}}^*\hat{a}_{\mathbf{k}}^\dagger, \tag{5.52}$$

and it follows that after the temporal variation of the mode frequency the vacuum state has population

$$\langle n_{\mathbf{k}}\rangle = \langle 0|\,\hat{b}_{\mathbf{k}}^\dagger\hat{b}_{\mathbf{k}}\,|0\rangle = |\beta_{\mathbf{k}}|^2\,. \tag{5.53}$$

Thus we find the spectrum of emitted quantum vacuum radiation by calculating the Bogoliubov coefficients $\beta_{\mathbf{k}}$. Now, it follows from Eq. (5.51) that

$$\begin{aligned}\beta_{\mathbf{k}} &= (g_{\mathbf{k}}^*, f_{\mathbf{k}}) \\ &= -\frac{e^{-i\omega_{\mathbf{k}}^{\text{out}}t}}{\sqrt{2\omega_{\mathbf{k}}^{\text{out}}}}\left[\omega_{\mathbf{k}}^{\text{out}} f_{\mathbf{k}} - i\partial_t f_{\mathbf{k}}\right].\end{aligned} \tag{5.54}$$

This is in some sense a measure of the difference between the out-mode frequency $\omega_{\mathbf{k}}^{\text{out}}$ and the instantaneous frequency of the mode function associated with $\hat{a}$ (i.e. annihilation of quanta). The latter is quantified by the ratio $i(\partial_t f_{\mathbf{k}})/f_{\mathbf{k}}$. In the case considered here, $\omega_{\mathbf{k}}^{\text{out}} = \omega_{\mathbf{k}}^{\text{in}} = \omega_{\mathbf{k}}$, and we finally arrive at the Bogoliubov β as given by

$$\beta_{\mathbf{k}} = -\frac{e^{-i\omega_{\mathbf{k}}t}}{\sqrt{2\omega_{\mathbf{k}}}}\left[\omega_{\mathbf{k}} f_{\mathbf{k}} - i\partial_t f_{\mathbf{k}}\right], \tag{5.55}$$

where $f_{\mathbf{k}}$ is given by the solution to

$$\ddot{f}_{\mathbf{k}} + \omega_{\mathbf{k}}^2(t) f_{\mathbf{k}} = 0, \tag{5.56}$$

with $\omega_{\mathbf{k}}^2(t)$ given by the real part of Eq. (5.42), and with the initial condition

$$f_{\mathbf{k}}(t\to-\infty) = \frac{e^{-i\omega_{\mathbf{k}}t}}{\sqrt{2\omega_{\mathbf{k}}}}. \tag{5.57}$$

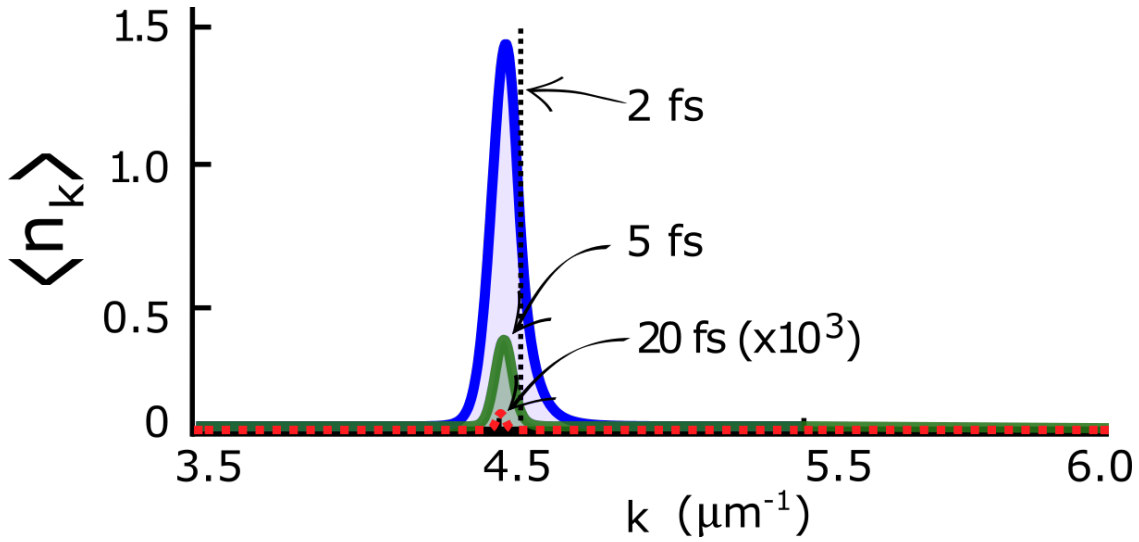

Figure 5.4: Spectrum of quantum vacuum radiation emitted in the ENZ metamaterial, using the change in refractive index from Fig. 5.3(c). Note that it is slightly displaced from $\omega_{\rm ENZ}$, which is denoted by the dashed vertical line. Figure adapted from Ref. [71].

Using this, we arrive at the spectrum seen in Fig. 5.4,[13] where we assume an intensity profile

$$I(t) \propto \mathrm{sech}^2(t/\sigma) \tag{5.58}$$

in Eq. (5.42).

Note that this should be understood as back-to-back emission of photon pairs from the vacuum state. We have here ignored the momentum $\mathbf{k}$ of each mode in the calculation, but this does not change the results. As a reminder, since we are considering the bulk, which is spatially uniform, the inclusion of sums over modes $\mathbf{k}$ would simply lead to the addition of a δ-function such that $\mathbf{k}_1 + \mathbf{k}_2 = 0$, where $\mathbf{k}_{1,2}$ is the momentum of first and second photon in the pair respectively [15]. It should be noted however, that this is a (minor) approximation given that most pump beams will vary slightly spatially.

As can be seen, the peak emission of quantum vacuum radiation is strongly associated with the frequency of zero real permittivity $\omega_{\rm ENZ}$. The reason for this is two-fold. Fig. 5.3 tells us that this is the point in the spectrum when both the background refractive index is the smallest and the temporal change in the refractive index is the largest. In turn, this allows for the largest relative change mode frequency $\Delta\omega_{\mathbf{k}}/\omega_{\mathbf{k}}$, which is the relevant quantity from which $\beta_{\mathbf{k}}$ is determined. Interestingly, this effect contradicts the usual conclusion that emission is centred around $1/\sigma$. In the context of analogue gravity, we should note that this is qual-

[13] In particular, to produce Fig. 5.4 we solve Eq. (5.56) with the initial condition in Eq. (5.57) under the assumption that $\omega^2_{\mathbf{k}}(t)$ is varied in time according to Eq. (5.58), using the *Maple*-software's built in numerical solvers of ordinary differential equations. The Bogoliubov $\beta_{\mathbf{k}}$ can then be extracted using Eq. (5.55), and the spectrum $\langle n_{\mathbf{k}} \rangle$ can be calculated.

itatively different from what we would expect from a scalar field in an expanding universe, where quantum emission would be expected to be strongly tied to the time-scale of driving $1/\sigma$.

If we take a step back, we arrived at this result by neglecting most dispersive effects. First, we should note that this removes the existence of multiple polariton modes, and we have therefore studied only intrabranch quantum vacuum radiation in this work. However, we also neglected the time-delayed response in order to arrive at Eq. (5.40). In particular, we assumed that $|\omega(\mathbf{K})| \simeq c\,|\mathbf{k}|$ throughout the dynamics in order to approximate

$$\frac{\omega_p^2}{\omega^2 + i\Gamma\omega} \simeq \frac{\omega_p^2}{c^2\,|\mathbf{k}|^2 + i\Gamma c\,|\mathbf{k}|}.$$

This is the expansion of the left hand side to the 0^{th} order in the difference $\omega - c\,|\mathbf{k}|$. Indeed, this is the most severe approximation made in this work, but within the range discussed in Fig. 5.4 it is easy to check that

$$-0.1 \lesssim \frac{|\omega(\mathbf{K})| - c|\mathbf{k}|}{c|\mathbf{k}|} \lesssim 0.4$$

for the most photon-like polariton mode. We can therefore assume that the results obtained in Ref. [71] are a decent approximation, and some of the qualitative conclusions are valid. In particular, it is reasonable to assume that emission will indeed be centred around ω_{ENZ}.

We should note that there is a second polariton mode in the system, associated with the matter degree of freedom, which oscillates at low frequency. We learned in Chapter 3 that low energy modes are most likely to be involved in interbranch vacuum radiation, and it is therefore feasible that this mode will play an interesting role in the physics of ENZ metamaterials also.

In addition to this, we have assumed that only the real part of the mode frequency $\omega_{\mathbf{k}}(t)$ plays a role, and the imaginary part will only act as a damping factor. This was necessary in order to formulate the theory in terms of mode operators. It is a physically motivated assumption, but it is nonetheless a crude approximation for the dissipative physics. In the next chapter (Ch. 6), we will return to this, and treat the dissipative physics with more care. Finally, we should note that we would expect this damping to reduce the average population $\langle n_{\mathbf{k}} \rangle$ by roughly a factor of 10 for each micron propagated in the medium. This will greatly reduce the number of potentially observable photons, unless they are out-coupled in an efficient manner.

5.3 Lessons from the intermission

It might be worth re-connecting the result of the previous section to the start of this chapter. We turned to ε-near-zero metamaterials in order to access large changes in the optical characteristics in time. However, whilst these materials have a rich phenomenology of quantum vacuum radiation, it obscured the connection to a scalar field in an expanding universe. Indeed, we found a spectrum of emitted radiation [Fig. 5.4] quite unlike the spectrum expected for a scalar field in an expanding/contracting universe [Fig. 5.1]. The approximations made in deriving the ENZ vacuum radiation spectrum further obscures any direct connection to a scalar field. However, purely at a level of the equations of motion we can still find some links, and an explanation for the qualitative difference between the spectra.

Each momentum mode of a massive scalar field obeys the equation of motion

$$\ddot{\phi}_{\mathbf{k}} + \left[|\mathbf{k}|^2 + m^2 a^2 - \frac{1}{2}\left(\frac{\ddot{a}}{a} - \frac{\dot{a}^2}{2a^2} \right) \right] \phi_{\mathbf{k}} = 0 \tag{5.59}$$

in a 2+1 dimensional expanding universe with metric

$$ds^2 = a(\eta)^2 \left[-dt^2 + dx^2 + dy^2 \right] \tag{5.60}$$

which is written in conformal time. We have here suitably re-scaled the scalar field in order to eliminate 1$^{\text{st}}$-order time-derivatives.[14] We can compare this to the mode equation for the electric field in Eq. (5.43). As discussed in the previous section, the quantum vacuum radiation is usually determined by a combination of the time-scale of the temporal variation in the mode frequency (say $1/\sigma$) and the relative amplitude of the mode frequency variation (say $\Delta\omega_{\mathbf{k}}/\omega_{\mathbf{k}}$). We noted that the latter effect completely suppresses the former in an ENZ material, and emission is peaked in the region where $\Delta\omega_{\mathbf{k}}/\omega_{\mathbf{k}}$ peaks. For scalar fields on the other hand, this ratio is firmly peaked at zero momentum: it is much easier to excite low energy modes than high energy ones. Therefore we expect the time-scale to dominate the emission spectra instead. Thus, ENZ physics is of little relevance to cosmology, but it is an interesting link.

Finally, we should note that time-dependent ε-near-zero metamaterials offer an intriguing window into quantum vacuum radiation that is worth exploring further. We expect that the approximations made will be valid to leading order, but the effects of dispersion and dissipation are to be explored further.

[14] We start with $\left[\nabla_\mu \nabla^\mu - m^2\right] \Phi = 0$ using the metric in Eq. (5.60), and we define $\phi = a^{1/2}\Phi$.

Chapter 6

Macroscopic QED as a trapped particle in a magnetic field

"All theoretical physics is in the end Gaussian integrals and harmonic oscillators - they're the only problems we seem able to solve!"

Prof. Luigi Del Debbio, tutorial 'Adv. Stat. Phys.', Higgs Centre, 2015

Moving beyond small variations to the refractive index, which we explored in Chapter 3 is a considerable task. In this chapter, we find that macroscopic quantum electrodynamics can be mapped to a quantum harmonic oscillator in a magnetic field — the wavenumber of light and the resonance will act as the two harmonic trap frequencies, and the dipolar coupling serves as a magnetic field. Whilst this trapped 'particle' in a magnetic field lives in functional space, it is still possible to transfer the intuition gained from other studies of the problem. In particular, we will show that the complete problem can be solved semi-analytically; that is, we can exactly solve the dynamics of the system in terms of some coupled ordinary differential equations. In the case of a static medium the equations can be solved exactly, whereas for more complicated scenarios we must rely on numerical methods. This chapter is based on research notes, which have yet to be compiled into a publication.

6.1 A return to the Hopfield action

Let us start by returning to the action outlined in Eq. (3.13) (p. 36). To recap, this is a phenomenological model that describes the electromagnetic vector potential, $\mathbf{A}$, coupled to a set of harmonic oscillators $\mathbf{R}_i$. The latter models an optical medium with resonances set by the natural oscillation frequencies Ω_i of the oscillators. We will refer to this model as the Hopfield model of macroscopic quantum electrodynamics. For simplicity, let us in this chapter focus on media that can be described by a single resonance frequency Ω, and we therefore need only to keep a single oscillator $\mathbf{R}$. Diamond is a good example of such a medium. Furthermore, let us also assume that we want to describe bulk media. As such we assume that the oscillator frequency Ω can depend on time but not space. In this case, Eq. (3.13)

(p. 36) reduces to

$$\begin{aligned} S_\gamma &= \int_{t_i}^{t_f} dt \int d^3x \, \frac{1}{2}\left[\dot{\mathbf{A}}^2 - (\boldsymbol{\nabla}\times\mathbf{A})^2\right], \\ S_R &= \int_{t_i}^{t_f} dt \int d^3x \, \frac{\rho}{2}\left[\dot{\mathbf{R}}^2 - \Omega^2(t)\mathbf{R}^2\right], \\ S_{\text{int}} &= \int_{t_i}^{t_f} dt \int d^3x \; (-\rho q) \; \dot{\mathbf{A}}\cdot\mathbf{R}, \end{aligned} \tag{6.1}$$

where once again ρ is the density of the oscillator $\mathbf{R}$, and q is its dipole moment. In this chapter, we will as before work in units where $c = 1$, $\varepsilon_0 = 1$, and $\hbar = 1$. In addition to this we will, for the purpose of notational simplicity, work in units of time scaled by $1/\Omega_{\text{ref}}$, where Ω_{ref} is some reference frequency. In other words, we will use the dimensionless time

$$\tau = \Omega_{\text{ref}}\, t,$$

as well as rescale both the vector potential $\mathbf{A}$ and the oscillator $\mathbf{R}$ as

$$\begin{aligned} \mathbf{A} &\to \mathbf{A}/\sqrt{\Omega_{\text{ref}}}, \\ \mathbf{R} &\to \mathbf{R}/\sqrt{\rho\Omega_{\text{ref}}}. \end{aligned}$$

We can then further expand the vector potential in some set of two polarisation vectors

$$\mathbf{A}(\mathbf{x}) = \sum_{\lambda=1,2} A_\lambda(\mathbf{x})\, \mathbf{e}_\lambda \tag{6.2}$$

where $\mathbf{e}_\lambda \cdot \mathbf{e}_{\lambda'} = \delta_{\lambda,\lambda'}$. Through this we find the simplified action which, written in momentum space,[1] takes the form

$$\begin{aligned} S_\gamma^{\mathbf{k}} &= \frac{1}{2}\int_0^T d\tau \; |\dot{A}_{\mathbf{k}}|^2 - k^2|A_{\mathbf{k}}|^2, \\ S_R &= \frac{1}{2}\int_0^T d\tau \; \dot{R}^2 - \Omega^2(\tau)R^2, \\ S_I^{\mathbf{k}} &= -\frac{g}{2}\int_0^T d\tau \; \left[\dot{A}_{\mathbf{k}} + \dot{A}_{\mathbf{k}}^*\right] R. \end{aligned} \tag{6.3}$$

Note that the full electromagnetic action is given by $S_{\gamma+I} = \sum_{\mathbf{k}} S_{\gamma+I}^{\mathbf{k}}$. However, we can here treat each spatial mode $\mathbf{k}$ independently, since we are considering a spatially uniform oscillator frequency Ω and no transition between spatial modes are

[1] Here we use the convention

$$f(\mathbf{x},t) = \int \frac{d^3k}{(2\pi)^3} e^{i\mathbf{k}\cdot\mathbf{x}} f_{\mathbf{k}}(t).$$

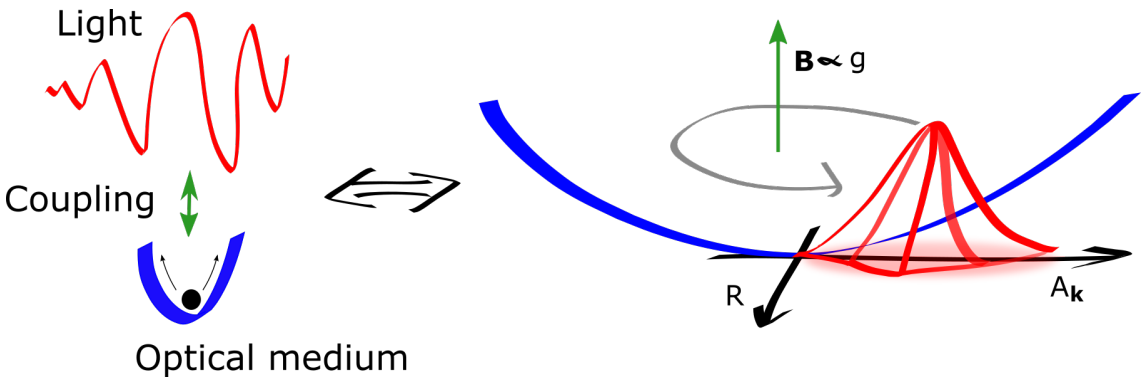

Figure 6.1: To the left is a representation of macroscopic quantum electrodynamics, as interpreted as light coupled to an harmonic oscillator. This is equivalent to considering a trapped particle in a magnetic field, as can be seen on the right hand side, where the position in the trap is the field amplitude and the coupling acts as a magnetic field.

therefore allowed.[2] With this in mind, we will in the following omit the superscript $\mathbf{k}$ in the action for notational simplicity. Also, we have here defined the scaled plasma frequency of the medium $g = \sqrt{\rho}q/\Omega_{\text{ref}}$, and symmetrised the interaction term for reasons we will discuss later. In order to keep notation simple, we have furthermore implicitly defined the unit-less variants of k and Ω from the unit-full quantities used in Eq. (6.1) by letting

$$\begin{aligned} k/\Omega_{\text{ref}} &\to k, \\ \Omega/\Omega_{\text{ref}} &\to \Omega. \end{aligned} \tag{6.4}$$

Finally, we have chosen $t_i = 0$ and $t_f = \Omega_{\text{ref}}T$ for similar reasons. This action will yield the familiar dispersion relation

$$-\mathbf{k}^2 + \omega^2\left(1 - \frac{g^2}{\omega^2 - \Omega^2}\right) = 0, \tag{6.5}$$

which is the reduction of Eq. (3.2) (p. 34) in Chapter 3 to a single resonance frequency. In this chapter, we will not switch to polariton variables, as was previously done in Chapter 3 (p. 45), but instead solve the system directly.

6.2 Connection to harmonic oscillators

As we will see, we can directly map the physics of macroscopic quantum electrodynamics to the physics of a trapped particle in a magnetic field, with the coupling playing the role of the magnetic field. Importantly, as the former is a well-studied problem [98, 144, 145], linked to quantum Hall physics [146] amongst other things, we can use the intuition obtained from these studies in understanding the physics

[2] This is further discussed in Section 2.2.3.

of macroscopic QED.

Let us start by defining a pair of real variables for the vector potential $A_{\mathbf{k}}$ such that

$$\begin{aligned} A_{\mathbf{k}} &= x_{\mathbf{k}} + iy_{\mathbf{k}}, \\ A^*_{\mathbf{k}} &= x_{\mathbf{k}} - iy_{\mathbf{k}}. \end{aligned} \tag{6.6}$$

The physical interpretation of these coordinates $x_{\mathbf{k}}$ and $y_{\mathbf{k}}$ is somewhat obtuse, but we should nonetheless note a few features. We can first note that $A_{\mathbf{k}}$ and $A^*_{\mathbf{k}}$ propagate in opposite directions. Therefore, interpreting the combination of $x_{\mathbf{k}}$ and $y_{\mathbf{k}}$ depends on the relative sign, where the same-sign-between-$x_{\mathbf{k}}$-and-$y_{\mathbf{k}}$ photon propagates in the $\mathbf{k}$-direction, and vice-versa. Also note that the magnitude of the vector potential is given as $|A_{\mathbf{k}}| = \sqrt{x^2_{\mathbf{k}} + y^2_{\mathbf{k}}}$, whereas its phase is determined by $\theta = \arctan\left(y_{\mathbf{k}}/x_{\mathbf{k}}\right)$.[3]

Regardless of the physical interpretation, these coordinates are a very useful representation. The action in Eq. (6.3) now becomes

$$\begin{aligned} S_{\gamma+R} &= \frac{1}{2}\int_0^T d\tau \ \left[\dot{x}^2_{\mathbf{k}} - k^2 x^2_{\mathbf{k}}\right] + \left[\dot{y}^2_{\mathbf{k}} - k^2 y^2_{\mathbf{k}}\right] + \left[\dot{R}^2 - \Omega^2 R^2\right] \\ S_I &= -\frac{g}{2}\int_0^T d\tau \ \left[\dot{A}_{\mathbf{k}} + \dot{A}^*_{\mathbf{k}}\right] R = -g\int_0^T d\tau \ \dot{x}_{\mathbf{k}} R = \frac{g}{2}\int_0^T d\tau \ \left(x_{\mathbf{k}}\dot{R} - \dot{x}_{\mathbf{k}} R\right), \end{aligned}$$

where we integrated by parts in the last step. We can now introduce the position and magnetic field vectors

$$\begin{aligned} \mathbf{q} &= (x_{\mathbf{k}}, y_{\mathbf{k}}, R) \\ \mathbf{B} &= (0, -g, 0)\,, \end{aligned} \tag{6.7}$$

respectively, as well as the trapping matrix

$$A^2 = \begin{pmatrix} k^2 & 0 & 0 \\ 0 & k^2 & 0 \\ 0 & 0 & \Omega^2 \end{pmatrix} \tag{6.8}$$

in order to rewrite the action further. After some algebra, this yields

$$S_{\gamma+R+I} = \int_0^T d\tau \ \frac{1}{2}\dot{\mathbf{q}}^2 - \frac{1}{2}\mathbf{q}\cdot A^2 \cdot \mathbf{q} + \frac{1}{2}\left(\mathbf{B}\times\mathbf{q}\right)\cdot\dot{\mathbf{q}}. \tag{6.9}$$

We can recognise this as a charged particle trapped in a quadratic potential in the presence of a magnetic field. A visual representation of this link can be found in Fig. 6.1. Interestingly, in this representation, the dipolar coupling between light and the oscillator acts as a magnetic field, whereas the respective field amplitude maps

[3]The vector potential can thus be decomposed as $A_{\mathbf{k}} = |A_{\mathbf{k}}|e^{i\theta}$.

onto a position in the harmonic well. Quantising this follows as usual, but we must take care to allow A^2 to be time-dependent. We will here use a generalisation of the work by Davies [147].

6.3 Quantisation

We now wish to quantise the Hopfield system in terms of the real variables introduced in Section 6.2. A path integral quantisation procedure is formally given by

$$\langle \mathbf{b}, T|\mathbf{a}, 0\rangle = \int_{\mathbf{q}(0)=\mathbf{a}}^{\mathbf{q}(T)=\mathbf{b}} \mathcal{D}\mathbf{q}\; e^{iS_{\gamma+R+I}[\mathbf{q}]}, \tag{6.10}$$

where $S_{\gamma+R+I}$ is the action given in Eq. (6.9). The path integral sums over all paths of $\mathbf{q}$ that start in position $\mathbf{a}$ at time $\tau = 0$ and finish in position $\mathbf{b}$ at time $\tau = T$.

However, as this is a quadratic action, it can be quantised by finding the classical action, and then calculating the Morette-van Hove determinant [98]. This procedure was discussed in detail in Section 2.1.4.2 (p. 20), as well as Section 3.3, of this thesis, and we will here go through similar steps. Therefore, if we let $\mathbf{q}(T) = \mathbf{b}$ and $\mathbf{q}(0) = \mathbf{a}$, then we find that the transition amplitude is given by

$$\langle \mathbf{b}, T|\mathbf{a}, 0\rangle = \frac{1}{(2\pi i)^{3/2}} \left| -\frac{\partial^2 S_{\mathrm{cl}}}{\partial b_j \partial a_k} \right|^{1/2} e^{iS_{\mathrm{cl}}}, \tag{6.11}$$

where S_{cl} is the action in Eq. (6.9) evaluated for the classical solution, and where $\partial/\partial b_j$ is shorthand for the derivative with respect to the j^{th} component of $\mathbf{b}$ (and likewise for $\mathbf{a}$). As a reminder, Eq. (6.11) gives the probability amplitude for the oscillator to start in position $\mathbf{a}$ at time $\tau = 0$ and finish in position $\mathbf{b}$ at time $\tau = T$. This can then be used to calculate the time-propagation of an initial wavepacket, as discussed in Section 2.1.2, and as we have previously done in Chapter 3 (see for instance p. 50). We must therefore first find the classical action in order to quantise this problem. And to do this, we must solve the classical equations of motion, given by

$$\ddot{\mathbf{q}} + \mathbf{B} \times \dot{\mathbf{q}} + A^2(s)\mathbf{q} = 0, \tag{6.12}$$

with boundary values $\mathbf{q}(T) = \mathbf{b}$ and $\mathbf{q}(0) = \mathbf{a}$. We can however, transform this to an initial value problem, by first defining the vector

$$\boldsymbol{\xi}(s) = \left(\mathbf{q}(s), \dot{\mathbf{q}}(s)\right), \tag{6.13}$$

where we note that $\boldsymbol{\xi}$ here is a 6-by-1 vector. The equations of motion can then be

written as

$$\dot{\boldsymbol{\xi}}(s) = \begin{pmatrix} 0 & \mathbb{I} \\ -A^2(s) & -B \end{pmatrix} \boldsymbol{\xi}(s), \tag{6.14}$$

where $\mathbb{I}$ is the identity matrix, and we have defined the matrix B such that $B\mathbf{z} = \mathbf{B} \times \mathbf{z}$ for all $\mathbf{z} \in \mathbb{R}^3$. In this case, this yields

$$B = \begin{pmatrix} 0 & 0 & -g \\ 0 & 0 & 0 \\ g & 0 & 0 \end{pmatrix}. \tag{6.15}$$

Furthermore, let us introduce the block matrix $\begin{pmatrix} E(s) & F(s) \\ G(s) & H(s) \end{pmatrix}$ whose elements E, F, G, H are matrices themselves such that

$$\boldsymbol{\xi}(s) = \begin{pmatrix} E(s) & F(s) \\ G(s) & H(s) \end{pmatrix} \boldsymbol{\xi}(0). \tag{6.16}$$

In this formalism, the equation of motion Eq. (6.14) can be written as

$$\begin{pmatrix} \dot{E}(s) & \dot{F}(s) \\ \dot{G}(s) & \dot{H}(s) \end{pmatrix} = \begin{pmatrix} 0 & \mathbb{I} \\ -A^2(s) & -B \end{pmatrix} \begin{pmatrix} E(s) & F(s) \\ G(s) & H(s) \end{pmatrix} \tag{6.17}$$

together with the initial values

$$\begin{pmatrix} E(0) & F(0) \\ G(0) & H(0) \end{pmatrix} = \begin{pmatrix} \mathbb{I} & 0 \\ 0 & \mathbb{I} \end{pmatrix}.$$

It now follows that

$$\begin{aligned} \dot{\mathbf{q}}(0) &= F^{-1}(T)\mathbf{q}(T) - F^{-1}(T)E(T)\mathbf{q}(0), \\ \dot{\mathbf{q}}(T) &= H(T)F^{-1}\mathbf{q}(T) + \left[G(T) - H(T)F^{-1}(T)E(T)\right]\mathbf{q}(0). \end{aligned}$$

If we assume that the effective magnetic field is constant, i.e. g does not change in time, we can show that

$$G(T) - H(T)F^{-1}(T)E(T) = -F^{-T}, \tag{6.18}$$

with which we find

$$\begin{aligned} \dot{\mathbf{q}}(0) &= F^{-1}(T)\mathbf{q}(T) - F^{-1}(T)E(T)\mathbf{q}(0), \\ \dot{\mathbf{q}}(T) &= H(T)F^{-1}\mathbf{q}(T) - F^{-T}(T)\mathbf{q}(0), \end{aligned} \tag{6.19}$$

where F^{-T} denotes the transpose of the inverse of F.[4]

As usual, the classical action in Eq. (6.9) can be integrated by parts, and after using the equation of motion, we find

$$S_{\rm cl} = \frac{1}{2}\left[\mathbf{q}(T)\cdot\dot{\mathbf{q}}(T) - \mathbf{q}(0)\cdot\dot{\mathbf{q}}(0)\right].$$

Finally, using Eq. (6.19), we find that

$$S_{\rm cl} = \frac{1}{2}\left[\mathbf{b}\cdot\dot{F}F^{-1}\cdot\mathbf{b} + \mathbf{a}\cdot F^{-1}E\cdot\mathbf{a} - 2\mathbf{a}\cdot F^{-1}\cdot\mathbf{b}\right]. \tag{6.20}$$

Here

$$\frac{d^2F}{ds^2} + B\frac{dF}{ds} + A^2(s)F = 0, \tag{6.21}$$

with $F(0) = 0$ and $\dot{F}(0) = I$, and

$$\frac{d^2E}{ds^2} + B\frac{dE}{ds} + A^2(s)E = 0, \tag{6.22}$$

with $E(0) = I$ and $\dot{E}(0) = 0$. For clarity, here we use

$$A^2 = \begin{pmatrix} k^2 & 0 & 0 \\ 0 & k^2 & 0 \\ 0 & 0 & \Omega^2(s) \end{pmatrix}, \qquad B = \begin{pmatrix} 0 & 0 & -g \\ 0 & 0 & 0 \\ g & 0 & 0 \end{pmatrix}.$$

This completely specifies the classical action in terms of matrix equations, which in

[4] In order to prove this, let us define

$$\begin{pmatrix} P & Q \\ R & S \end{pmatrix} = \begin{pmatrix} E & F \\ G & H \end{pmatrix}^{-1}.$$

Using Eq. (6.17), and known rules regarding the algebra of matrices, we find that

$$\frac{d}{ds}\begin{pmatrix} P & Q \\ R & S \end{pmatrix} = -\begin{pmatrix} P & Q \\ R & S \end{pmatrix}\begin{pmatrix} 0 & \mathbb{I} \\ -A^2(s) & -B \end{pmatrix}, \quad \begin{pmatrix} P(0) & Q(0) \\ R(0) & S(0) \end{pmatrix} = \begin{pmatrix} \mathbb{I} & 0 \\ 0 & \mathbb{I} \end{pmatrix}.$$

In particular, we find that $Q(s)$ satisfies the following equation of motion

$$\ddot{Q} + QA^2(s) - \dot{Q}B = 0$$

where $Q(0) = 0$ and $\dot{Q}(0) = -1$. For this we had to assume that $B \equiv$ constant matrix. In a similar manner we can show that F^T satisfies

$$\ddot{F}^T + F^TA^2(s) - \dot{F}^TB = 0$$

where $F^T(0) = 0$ and $\dot{F}^T(0) = 1$. Here we used that $\left(A^2\right)^T = A^2$ and $B^T = -B$. Now we see that since $-F^T(s)$ and $Q(s)$ satisfy the same equation of motion with the same initial conditions, then by uniqueness they must be the same function. Thus

$$-F^T = Q = -\left(E - FH^{-1}G\right)^{-1}FH^{-1} \Rightarrow -F^{-T}(s) = G(s) - H(s)F^{-1}(s)E(s).$$

general will have to be solved numerically. Throughout this chapter, equations of the form seen in Eqns. (6.21) and (6.22) will be solved numerically using an explicit 4^{th}-order Runge-Kutta method [148, 149], a solver which was written in *MATLAB* for the purpose. The transition amplitude now follows, and we find that

$$\langle \mathbf{b}, T|\mathbf{a}, 0\rangle = \frac{\sqrt{|F^{-1}|}}{(2\pi i)^{3/2}} e^{iS_{\text{cl}}}. \tag{6.23}$$

6.3.1 Comments on the transition amplitude

Importantly, it is easy to check that when $g \to 0$, the transition amplitude in Eq. (6.23) reduces to the transition amplitude for three uncoupled harmonic oscillators. Likewise, when $k \to 0$ and $\Omega \to 0$, we get a free particle in a magnetic field. However, and curiously, there is an imbalance between the real part $x_{\mathbf{k}}$ and imaginary part $y_{\mathbf{k}}$ of $A_{\mathbf{k}}$. In general, the action is rather complicated, but the $y_{\mathbf{k}}^2$-term always has the simple coefficient $\frac{k}{2\sin kT}\cos kT$ of a harmonic oscillator, whereas the corresponding coefficient for $x_{\mathbf{k}}^2$ is much more complex. This seems to be related to the uneven coupling, where $y_{\mathbf{k}}$ does not couple directly to R. Nonetheless, most terms have time-dependences that involve the roots of the dispersion relation Eq. (6.5), which hints that the polaritons are well described by this representation.

Also, we could have chosen a non-symmetrised coupling in the original action Eq. (6.3), such that

$$S_I = -g\int_0^T d\tau\ \dot{A}_{\mathbf{k}} R.$$

This would introduce an imaginary effective magnetic field that couples $y_{\mathbf{k}}$ and R. We can still solve the problem, as it is defined as long as A^2 is positive definite, but the solution looks quite different. The sought after roots of the dispersion relation are, for example, no longer present. The same physics should be represented, just in somewhat oblique terms. In this case, since the difference between the two versions of the action is a total derivative, the transition amplitudes should be connected by a gauge transformation. This is related to the fact that we are dealing with an effective functional 'gauge' field, whose curl yields $\mathbf{B}$.

6.4 The polariton ground state

As it will be useful later, let us compute the ground state wavefunction from the transition amplitude in Eq. (6.23). By definition of the transition amplitude [3] in Eq. (6.23), it can always (for time-independent systems) be expanded in terms of the energy-space wavefunctions $\Psi_{mnp}(\mathbf{q})$. There are three indices here, since we are working with three degrees of freedom $x_{\mathbf{k}}$, $y_{\mathbf{k}}$ and R. Therefore, we can expand

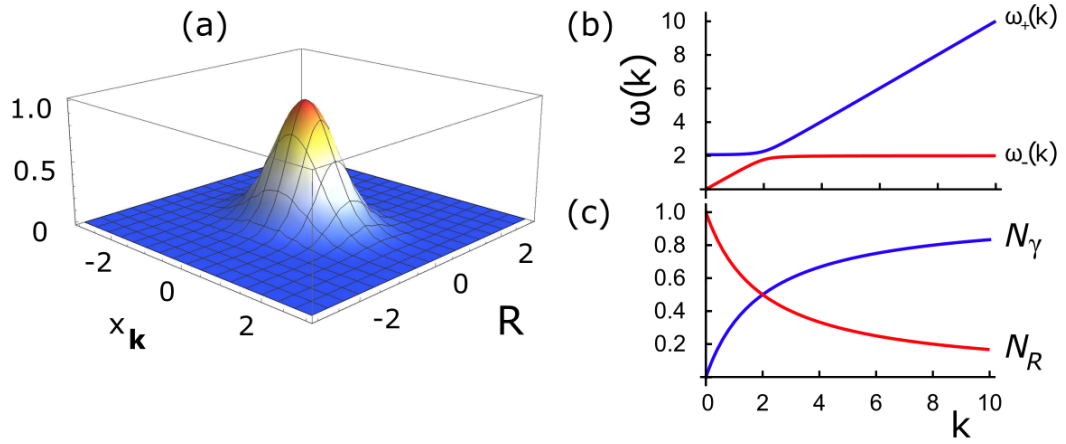

Figure 6.2: **(a)** Unnormalised ground state for $k = 1$, $\Omega = 2$ and $g = 1/2$ in normalised units. As we change k, the width in the photon direction $x_{\mathbf{k}}$ changes. **(b)** Polariton modes in the system. **(c)** Coefficients governing the degree to which the ground state is photon- or matter-like. For instance, at high momenta k, the system is mostly photon like, as N_γ approaches unity and N_R decays to zero.

Eq. (6.23) as

$$\langle \mathbf{b}, T|\mathbf{a}, 0\rangle = \sum_{mnp} e^{-iE_{mnp}T}\Psi^*_{mnp}(\mathbf{b})(\mathbf{q})\Psi_{mnp}(\mathbf{a}). \tag{6.24}$$

If we let $T \to -i\beta$, then

$$\langle \mathbf{b}, -i\beta|\mathbf{a}, 0\rangle = \sum_{mnp} e^{-E_{mnp}\beta}\Psi^*_{mnp}(\mathbf{b})\Psi_{mnp}\mathbf{a} \to e^{-E_{000}\beta}\Psi^*_{000}(\mathbf{b})\Psi_{000}(\mathbf{a}) \text{ as } \beta \to \infty, \tag{6.25}$$

and we can thus extract the ground state wavefunction $\Psi_0(\mathbf{q}) \equiv \Psi_{000}(\mathbf{q})$ from Eq. (6.25) in the limit when $\beta \to \infty$. In other words, in the limit of $\beta \to \infty$, only the ground state remains in the transition amplitude as this decays the slowest. In practise, it is simpler to set $\mathbf{a} = \mathbf{0}$ and then compute the unnormalised ground state wavefunction, which can be done if we ignore the normalisation of the transition amplitude. Naturally, in this we will let $A^2(s) \equiv A^2 =$ constant in order to have a well-defined lowest energy state. We should also note that the dispersion relation in Eq. (6.5) has two solutions $\omega^2_\pm(\mathbf{k})$, given by

$$\omega^2_\pm(\mathbf{k}) = \frac{1}{2}\left(k^2 + \Omega^2 + g^2 \pm \sqrt{(k^2 + \Omega^2 + g^2)^2 - 4k^2\Omega^2}\right). \tag{6.26}$$

These are the natural excitation modes of the system, defining the polaritons we found in Chapter 3 (p. 46), and will be important in the following. An example can be seen in Fig. 6.2(b) for $\Omega = 2$ and $g = 1/2$.

If we return to the classical action in Eq. (6.20), then setting $\mathbf{a} = \mathbf{0}$ yields

$$S_{\text{cl}} = \frac{1}{2}\left[\mathbf{b}\cdot\dot{F}(T)F^{-1}(T)\cdot\mathbf{b}\right] \to \frac{i}{2}\left[\mathbf{b}\cdot\dot{F}(-i\beta)F^{-1}(-i\beta)\cdot\mathbf{b}\right],$$

where we also let $T \to -i\beta$ in the last step. This enters into the transition amplitude as iS_{cl}, implying that

$$\langle \mathbf{b}, -i\beta|\mathbf{0}, 0\rangle \propto \exp\left(-\frac{1}{2}\left[\mathbf{b}\cdot\dot{F}(-i\beta)F^{-1}(-i\beta)\cdot\mathbf{b}\right]\right) \to \Psi_0^{\text{un}}(\mathbf{b}) \text{ as } \beta\to\infty,$$

where we with $\Psi_0^{\text{un}}(\mathbf{b})$ denote the unnormalised version of $\Psi_0(\mathbf{b})$. We can therefore define the ground state matrix $\mathcal{G}$ as

$$\mathcal{G} = \lim_{\beta\to\infty}\left[\dot{F}(-i\beta)F^{-1}(-i\beta)\right].$$

Given F is the solution to Eq. (6.21), we find that this matrix is given by

$$\mathcal{G} = \begin{pmatrix} N_\gamma\left(\omega_+ + \omega_-\right) & 0 & ig\left(\frac{k-\Omega}{k+\Omega}\right) \\ 0 & k & 0 \\ ig\left(\frac{k-\Omega}{k+\Omega}\right) & 0 & N_R\left(\omega_+ + \omega_-\right) \end{pmatrix}, \tag{6.27}$$

where N_γ and N_R are coefficients bounded between 0 and 1. Specifically,

$$N_\gamma = \left(\frac{k}{\Omega}\right)\left(\frac{g^2+(k+\Omega)^2}{2\left(k+\Omega\right)^2} - \frac{g^2+k^2-\Omega^2}{2\left(g^2+(k-\Omega)^2\right)\left(k+\Omega\right)^2}\left(\omega_+-\omega_-\right)^2\right), \tag{6.28}$$

$$N_R = \left(\frac{\Omega}{k}\right)\left(\frac{g^2+(k+\Omega)^2}{2\left(k+\Omega\right)^2} - \frac{g^2-k^2+\Omega^2}{2\left(g^2+(k-\Omega)^2\right)\left(k+\Omega\right)^2}\left(\omega_+-\omega_-\right)^2\right). \tag{6.29}$$

As can be seen in Fig. 6.2(c), where N_γ and N_R are plotted for $\Omega = 2$ and $g = 1/2$, we can interpret these coefficients as corresponding physically to the proportion of photon-component versus matter-component present in the ground state.

We have thus shown that the ground state wavefunction is given by

$$\Psi_0(\mathbf{q}) \propto e^{-\frac{1}{2}\mathbf{q}\cdot\mathcal{G}\cdot\mathbf{q}}.$$

This can then be normalised such that

$$\int d^3q\,|\Psi_0(\mathbf{q})|^2 = 1,$$

from which we find the ground state wavefunction

$$\Psi_0(\mathbf{q}) = \left(|\text{Re}\left[\mathcal{G}\right]|\pi^{-3}\right)^{1/4} e^{-\frac{1}{2}\mathbf{q}\cdot\mathcal{G}\cdot\mathbf{q}}. \tag{6.30}$$

The normalisation is found in the usual manner, where $\text{Re}\left[\mathcal{G}\right]$ is the real part of $\mathcal{G}$.

A plot of a sample (unnormalised) ground state can be seen in Fig. 6.2(a) for $k = 1$, $\Omega = 2$ and $g = 1/2$ in normalised units.

6.4.1 The bare/strongly coupled ground state

Some properties of Eq. (6.27) are noteworthy. When the light-matter coupling goes to zero with $g \simeq 0$, the ground state matrix reduces to the diagonal

$$\mathcal{G}_{\text{bare}} = \begin{pmatrix} k & 0 & 0 \\ 0 & k & 0 \\ 0 & 0 & \Omega \end{pmatrix}, \tag{6.31}$$

as expected for three independent harmonic oscillators. This is the bare ground state of the light-matter vacuum.

In the opposite limit, i.e. the strong-coupling case when $g \gg k, \Omega$, we have to be a bit more careful due to the off-diagonal terms in Eq. (6.27). This is related to the degeneracy of the lowest lying Landau level, where only the co-rotating (ω_+) polariton mode contributes [150].[5] We find the simplest case when $k = \Omega$, given by

$$\mathcal{G} \simeq \mathcal{G}_{\text{Landau}} = \begin{pmatrix} g/2 + \frac{k^2}{g} & 0 & 0 \\ 0 & k & 0 \\ 0 & 0 & g/2 + \frac{k^2}{g} \end{pmatrix}. \tag{6.32}$$

As expected, in the limit of $k/g \to 0$, this is the Landau ground state [151] for a particle in a homogeneous magnetic field.

6.5 Vacuum persistence amplitude

It is now fairly straightforward (at least formally) to calculate the vacuum persistence amplitude, i.e. the probability amplitude that the system remains in the vacuum state after a period during which the oscillator frequency Ω is time-dependent (and subsequently $A^2(s)$ is not constant). It is worth noting that we can ignore the $y_{\mathbf{k}}$ degree of freedom, as it is unaffected by changes to the medium. This reduces the problem to 2-by-2 matrices, simplifying the algebra.

We want to calculate

$$\langle 0|0\rangle = \int_{-\infty}^{\infty} d^3b\, d^3a\, \Psi_0^*(\mathbf{b})\, \langle \mathbf{b}, T|\mathbf{a}, 0\rangle\, \Psi_0(\mathbf{a}). \tag{6.33}$$

This is simply Gaussian integrals, and can be computed. However, we should note

[5] Note that both the co-rotating (ω_+) and the counter-rotating (ω_-) polariton modes contribute to the energy of a harmonic oscillator in a magnetic field. This is not the case for a free particle in a magnetic field ($k \to \Omega \to 0$), where only the co-rotating mode contributes [150]. This is because in this limit Eq. (6.26) becomes $\omega_\pm^2 = \frac{1}{2}\left(g^2 \pm |g^2|\right)$, from which it follows that $\omega_- = 0$.

that whilst it involves positive definite matrices (this has been confirmed numerically), they are not symmetric. We can still solve the integral, but the standard result for a N-dimensional Gaussian integral is altered slightly to become

$$\int_{-\infty}^{\infty} d^N u \; e^{-\frac{1}{2}\mathbf{u}\cdot A\cdot\mathbf{u}+\mathbf{J}\cdot\mathbf{u}} = \sqrt{\frac{(2\pi)^N}{|A_{\rm sym}|}} e^{\frac{1}{2}\mathbf{J}\cdot A^{-1}_{\rm sym}\cdot\mathbf{J}}, \tag{6.34}$$

where $A_{\rm sym} = \left(A + A^{\rm T}\right)/2$ is the symmetric part of A. After reducing to 2-dimensions and some algebra,[6] we find that the vacuum persistence amplitude is given by

$$\langle 0|0\rangle = \left(\frac{2}{i}\right) \sqrt{\frac{|{\rm Re}\left[\mathcal{G}\right]|\,|F^{-1}|}{|\Sigma_F|_{\rm sym}\left|\Sigma_E + F^{-1}\left(\Sigma_F\right)^{-1}_{\rm sym} F^{-T}\right|_{\rm sym}}}, \tag{6.35}$$

where $\Sigma_F = \mathcal{G}^* - i\dot{F}F^{-1}$, $\Sigma_E = \mathcal{G} - iF^{-1}E$, and the subscript 'sym' denotes taking only the symmetric part. The problem is therefore reduced to solving a coupled set of ordinary differential equations and a somewhat significant amount of matrix algebra. Specifically, we first want to solve Eqns. (6.21) and (6.22) where

$$A^2 = \begin{pmatrix} k^2 & 0 \\ 0 & \Omega^2(s) \end{pmatrix}, \qquad B = \begin{pmatrix} 0 & -g \\ g & 0 \end{pmatrix}. \tag{6.36}$$

This is best done numerically, and we will here use a $4^{\rm th}$-order Runge-Kutta method to do so, but it is worth considering the physics implied by the structure of Eq. (6.35).

First of all, let us note that the matrices F and E are the two independent solution to the second order equation in Eq. (6.12), in that any solution to Eq. (6.12) can be constructed as

$$\mathbf{q}(s) = F(s)\mathbf{c}_1 + E(s)\mathbf{c}_2, \tag{6.37}$$

where $\mathbf{c}_{1,2}$ are constant vectors. This is similar to the orthonormal functions in Eq. (2.33) (p. 13), which in turn is used to expand the position operator $\hat{x}$ in terms of ladder operators $\hat{a}$ and $\hat{a}^\dagger$ in Eq. (2.35). However, F and E are not orthonormal according to the norm in Eq. (2.32), although orthonormal functions could be constructed from F and E. Now, we should further note the similarity of these matrices to the Bogoliubov β-coefficients that we calculated in Chapter 5. In particular, recall Eq. (5.55) (p. 107), which we will for clarity repeat here:

$$\beta_{\mathbf{k}} = -\frac{e^{-i\omega_{\mathbf{k}}t}}{\sqrt{2\omega_{\mathbf{k}}}}\left[\omega_{\mathbf{k}} f_{\mathbf{k}} - i\partial_t f_{\mathbf{k}}\right].$$

[6] Note that $\int_{-\infty}^{\infty} d^N u \; d^N v \; e^{-\frac{1}{2}\mathbf{u}\cdot A\cdot\mathbf{u}} e^{\mathbf{u}\cdot B\cdot\mathbf{v}} e^{-\frac{1}{2}\mathbf{v}\cdot C\cdot\mathbf{v}} = \frac{(2\pi)^N}{\sqrt{|C_{\rm sym}|\left|A - BC^{-1}_{\rm sym}B^T\right|_{\rm sym}}}$.

This Bogoliubov β-coefficient is a measure of the difference between the ground state frequency $\omega_{\mathbf{k}}$ and the instantaneous frequency $(-i\partial_t f_{\mathbf{k}})/f_{\mathbf{k}}$. It further relates to the number of excitations in the system through $\langle n_{\mathbf{k}}\rangle = |\beta_{\mathbf{k}}|^2$. We can then note that both $\mathcal{G}$ and $-i\dot{F}F^{-1}$ are matrices of frequencies, the former containing the ground state frequencies whereas the latter represents the instantaneous frequencies in the system. Hence $|\Sigma_F|_{\text{sym}}$ is a measure of the difference between the instantaneous frequency $(-i\dot{F}F^{-1})$ and ground state frequency $(\mathcal{G})$. This holds true similarly for $-iF^{-1}E$. It thus stands to reason that both $|\Sigma_F|_{\text{sym}}$ and $|\Sigma_E|_{\text{sym}}$ are related to the Bogoliubov β-coefficients, and we should not be surprised to see them in the vacuum persistence amplitude.

6.5.1 Periodic modulation

We can now compute the vacuum persistence amplitude by numerically solving Eqns. (6.21) and (6.22) using a 4^{th}-order Runge-Kutta method, and from $1-|\langle 0|0\rangle|^2$ extract the probability to excite quanta in the system. Inspired by Chapter 3,[7] we will consider a time-dependent resonance frequency of the form

$$\Omega^2(s) = \Omega_0^2\left(1 + \left[\alpha_1\cos\nu_1 s + \alpha_2\cos\nu_2 s\right]e^{-\left[s^2/(2\sigma^2)\right]^N}\right), \tag{6.38}$$

where α_i and ν_i are the amplitudes and frequencies of the modulation. Also, σ denotes the duration of the interval in which we modulate the medium, and N is the order of super-Gaussian used (in order to have sharp turn-on/off times). An example of this can be seen in Fig. 6.3(a) for the medium parameters $\Omega_0 = 3$ and $g = 2$, which is modulated using $\alpha_1 = \alpha_2 = 0.1$ for the duration $\sigma = 100$ at frequencies $\nu_1 = 1$ and $\nu_2 = 0.8$. Here we have chosen $N = 10$.

This modulation of the medium resonance frequency produces vacuum radiation, the spectrum of which can be seen in Fig. 6.3(b) (solid blue). At a maximum relative modulation amplitude of 0.1, it can be argued to be slightly non-perturbative. Interestingly, the character of the spectrum is identical to the result of the one found in Chapter 3 [Fig. 3.4, p. 67], where we discussed frequency mixing processes for vacuum radiation at a perturbative level. Note that the spectrum has multiple resonances at mixed modulation frequencies.

As can be seen in Fig. 6.3(b) (dashed green), when we increase the modulation amplitude to $\alpha_1 = \alpha_2 = 0.3$, further resonances become visible in the spectrum. This is not captured qualitatively by 2^{nd}-order perturbation theory, they are higher-order mixing processes, similar to a nonlinear optics spectrum [53]. Note that for this choice of modulation frequencies (ν_1 and ν_2), we access mostly resonances with the ω_- branch. For example, quanta are excited when $\omega_-(\mathbf{k}) = \nu_1/2$. This is the case for both amplitudes chosen. Physically, this means that we are only driving

[7] In particular Eq. (3.49) along with Eq. (3.66).

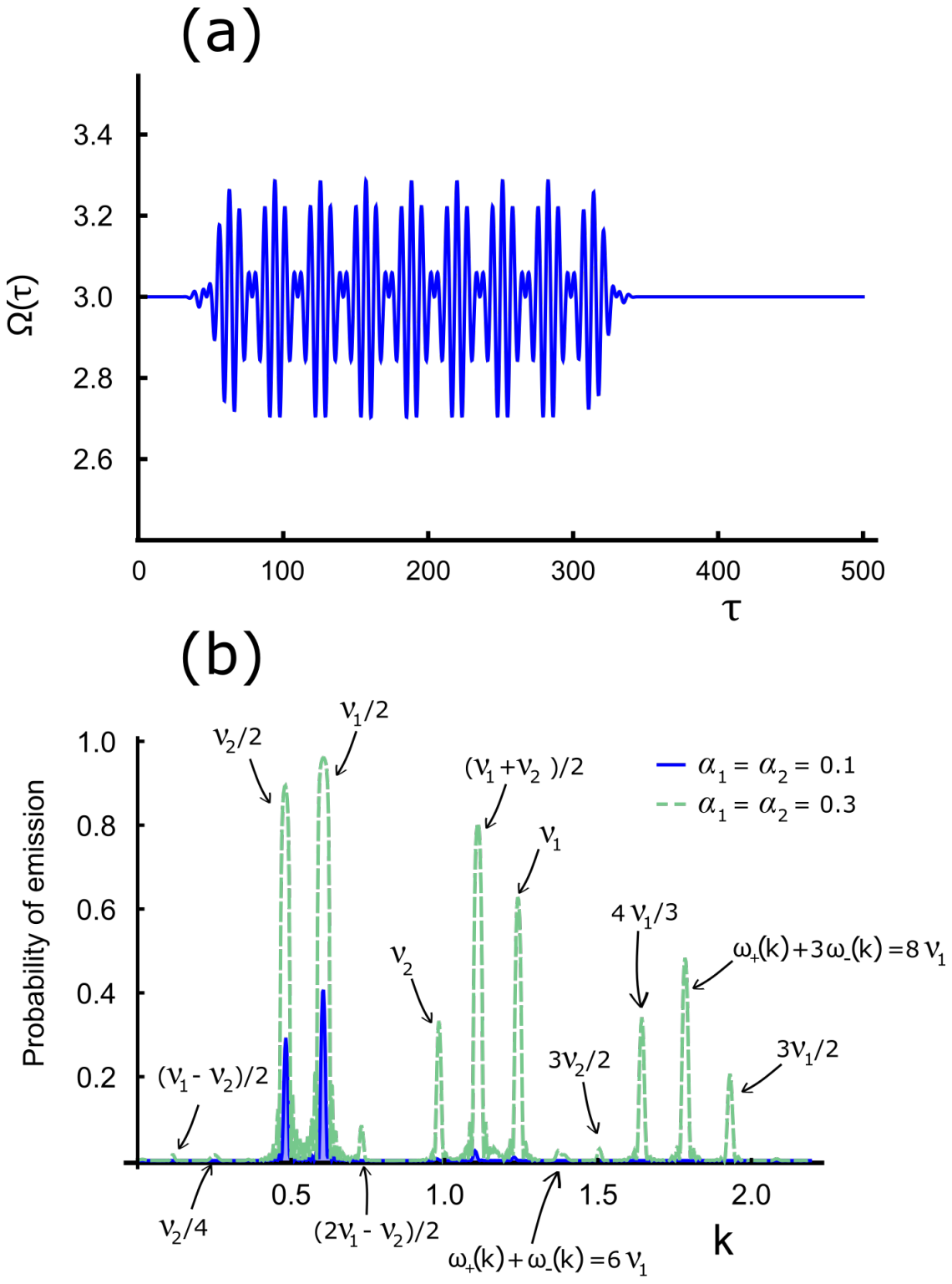

Figure 6.3: **(a)** Modulation of the medium resonance frequency. Here we use $\Omega = 3$ and $g = 2$, and modulated using $\alpha_1 = \alpha_2 = 0.1$ for $\sigma = 100$ with $N = 10$, with $\nu_1 = 1$ and $\nu_2 = 0.8$. **(b)** Vacuum radiation spectrum produced by a time-dependent medium. Here two different amplitudes were used, $\alpha_1 = \alpha_2 = 0.1$ (solid blue) and $\alpha_1 = \alpha_2 = 0.3$ (dashed green). The mixing processes have been labelled accordingly. For this choice of ν_1 and ν_2, we mainly access resonances related to the ω_- branch and have therefore omitted the polariton frequency label unless necessary. In other words, the quanta is excited when for instance $\omega_-(k) = \nu_1/2$.

the photon-like degree of freedom. It is interesting to note that we would expect a larger response from the matter-like degree of freedom, as we are modulating the matter parameters.

6.5.1.1 Classical parametric resonances

Differently to a nonlinear system, the quantum behaviour of the macroscopic QED system is solely determined by the classical solution. This follows from its linearity, as we discussed in Chapter 3. We should therefore be able to understand the resonances discussed in the previous section in the context of classical parametric resonances. This becomes apparent especially if we consider the classical equations of motion in Eq. (6.12), which can be rewritten as

$$\begin{aligned} \ddot{x}_{\mathbf{k}} + k^2 x_{\mathbf{k}} &= -g\dot{R}, \\ \ddot{R} + \Omega^2 \left[1 + f(t)\right] R &= g\dot{x}_{\mathbf{k}}, \end{aligned} \tag{6.39}$$

where we have ignored the equation of motion for $y_{\mathbf{k}}$ as it is uncoupled to matter (and its solution is simply that of a harmonic oscillator). Here, $f(t)$ contains the time-dependence of the resonance frequency of the medium. The formalism of this chapter lends itself to the stability analysis commonly performed when considering parametric resonances.

As is outlined in a book by Arnol'd [152], we are interested in the stability of the matrix $\mathcal{M}$ that connects the system at time $t = 0$ to the later time $t = \tau$, where τ is the period of the modulation, i.e. we look for the matrix $\mathcal{M}$ such that

$$\boldsymbol{\xi}(\tau) = \mathcal{M}\boldsymbol{\xi}(0),$$

where $\boldsymbol{\xi}$ is given by Eq. (6.13). Interestingly, this matrix $\mathcal{M}$ is given by

$$\mathcal{M} = \begin{pmatrix} E(\tau) & F(\tau) \\ G(\tau) & H(\tau) \end{pmatrix}, \tag{6.40}$$

which has already been used extensively. Suppose that we consider a single-frequency modulation such that $f(t) = \alpha \cos(\nu t)$. Then the equation of motion in Eq. (6.39) is the same at times $t = 0$ and $t = 2\pi/\nu$. Therefore $\tau = 2\pi/\nu$.

From Ref. [152], we learn that this map is stable if all eigenvalues of $\mathcal{M}$ are complex, and can therefore be reduced to a rotation, whereas it is unstable if at least one of the eigenvalues is real. As was noted in Ref. [147], the eigenvalues of $\mathcal{M}$ are given by $\exp\left(\pm i\omega_{\pm}\tau\right)$ for a general period τ. This follows because $\pm i\omega_{\pm}$ are the eigenvalues of

$$\begin{pmatrix} 0 & \mathbb{I} \\ -A^2 & -B \end{pmatrix}$$

and from Eq. (6.17) we find that $\exp(\pm i\omega_\pm \tau)$ are the eigenvalues of $\mathcal{M}$. Thus, we see that at least one of the eigenvalues of $\mathcal{M}$ is real when $\exp(\pm i2\pi\omega_\pm/\nu) = \pm 1$, that is, when

$$\omega_\pm = \frac{n\nu}{2}$$

for $n = \mathbb{Z}$. From this we find that we expect quantum vacuum radiation to be emitted when

$$\omega_\pm = \nu/2,\ \nu,\ 3\nu/2,\ 2\nu,\ 5\nu/2, ...$$

at decreasing amplitude. Interestingly, it is not straightforward to analyse the two-frequency modulation in Eq. (6.38) within this framework. This is because the two-frequency modulation is not strictly periodic in either $\tau = 2\pi/\nu_1$ or $\tau = 2\pi/\nu_2$.

6.5.1.2 Fock-Darwin spectrum

Whilst it is possible to understand the spectrum of emitted quantum vacuum radiation in terms of classical parametric resonances, another interpretation might be more natural. In this chapter, we have shown that the dynamics of macroscopic quantum electrodynamics can be directly linked to the dynamics of a harmonically trapped particle in a magnetic field. It follows that it must be possible to decompose any wavefunction into a weighted superposition of the energy state wavefunctions. Now, the energy state space of a trapped particle in a magnetic field is well-studied, and its spectrum is often called the Fock-Darwin spectrum [144, 145]. As is also pointed out in Ref. [147], the states have energies

$$E_{mn} = \left(m + \frac{1}{2}\right)\omega_+ + \left(n + \frac{1}{2}\right)\omega_-,$$

where m and n are positive integers. Therefore, after the modulation of the resonance frequency the final state wavefunction can be decomposed as

$$\Psi(\mathbf{q}) = \sum_{m,n} c_{mn}\Psi_{mn}(\mathbf{q})e^{-iE_{mn}},$$

where $\Psi_{mn}(\mathbf{q})$ is the wavefunction for the state with energy E_{mn}. Here we only have two indices m and n, as compared to three in Eq. (6.24) as we ignore the $y_\mathbf{k}$ degree of freedom, seeing that it is decoupled from the rest of the system. From this we can conclude that quantum vacuum radiation must fulfil

$$\begin{aligned} \Delta E &= \text{energy supplied}, \\ m\omega_+ + n\omega_- &= \text{energy supplied}, \end{aligned}$$

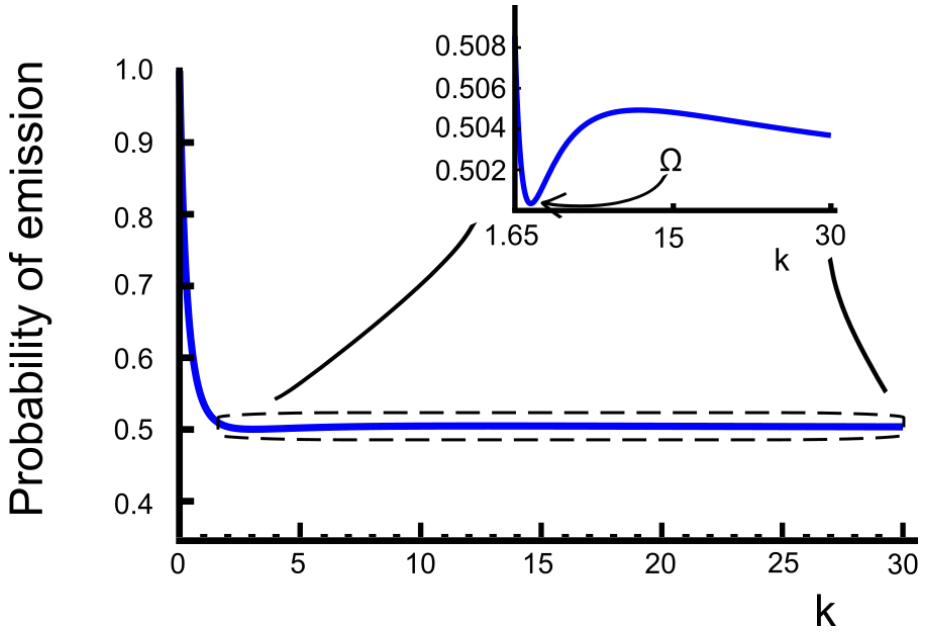

Figure 6.4: Spectrum of a quench.

where m and n are the number of ω_+–polaritons and ω_-–polaritons respectively.

6.5.2 The Schrödinger equation and quenches

So far we have solved the problem for a general oscillator frequency $\Omega(\tau)$ in a path integral language. In the case of quenches,[8] however, we can find a simple answer using the Schrödinger equation. As can be seen, we can use familiar quantum mechanics to solve this quantum field theory problem.

It is easy to see that for the action in Eq. (6.9), we have the Schrödinger equation

$$i\frac{\partial\Psi}{\partial\tau} = \left[-\frac{1}{2}\left(\boldsymbol{\nabla} - i\boldsymbol{\mathcal{A}}\right)^2 + \frac{1}{2}k^2\left(x_{\mathbf{k}}^2 + y_{\mathbf{k}}^2\right) + \frac{1}{2}\Omega^2(\tau)R^2\right]\Psi, \tag{6.41}$$

where we have defined an effective 'gauge' potential $\boldsymbol{\mathcal{A}} = (-gR, 0, gx_{\mathbf{k}})/2$ written in symmetric 'gauge', and where $\boldsymbol{\nabla} = (\partial_{x_{\mathbf{k}}}, \partial_{y_{\mathbf{k}}}, \partial_R)$. Using the Schrödinger equation, it is straightforward to obtain the vacuum persistence amplitude in the case of a quench. Note that this should be seen as a mathematical exercise, useful in order to gain intuition about the system. In reality, no perfect quench is possible.[9] Eq. (6.41) also highlights that we can interpret the dynamics in terms of a functional gauge field $\boldsymbol{\mathcal{A}}$. As we mentioned earlier, we are free to choose another 'gauge' corresponding to the addition of a total derivative to the action, at the cost of a phase change.

6.5.2.1 Quench to bare vacuum

We can thus address the typical scenario of a quench between the polariton vacuum and the bare vacuum, which was considered in a cavity scenario in, for example, Ref. [84]. From the Schrödinger equation we can immediately see that if we change the optical parameters abruptly then the vacuum persistence amplitude is given by

$$\langle 0|0\rangle = \left(\frac{|\mathrm{Re}\left[\mathcal{G}_i\right] \mathrm{Re}\left[\mathcal{G}_f\right]|}{\left(|\mathcal{G}_f^* + \mathcal{G}_i|/2\right)^2} \right)^{1/4},$$

where $\mathcal{G}_i$ and $\mathcal{G}_f$ is $\mathcal{G}$ at the initial time $\tau = 0$ and the final time $\tau = T$, respectively.

Suppose now that we start in the polariton vacuum state described in Section 6.4 at $\tau = 0$, and then quench $g \to 0$ at $\tau = T$. Then we find

$$\langle 0|0\rangle = \sqrt{\frac{\sqrt{4k\Omega N_\gamma N_R}\left(k+\Omega\right)^2\left(\omega_+ + \omega_-\right)}{g^2\left(k-\Omega\right)^2 + \left(k+\Omega\right)^2\left[N_\gamma\left(\omega_+ + \omega_-\right) + k\right]^2\left[N_R\left(\omega_+ + \omega_-\right) + \Omega\right]}}. \quad (6.42)$$

As a reminder, here $N_{\gamma,R}$ are the coefficients seen in Eqns. (6.28)-(6.29), which determines the relative composition of the polariton ground state in terms of 'photon-like' and 'matter-like' fluctuations respectively. This amplitude has the same general structure as the full amplitude in Eq. (6.35), where the important quantity is the difference between initial ground state frequencies ($\mathcal{G}$) and the final ground state frequencies $[-i\dot{F}F^{-1}(T)]$. The probability spectrum, i.e. $1 - |\langle 0|0\rangle|^2$, for such a quench can be seen in Fig. 6.4, where we have chosen $g = 2$ and $\Omega = 3$, similarly to the periodically driven example in Section 6.5.1.

Whilst the general structure of the vacuum persistence amplitude in Eq. (6.42) is very similar to the generic case in Eq. (6.35), the actual spectrum seen in Fig. 6.4 and Fig. 6.3 respectively, is vastly different. The origin of this is two-fold. The quench has no preferential frequency into which quantum vacuum radiation can be emitted. Therefore, we expect fairly homogeneous emission across the spectrum. However, there is still some dependence on k, specifically a small suppression of emission for $k = \Omega$, as can be seen in the inset of Fig. 6.4.

This depends strongly on the ratio of N_γ and N_R, which essentially counts the degree to which the ground state is 'photon-like' or 'matter-like', respectively. In the $k \ll \Omega$ regime, the energy cost of exciting n photons ($\propto nk$) after the quench is much smaller than the respective cost for the matter degree of freedom ($\propto n\Omega$). Hence, photons are preferentially emitted after the quench, and the small energy cost leads to the close to unity probability of emission seen in Fig. 6.4. On the opposite side of the spectrum, photons carry a higher energy cost than matter quanta. However, the emission is suppressed in general by the fact that the energy cost of each matter

[8] Abrupt changes to the parameters.

[9] For one, the changes needed might be quicker than the speed of light, which is clearly unphysical!

quantum is still considerable. In the special case of $k = \Omega$, the photon and matter quanta are degenerate and this balance reduces the total number of emitted quanta.

6.6 Direct driving

We have so far in the chapter explored the physics of a time-dependent resonance frequency, which has links to parametric driving (see Section 6.5.1.1). Let us now turn to direct driving, similarly to what was done in Section 3.4.1 where we studied the emission of quanta due to free currents in the system. We will here consider direct driving of the matter degree of freedom, rather than the electromagnetic degree of freedom. The reason for this will become clear in Section 6.7, but we can physically imagine such a driving to originate from an external classical electromagnetic field. It is, however, straightforward to generalise to include free currents. If we return to the action in Eq. (6.3) and include a driving term $J_R(\tau)$, we find the action

$$\begin{aligned} S_\gamma &= \frac{1}{2}\int_0^T d\tau\ |\dot{A}_{\mathbf{k}}|^2 - k^2|A_{\mathbf{k}}|^2, \\ S_R &= \frac{1}{2}\int_0^T d\tau\ \dot{R}^2 - \Omega^2(\tau)R^2 + J_R(\tau)R, \\ S_I &= -\frac{g}{2}\int_0^T d\tau\ \left[\dot{A}_{\mathbf{k}} + \dot{A}^*_{\mathbf{k}}\right] R. \end{aligned} \tag{6.43}$$

This is our starting point, but it follows in a straightforward fashion that we can re-write it into the action of a driven and harmonically trapped particle in a magnetic field by the same procedure as was done in Section 6.2. From this we find,

$$S_{\gamma+R+I} = \int_0^T d\tau\ \frac{1}{2}\dot{\mathbf{q}}^2 - \frac{1}{2}\mathbf{q}\cdot A^2\cdot\mathbf{q} + \frac{1}{2}\left(\mathbf{B}\times\mathbf{q}\right)\cdot\dot{\mathbf{q}} + \mathbf{J}\cdot\mathbf{q}, \tag{6.44}$$

where we have defined the driving force vector

$$\mathbf{J} = (0, 0, J_R)\,, \tag{6.45}$$

along with the $\mathbf{q}$, $\mathbf{B}$ and A^2 defined as in Eqns. (6.7) and (6.8), respectively. From this action, we find the equation of motion

$$\ddot{\mathbf{q}} + B\dot{\mathbf{q}} + A^2(s)\mathbf{q} = \mathbf{J}, \tag{6.46}$$

where we have defined the matrix B as in Eq. (6.15). We can now also define $\boldsymbol{\xi}$ as before [Eq. (6.13)] in order to find the equation of motion

$$\dot{\boldsymbol{\xi}}(s) = \begin{pmatrix} 0 & \mathbb{I} \\ -A^2(s) & -B \end{pmatrix}\boldsymbol{\xi}(s) + \boldsymbol{\sigma}, \tag{6.47}$$

where we have also introduced the new driving force vector

$$\boldsymbol{\sigma} = (0, \mathbf{J})\,. \tag{6.48}$$

We can now solve the equation of motion in Eq. (6.46), using the solution to the homogeneous problem ($\boldsymbol{\sigma} = 0$) that we studied in Section 6.2. For the sake of notational simplicity, let us define the matrix

$$\mathcal{T}(s) = \begin{pmatrix} 0 & \mathbb{I} \\ -A^2(s) & -B \end{pmatrix}.$$

Suppose we re-write the equation of motion as

$$\dot{\boldsymbol{\xi}} - \mathcal{T}(s)\boldsymbol{\xi} = \boldsymbol{\sigma},$$

from which it follows that (at least formally)

$$\frac{d}{ds}\left[\exp\left(-\int_0^s dt\;\mathcal{T}(t)\right)\boldsymbol{\xi}(s)\right] = \exp\left(-\int_0^s dt\;\mathcal{T}(t)\right)\boldsymbol{\sigma}(s).$$

After some elementary algebra we find the formal solution

$$\begin{aligned}\boldsymbol{\xi}(s) = &\left[\exp\left(-\int_0^s dt\;\mathcal{T}(t)\right)\right]^{-1}\boldsymbol{\xi}(0) \\ &+ \left[\exp\left(-\int_0^s dt\;\mathcal{T}(t)\right)\right]^{-1}\int_0^s dt\left[\exp\left(-\int_0^t dt'\;\mathcal{T}(t')\right)\right]\boldsymbol{\sigma}(s).\end{aligned} \tag{6.49}$$

We can now notice that the first line is simply the formal homogeneous solution, which we solved in Section 6.2 in terms of the matrices $E(s)$, $F(s)$, $G(s)$ and $H(s)$ [Eq. (6.16)]. Therefore, it is useful to define

$$\left[\exp\left(-\int_0^s dt\;\mathcal{T}(s)\right)\right]^{-1} \equiv \begin{pmatrix} E(s) & F(s) \\ G(s) & H(s) \end{pmatrix},$$

and its inverse

$$\left[\exp\left(-\int_0^s dt\;\mathcal{T}(t)\right)\right] = \begin{pmatrix} E(s) & F(s) \\ G(s) & H(s) \end{pmatrix}^{-1} \equiv \begin{pmatrix} P(s) & Q(s) \\ R(s) & S(s) \end{pmatrix}.$$

Note that we can express

$$\begin{aligned}\begin{pmatrix} P(s) & Q(s) \\ R(s) & S(s) \end{pmatrix} &= \begin{pmatrix} E(s) & F(s) \\ G(s) & H(s) \end{pmatrix}^{-1} \\ &= \begin{pmatrix} E^{-1} + E^{-1}F\left[H - GE^{-1}F\right]^{-1}E^{-1} & -E^{-1}F\left[H - GE^{-1}F\right]^{-1} \\ -\left[H - GE^{-1}F\right]^{-1}GE^{-1} & \left[H - GE^{-1}F\right]^{-1} \end{pmatrix},\end{aligned} \tag{6.50}$$

where we have suppressed the s-dependence for notational simplicity. In particular, from this we find

$$\begin{aligned} Q(s) &= -E^{-1}(s)F(s)\left[H(s) - G(s)E^{-1}(s)F(s)\right]^{-1} \\ S(s) &= \left[H(s) - G(s)E^{-1}(s)F(s)\right]^{-1}. \end{aligned} \tag{6.51}$$

This form will be important for computations. We have thus found the full solution of the driven equation of motion in Eq. (6.46) in terms of the differential equations discussed in Section 6.2. Specifically, we have

$$\boldsymbol{\xi}(s) = \begin{pmatrix} E(s) & F(s) \\ G(s) & H(s) \end{pmatrix}\boldsymbol{\xi}(0) + \begin{pmatrix} E(s) & F(s) \\ G(s) & H(s) \end{pmatrix}\int_0^s dt \begin{pmatrix} P(t) & Q(t) \\ R(t) & S(t) \end{pmatrix}\boldsymbol{\sigma}(t). \tag{6.52}$$

From this, we can extract the solution $\mathbf{q}(s)$ of the driven dynamics, i.e. the classical solution to the driven Hopfield equations. This yields

$$\begin{aligned}\mathbf{q}(s) = &\left[E(s) - F(s)F^{-1}(T)E(T)\right]\mathbf{a} + \left[F(s)F^{-1}(T)\right]\mathbf{b} \\ &+ E(s)\left(\int_0^s dt\, Q(t)\mathbf{J}(t)\right) - F(s)F^{-1}(T)E(T)\left(\int_0^T dt\, Q(t)\mathbf{J}(t)\right) \\ &- F(s)\int_s^T dt\, S(t)\mathbf{J}(t).\end{aligned} \tag{6.53}$$

Interestingly, we can separate this into the homogeneous $\mathbf{q}_{\mathrm{H}}$ and inhomogeneous solution $\mathbf{q}_{\mathrm{I}}$ as

$$\begin{aligned}\mathbf{q}_{\mathrm{H}}(s) &= \left[E(s) - F(s)F^{-1}(T)E(T)\right]\mathbf{a} + \left[F(s)F^{-1}(T)\right]\mathbf{b}, \\ \mathbf{q}_{\mathrm{I}}(s) &= E(s)\left(\int_0^s dt\, Q(t)\mathbf{J}(t)\right) - F(s)F^{-1}(T)E(T)\left(\int_0^T dt\, Q(t)\mathbf{J}(t)\right) \\ &\quad - F(s)\int_s^T dt\, S(t)\mathbf{J}(t),\end{aligned} \tag{6.54}$$

where we find the solution in Eq. (6.53) by $\mathbf{q}(s) = \mathbf{q}_{\rm H}(s) + \mathbf{q}_{\rm I}(s)$. Importantly, in this construction we find that

$$\begin{aligned} \mathbf{q}_{\rm H}(0) = \mathbf{a}, \quad \mathbf{q}_{\rm H}(T) = \mathbf{b}, \\ \mathbf{q}_{\rm I}(0) = \mathbf{q}_{\rm I}(T) = 0. \end{aligned} \tag{6.55}$$

In other words, the boundary conditions are, by construction, taken into account by the homogeneous solution. We can substitute this solution into the action in Eq. (6.44), separating the solution into homogeneous and inhomogeneous parts as

$$\begin{aligned} S_{\rm cl} &= S_{\gamma+R+I}[\mathbf{q}_{\rm H} + \mathbf{q}_{\rm I}] \\ &= \frac{1}{2}\left[\mathbf{q}_{\rm H}\dot{\mathbf{q}}_{\rm H}\right]_0^T + \int_0^T d\tau\ \mathbf{J}\cdot\left(\mathbf{q}_{\rm H} + \frac{1}{2}\,\mathbf{q}_{\rm I}\right), \end{aligned} \tag{6.56}$$

where we used the fact that

$$\begin{aligned} \int_0^T d\tau\ (\mathbf{B}\times\mathbf{q})\cdot\dot{\mathbf{q}} &= \left[(\mathbf{B}\times\mathbf{q})\cdot\mathbf{q}\right]_0^T - \int_0^T d\tau\ (\mathbf{B}\times\dot{\mathbf{q}})\cdot\mathbf{q} \\ &= -\int_0^T d\tau\ (\mathbf{B}\times\dot{\mathbf{q}})\cdot\mathbf{q} \end{aligned}$$

since $(\mathbf{B}\times\mathbf{q}) \perp \mathbf{q}$ and

$$\int_0^T d\tau\ (\mathbf{B}\times\dot{\mathbf{q}}_{\rm H})\cdot\mathbf{q}_I = \int_0^T d\tau\ (\mathbf{B}\times\dot{\mathbf{q}}_{\rm I})\cdot\mathbf{q}_H,$$

using the boundary conditions in Eq. (6.55). Finally, substituting the classical solution of the Hopfield equations in Eq. (6.53) into the action in Eq. (6.56) yields

$$\begin{aligned} S_{\rm cl}\left[\mathbf{J}\right] =& \frac{1}{2}\left[\mathbf{b}\cdot\dot{F}F^{-1}\cdot\mathbf{b} + \mathbf{a}\cdot F^{-1}E\cdot\mathbf{a} - 2\mathbf{a}\cdot F^{-1}\cdot\mathbf{b}\right] \\ &+ \int_0^T ds\ \mathbf{J}(s)\cdot\left(\left[E(s) - F(s)F^{-1}(T)E(T)\right]\mathbf{a} + F(s)F^{-1}(T)\mathbf{b}\right) \\ &- \frac{1}{2}\int_0^T ds\int_0^s dt\ \mathbf{J}(s)\cdot\Big[S^T(s)F^T(t) + F(s)F^{-1}(T)E(T)Q(t) \\ &\qquad + Q^T(s)E^T(T)F^{-T}(T)F^T(t) - E(s)Q(t)\Big]\cdot\mathbf{J}(t), \end{aligned} \tag{6.57}$$

in which we used the identity

$$\int_0^T ds\int_0^s dt\ f(t,s) = \int_0^T ds\int_s^T dt\ f(s,t). \tag{6.58}$$

In order to simplify notation, and also provide some physical intuition, let us define the classical propagator

$$\Delta(s,t) = \theta(s-t)\Big[S^T(s)F^T(t) + F(s)F^{-1}(T)E(T)Q(t) \\ + \; Q^T(s)E^T(T)F^{-T}(T)F^T(t) - E(s)Q(t)\Big]. \quad (6.59)$$

This propagator is the Green's function for the classical Hopfield equations, that is, it is the solution to

$$\left[\mathbb{I}\partial_s^2 + B\partial_s + A^2(s)\right]\Delta(s,t) = \mathbb{I}\delta(s-t),$$

with boundary conditions $\Delta(0,t) = \Delta(T,t) = 0$, and where $\mathbb{I}$ is the identity matrix as before. Notably, time-reversal symmetry is broken since the light-matter coupling acts as a 'magnetic field', and we expect $\Delta(s,t) \neq \Delta(t,s)$. Finally, we find the driven action

$$S_{\mathrm{cl}}[\mathbf{J}] = \frac{1}{2}\left[\mathbf{b}\cdot\dot{F}F^{-1}\cdot\mathbf{b} + \mathbf{a}\cdot F^{-1}E\cdot\mathbf{a} - 2\mathbf{a}\cdot F^{-1}\cdot\mathbf{b}\right] \\ + \int_0^T ds\, \mathbf{J}(s)\cdot\left\{\left[E(s) - F(s)F^{-1}(T)E(T)\right]\mathbf{a} + F(s)F^{-1}(T)\mathbf{b}\right\} \\ - \frac{1}{2}\int_0^T ds\int_0^T dt\, \mathbf{J}(s)\cdot\Delta(s,t)\cdot\mathbf{J}(t). \quad (6.60)$$

Importantly, it is straightforward to show that this action reduces to the expected harmonic oscillator action when we let the light-matter coupling g go to zero.[10]

Given that we have mapped the dynamics to the harmonic oscillator in a magnetic field, the classical action of the driven Hopfield model of macroscopic QED in Eq. (6.60) contains few surprises. The driving simply adds a constant shift to the action.

6.6.1 Quantisation

It is well-known that a driving term $\mathbf{J}$ does not couple to the quantum fluctuations in a harmonic oscillator [3], meaning that it does not contribute to the normalisation

[10] In the case of $g \to 0$, the classical action in Eq. (6.60) reduces to

$$S_{\mathrm{cl}}[\mathbf{J}] = \frac{1}{2}\left[[\mathbf{b}+\mathbf{a}]\cdot\begin{pmatrix} k\frac{\cos kT}{\sin kT} & 0 \\ 0 & \Omega\frac{\cos\Omega T}{\sin\Omega T}\end{pmatrix}\cdot[\mathbf{b}+\mathbf{a}] - 2\mathbf{a}\cdot\begin{pmatrix} \frac{k}{\sin kT} & 0 \\ 0 & \frac{\Omega}{\sin\Omega T}\end{pmatrix}\cdot\mathbf{b}\right] \\ + \int_0^T ds\,\mathbf{J}(s)\cdot\left[\begin{pmatrix} \frac{\sin ks}{\sin kT} & 0 \\ 0 & \frac{\sin\Omega s}{\sin\Omega T}\end{pmatrix}\cdot\mathbf{b} + \begin{pmatrix} \frac{\sin k(T-s)}{\sin kT} & 0 \\ 0 & \frac{\sin\Omega(T-s)}{\sin\Omega T}\end{pmatrix}\cdot\mathbf{a}\right] \\ - \int_0^T ds\int_0^s dt\,\mathbf{J}(s)\cdot\begin{pmatrix} \frac{\sin kt\sin k(T-s)}{k\sin kT} & 0 \\ 0 & \frac{\sin\Omega t\sin\Omega(T-s)}{\Omega\sin\Omega T}\end{pmatrix}\cdot\mathbf{J}(t),$$

where we have as usual omitted the $y_{\mathbf{k}}$ degree of freedom (which is a $x_{\mathbf{k}}$-replica in this case).

factor of the transition amplitude $\langle \mathbf{b}, T|\mathbf{a}, 0\rangle_{\mathbf{J}}$. This is also true for a harmonic oscillator in a magnetic field, and thus also the case for the Hopfield system. We can see this by separating the coordinate $\mathbf{q}$ into classical $\mathbf{q}_{\rm cl}$ and quantum parts $\boldsymbol{\eta}$ as in $\mathbf{q} = \mathbf{q}_{\rm cl} + \boldsymbol{\eta}$, where $\boldsymbol{\eta}(0) = \boldsymbol{\eta}(T) = 0$, and substitute this into the action in Eq. (6.44). This yields

$$S[\mathbf{q}, \mathbf{J}] = S[\boldsymbol{\eta}, 0] + S_{\rm cl}[\mathbf{q}_{\rm cl}, \mathbf{J}],$$

and the formal path integral in Eq. (6.10) reduces to

$$\langle \mathbf{b}, T|\mathbf{a}, 0\rangle_{\mathbf{J}} = e^{iS_{\rm cl}[\mathbf{q}_{\rm cl}, \mathbf{J}]} \int_{\boldsymbol{\eta}(0)=0}^{\boldsymbol{\eta}(T)=0} \mathcal{D}\boldsymbol{\eta}\; e^{iS_{\gamma+R+I}[\boldsymbol{\eta}, 0]}. \tag{6.61}$$

For our purposes however, the quantum fluctuations are taken into account in the Morette-Van Hove determinant $\mathbb{D}$, seen in the pre-factor of Eq. (6.10). In a generic N-dimensional system, this determinant is given by

$$\mathbb{D} = \frac{1}{(2\pi i)^{N/2}} \left| -\frac{\partial^2 S_{\rm cl}}{\partial b_j \partial a_k} \right|^{1/2}. \tag{6.62}$$

As can be seen, only terms in the classical action that contain both $\mathbf{a}$ and $\mathbf{b}$ will contribute, and thus the determinant will not contain any terms proportional to $\mathbf{J}$. Finally, it follows that the driven transition amplitude is given by

$$\langle \mathbf{b}, T|\mathbf{a}, 0\rangle_{\mathbf{J}} = \frac{\sqrt{|F^{-1}|}}{(2\pi i)^{3/2}} \exp\left(iS_{\rm cl}\left[\mathbf{q}_{\rm cl}, \mathbf{J}\right]\right), \tag{6.63}$$

with $S_{\rm cl}$ given in Eq. (6.60).

6.6.2 Driven vacuum persistence amplitude

Let us start by calculating the vacuum expectation value for the driven Hopfield system. This follows similarly to Eq. (6.33), but where we now wish to use the driven transition amplitude from Eq. (6.63) instead of the one in Eq. (6.23). In other words, we want to compute

$$\langle 0|0\rangle_{\mathbf{J}} = \int_{-\infty}^{\infty} d^3b\; d^3a\; \Psi_0^*(\mathbf{b})\, \langle \mathbf{b}, T|\mathbf{a}, 0\rangle_{\mathbf{J}}\, \Psi_0(\mathbf{a}), \tag{6.64}$$

where the ground state wavefunction Ψ_0 was found in Eq. (6.30). Since this is in the form of Gaussian integrals, we can use the relation in Eq. (6.34). However, due to the algebraic complexity, let us proceed step-by-step. It is useful, for reasons that

will soon become clear, to first evaluate the integrals

$$\begin{aligned}\int_{-\infty}^{\infty} d^N u\, d^N v\, e^{-\frac{1}{2}\mathbf{u}\cdot A\cdot\mathbf{u}+\mathbf{J}\cdot\mathbf{u}} e^{\mathbf{u}\cdot B\cdot\mathbf{v}} e^{-\frac{1}{2}\mathbf{v}\cdot C\cdot\mathbf{v}+\mathbf{K}\cdot\mathbf{v}} \\ = (2\pi)^N \left(\sqrt{|C_{\text{sym}}|\left|A-BC_{\text{sym}}^{-1}B^T\right|_{\text{sym}}}\right)^{-1} \\ \times e^{\frac{1}{2}\mathbf{K}\cdot\left(C_{\text{sym}}^{-1}+C_{\text{sym}}^{-1}B^T\left[A-BC_{\text{sym}}^{-1}B^T\right]_{\text{sym}}^{-1}BC_{\text{sym}}^{-1}\right)\cdot\mathbf{K}} \\ \times e^{\frac{1}{2}\mathbf{J}\cdot\left(A-BC_{\text{sym}}^{-1}B^T\right)_{\text{sym}}^{-1}\cdot\mathbf{J}} \\ \times e^{\mathbf{J}\cdot\left(A-BC_{\text{sym}}^{-1}B^T\right)_{\text{sym}}^{-1}BC_{\text{sym}}^{-1}\cdot\mathbf{K}} \qquad (6.65)\end{aligned}$$

$$(6.66)$$

as well as

$$\begin{aligned}\int_{-\infty}^{\infty} d^N u\, d^N v\, e^{-\frac{1}{2}\mathbf{u}\cdot A\cdot\mathbf{u}+\mathbf{J}\cdot\mathbf{u}} e^{\mathbf{u}\cdot B\cdot\mathbf{v}} e^{-\frac{1}{2}\mathbf{v}\cdot C\cdot\mathbf{v}+\mathbf{K}\cdot\mathbf{v}} \\ = (2\pi)^N \left(\sqrt{|A_{\text{sym}}|\left|C-B^TA_{\text{sym}}^{-1}B\right|_{\text{sym}}}\right)^{-1} \\ \times e^{\frac{1}{2}\mathbf{K}\cdot\left(C-B^TA_{\text{sym}}^{-1}B\right)_{\text{sym}}^{-1}\cdot\mathbf{K}} \\ \times e^{\frac{1}{2}\mathbf{J}\cdot\left(A_{\text{sym}}^{-1}+A_{\text{sym}}^{-1}B\left[C-B^TA_{\text{sym}}^{-1}B\right]_{\text{sym}}^{-1}B^TA_{\text{sym}}^{-1}\right)\cdot\mathbf{J}} \\ \times e^{\mathbf{K}\cdot\left(C-B^TA_{\text{sym}}^{-1}B\right)_{\text{sym}}^{-1}B^TA_{\text{sym}}^{-1}\cdot\mathbf{J}}, \qquad (6.67)\end{aligned}$$

where we find either (6.65) or (6.67) depending on which integral ($\mathbf{u}$ or $\mathbf{v}$) we evaluate first. From this we can establish some useful matrix identities, i.e. that

$$\begin{aligned}C_{\text{sym}}^{-1}+C_{\text{sym}}^{-1}B^T\left[A-BC_{\text{sym}}^{-1}B^T\right]_{\text{sym}}^{-1}BC_{\text{sym}}^{-1} &= \left(C-B^TA_{\text{sym}}^{-1}B\right)_{\text{sym}}^{-1}, \\ A_{\text{sym}}^{-1}+A_{\text{sym}}^{-1}B\left[C-B^TA_{\text{sym}}^{-1}B\right]_{\text{sym}}^{-1}B^TA_{\text{sym}}^{-1} &= \left(A-BC_{\text{sym}}^{-1}B^T\right)_{\text{sym}}^{-1}, \\ \left(C-B^TA_{\text{sym}}^{-1}B\right)_{\text{sym}}^{-1}B^TA_{\text{sym}}^{-1} &= C_{\text{sym}}^{-T}B^T\left(A-BC_{\text{sym}}^{-1}B^T\right)_{\text{sym}}^{-T}, \qquad (6.68)\end{aligned}$$

where we have to assume that the arbitrary matrices A and C are positive definite (but not necessarily symmetric) and suitably invertible.[11] The simplest form of this integral is thus

$$\begin{aligned}\int_{-\infty}^{\infty} d^N u\, d^N v\, e^{-\frac{1}{2}\mathbf{u}\cdot A\cdot\mathbf{u}+\mathbf{J}\cdot\mathbf{u}} e^{\mathbf{u}\cdot B\cdot\mathbf{v}} e^{-\frac{1}{2}\mathbf{v}\cdot C\cdot\mathbf{v}+\mathbf{K}\cdot\mathbf{v}} &= \frac{(2\pi)^N}{\sqrt{|C_{\text{sym}}|\left|A-BC_{\text{sym}}^{-1}B^T\right|_{\text{sym}}}} \\ &\times e^{\frac{1}{2}\mathbf{K}\cdot\left(C-B^TA_{\text{sym}}^{-1}B\right)_{\text{sym}}^{-1}\cdot\mathbf{K}} \\ &\times e^{\frac{1}{2}\mathbf{J}\cdot\left(A-BC_{\text{sym}}^{-1}B^T\right)_{\text{sym}}^{-1}\cdot\mathbf{J}} \\ &\times e^{\mathbf{J}\cdot\left(A-BC_{\text{sym}}^{-1}B^T\right)_{\text{sym}}^{-1}BC_{\text{sym}}^{-1}\cdot\mathbf{K}}, \qquad (6.69)\end{aligned}$$

[11] By suitably invertible we mean that A, C, $C-B^TA^{-1}B$ as well as $A-BC^{-1}B^T$ are invertible.

which is the version we will use from here on. We can now use this to compute the driven vacuum persistence amplitude by identifying

$$\begin{aligned}
A &\to \Sigma_F \equiv \mathcal{G}^* - i\dot{F}F^{-1}, \\
B &\to -iF^{-1}, \\
C &\to \Sigma_E \equiv \mathcal{G} - iF^{-1}E, \\
\mathbf{J} &\to i\int_0^T ds\; F^{-T}F^T(s)\mathbf{J}(s), \\
\mathbf{K} &\to i\int_0^T ds\; \left[E^T(s) - E^TF^{-T}F^T(s)\right]\mathbf{J}(s),
\end{aligned}$$

where we should remember to check that $\mathcal{G}^* - i\dot{F}F^{-1}$ and $\mathcal{G} - iF^{-1}E$ are indeed positive definite. This is best done numerically, after F and E have been computed. Note that for notational simplicity, a matrix is implicitly assumed to be evaluated at $\tau = T$ whenever the argument is omitted. Finally, we arrive at the driven vacuum persistence amplitude

$$\begin{aligned}
\langle 0|0\rangle_{\mathbf{J}} = \langle 0|0\rangle \exp\Bigg(-\frac{1}{2}\int_0^T ds \int_0^T dt\; \mathbf{J}(s)\Big[& F(s)F^{-1}\left(\mathcal{S}/\Sigma_E\right)^{-1}_{\text{sym}} F^{-T}F^T(t) \\
& + \left\{E(s) - F(s)F^{-1}E\right\}\left(\mathcal{S}/\Sigma_F\right)^{-1}_{\text{sym}}\left\{E^T(t) - E^TF^{-T}F^T(t)\right\}\Big]\mathbf{J}(t)\Bigg) \\
\times\; \exp\Bigg(-\frac{i}{2}\int_0^T ds \int_0^T dt\; \mathbf{J}(s)\Big[& \Delta(s,t) \\
& - 2F(s)F^{-1}\left(\mathcal{S}/\Sigma_E\right)^{-1}_{\text{sym}} F^{-1}\left(\Sigma_E\right)^{-1}_{\text{sym}}\left\{E^T(t) - E^TF^{-T}F^T(t)\right\}\Big]\mathbf{J}(t)\Bigg),
\end{aligned} \tag{6.70}$$

where $\langle 0|0\rangle$ is the $\mathbf{J} = 0$ vacuum persistence amplitude from Eq. (6.35), and where we have introduced the matrix

$$\mathcal{S} = \begin{pmatrix} \Sigma_F & -iF^{-1} \\ -iF^{-T} & \Sigma_E \end{pmatrix}, \tag{6.71}$$

as well as the symmetrised Schur complements [153]

$$\begin{aligned}
\left(\mathcal{S}/\Sigma_F\right)_{\text{sym}} &= \left(\Sigma_E + F^{-T}\left(\Sigma_F\right)^{-1}_{\text{sym}} F^{-1}\right)_{\text{sym}}, \\
\left(\mathcal{S}/\Sigma_E\right)_{\text{sym}} &= \left(\Sigma_F + F^{-1}\left(\Sigma_E\right)^{-1}_{\text{sym}} F^{-T}\right)_{\text{sym}}.
\end{aligned} \tag{6.72}$$

Whilst the expression in Eq. (6.70) is complicated, it is nonetheless calculable and entirely expressable in terms of the ground state matrix $\mathcal{G}$ from Eq. (6.27), and the propagation matrices F and E as defined in Eqns. (6.21) and (6.22) respectively.

Let us, for notational simplicity, define the Fock space propagator

$$\begin{aligned}\Delta_{00}(s,t) = i\Delta(s,t) &+ F(s)F^{-1}\left(\mathcal{S}/\Sigma_E\right)^{-1}_{\text{sym}} F^{-T}F^T(t) \\ &+ \left\{E(s) - F(s)F^{-1}E\right\}\left(\mathcal{S}/\Sigma_F\right)^{-1}_{\text{sym}}\left\{E^T(t) - E^TF^{-T}F^T(t)\right\} \\ &- 2iF(s)F^{-1}\left(\mathcal{S}/\Sigma_E\right)^{-1}_{\text{sym}} F^{-1}\left(\Sigma_E\right)^{-1}_{\text{sym}}\left\{E^T(t) - E^TF^{-T}F^T(t)\right\},\end{aligned} \tag{6.73}$$

in analogy with the standard result for a harmonic oscillator [3] and Eq. (3.43) in Chapter 3. We can therefore express the driven vacuum persistence amplitude as

$$\langle 0|0\rangle_{\mathbf{J}} = \langle 0|0\rangle \exp\left(-\frac{1}{2}\int_0^T ds \int_0^T dt\ \mathbf{J}(s)\Delta_{00}(s,t)\mathbf{J}(t)\right). \tag{6.74}$$

In order to bring the field-point propagator $\Delta(s,t)$ and the Fock space propagator $\Delta_{00}(s,t)$ to the same form, it is convenient to define the symmetrised Fock space propagator

$$\Delta^{\text{sym}}_{00}(s,t) = \Delta_{00}(s,t) + \Delta_{00}(t,s). \tag{6.75}$$

This brings the vacuum persistence amplitude into the form

$$\langle 0|0\rangle_{\mathbf{J}} = \langle 0|0\rangle \exp\left(-\frac{1}{2}\int_0^T ds \int_0^s dt\ \mathbf{J}(s)\Delta^{\text{sym}}_{00}(s,t)\mathbf{J}(t)\right), \tag{6.76}$$

where we used the integral identity in Eq. (6.58). This will be a handy notation for computations.[12] We can directly see that any driving force $\mathbf{J}$ will exponentially suppress the vacuum persistence. Unsurprisingly, the vacuum is unstable when driven.

6.6.3 Correlators

We are mostly interested in vacuum-correlators, and so we can use the vacuum persistence amplitude in Eq. (6.70) as a basis when calculating the correlators. As discussed briefly in Section 3.4.2.3 of Chapter 3, we can calculate the two-point correlator as

$$\begin{aligned}\langle 0|q_i(\tau)q_j(\tau')|0\rangle &= \frac{\delta}{i\delta J_i(\tau)}\frac{\delta}{i\delta J_j(\tau')}\langle 0|0\rangle\, e^{-\frac{1}{2}\int_0^T ds\int_0^s dt\ \mathbf{J}(s)\Delta^{\text{sym}}_{00}(s,t)\mathbf{J}(t)}\Big|_{\mathbf{J}=0} \\ &= \langle 0|0\rangle\,\theta(\tau-\tau')\left[\Delta^{\text{sym}}_{00}(\tau,\tau')\right]_{ij},\end{aligned} \tag{6.77}$$

[12] In this form it is easy to confirm that when $g \to 0$ and for time-independent Ω, we find the usual harmonic oscillator amplitude

$$\langle 0|0\rangle_{\mathbf{J}} = \langle 0|0\rangle \exp\left(-\frac{1}{2}\int_0^T ds\int_0^s dt\ \mathbf{J}(s)\begin{pmatrix} e^{-ik(s-t)}/k & 0 \\ 0 & e^{-i\Omega(s-t)}/\Omega\end{pmatrix}\mathbf{J}(t)\right).$$

for $\tau, \tau' \in [0, T]$, where q_i refers to the i^{th} component of $\mathbf{q}$ (similarly for J_i), and where $[\Delta_{00}^{\text{sym}}(\tau, \tau')]_{ij}$ refers to the i^{th} column and j^{th} row of Δ_{00}^{sym}. Thus we find a physical interpretation of Δ_{00}^{sym} in terms of the field-field correlator. Note that the free vacuum persistence amplitude $\langle 0|0\rangle$ is not necessarily unity for all times. In fact, from Section 6.5, we know that it is not when the resonance frequency of the medium depends on time.

6.7 A damped harmonic oscillator

In order to properly model many materials, it is crucial to also include dissipation. This has been ignored in the treatment so far, restricting the use to materials where absorption can be neglected. Whilst this is indeed the case far away from the resonance frequency in most materials, the models simply are not valid close to the resonance frequencies. In order to remedy this, let us first study the dynamics of a damped harmonic oscillator. The lessons learned from this can then be applied to the matter degree of freedom in the model for an optical medium.

As this is a type of open quantum system, we will require the introduction of a reservoir into which energy can be dissipated. We will here model this reservoir as a free field living in an auxiliary dimension ζ. This is similar to the Lamb model [154] of the quantum Langevin equation for a damped harmonic oscillator studied also in many different works, such as [155–161]. The general framework of including a bath to absorb energy is used in a variety of scenarios relating to open quantum systems, most commonly through a master equation [56, 162–164] but also its (Keldysh) path integral representation [165] (and references therein). Applications of this are ubiquitous, but include lossy cavities [56, 166, 167] and the damped dynamical Casimir effect [168, 169].[13] In particular, we will be using the version introduced by Unruh and Zurek [170] where the harmonic oscillator is coupled to the free scalar field by a derivative coupling in order to explicitly break time-reversal symmetry.

Let us start at the action, given here by

$$\begin{aligned} S_R &= \frac{1}{2}\int_0^T d\tau\ \dot{R}^2 - \Omega^2 R^2, \\ S_D &= \frac{1}{2}\int_0^T d\tau \int d\zeta\ \dot{D}^2 - (\partial_\zeta D)^2\,, \\ S_{\text{int}} &= \int_0^T d\tau \int d\zeta\ \mu \dot{D}(\zeta,\tau)\delta(\zeta)R(\tau), \end{aligned} \tag{6.78}$$

where we used the same normalised units as previously in the chapter. Here D is the free scalar field playing the role of reservoir. It propagates only in the auxiliary (1-dimensional) ζ-axis, and the coupling in S_{int} ensures that energy is deposited at the origin $\zeta = 0$. In particular, the δ-function at the origin of the ζ-axis ensures that

[13] This is not by any means an exhaustive list!

energy is emitted into ζ-space, and no energy that has been previously emitted can be re-absorbed.[14] Furthermore, the derivative in time explicitly breaks the time-reversal symmetry of the system. Because of this nature, we will refer to the field D as the dissipator. It follows that the equations of motion are

$$\begin{aligned} \ddot{R} + \Omega^2 R &= \mu \dot{D}(0,\tau), \\ \ddot{D} - \partial_\zeta^2 D &= -\mu \delta(\zeta)\dot{R}(\tau). \end{aligned} \tag{6.79}$$

We can most easily solve this system by using the Green's function for the dissipator D, which satisfies

$$\left[\partial_t^2 - \partial_\zeta^2\right] G_D(\tau - \tau', \zeta - \zeta') = \delta(\zeta - \zeta')\delta(\tau - \tau').$$

This is well-known [1, 170] and given by

$$G_D(\tau - \tau', \zeta - \zeta') = \frac{1}{2}\theta\left(\tau - \tau' - |\zeta - \zeta'|\right),$$

where we have chosen the retarded Green's function out of physical considerations.[15] The full solution for the dissipator is therefore

$$D(\zeta,\tau) = D_H(\zeta,\tau) - \frac{\mu}{2}\int_0^T d\tau'\, \theta(\tau - \tau' - |\zeta|)\dot{R}(\tau'), \tag{6.80}$$

where $D_H(\zeta,\tau)$ satisfies the homogeneous equation of motion. By substituting this back into the equation of motion for R in Eq. (6.79) we find

$$\ddot{R} + \frac{\mu^2}{2}\dot{R} + \Omega^2 R = \mu \dot{D}_H(0,\tau). \tag{6.81}$$

The form of the damping is a direct consequence of the δ-function in the coupling S_{int}, and would take a considerably more complicated form otherwise. This is clearly a damped harmonic oscillator driven by the fluctuations in the dissipator. As such, it takes the form of the quantum Langevin equation when

$$\langle \dot{D}(0,\tau)\dot{D}(0,\tau')\rangle \propto \delta(\tau - \tau'), \tag{6.82}$$

which is indeed the case if we let D_H be a thermal field at high temperature. To bring this into a familiar form, let us define the dissipation rate $\gamma = \mu^2/4$, with which we find

$$\ddot{R} + 2\gamma\dot{R} + \Omega^2 R = 2\sqrt{\gamma}\dot{D}_H(0,\tau). \tag{6.83}$$

[14] The energy will simply propagate out towards $\zeta = \infty$.

[15] We are interested in whether energy is being emitted into the auxiliary space ζ, not energy being absorbed from it. The latter would involve the advanced Green's function.

For now, let us ignore the driving and focus on the homogeneous version of Eq. (6.83). We will treat the driving later. As such, let us for now assume that $D_H \equiv 0$.

We wish to quantise the above system by computing the path integral

$$\langle R_b, T | R_a, 0 \rangle = \int_{R(0)=R_a}^{R(T)=R_b} \mathcal{D}R \exp\left[iS_{R+D+\text{int}}\right], \tag{6.84}$$

where we are treating only the inhomogeneous part of the dissipator. As we are dealing with a quadratic action, in order to compute this we want to find the solution to the classical equation of motion Eq. (6.83) with boundary conditions $R(0) = R_a$ and $R(T) = R_b$. It is easy to show that the action in Eq. (6.78) can be reduced to the usual

$$S_{R+D+\text{int}} = \frac{1}{2}\left[\dot{R}R\right]_0^T + \frac{1}{2}\int d\zeta \ \left[\dot{D}D\right]_0^T,$$

by integrating by parts. If we consider only the homogeneous part of R together with the inhomogenoeus part of the dissipator (as we are not interested in the dynamics of the dissipator), we find

$$S_{R+D+\text{int}} = \frac{1}{2}\left[\dot{R}R\right]_0^T + \frac{\gamma}{2}\left(R_b - R_a\right)^2,$$

where R obeys

$$\ddot{R} + 2\gamma\dot{R} + \Omega^2 R = 0 \tag{6.85}$$

with boundary conditions $R(0) = R_a$ and $R(T) = R_b$. The solution to Eq. (6.85) with these boundary conditions is

$$R(t) = \frac{1}{\sin\chi T}\left[-R_a e^{-\gamma t}\sin\chi(t-T) + R_b e^{-\gamma(t-T)}\sin\chi t\right], \tag{6.86}$$

where we use $\chi = \sqrt{\Omega^2 - \gamma^2}$. This in turn leads to the action

$$S_{\text{cl}} = \frac{\chi}{2\sin\chi T}\left[\left(R_b^2 + R_a^2\right)\cos\chi T - 2R_b R_a \cosh\gamma T + 2R_a(R_a - R_b)\sin\chi T\right]. \tag{6.87}$$

Interestingly, in the limit of $\Omega \to 0$ we have to be a bit careful, as the correct action is

$$S_{\text{cl}}^{\Omega\to 0} = \frac{\gamma}{2}\left[\left(R_b - R_a\right)^2 \coth\gamma T + 2R_a(R_a - R_b)\right], \tag{6.88}$$

which is not the same as the $\Omega \to 0$ of Eq. (6.87). This is because if we naïvely take this limit we cross a branch cut, as is common when some sort of damping is included (see for instance the inverted harmonic oscillator in Ref. [98]). Let us focus

on the damped free particle, as it can tell us a bit about the role of each term. It is straightforward to find the transition amplitude

$$\langle R_b, T|R_a, 0\rangle = \sqrt{\frac{\gamma}{2\pi i}\left(1+\coth\gamma T\right)}e^{iS_{\rm cl}^{\Omega\to 0}} \tag{6.89}$$

where we used the Morette-Van Hove determinant from Eq. (6.62) in order to compute the normalisation. If we start with a Gaussian wavefunction with width σ and initial momentum p_0,

$$\psi(R) \propto e^{-\frac{R^2}{2\sigma^2}}e^{ip_0R}, \tag{6.90}$$

we find that

$$\langle R\rangle(T\to\infty) = \frac{p_0}{2\gamma}. \tag{6.91}$$

This matches what is expected from the classical damped free particle.[16] If the last term in the action in Eq. (6.88) is ignored, i.e. the contribution from the dissipator, then we get the incorrect result of $\langle R\rangle(T\to\infty) = p_0/\gamma$. In other words, we cannot simply neglect the dissipator dynamics in the action. This is not the full story, however, as we have presently ignored the driving term $2\sqrt{\gamma}\dot{D}_H(0,\tau)$.

Including this driving term into the dynamics of R is fairly straightforward as we can adopt the general solution we found in Eq. (6.54). In this case, we find

$$\begin{aligned} R_{\rm H}(s) &= \left[E(s) - F(s)F^{-1}(T)E(T)\right]R_a + \left[F(s)F^{-1}(T)\right]R_b, \\ R_{\rm I}(s) &= E(s)\left(\int_0^s dt\; Q(t)\hat{\xi}(t)\right) - F(s)F^{-1}(T)E(T)\left(\int_0^T dt\; Q(t)\hat{\xi}(t)\right) \\ &\quad - F(s)\int_s^T dt\; S(t)\hat{\xi}(t), \end{aligned} \tag{6.92}$$

where we have defined $\hat{\xi}(t) = 2\sqrt{\gamma}\dot{D}_H(0,\tau)$ for notational simplicity. Here the matrices E, F, G, and H reduce to scalars and we have the equation of motion

$$\begin{pmatrix} \dot{E}(s) & \dot{F}(s) \\ \dot{G}(s) & \dot{H}(s) \end{pmatrix} = \begin{pmatrix} 0 & 1 \\ -\Omega^2 & -2\gamma \end{pmatrix}\begin{pmatrix} E(s) & F(s) \\ G(s) & H(s) \end{pmatrix} \tag{6.93}$$

[16] In the classical limit, we have

$$\ddot{R}_{\rm cl} + 2\gamma\dot{R}_{\rm cl} = 0,$$

whose solution for $R_{\rm cl}(0) = 0$ and $\dot{R}_{\rm cl} = p_0$ is

$$R_{\rm cl}(\tau) = \frac{p_0}{2\gamma}\left(1-e^{-2\gamma\tau}\right) \xrightarrow{\tau\to\infty} \frac{p_0}{2\gamma}.$$

together with the initial values

$$\begin{pmatrix} E(0) & F(0) \\ G(0) & H(0) \end{pmatrix} = \begin{pmatrix} 1 & 0 \\ 0 & 1 \end{pmatrix}.$$

However, we cannot directly adopt the action found in Eq. (6.60), as we can no longer equate $G - HF^{-1}E = -F^{-T}$. This required $B = -B^T$ in Eq. (6.15), which is here given by $B = 2\gamma$. Clearly this cannot be satisfied as $2\gamma \neq -2\gamma$ unless $\gamma = 0$. Nonetheless, the action can be written as

$$\begin{aligned} S_{\rm cl}\left[\hat{\xi}\right] = \frac{1}{2}\Big[R_b\left(\dot{F}F^{-1}\right)R_b + R_a\left(F^{-1}E\right)R_a - R_a\left(F^{-1} + E^TF^{-T}H^T - G^T\right)R_b\Big] \\ + \int_0^T ds\,\hat{\xi}(s)\cdot\left\{\left[E(s) - F(s)F^{-1}E\right]R_a + F(s)F^{-1}R_b\right\} \\ + \frac{\gamma}{2}\left(R_b - R_a\right)^2 - \frac{1}{2}\int_0^T ds\int_0^T dt\,\hat{\xi}(s)\Delta(s,t)\hat{\xi}(t), \end{aligned} \tag{6.94}$$

where we kept the transpose notation despite dealing with scalars as this will be useful when we generalise this to the Hopfield system. As expected, when $\hat{\xi} \to 0$ we arrive at the action of Eq. (6.87). Thus we find the transition amplitude

$$\begin{aligned} \langle R_b, T|R_a, 0\rangle_{\hat{\xi}} &= \sqrt{\frac{\gamma}{2\pi i}\left(1 + \frac{1}{2\gamma}\left[F^{-1} + E^TF^{-T}H^T - G^T\right]\right)}e^{iS_{\rm cl}[\hat{\xi}]} \\ &= \sqrt{\frac{1}{2\pi i}\left(\gamma + \frac{\chi}{\sin\chi T}\cosh\gamma T\right)}e^{iS_{\rm cl}[\hat{\xi}]}. \end{aligned} \tag{6.95}$$

We now want to integrate over all configurations of the dissipator D_H in order to take the fluctuations into account. Whilst we can perform the path integral over D, it is simpler to deal with $\hat{\xi}(\tau) = 2\sqrt{\gamma}\dot{D}_H(0,\tau)$ directly. This is akin to the Martin-Siggia-Rose formalism for stochastic path integrals [171], although we should note that we do not restrict ourselves to the high-temperature limit just yet. In other words, we can now integrate over $\hat{\xi}$ such that the correlation function for $\hat{\xi}$ is [154]

$$\frac{1}{2}\langle\hat{\xi}(s)\hat{\xi}(t) + \hat{\xi}(t)\hat{\xi}(s)\rangle = -2\gamma k_B\mathbb{T}\frac{d}{ds}\coth\left[\pi k_B\mathbb{T}\left(s-t\right)\right] \equiv K_{\mathbb{T}}(s,t) + K_{\mathbb{T}}(t,s), \tag{6.96}$$

where $\mathbb{T}$ is the temperature of the bath and k_B is the Boltzmann constant. In the high-temperature limit, we have

$$K_{\mathbb{T}}(s,t) \overset{\mathbb{T}\to\infty}{\sim} 4\gamma k_B\mathbb{T}\delta(s-t), \tag{6.97}$$

corresponding to the classical Langevin limit. On the other hand, when $T \to 0$ the

noise is dominated by quantum fluctuations in the dissipator, and we find

$$K_{\mathbb{T}}(s,t) \overset{\mathbb{T}\to 0}{\sim} \frac{\gamma}{\pi}\frac{1}{(s-t)^2}. \tag{6.98}$$

We can compute the correlation function in Eq. (6.96) through the path integral

$$\begin{aligned}\frac{1}{2}\langle\hat{\xi}(\tau)\hat{\xi}(\tau')+\hat{\xi}(\tau')\hat{\xi}(\tau)\rangle &= \int \mathcal{D}\hat{\xi}\ \hat{\xi}(\tau)\hat{\xi}(\tau')\exp\left[-\int_0^T ds\int_0^T dt\ \frac{1}{2}\hat{\xi}(s)K_{\mathbb{T}}^{-1}(s,t)\hat{\xi}(t)\right]\\ &= \frac{\delta^2}{i\delta f(s) i\delta f(t)}\int \mathcal{D}\hat{\xi}\ e^{-\int_0^T ds\ dt\ \frac{1}{2}\hat{\xi}(s)K_{\mathbb{T}}^{-1}(s,t)\hat{\xi}(t)}\\ &\qquad\qquad \times e^{i\int_0^T ds\ f(s)\hat{\xi}(s)}\Big|_{f=0}\\ &= \frac{\delta^2}{i\delta f(s) i\delta f(t)}\exp\left(-\int_0^T ds\ dt\ \frac{1}{2}f(s)K_{\mathbb{T}}(s,t)f(t)\right)\Big|_{f=0},\end{aligned} \tag{6.99}$$

where we define $K_{\mathbb{T}}^{-1}$ as the functional inverse of $K_{\mathbb{T}}$,[17] and where we have normalised such that the path integral with $f=0$ equals unity. We can use this to define averages with respect to the noise, which we will denote as $\langle\langle ...\rangle\rangle$. In this way we can compute the noise averaged transition amplitude

$$\langle\langle R_b,T|R_a,0\rangle\rangle = \int \mathcal{D}\hat{\xi}\ \langle R_b,T|R_a,0\rangle_{\hat{\xi}}\ \exp\left[-\int_0^T ds\int_0^T dt\ \frac{1}{2}\hat{\xi}(s)K_{\mathbb{T}}^{-1}(s,t)\hat{\xi}(t)\right]. \tag{6.100}$$

It is fairly straightforward to formally compute this, yielding

$$\langle\langle R_b,T|R_a,0\rangle\rangle = \sqrt{\frac{\det K_{\mathbb{T}}^{-1}}{\det\left(K_{\mathbb{T}}^{-1}+i\Delta\right)^{-1}}}\sqrt{\frac{1}{2\pi i}\left(\gamma+\frac{\chi}{\sin\chi T}\cosh\gamma T\right)}\exp\left[iS_{\rm cl}\right], \tag{6.101}$$

where 'det' is the functional determinant (as discussed in Chapter 2), and we have defined the combined propagator $\left(K_{\mathbb{T}}^{-1}+i\Delta\right)^{-1}$ as the inverse of $K_{\mathbb{T}}^{-1}+i\Delta$. Also,

[17] $K_{\mathbb{T}}^{-1}$ is defined implicitly though Eq. (6.96), as we never need to find the explicit form of it. In the high-temperature limit however, we can note that $K_{\mathbb{T}}^{-1}=\delta(s-t)/(4\gamma k_B\mathbb{T})$.

from Eq. (6.101) we find the noise averaged classical action is given by

$$\begin{aligned} S_{\rm cl} = \frac{1}{2}\Big[R_b\left(\dot{F}F^{-1}\right)R_b + R_a\left(F^{-1}E\right)R_a - R_a\left(F^{-1} + E^T F^{-T} H^T - G^T\right)R_b\Big] \\ + \frac{i}{2}\int_0^T ds \int_0^T dt\ \left\{\left[E^T(s) - E^T F^{-T} F(s)^T\right]R_a + F^{-T}F^T(s)R_b\right\} \\ \times \quad \left(\frac{1}{K_{\mathbb{T}}^{-1} + i\Delta}\right)(s,t)\left\{\left[E(t) - F(t)F^{-1}E\right]R_a + F(t)F^{-1}R_b\right\} \\ + \quad \frac{\gamma}{2}\left(R_b - R_a\right)^2 . \end{aligned} \tag{6.102}$$

At this point, we have yet to make any approximation of the dissipator dynamics. As can be seen, this defines a time-nonlocal action whose memory kernel is given by $\left(K_{\mathbb{T}}^{-1} + i\Delta\right)^{-1}$. We can formally compute this memory kernel perturbatively[18] as

$$\left(\frac{1}{K_{\mathbb{T}}^{-1} + i\Delta}\right)(s,t) \simeq K_T(s,t) + i\int ds' \int dt'\ K_{\mathbb{T}}(s,s')\Delta(s',t')K_{\mathbb{T}}(t',t) + ... \quad . \tag{6.103}$$

This corresponds to a perturbation series quantifying the degree to which the bath dynamics are affected by the oscillator. Let us for now truncate this expansion at the $0^{\rm th}$ order in γ, where the bath is unaffected by the oscillator, in order to get a feeling for the physics. Furthermore, let us also work in the high-temperature limit, such that the bath correlations reduce to a δ-function. In this limit, we find

$$\left(\frac{1}{K_{\mathbb{T}}^{-1} + i\Delta}\right)(s,t) \overset{\gamma \text{ small}}{\simeq} K_T(s,t) \overset{\text{high } \mathbb{T}}{\simeq} 4\gamma k_B \mathbb{T}\delta(s-t), \tag{6.104}$$

where the last step follows from Eq. (6.97). Hence, we find

$$\sqrt{\frac{\det K_{\mathbb{T}}^{-1}}{\det\left(K_{\mathbb{T}}^{-1} + i\Delta\right)^{-1}}} \simeq 1$$

and

$$\begin{aligned} &\int_0^T ds \int_0^T dt\ \left\{\left[E^T(s) - E^T F^{-T} F(s)^T\right]R_a + F^{-T}F^T(s)R_b\right\} \\ &\qquad \times \quad \left(\frac{1}{K_{\mathbb{T}}^{-1} + i\Delta}\right)(s,t)\left\{\left[E(t) - F(t)F^{-1}E\right]R_a + F(t)F^{-1}R_b\right\} \\ &\simeq 4\gamma k_B \mathbb{T}\int_0^T ds \Big(\left[E(s) - F(s)F^{-1}E\right]R_a + F^{-T}F^T(s)R_b\Big)^2 \\ &= 4\gamma k_B \mathbb{T}\int_0^T ds\left[R_{\rm H}(s)\right]^2 , \end{aligned} \tag{6.105}$$

where $R_H(s)$ is the solution to the homogeneous equations of motion for the oscil-

[18] Note that it is also possible to solve it non-perturbatively in a Dyson equation fashion [4].

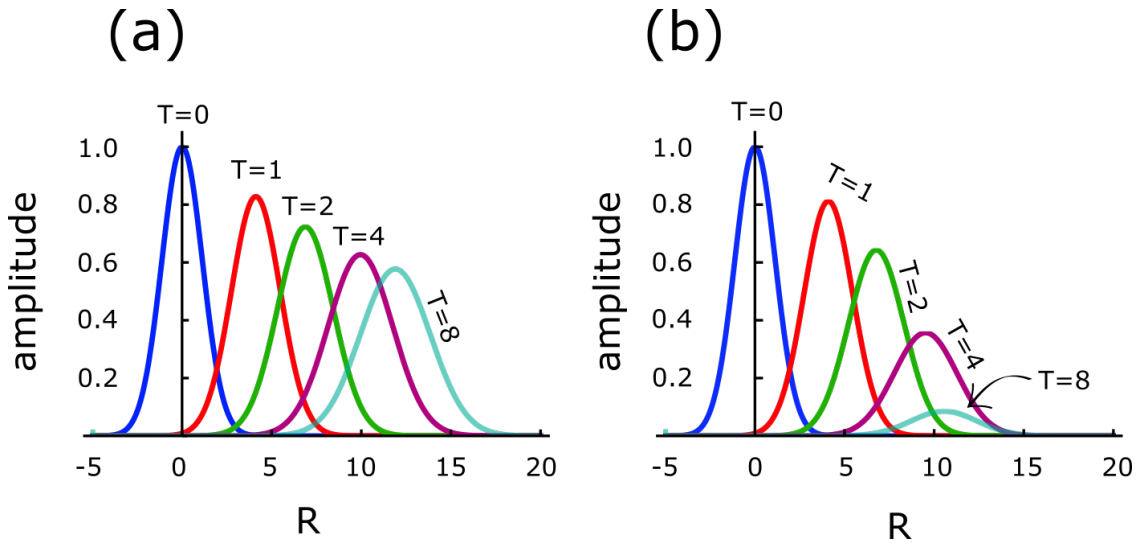

Figure 6.5: **(a)** Unitary evolution of the wavepacket. **(b)** Non-unitary evolution with $k_B\mathbb{T} \simeq 1/255$ (that is 300 K with a reference frequency $\Omega_{\text{ref}} = 10$ fs^{-1})

lator, seen in Eq. (6.86). This term is responsible for the loss of unitarity, since Eq. (6.105) enters the action in Eq. (6.102) with a factor of i, meaning that this 'phase' term in the propagator in Eq. (6.101) becomes a decay rate. We can now rewrite the noise averaged classical action as

$$S_{\text{cl}} = \frac{1}{2}\Big[R_b\left(\dot{F}F^{-1}+\gamma\right)R_b + R_a\left(F^{-1}E+\gamma\right)R_a \tag{6.106}$$
$$- R_a\left(F^{-1}+E^TF^{-T}H^T-G^T+2\gamma\right)R_b + i4\gamma k_BT\int_0^T ds\,[R_{\text{H}}(s)]^2\Big].$$

Here the first three terms govern the phase acquired ($\exp iS_{\text{cl}}$) by a wavepacket during propagation. This is unitary evolution. The 4$^{\text{th}}$-term of Eq. (6.106), on the other hand, leads to a decay rate — non-unitary evolution. Finally we arrive at the transition amplitude

$$\langle\langle R_b, T|R_a, 0\rangle\rangle = \sqrt{\frac{1}{2\pi i}\left(\gamma + \frac{\chi}{\sin\chi T}\cosh\gamma T\right)}e^{iS_{\text{cl}}}. \tag{6.107}$$

We can see a comparison of the unitary to non-unitary propagation of an initial state of the form of Eq. (6.90) in Fig. 6.5(a) and Fig. 6.5(b) respectively. As can be seen, the main effect of the 4$^{\text{th}}$-term in Eq. (6.106), which originates from the thermal fluctuations, is the loss of amplitude.

6.8 Vacuum radiation in absorbing media

Let us now take what we have learned from the damped harmonic oscillator and apply this to study quantum vacuum radiation in absorbing media. The idea here is to couple the oscillator, which is responsible for dispersion, to a reservoir in order to

induce damping. We can more or less apply the same procedure as in Section 6.7 in order to do this, but with some caveats. Also, we should note that other approaches to macroscopic quantum electrodynamics in absorbing media, the most prominent of which is by Huttner and Barnett [60], are very similar in spirit, building on the same idea of coupling the oscillator to a reservoir.

If we now return to the Hopfield action in Eq. (6.1), we want to further couple the harmonic oscillator $\mathbf{R}$ (which sets the resonance frequencies of the medium) to the bath degree of freedom. Our starting point is thus the action

$$\begin{aligned} S_\gamma &= \int_{t_i}^{t_f} dt \int d^3x \, \frac{1}{2}\left[\dot{\mathbf{A}}^2 - (\boldsymbol{\nabla}\times\mathbf{A})^2\right] \\ S_R &= \int_{t_i}^{t_f} dt \int d^3x \, \frac{\rho}{2}\left[\dot{\mathbf{R}}^2 - \Omega^2(t)\mathbf{R}^2\right] \\ S_D &= \int_{t_i}^{t_f} dt \int d\zeta \;\; \frac{1}{2}\left[\dot{D}^2 - (\partial_\zeta D)^2\right] \\ S_{\text{int,A}} &= \int_{t_i}^{t_f} dt \int d^3x \;\; (-\rho q) \;\; \dot{\mathbf{A}}\cdot\mathbf{R} \\ S_{\text{int,D}} &= \int_{t_i}^{t_f} dt \int d\zeta \; \dot{D}(\zeta,\tau)\delta(\zeta) \; \boldsymbol{\mu}\cdot\mathbf{R}(\tau), \end{aligned} \tag{6.108}$$

where $\boldsymbol{\mu}$ is a vector chosen along the polarisation directions in Eq. (6.2). The rationale behind choosing $\boldsymbol{\mu}$ in this way is to ensure that both polarisations are damped equally. Furthermore, we should note that this is possible because we have, when deriving Eq. (6.1), chosen to work with a spatially uniform oscillator $\mathbf{R}$ such that $\boldsymbol{\nabla}\cdot\mathbf{R} = 0$, which means that the oscillator also satisfies the Coulomb gauge condition. Further discussion of this can be found in Section 3.1 (p. 35). As before, we can expand into the polarisation directions $\mathbf{e}_\lambda$, re-define the fields and time-coordinates to scale it into dimensionless form, and split up the vector potential into real and imaginary parts $A_\mathbf{k} = x_\mathbf{k} + iy_\mathbf{k}$. This yields

$$\begin{aligned} S_{\gamma+R+I} &= \int_0^T d\tau \; \frac{1}{2}\dot{\mathbf{q}}^2 - \frac{1}{2}\mathbf{q}\cdot A^2\cdot\mathbf{q} + \frac{1}{2}\left(\mathbf{B}\times\mathbf{q}\right)\cdot\dot{\mathbf{q}} \\ S_D &= \int_0^T d\tau \int d\zeta \;\; \frac{1}{2}\left[\dot{D}^2 - (\partial_\zeta D)^2\right] \\ S_{\text{int,D}} &= \int_0^T d\tau \int d\zeta \; \dot{D}(\zeta,\tau)\delta(\zeta) \; \mu R(\tau), \end{aligned} \tag{6.109}$$

where

$$\begin{aligned} \mathbf{q} &= (x_\mathbf{k}, y_\mathbf{k}, R) \\ \mathbf{B} &= (0, -g, 0)\,. \end{aligned} \tag{6.110}$$

First of all, let us, as usual, ignore the $y_\mathbf{k}$ degree of freedom, as it is not coupled to

the matter degree of freedom. What follows is an extension of the method used in Section 6.7 to consider a 2-dimensional coordinate $\mathbf{q}$, rather than R. In particular, we consider only the retarded Green's function for the dissipator D. In this way, we can arrive at the equation of motion

$$\ddot{\mathbf{q}} + B_\gamma \dot{\mathbf{q}} + A^2(s)\mathbf{q} = \mathbf{J}, \tag{6.111}$$

where $\mathbf{J} = \left(0, \hat{\xi}\right)$ and

$$A^2 = \begin{pmatrix} k^2 & 0 \\ 0 & \Omega^2(s) \end{pmatrix}, \quad B_\gamma = \begin{pmatrix} 0 & -g \\ g & 2\gamma \end{pmatrix}, \tag{6.112}$$

where $\gamma = \mu^2/4$. Note that B_0, i.e. B_γ in the case when $\gamma = 0$, is the matrix we considered in the undamped case in Section 6.5 [Eq. (6.36)]. By introducing $\hat{\xi}$, we have a driven-damped system, which we can solve in the same manner as previously in terms of the matrices E, F, G, and H. In this case we have the equation of motion

$$\begin{pmatrix} \dot{E}(s) & \dot{F}(s) \\ \dot{G}(s) & \dot{H}(s) \end{pmatrix} = \begin{pmatrix} 0 & \mathbb{I} \\ -A^2(s) & -B_\gamma \end{pmatrix} \begin{pmatrix} E(s) & F(s) \\ G(s) & H(s) \end{pmatrix} \tag{6.113}$$

together with the initial values

$$\begin{pmatrix} E(0) & F(0) \\ G(0) & H(0) \end{pmatrix} = \begin{pmatrix} \mathbb{I} & 0 \\ 0 & \mathbb{I} \end{pmatrix}.$$

We can now go through the same procedure as in Section 6.7, but with the introduction of the matrix

$$\Gamma = \begin{pmatrix} 0 & 0 \\ 0 & \gamma \end{pmatrix}. \tag{6.114}$$

Finally we arrive at the action of the driven-dissipative Hopfield system

$$\begin{aligned} S_{\mathrm{cl}}\left[\hat{\xi}\right] = \frac{1}{2}\Big[& \mathbf{b}\left(\dot{F}F^{-1} + \Gamma\right)\mathbf{b} + \mathbf{a}\left(F^{-1}E + \Gamma\right)R_a \\ & - \mathbf{a}\left(F^{-1} + E^T F^{-T} H^T - G^T + 2\Gamma\right)\mathbf{b}\Big] \\ & + \int_0^T ds\, \mathbf{J}(s) \cdot \left\{\left[E(s) - F(s)F^{-1}E\right]\mathbf{a} + F(s)F^{-1}\mathbf{b}\right\} \\ & - \frac{1}{2}\int_0^T ds \int_0^T dt\, \mathbf{J}(s) \cdot \Delta(s,t) \cdot \mathbf{J}(t), \end{aligned} \tag{6.115}$$

where, as a reminder, the driving force

$$\mathbf{J} = \left(0, \hat{\xi}\right) \tag{6.116}$$

is of the stochastic nature explored in the end of Section 6.7. Also, we have introduced the classical propagator

$$\Delta(s,t) = \theta(s-t)\Big[S^T(s)F^T(t) + F(s)F^{-1}(T)E(T)Q(t) \\ + \; Q^T(s)E^T(T)F^{-T}(T)F^T(t) - E(s)Q(t)\Big], \tag{6.117}$$

which is the solution to

$$\left[\mathbb{I}\partial_s^2 + B_\gamma \partial_s + A^2(s)\right]\Delta(s,t) = \mathbb{I}\delta(s-t). \tag{6.118}$$

The transition amplitude now becomes

$$\langle \mathbf{b}, T|\mathbf{a}, 0\rangle_{\hat{\xi}} = \frac{\sqrt{|\mathcal{F}^{-1}|}}{2\pi i}\exp\left(iS_{\rm cl}\left[\hat{\xi}\right]\right), \tag{6.119}$$

where we used the Morette-van Hove determinant to calculate the pre-fractor of the path integral. Also we have here defined the matrix

$$\mathcal{F}^{-1} \equiv \frac{1}{2}\left(F^{-1} + E^T F^{-T} H^T - G^T + 2\Gamma\right) \tag{6.120}$$

for notational convenience. Note that as $\gamma \to 0$ then $\mathcal{F}^{-1} \to F^{-1}$, because $\Gamma = 0$ and $B_0 = -B_0^T$ in this limit, and thus Eq. (6.18) can be used.

6.8.1 Vacuum persistence amplitude

Suppose now we want to calculate the persistence amplitude of the ground state of the damped system. Let us for this calculation assume that the ground state is given by Eq. (6.30), i.e. that it has the same form as the un-damped ground state. We will return to the physical relevance of this shortly. As in Section 6.6, this involves calculating an integral of the form of Eq. (6.69), but where

$$\begin{aligned}
A &\to \Sigma_F^\gamma \equiv \mathcal{G}^* - i\dot{F}F^{-1} - i\Gamma, \\
B &\to -i\mathcal{F}^{-1}, \\
C &\to \Sigma_E^\gamma \equiv \mathcal{G} - iF^{-1}E - i\Gamma, \\
\mathbf{J} &\to i\int_0^T ds\; F^{-T}F^T(s)\mathbf{J}(s), \\
\mathbf{K} &\to i\int_0^T ds\; \left[E^T(s) - E^T F^{-T}F^T(s)\right]\mathbf{J}(s).
\end{aligned}$$

The rest follows analogously to Section 6.6. For notational simplicity let us furthermore define

$$\mathcal{S}^\gamma = \begin{pmatrix} \Sigma_F^\gamma & -i\mathcal{F}^{-1} \\ -i\mathcal{F}^{-T} & \Sigma_E^\gamma \end{pmatrix}, \tag{6.121}$$

the symmetrised Schur complements

$$\begin{aligned} (\mathcal{S}^\gamma/\Sigma_F)_{\text{sym}} &= \left(\Sigma_E^\gamma + \mathcal{F}^{-T}\,(\Sigma_F^\gamma)^{-1}_{\text{sym}}\,\mathcal{F}^{-1}\right)_{\text{sym}}, \\ (\mathcal{S}^\gamma/\Sigma_E)_{\text{sym}} &= \left(\Sigma_F^\gamma + \mathcal{F}^{-1}\,(\Sigma_E^\gamma)^{-1}_{\text{sym}}\,\mathcal{F}^{-T}\right)_{\text{sym}}, \end{aligned} \tag{6.122}$$

as well as the Fock space propagator

$$\begin{aligned} \Delta_{00}^\gamma(s,t) = i\Delta(s,t) &+ F(s)F^{-1}\,(\mathcal{S}/\Sigma_E^\gamma)^{-1}_{\text{sym}}\,F^{-T}F^T(t) \\ &+ \left\{E(s) - F(s)F^{-1}E\right\}(\mathcal{S}/\Sigma_F^\gamma)^{-1}_{\text{sym}}\left\{E^T(t) - E^TF^{-T}F^T(t)\right\} \\ &- 2iF(s)F^{-1}\,(\mathcal{S}/\Sigma_E^\gamma)^{-1}_{\text{sym}}\,F^{-1}\,(\Sigma_E^\gamma)^{-1}_{\text{sym}}\left\{E^T(t) - E^TF^{-T}F^T(t)\right\}. \end{aligned} \tag{6.123}$$

This yields the vacuum persistence amplitude

$$\langle 0|0\rangle_{\hat\xi}^\gamma = \langle 0|0\rangle^\gamma \exp\left(-\frac{1}{2}\int_0^T ds \int_0^s dt\ \mathbf{J}(s)\Delta_{00}^{\text{sym},\gamma}(s,t)\mathbf{J}(t)\right), \tag{6.124}$$

where

$$\langle 0|0\rangle^\gamma = \left(\frac{2}{i}\right)\sqrt{\frac{|\text{Re}\,[\mathcal{G}]\,|\,|\mathcal{F}^{-1}|}{|\Sigma_F^\gamma|_{\text{sym}}\left|\Sigma_E^\gamma + \mathcal{F}^{-1}\,(\Sigma_F^\gamma)^{-1}_{\text{sym}}\,\mathcal{F}^{-T}\right|_{\text{sym}}}}, \tag{6.125}$$

and where we have defined

$$\Delta_{00}^{\text{sym},\gamma}(s,t) = \Delta_{00}^\gamma(s,t) + \Delta_{00}^\gamma(t,s). \tag{6.126}$$

We can finally average over the noise $\hat\xi$ by computing

$$\langle\langle 0|0\rangle\rangle^\gamma = \langle 0|0\rangle^\gamma \int \mathcal{D}\hat\xi\ e^{-\int_0^T ds\int_0^T dt\ \frac{1}{2}\hat\xi(s)\left(K_{\mathbb{T}}^{-1}(s,t) + \theta(s-t)\left[\Delta_{00}^{\text{sym},\gamma}(s,t)\right]_{2,2}\right)\hat\xi(t)}, \tag{6.127}$$

where $\left[\Delta_{00}^{\text{sym},\gamma}(s,t)\right]_{2,2}$ is the element of the propagator in Eq. (6.123) related to the oscillator dynamics R. This yields

$$\langle\langle 0|0\rangle\rangle^\gamma = \langle 0|0\rangle^\gamma \sqrt{\frac{\det K_{\mathbb{T}}^{-1}}{\det\left[K_{\mathbb{T}}^{-1} + \left[\Delta_{00}^{\text{sym},\gamma}\right]_{2,2}\right]^{-1}}}. \tag{6.128}$$

The functional determinant can be re-written as

$$\sqrt{\frac{\det K_{\mathbb{T}}^{-1}}{\det\left[K_{\mathbb{T}}^{-1}+\left[\Delta_{00}^{\mathrm{sym},\gamma}\right]_{2,2}\right]^{-1}}}=\det\left[1+K_{\mathbb{T}}\left[\Delta_{00}^{\mathrm{sym},\gamma}\right]_{2,2}\right]^{-1/2}$$
$$=\exp\left[-\frac{1}{2}\,\mathrm{Tr}\,\log\left(1+K_{\mathbb{T}}\left[\Delta_{00}^{\mathrm{sym},\gamma}\right]_{2,2}\right)\right]. \qquad (6.129)$$

Now the exponent can be approximated as [172]

$$\mathrm{Tr}\left[\log\left(1+K_{\mathbb{T}}\left[\Delta_{00}^{\mathrm{sym},\gamma}\right]_{2,2}\right)\right]\simeq\mathrm{Tr}\left[K_T\left[\Delta_{00}^{\mathrm{sym},\gamma}\right]_{2,2}\right]$$
$$=\int_0^T ds\int_0^s dt\;K_{\mathbb{T}}(s,t)\left[\Delta_{00}^{\mathrm{sym},\gamma}(t,s)\right]_{2,2}$$
$$=4\gamma k_B\mathbb{T}\int_0^T ds\left[\Delta_{00}^{\mathrm{sym},\gamma}(s,s)\right]_{2,2} \qquad (6.130)$$

by expanding $\log(1+x)\simeq x$ for $x\ll 1$. This can be further simplified if we consider the form of $\left[\Delta_{00}^{\mathrm{sym},\gamma}(s,s)\right]_{2,2}$ [Eq. (6.123)]. It can be shown that the equal time Fock space propagator is a measure of the ground state fluctuations. In particular, the $(2,2)$-component measures the fluctuations in the matter degree of freedom R. These fluctuations will be proportional to the inverse of the ground state energy. For instance, if we let the plasma frequency g go to zero, where the relevant ground state energy is Ω, we know that $\left[\Delta_{00}^{\mathrm{sym},\gamma}(s,s)\right]_{2,2}=1/\Omega$. Therefore, if we consider a time-independent dielectric (where Ω is a constant) we find

$$\frac{1}{2}\left[\Delta_{00}^{\mathrm{sym},\gamma}(s,s)\right]_{2,2}=\int d^2q\;R^2\left|\Psi_0(\mathbf{q})\right|^2=\frac{1}{2N_R\left(\omega_++\omega_-\right)}.$$

It is thus reasonable to estimate $\left[\Delta_{00}^{\mathrm{sym},\gamma}(s,s)\right]_{2,2}\simeq 1/\left[N_R\left(\omega_++\omega_-\right)\right]$ also in the time-dependent dielectric. As a reminder, the coefficient N_R [Eq. (6.29)] determines the degree to which the ground state is matter-like. Hence we find

$$\sqrt{\frac{\det K_{\mathbb{T}}^{-1}}{\det\left(K_{\mathbb{T}}^{-1}+\left[\Delta_{00}^{\mathrm{sym},\gamma}\right]_{2,2}\right)^{-1}}}\simeq e^{-2\gamma\,k_B\mathbb{T}\,T/\left[N_R(\omega_++\omega_-)\right]}. \qquad (6.131)$$

The thermal noise thus introduces a weak exponential decay of the persistence amplitude. We can expect this exponential decay to be significant at timescales of $T\simeq\omega_\pm/2\gamma k_B\mathbb{T}$. In the optical regime where $\omega_\pm\gg k_B\mathbb{T}$, and with a small damping factor γ, this is much longer than any other timescale in the system.[19] For notational

[19]For instance, we find that room temperature (300 K) corresponds to $k_B\mathbb{T}\simeq 1/76$ with a reference frequency $\Omega_{\mathrm{ref}}=2\pi/210$ nm. If we further assume $\gamma=0.1$ and $N_R\left(\omega_++\omega_-\right)\simeq 3$ then the relevant timescale is $T\simeq 1140$.

simplicity, let us define the thermal decay rate

$$\gamma_{\text{th}} = 4\gamma\, k_B \mathbb{T} / \left[N_R \left(\omega_+ + \omega_- \right) \right].$$

At short timescales, we can nonetheless approximate

$$\sqrt{\frac{\det K_{\mathbb{T}}^{-1}}{\det\left(K_{\mathbb{T}}^{-1} + [\Delta_{00}^{\text{sym},\gamma}]_{2,2} \right)^{-1}}} \simeq 1, \tag{6.132}$$

but for longer times we find the damped vacuum persistence amplitude is given by

$$\langle\langle 0|0 \rangle\rangle^{\gamma} = \left(\frac{2}{i} \right) \sqrt{\frac{|\text{Re}\left[\mathcal{G}\right]|\,|\mathcal{F}^{-1}|}{|\Sigma_F^{\gamma}|_{\text{sym}} \left| \Sigma_E^{\gamma} + \mathcal{F}^{-1} \left(\Sigma_F^{\gamma}\right)_{\text{sym}}^{-1} \mathcal{F}^{-T} \right|_{\text{sym}}}} e^{-\gamma_{\text{th}} T/2}, \tag{6.133}$$

where, as a reminder, $\Sigma_F = \mathcal{G}^* - i\dot{F}F^{-1}$, $\Sigma_E = \mathcal{G} - iF^{-1}E$ with $\mathcal{G}$ given in Eq. (6.27) and $\mathcal{F}^{-1}$ as seen in Eq. (6.120). Furthermore, the propagation matrices F, E, H and G are obtained from Eq. (6.113).

Let us now return to the physical interpretation of this amplitude. From the above, it is clear that this amplitude will reduce with time, eventually reaching zero, as it continually dissipates energy into the bath D. Clearly this is not a good description of the ground state of the damped Hopfield system. This is related to the fact that we are treating the coupling to the bath perturbatively. Energy is allowed to flow away from the system and into the bath, but the energy flow back into the system is very small and of thermal nature.[20] For the latter, we are assuming that the temperature of the bath is at much lower energy than than the characteristic energy of the oscillator $\hbar\Omega$. This is a reasonable assumption for optical systems as typical optical energies of 1.5 eV are about ~ 60 times larger than room temperature (~ 300 K) energies.

Nonetheless, we would expect the ground state to persist. Suppose we first consider a static resonance frequency $\Omega^2(s) \equiv \Omega_0^2$ for some constant Ω_0. With the oscillator still coupled to the bath, we would from this computation expect the ground state to decay according to Eq. (6.133). We will call this amplitude $\langle\langle 0|0 \rangle\rangle^{\gamma}_{\text{static}}$, with the subscript 'static' implying a time-constant resonance frequency Ω^2. However, we can ensure that the ground state persists by renormalising the vacuum persistence to unity. This would involve simply dividing by Eq. (6.133) by itself.

Let us now return to a time-dependent resonance frequency $\Omega^2(s)$. Since a room temperature thermal state contains mostly the ground state,[21] we can also renormalise the modulated vacuum persistence amplitude (denoted as $\langle\langle 0|0 \rangle\rangle^{\gamma}_{\text{mod}}$)

[20] In the zero temperature limit, it would be appropriate to drive the system by the quantum fluctuations, as discussed briefly in Section 6.7.

[21] The relative population of the first excited state would be $\simeq e^{-60}$.

with respect to the static vacuum persistence amplitude. In other words, we only care about changes with respect to the static ground state. Physically, this implies that we assume that only states above the ground state are dissipated into the bath. In this way we can still extract information about quantum vacuum radiation by considering

$$P(\text{radiation}) = 1 - \left|\langle\langle 0|0\rangle\rangle^{\gamma}_{\text{mod}}\right|^2 / \left|\langle\langle 0|0\rangle\rangle^{\gamma}_{\text{static}}\right|^2 . \tag{6.134}$$

The polaritons that are excited from the vacuum state can however be absorbed by the bath, and we expect the long time dynamics of this probability to return to zero. This is in line of expectations for radiation in an absorbing medium. If the radiation can couple out before being absorbed, it can be observed.

6.8.2 Excitation probability

Unfortunately, extracting information about the quantum vacuum radiation from the vacuum persistence amplitude in this case is troublesome. This is because the normalisation procedure is prone to amplify numerical noise, since the matrices involved can quickly become near-singular due to the damping.[22] Instead, we can calculate the probability amplitude of starting in the vacuum state and finishing in an excited state. In particular, we are interested in the transition amplitude to excited states of the form

$$\Psi_2^{\text{ph}}(\mathbf{q}) = \left(\left|\text{Re}\left[\mathcal{G}\right]|\pi^{-2}\right)^{1/4}\left[2\text{Re}\left[\mathcal{G}\right]_{1,1}x_{\mathbf{k}}^2 - 1\right]e^{-\frac{1}{2}\mathbf{q}\cdot\mathcal{G}\cdot\mathbf{q}} \tag{6.135}$$

or

$$\Psi_2^{\text{m}}(\mathbf{q}) = \left(\left|\text{Re}\left[\mathcal{G}\right]|\pi^{-2}\right)^{1/4}\left[2\text{Re}\left[\mathcal{G}\right]_{2,2}R^2 - 1\right]e^{-\frac{1}{2}\mathbf{q}\cdot\mathcal{G}\cdot\mathbf{q}}. \tag{6.136}$$

The former [Eq. (6.135)] is a photon-like excited state containing two polaritons, whereas the latter [Eq. (6.135)] is matter-like. Here $\text{Re}\left[\mathcal{G}\right]_{i,j}$ is the (i,j)-component of the real part of $\mathcal{G}$. It is straightforward to show that the relevant transition amplitude can be calculated from the (un-renormalised) vacuum persistence amplitude by

$$\begin{aligned}\langle\langle 2|0\rangle\rangle^{\text{ph/m}} &= \int_{-\infty}^{\infty} d^3b\, d^3a\, \left[\Psi_2^{\text{ph/m}}(\mathbf{b})\right]^* \langle \mathbf{b}, T|\mathbf{a}, 0\rangle\, \Psi_0(\mathbf{a}) \\ &= -2\frac{\partial}{\partial\text{Re}\left[\mathcal{G}\right]_{1,1/2,2}}\langle\langle 0|0\rangle\rangle^{\gamma} \\ &= \langle\langle 0|0\rangle\rangle^{\gamma}\left[\left(\mathcal{S}^{\gamma}/\Sigma_E\right)_{\text{sym}}\right]_{2,2/1,1}\Big/\left|\left(\mathcal{S}^{\gamma}/\Sigma_E\right)_{\text{sym}}\right| .\end{aligned} \tag{6.137}$$

[22] In particular, the calculation of $\mathcal{F}^{-1}$ is troublesome with near-singular matrices.

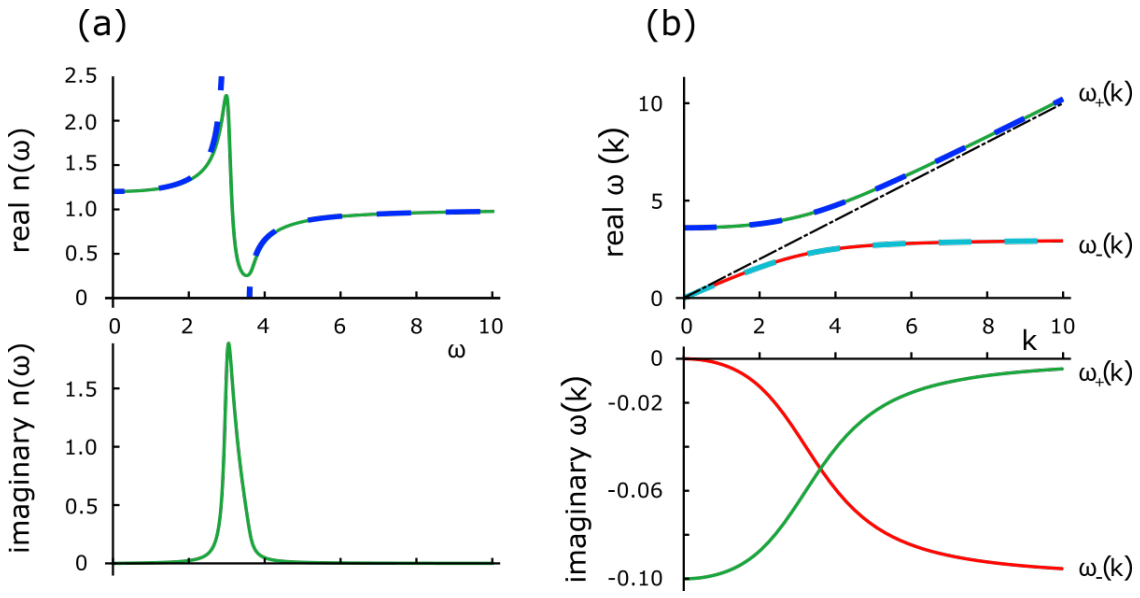

Figure 6.6: **(a)** Real and imaginary part of the refractive index for $\Omega = 3$, $g = 2$ and $\gamma = 0.1$. This can correspond to a variety of media with a single resonance frequency, since the reference frequency Ω_{ref} is not specified. However, it is the relation between the parameters Ω, g and γ that determines the physics. **(b)** Corresponding real and imaginary parts of the polariton frequencies $\omega_\pm$. Dashed lines represent the effective dispersion relation using the resonance frequency in Eq. (6.139). The differing signs between the imaginary parts of the refractive index and polariton frequency are due to the differing sign conventions for the space and time Fourier transforms.

Here we implicitly average over the thermal noise $\hat{\xi}$ in the first line. Note that we must do a bit of renormalisation here also, this time subtracting off the contribution from free (static) dynamics. This is because 2-polariton states is also absorbed by the bath, and the overlap with the ground state consequently increases. It should be noted that this procedure is also prone to noise, but considerably less.

Let us now consider the same optical medium that we used in Section 6.5, i.e. $\Omega = 3$ and $g = 2$, but with a damping term of $\gamma = 0.1$. This has the dispersion relation determined by

$$-\mathbf{k}^2 + \omega^2 \left(1 - \frac{g^2}{\omega^2 + 2\gamma i\omega - \Omega^2}\right) = 0. \tag{6.138}$$

The refractive index of this is shown in Fig. 6.6(a), determined by solving Eq. (6.138) for $k(\omega)$, with the corresponding polariton frequencies $\omega_\pm$ seen in Fig. 6.6(b). In particular, the real part of the polariton frequencies $\omega_\pm$ is given by Eq. (6.26) with a shifted resonance frequency

$$\Omega \to \sqrt{\Omega^2 - (2\gamma)^2}. \tag{6.139}$$

As a simple example, let us now modulate the medium with a single frequency ν at

amplitude α for some time σ such that

$$\Omega^2(s) = \Omega_0^2 \left[1 + \alpha \cos(\nu s)\, e^{-s^2/2\sigma^2}\right]. \tag{6.140}$$

The result can be seen in Fig. 6.7, where we consider wavenumber $k = 2$. Interestingly, if we compare the unitary and damped evolution we see that the damping does not contribute to the excitation dynamics, but simply shifts the polariton frequencies. After the polaritons are excited, however, the damping serves to reduce the overall amplitude. Specifically, we can take the damping into account by multiplying the unitary evolution by $\exp(-\gamma_\pm \tau)$,[23] where

$$\gamma_\pm = |\mathrm{Im}[\omega_\pm]|.$$

The damping rate will depend on the kind of excitation in the system. In the example chosen, we modulate at $2\omega_+$ and would therefore expect to predominately excite polaritons oscillating at ω_+. It is this decay rate that we see. We should note that the type of excitation studied here is not the pure co-rotating (ω_+) nor counter-rotating (ω_-) excited state.[24] In fact, both the photon-like state and the matter-like state contains a mix of both polariton modes.[25] This means that the probability of observing such a state will be damped by the maximum damping rate in the system.

Therefore, we finally find that we can solve the problem of numerical noise[26] by computing unitary dynamics, and afterwards subject the radiation to damping. The unitary dynamics is here simply solving Eq. (6.113) with $\gamma = 0$ everywhere, but with a shifted resonance frequency according to Eq. (6.139). For long time-dynamics, we must also include the damping γ_{th} due to the thermal noise. In short, we have

$$|\langle\langle 2|0\rangle\rangle^\gamma|^2 = |\langle 2|0\rangle|^2_{\mathrm{renorm}}\, e^{-\gamma_\pm \tau_{\mathrm{out}}} e^{-\gamma_{\mathrm{th}} \tau_{\mathrm{out}}}, \tag{6.141}$$

where $\langle 2|0\rangle_{\mathrm{renorm}}$ is the unitary evolution using the renormalised oscillation frequency in Eq. (6.139). Here τ_{out} is the time taken for the polaritons to exit the medium. This is in line with our discussion in Chapter 5, as well as Ref. [71]. It follows that we can extract information from the unitary evolution of the vacuum persistence amplitude in the same manner, such that the probability of emission becomes

$$P_{\mathrm{damped}} = \left(1 - |\langle 0|0\rangle|^2_{\mathrm{renorm}}\right) e^{-\gamma_\pm \tau_{\mathrm{out}}} e^{-\gamma_{\mathrm{th}} \tau_{\mathrm{out}}}, \tag{6.142}$$

where τ_{out} is an estimate of the time taken for any excitation to leave the medium,

[23] Here we can ignore the thermal noise as it is only relevant at much longer timescales.

[24] The actual wavefunctions are considerably more complicated and can be found in Ref. [173].

[25] They are nonetheless eigenstates of the system.

[26] As mentioned, this numerical noise originates from the fact that Eq. (6.113) yields near-singular matrices, especially at long time-scales due to the damping factor.

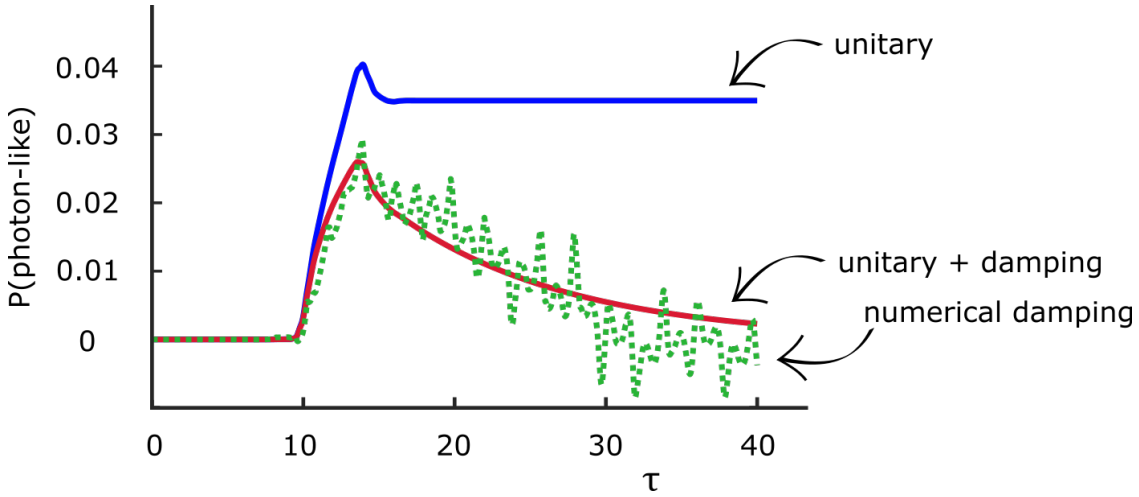

Figure 6.7: Probability of exciting a photon-like excitation by modulating the medium with $\nu = 2\omega_+$ and amplitude $\alpha = 0.9$, where $\Omega = 3$, $g = 2$ and $\gamma = 0.1$. The solid blue line is the the unitary dynamics with a shifted resonance frequency, and solid red denotes the unitary dynamics combined with damping determined by Eq. (6.141), whereas dashed green is the fully numerical solution. For this, we used a 4^{th}-order Runge-Kutta method to solve Eq. (6.113) with the above parameters specified for the medium. In particular, we consider a close to resonance wavenumber $k = 2$. Here we used the decay rate determined by $\text{Im}\,[\omega_+]$ on the unitary evolution. Naturally, the probabilities less than zero are noise and should be ignored.

usually directly proportional to the system size. For instance, for a medium of physical width L this time scale would be given by $\tau_{\text{out}} = \Omega_{\text{ref}} L$, where L should be given in units of $c = 1$.

We can therefore qualitatively expect the same behaviour as already discussed in Section 6.5, but where the overall extracted quantum vacuum radiation is reduced by a factor of $\sim \exp\left(-\gamma\tau_{\text{out}}\right)$. Here it is useful to give an estimate for the time τ_{out}. Suppose that we set the reference frequency $\Omega_{\text{ref}} \simeq 3$ fs^{-1} (such that the resonance frequency $\Omega = 3\Omega_{\text{ref}} \simeq 2\pi/210$ nm), where it is useful to recall Eq. (6.4) to see how the scaling factor enters. In this case, a medium of width 10 μm corresponds to $\tau_{\text{out}} \simeq 100$.

Let us now study three examples, first of all re-analysing the bichromatic driving we studied in Section 6.5, followed by a simulation of an expanding/contracting universe in the spirit of Section 5.1 from Chapter 5, and finish by a model of ENZ metamaterials similar to Section 5.2 of the same chapter.

6.8.3 Periodic modulation

Let us now return to periodic modulation, specifically the bichromatic modulation we studied in Section 6.5, and study how the damping affects the quantum vacuum radiation. We use the same medium as in the previous section,[27] whose optical characteristics can be seen in Fig. 6.6. Let us therefore return to modulating the

[27] That is, $\Omega = 3$, $g = 2$ and a damping rate of $\gamma = 0.1$.

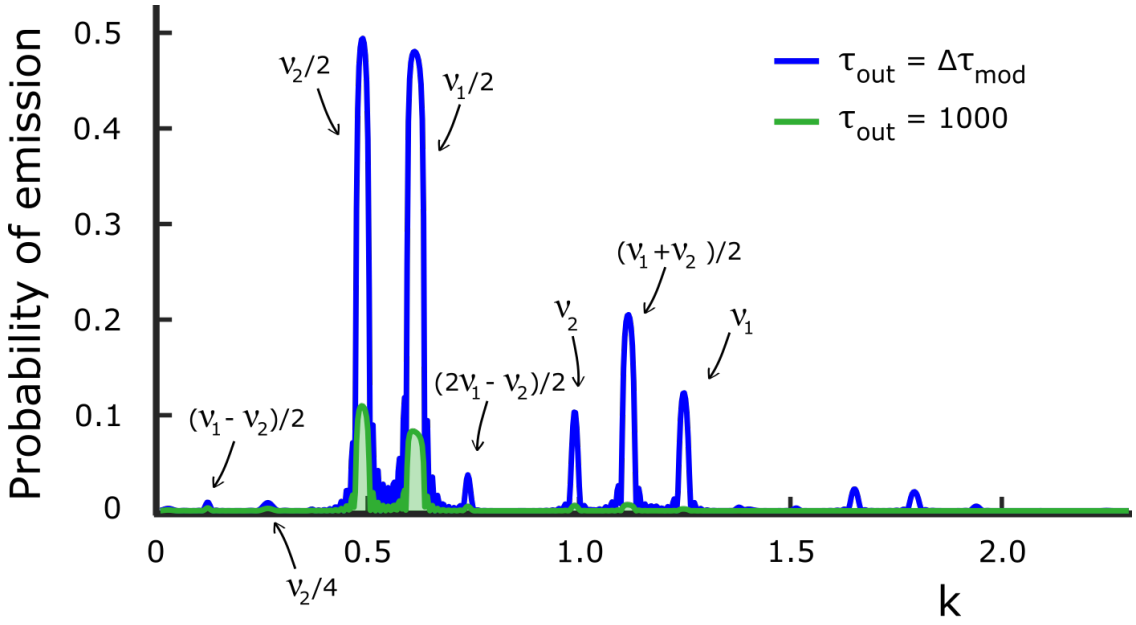

Figure 6.8: Probability of exciting polaritons from the vacuum state as measured at different times. $\tau_{\text{out}} = \Delta\tau_{\text{mod}}$ is the probability of observing quantum vacuum radiation emission directly after the modulation finishes, whereas $\tau_{\text{out}} = 1000$ is an estimate of surviving vacuum radiation as it exits the medium. Note the similarity to Fig. 6.3 (b).

resonance frequency as seen in Eq. (6.38). To re-cap, this is a time-dependent resonance frequency of the form

$$\Omega^2(s) = \Omega_0^2 \left(1 + \left[\alpha_1 \cos \nu_1 s + \alpha_2 \cos \nu_2 s\right] e^{-\left[s^2/(2\sigma^2)\right]^N}\right),$$

where α_i, ν_i, σ are the amplitudes, frequencies and duration of the modulation, respectively. Also, here N is the order of super-Gaussian. In Fig. 6.8 we see the resulting spectrum for $\alpha_1 = \alpha_2 = 0.3$, as well as $\nu_1 = 1$ and $\nu_2 = 0.8$ for a period of $\sigma = 100$ with $N = 10$. When compared to Fig. 6.3, we seen that the emitted radiation is essentially the same as without damping, albeit slightly shifted as expected due to the renormalised resonance frequency. However, the emission closer to the resonance frequency is quickly absorbed, and is thus unlikely to be observed.

6.8.4 Back to the expanding universe

Once again, we use the same medium as seen in Fig. 6.6. As opposed to the periodic modulation however, we now temporally vary the resonance frequency as

$$\Omega^2(s) = \Omega_0^2 \left(1 + \alpha \operatorname{sech} s/\sigma\right). \tag{6.143}$$

Depending on the sign of α, the permittivity ε either increases ($\text{sgn}(\alpha) = -1$) or decreases ($\text{sgn}(\alpha) = 1$) with time, connecting either to an expanding or a contracting spacetime, as discussed in Section 5.1 [specifically Eq. (5.27)]. As we mentioned

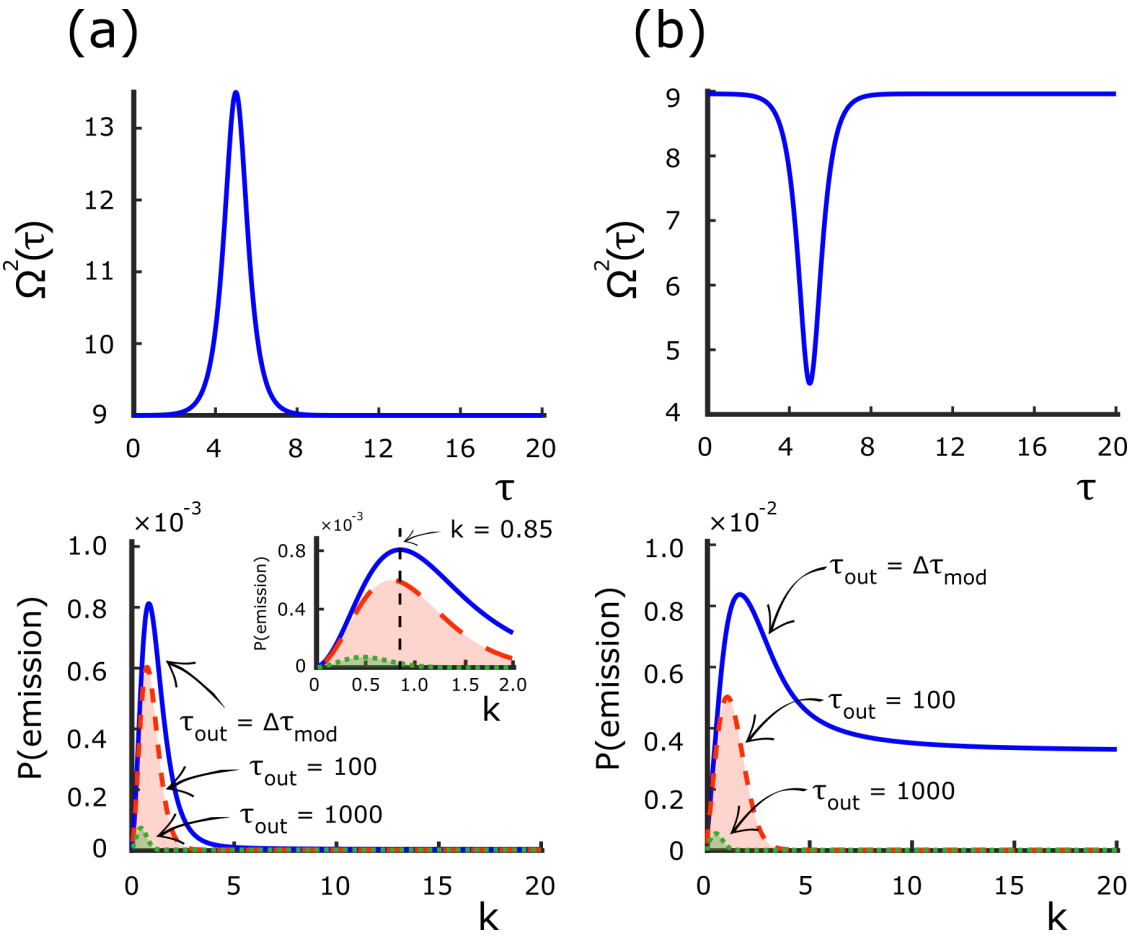

Figure 6.9: Probability of exciting polaritons from the vacuum state as measured at different times. We note here that the changes in resonance frequency are far into the non-perturbative regime. **(a)** A contracting 'universe'. Emission is centred around $\omega_- \simeq 0.38/\sigma$ [$k \simeq 0.85$], as seen in the inset. The duration of the temporal modulation is $\Delta\tau_{\rm mod}$. **(b)** An expanding 'universe'. Note the shifted peak emission at $k \simeq 1.8$, as compared to the contracting 'universe' in (a).

there, from a perturbative analysis we expect the emission to be centred around

$$\omega_- \simeq 0.38/\sigma. \tag{6.144}$$

This is indeed what we see in Fig. 6.9(a), i.e. for the analogue contracting spacetime where the permittivity decreases ($\mathrm{sgn}(\alpha) = 1$). Interestingly however, in the second case seen in Fig. 6.9(b), where the analogue spacetime expands ($\mathrm{sgn}(\alpha) = -1$) we see something different. Instead the emission is peaked at a higher frequency. This is a non-perturbative effect, related to the fact that the change in the permittivity is strongly peaked around the instantaneous resonance frequency $(1 \pm \alpha)\,\Omega_0$ at $s = 0$.

In the contracting 'universe', i.e. when the permittivity decreases in time, the change in permittivity is fairly flat close to $1/\sigma$, as the resonance frequency is moved further away. In the expanding 'universe', on the other hand, the resonance moves closer to $1/\sigma$, and consequently the peak permittivity variation is at a frequency

comparable to, but still different from, $1/\sigma$. As discussed in Section 5.3, we expect quantum emission to be maximised close to either the frequency set by the inverse of the modulation time σ or around the maximum of $\Delta\varepsilon/\varepsilon$. When $\mathrm{sgn}(\alpha) = -1$, both effects overlap considerably. In Fig. 6.9(b), the change in permittivity wins out, and the peak emission moves close to the $s = 0$ resonance frequency, which is here $\Omega(s = 0) \simeq 1.5$. This also explains the order of magnitude increase in the emission. In both cases we used $|\alpha| = 0.5$. The absorption however makes the probability of observing the quantum vacuum radiation more likely at lower frequencies. This is simply because the ω_-–polariton mode has a low damping rate at low frequencies, as these polaritons are mostly photon-like.

6.8.5 A slightly-less crude model of an ENZ material

Finally, let us attempt a model of an ε-near-zero metamaterial, as in Section 5.2. In our case, we have a permittivity given by

$$\varepsilon(\omega) = 1 - \frac{g^2}{\omega^2 + 2i\gamma\omega - \Omega^2}. \tag{6.145}$$

It is possible to model a medium with a real permittivity that crosses zero if the dominating frequency is the plasma frequency g. This corresponds to the strong-coupling limit, where the light-matter coupling dominates the physics. Interestingly, if we return to thinking of the light-matter coupling as an effective magnetic field, we see that the physics will be dominated by the effective Landau levels. Specifically, if we choose

$$\begin{aligned} \gamma &= 0.2, \\ \Omega &\simeq 4.2\gamma, \\ g &= 42\gamma, \end{aligned} \tag{6.146}$$

we find the permittivity seen in Fig. 6.10(a). Note the similarity to the actual ENZ metamaterials in Fig. 5.3. Here we find the crossing point $\omega_{\mathrm{ENZ}} \simeq \sqrt{g^2 - (2\gamma)^2} \simeq 4.4$.[28] In addition to this, we should take into account that the change in the permittivity is strongly peaked around ω_{ENZ}. We can do this by choosing a change in the oscillator frequency of the form

$$\Omega^2(s) = \Omega_0^2 \left[1 - \alpha(k)\,\mathrm{sech}(s/\sigma)\right], \tag{6.147}$$

[28] This follows from Eq. (5.31), as here $\varepsilon_\infty = 1$.

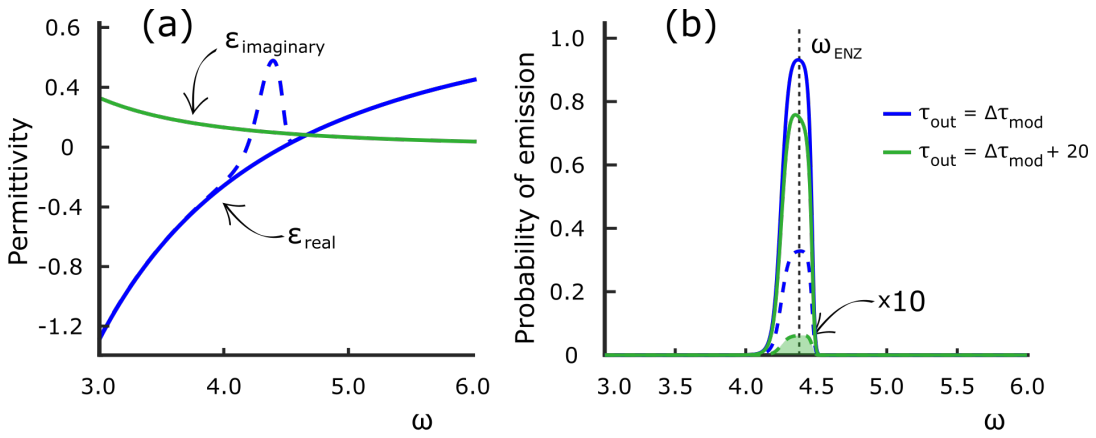

Figure 6.10: **(a)** Permittivity of the ε-near-zero metamaterial. Note the crossing point $\omega_{\mathrm{ENZ}} \simeq 4.4$ where the real permittivity goes to zero. Solid lines is the background permittivity, with blue the real part and green the imaginary part. Dashed blue denotes the maximum shift in the real permittivity due to the modulation. **(b)** Probability of exciting polaritons from the vacuum state. Blue is the initial probability directly after the modulation (whose duration is $\Delta\tau_{\mathrm{mod}}$), whereas green is the damped probability of observing the radiation after some time. Solid and dashed lines is the probability of observing ω_+–polaritons (matter-like) and ω_-–polaritons (photon-like) respectively.

where $\alpha(k)$ is given by

$$\alpha(k) = \alpha_0 \exp\left[-\frac{(k-k_{\mathrm{ENZ}})^2}{2\Delta_\omega^2}\right], \tag{6.148}$$

with $k_{\mathrm{ENZ}} = \mathrm{Re}\left[\sqrt{\varepsilon(\omega_{\mathrm{ENZ}})}\right] \times \omega_{\mathrm{ENZ}}$ being the in-material wavenumber corresponding to the ENZ frequency ω_{ENZ}. Interestingly, however, in order to model a medium where the change to the permittivity is of the order of unity in this manner, we must choose $\alpha_0 \simeq 50$ in Eq. (6.148). We find the resulting permittivity in the dashed line of Fig. 6.10(a), where we also set $\Delta_\omega = 0.1$. The result is that the matter degree of freedom turns from a harmonic oscillator to an inverted oscillator during the modulation. This will naturally excite polaritons from the vacuum state around the ε-near-zero frequency. This can be seen in Fig. 6.10(b), where the probability of emission is close to unity around ω_{ENZ}, in agreement with Section 5.2. Here we used $\sigma = 1/2$.

In addition to this we should note that the $1/\sigma$ chosen here is of the same order of magnitude as the ω_-–polariton, which is, in this case, the matter-like polariton as we are beyond the resonance frequency of the medium. The ω_+–polariton is, on the other hand, the photon-like mode, as discussed in Section 5.2. As we invert the oscillator, we would expect both polariton modes to be highly populated after the modulation.

The medium is however absorbing and both polariton modes are damped around

$\omega_{\rm ENZ}$, with the photon-like ω_+–polariton experiencing a higher rate of absorption. We see this in the green solid and dashed lines in Fig. 6.10(b) for the photon-like ω_+–mode and the matter-like ω_-–mode respectively. Nonetheless, this does not qualitatively change the spectrum, and the quantum vacuum radiation is centred around $\omega_{\rm ENZ}$. We should note however, that the damping of the photon-like ω_+–polaritons will preferentially leave polaritons at lower frequencies. This is qualitatively similar to what we found in Section 5.2, where the peak emission of photons was found to be slightly shifted to lower frequencies with respect to $\omega_{\rm ENZ}$.

6.9 Conclusions from a non-perturbative analysis

In this chapter, we found that the Hopfield model for macroscopic quantum electrodynamics can be mapped to a trapped particle in a magnetic field. This opens up a wide range of topics to be explored, and allowed for the solution of the problem in a non-perturbative manner. Here we focused on the quantum vacuum radiation from periodic modulation, essentially extending Chapter 3 to a non-perturbative setting where the changes to the medium properties can be of similar order to the background. We also extended the discussion to absorbing media, and connected the discussion briefly to analogue gravity and ε-near-zero materials that we explored in Chapter 5.

Starting with the periodic modulation, we confirmed what we found from the perturbative analysis in Chapter 3, i.e. that quantum vacuum radiation can be emitted whenever

$$m\omega_+ + n\omega_- = p\nu_1 + q\nu_2, \tag{6.149}$$

where m, n are positive integers whereas p, q can be both positive and negative. This is the case for a bichromatic drive oscillating at frequencies ν_1 and ν_2. The damping does not change this behaviour, but tends to strongly damp modes close to the resonance frequency, as expected. This means that quantum vacuum radiation close to the resonance frequency is unlikely to be observed. Instead, the damping rate serves to renormalise the resonance frequency such that $\Omega^2 \to \Omega^2 - (2\gamma)^2$.

Similarly, for a modulation that is aimed to model an expanding/contracting universe in the manner we discussed in Chapter 5, we can confirm that quantum vacuum radiation is peaked when

$$\omega_\pm \simeq 0.38/\sigma, \tag{6.150}$$

where σ is the characteristic time associated with expansion and contraction. This is the case when the change in permittivity is relatively uniform over the spectrum. If the permittivity change becomes peaked in some region on similar frequency-scale

as $1/\sigma$, the peak emission of quantum vacuum radiation shifts accordingly.

We find the latter physics again when we discuss ε-near-zero metamaterials. We know from experimental data (Ref. [71]) that the change in permittivity is strongly peaked around the frequency where the real permittivity crosses zero (ω_{ENZ}). To model this, we let the change in resonance frequency be peaked around these wavelengths. Subsequently, we found quantum vacuum radiation preferentially emitted around ω_{ENZ}. However, in order to model large changes to the permittivity of order unity we had to allow the modulation to invert the resonance of the matter degree of freedom. For some short time, the matter degree of freedom behaves as an inverted oscillator. These are unstable, and it comes as no surprise that this allows for near-unity probability of emission of quantum vacuum radiation. Whilst the results are similar to what we found in Chapter 5, perhaps a more sophisticated model of ε-near-zero metamaterials is warranted. In particular, since these are reasonably strongly-damped materials, we should expect the approximations made in deriving the damped vacuum persistence amplitude to break down. Nonetheless, the analysis presented here suggests that these materials are a promising experimental candidate for quantum vacuum radiation.

As a final remark, there is much that can be explored in macroscopic quantum electrodynamics if we think of it as a trapped particle in a magnetic field. Certainly it would be interesting if a functional variant of quantum Hall or topological physics could be realised in this manner. This would of course require the study of much more complicated media.

Chapter 7

Concluding remarks

"If I haven't seen as far as others,
it's because giants have been standing on my shoulders..."

Prof. Alejandro Jenkins, offhand remark about theses,
local pub in Edinburgh, May 2019

The pressing question now finally becomes, from this thesis, what have we learned about quantum vacuum radiation in optical media? That is what we will attempt to answer in this chapter. The aim here is not to go into any sort of detail, but rather to try link together the progress so far.

In this thesis we have built models for quantum vacuum radiation in optical media from first principles, starting with an action for the electromagnetic field coupled to some matter degree of freedom representing the optical medium. We then used this to study the radiation emitted from the vacuum state when some optical parameter varies temporally. Our aim was to build models applicable to optical experiments of bulk media or the bulk response of structured media, specifically in thin sheets and fibres, respectively. As such, we adopted a formalism of macroscopic quantum electrodynamics focused on optical media that could account for dispersion relations of the form

$$-|\mathbf{k}|^2 + \omega^2\left(1 - \frac{g^2}{\omega^2 + 2\gamma i\omega - \Omega^2}\right) = 0. \tag{7.1}$$

Here g is the plasma frequency of the medium, Ω its resonance frequency with γ being the damping rate. Time-dependent optical media can then be modelled by letting the previously mentioned parameters vary with time. We focused on the resonance frequency Ω, as we found it sufficient to model the experiments of interest.

After some introductory remarks and background theory in Chapters 1 and 2 respectively, we approached quantum vacuum radiation in Chapter 3 by supposing that the time-dependent changes to the medium were small enough to be treated analytically. From this we learned that the physics is well described by the collective light-matter excitations of the medium, namely the polaritons. Any excitation can be explained as transitions between the different polariton branches. However, we also have to keep in mind the nature of the medium, in particular the retarded

response. This becomes apparent at next-to-leading order in perturbation theory, where the probability amplitudes depend on past events. This latter effect allows the quantum vacuum radiation to be stimulated also by interference patterns in the temporal modulation, as opposed to being directly linked to the spectrum of the modulation. Interestingly, we found that the quantum vacuum radiation spectrum took on a character similar to what is observed in nonlinear optics, where sum and difference frequency generation is commonplace.

We then, in Chapter 4, applied this framework to analyse a fibre optics experiment. In this experiment, one of the dispersive parameters of the fibre was modulated in space and driven by a strong pump pulse. The pump pulse is responsible for creating a travelling refractive index perturbation, as well as a polarisation wave. Both effects can be modelled using the framework that we established in Chapter 3, and we found good agreement between the experimental results and the predicted quantum vacuum radiation (in fact they match exactly). In particular, we learn from the model that the photon pairs measured in the experiment are excited from the vacuum state by the beating pattern formed by the fibre modulation and the travelling polarisation wave of the pump. We must therefore conclude that the retarded response of the medium, and the subsequent frequency mixing processes, are required to describe the physics correctly.

The framework can also be applied to other scenarios, which is what we explored in Chapter 5. In the first part of the chapter, we explored some analogue gravity, specifically studying the photon pair production from an emulated expanding 'spacetime'. Whilst the effective 'spacetime' is of little cosmological relevance, we found that it serves as an interesting description of the low-energy physics of light in an optical medium.

Later in the chapter we turned to an experiment which cannot faithfully be described using the perturbative framework. Here we studied a so-called ε-near-zero metamaterial, a material whose permittivity ε passes through zero at some frequency ω_{ENZ}. In such a material it is known that the nonlinear response can change the refractive index from $\mathcal{O}(0.1)$ to $\mathcal{O}(1)$ — a highly non-perturbative setting. Through an analysis that neglects the time-nonlocal response, we found that the quantum vacuum radiation in this case becomes strongly centred around ω_{ENZ}.

We returned to this problem in Chapter 6, where we created a framework capable of taking into account both non-perturbative changes to the permittivity, as well as the time-nonlocal character of optical dispersion. Interestingly, we found that our formulation of macroscopic quantum electrodynamics could be mapped to a harmonically trapped particle in a magnetic field. Even if this is a 'particle' in functional space as opposed to real space, this allowed us to use much of the intuition from quantum mechanics to study quantum vacuum radiation. Subsequently we studied a sample of non-perturbative settings, including a bichromatic driving in the spirit of Chapter 3, an expanding 'spacetime' similar to Chapter 5 as well as a

model of an ε-near-zero metamaterial.

In the first case, we confirmed some of the results obtained in the perturbative setting, and furthermore expanded the spectrum to include further mixed-frequency resonances. This yielded the general energy conservation condition of

$$m\omega_+ + n\omega_- = p\nu_1 + q\nu_2 \tag{7.2}$$

where $m, n \in \mathbb{Z}^+$ whereas $p, q \in \mathbb{Z}$. Here ω_+ and ω_- are the polariton frequencies of the co-rotating and counter-rotating polariton branch respectively, and $\nu_{1,2}$ are the two frequencies of the bichromatic modulation. It is not hard to generalise this to include further frequencies in the drive, and we can imagine driving quantum vacuum radiation from a multitude of 'interference'-frequencies, since $p, q, ...$ are allowed to be both positive and negative.

In the cases of analogue gravity and ENZ metamaterials, we found results that were largely in agreement with the treatment in previous chapters — fascinatingly, in ENZ metamaterials the time-nonlocal response is not all that important. We should note here that if we return to thinking of this as particles and magnetic fields, we realise that the physics is dominated by the magnetic field, and therefore transitions between the effective Landau levels. The indifference of quantum vacuum radiation to the time-nonlocal response in ENZ metamaterials is perhaps not so surprising in light of this.

All in all, quantum vacuum radiation from time-dependent optical media can come in all shapes and colours. Sometimes we have to recall its time-nonlocal origin, and other times we can think of it as a trapped particle in a magnetic field! Especially in the latter interpretation is there bound to be new physics to explore.

Veni, bibi, scripsi — said Harold the Hypothetically Attentive Reader Of Limitless Discernment.

Bibliography

[1] J. D. Jackson, *Classical electrodynamics* (Wiley, 1999).

[2] R. Loudon, *The Quantum Theory of Light* (OUP Oxford, 2000) Chap. 4.

[3] R. Feynman, A. Hibbs, and D. Styer, *Quantum Mechanics and Path Integrals: Emended Edition* (Dover Publications, 2010).

[4] M. Srednicki, *Quantum Field Theory* (Cambridge University Press, 2007) Chap. 1 & 8.

[5] A. Altland and B. D. Simons, *Condensed Matter Field Theory* (Cambridge University Press, 2010).

[6] G. T. Moore, Journal of Mathematical Physics **11**, 2679 (1970).

[7] J. R. Johansson, G. Johansson, C. M. Wilson, and F. Nori, Phys. Rev. Lett. **103**, 147003 (2009).

[8] C. Wilson, G. Johansson, A. Pourkabirian, M. Simoen, J. Johansson, T. Duty, F. Nori, and P. Delsing, Nature **479**, 376 (2011).

[9] D. A. R. Dalvit, P. A. M. Neto, and F. D. Mazzitelli, "Fluctuations, dissipation and the dynamical casimir effect," in *Casimir Physics*, edited by D. Dalvit, P. Milonni, D. Roberts, and F. da Rosa (Springer Berlin Heidelberg, Berlin, Heidelberg, 2011) pp. 419–457.

[10] P. D. Nation, J. R. Johansson, M. P. Blencowe, and F. Nori, Rev. Mod. Phys. **84**, 1 (2012).

[11] C. Eberlein, Phys. Rev. Lett. **76**, 3842 (1996).

[12] C. S. Unnikrishnan and S. Mukhopadhyay, Phys. Rev. Lett. **77**, 4690 (1996).

[13] N. García and A. P. Levanyuk, Phys. Rev. Lett. **78**, 2268 (1997).

[14] A. Lambrecht, M.-T. Jaekel, and S. Reynaud, Phys. Rev. Lett. **78**, 2267 (1997).

[15] N. Birrel and P. Davies, *Quantum Field Theory in curved space-time* (Cambridge University Press, Cambridge, 1982).

[16] P. Candelas and D. J. Raine, Journal of Mathematical Physics **17**, 2101 (1976).

[17] P. Candelas and D. Deutsch, Proceedings of the Royal Society of London. A. Mathematical and Physical Sciences **354**, 79 (1977).

[18] P. C. Davies and S. A. Fulling, Proceedings of the Royal Society of London. A. Mathematical and Physical Sciences **356**, 237 (1977).

[19] W. G. Unruh, Phys. Rev. Lett. **46**, 1351 (1981).

[20] W. G. Unruh and R. M. Wald, Phys. Rev. D **25**, 942 (1982).

[21] S. W. Hawking, Nature **248**, 30 (1974).

[22] S. W. Hawking, Communications in Mathematical Physics **43**, 199 (1975).

[23] H. Stephani, D. Kramer, M. MacCallum, C. Hoenselaers, and E. Herlt, *Exact solutions of Einstein's field equations* (Cambridge University Press, 2003) Chap. 14.

[24] C. Barcelo, S. Liberati, and M. Visser, Living reviews in relativity **14**, 3 (2011).

[25] P. O. Fedichev and U. R. Fischer, Phys. Rev. A **69**, 033602 (2004).

[26] A. Prain, S. Fagnocchi, and S. Liberati, Phys. Rev. D **82**, 105018 (2010).

[27] C. Barceló, S. Liberati, and M. Visser, Phys. Rev. A **68**, 053613 (2003).

[28] M. Uhlmann, Y. Xu, and R. Schützhold, New Journal of Physics **7**, 248 (2005).

[29] R. Schützhold, M. Uhlmann, L. Petersen, H. Schmitz, A. Friedenauer, and T. Schätz, Phys. Rev. Lett. **99**, 201301 (2007).

[30] M. Wittemer, F. Hakelberg, P. Kiefer, J.-P. Schröder, C. Fey, R. Schützhold, U. Warring, and T. Schaetz, arXiv preprint arXiv:1903.05523 (2019).

[31] N. Westerberg, S. Cacciatori, F. Belgiorno, F. Dalla Piazza, and D. Faccio, New Journal of Physics **16**, 075003 (2014).

[32] J. Steinhauer, Nature Physics **12**, 959 (2016).

[33] J. R. Muñoz de Nova, K. Golubkov, V. I. Kolobov, and J. Steinhauer, Nature **569**, 688 (2019).

[34] J. Hu, L. Feng, Z. Zhang, and C. Chin, Nature Physics **15**, 785–789 (2019).

[35] J. Drori, Y. Rosenberg, D. Bermudez, Y. Silberberg, and U. Leonhardt, Phys. Rev. Lett. **122**, 010404 (2019).

[36] L. Parker, Phys. Rev. **183**, 1057 (1969).

[37] T. Jacobson, in *Lectures on Quantum Gravity* (Springer, 2005) pp. 39–89.

[38] L. Ford, in *General Relativity and Gravitation* (World Scientific, 2002) pp. 490–493.

[39] V. F. Mukhanov and S. Winitzki, Lecture notes (2005).

[40] V. I. Arnol'd, *Mathematical methods of classical mechanics*, Vol. 60 (Springer Science & Business Media, 2013).

[41] C. Hsu, Journal of Applied Mechanics **30**, 367 (1963).

[42] A. H. Nayfeh and D. T. Mook, The Journal of the Acoustical Society of America **62**, 375 (1977).

[43] R. Baskaran and K. L. Turner, Journal of Micromechanics and Microengineering **13**, 701 (2003).

[44] A. Ganesan, C. Do, and A. Seshia, EPL (Europhysics Letters) **119**, 10002 (2017).

[45] J. Jin and Z. Song, Journal of Fluids and Structures **20**, 763 (2005).

[46] J. G. Vioque, A. R. Champneys, and M. Truman, SeMA Journal **51**, 63 (2010).

[47] Y. M. Shukrinov, H. Azemtsa-Donfack, I. Rahmonov, and A. Botha, Low Temperature Physics **42**, 446 (2016).

[48] M. Castellanos-Beltran, K. Irwin, G. Hilton, L. Vale, and K. Lehnert, Nature Physics **4**, 929 (2008).

[49] A. A. Svidzinsky, L. Yuan, and M. O. Scully, Phys. Rev. X **3**, 041001 (2013).

[50] D. C. Burnham and D. L. Weinberg, Phys. Rev. Lett. **25**, 84 (1970).

[51] T. E. Keller and M. H. Rubin, Phys. Rev. A **56**, 1534 (1997).

[52] Y. Shih, Reports on Progress in Physics **66**, 1009 (2003).

[53] R. W. Boyd, *Nonlinear Optics* (Academic Press, 2003) Chap. 1.

[54] E. Hecht, *Optics*, 3rd ed. (Pearson, 2002) Chap. 3.

[55] L. D. Landau, J. Bell, M. Kearsley, L. Pitaevskii, E. Lifshitz, and J. Sykes, *Electrodynamics of continuous media*, Vol. 8 (Elsevier, 2013).

[56] G. S. Agarwal, *Quantum optics* (Cambridge University Press, 2012).

[57] L. Knoll, S. Scheel, and D.-G. Welsch, arXiv: quant-ph/0006121 (2003).

[58] S. Scheel and S. Buhmann, Acta Physica Slovaca **58**, 675 (2008).

[59] J. J. Hopfield, Phys. Rev. **112**, 1555 (1958).

[60] B. Huttner and S. M. Barnett, Phys. Rev. A **46**, 4306 (1992).

[61] T. G. Philbin, New Journal of Physics **12**, 123008 (2010).

[62] W. M. Simpson and U. Leonhardt, *Forces of the quantum vacuum: An Introduction to Casimir Physics* (World Scientific Publishing Company, 2015).

[63] M. Silveri, J. Tuorila, E. Thuneberg, and G. Paraoanu, Reports on Progress in Physics **80**, 056002 (2017).

[64] K. Brown, A. Lowenstein, and H. Mathur, Phys. Rev. A **99**, 022504 (2019).

[65] E. Yablonovitch, Phys. Rev. Lett. **62**, 1742 (1989).

[66] J. T. Mendonça, A. Guerreiro, and A. M. Martins, Phys. Rev. A **62**, 033805 (2000).

[67] J. T. Mendonça, *Theory of photon acceleration* (CRC Press, 2000).

[68] J. T. Mendonça and P. K. Shukla, Physica Scripta **65**, 160 (2002).

[69] J. T. Mendonça and A. Guerreiro, Phys. Rev. A **72**, 063805 (2005).

[70] S. Liberati, A. Prain, and M. Visser, Phys. Rev. D **85**, 084014 (2012).

[71] A. Prain, S. Vezzoli, N. Westerberg, T. Roger, and D. Faccio, Phys. Rev. Lett. **118**, 133904 (2017).

[72] V. Dodonov and A. Dodonov, *Journal of Physics: Conference Series*, **99**, 012006 (2008).

[73] F. Belgiorno, S. Cacciatori, and F. Dalla Piazza, Physica Scripta **91**, 015001 (2015).

[74] S. Finazzi and I. Carusotto, Phys. Rev. A **87**, 023803 (2013).

[75] D. Mills and E. Burstein, Reports on Progress in Physics **37**, 817 (1974).

[76] M. Artoni and J. L. Birman, Phys. Rev. B **44**, 3736 (1991).

[77] A. Reiserer and G. Rempe, Rev. Mod. Phys. **87**, 1379 (2015).

[78] S. Portolan, L. Einkemmer, Z. Vörös, G. Weihs, and P. Rabl, New Journal of Physics **16**, 063030 (2014).

[79] H. Deng, H. Haug, and Y. Yamamoto, Rev. Mod. Phys. **82**, 1489 (2010).

[80] I. Carusotto and C. Ciuti, Rev. Mod. Phys. **85**, 299 (2013).

[81] M. Aspelmeyer, T. J. Kippenberg, and F. Marquardt, Rev. Mod. Phys. **86**, 1391 (2014).

[82] M.-A. Lemonde and A. A. Clerk, Phys. Rev. A **91**, 033836 (2015).

[83] P. Törmä and W. L. Barnes, Reports on Progress in Physics **78**, 013901 (2014).

[84] C. Ciuti, G. Bastard, and I. Carusotto, Phys. Rev. B **72**, 115303 (2005).

[85] S. D. Liberato, C. Ciuti, and I. Carusotto, Phys. Rev. Lett. **98**, 103602 (2007).

[86] A. Auer and G. Burkard, Phys. Rev. B **85**, 235140 (2012).

[87] R. Stassi, A. Ridolfo, O. Di Stefano, M. J. Hartmann, and S. Savasta, Phys. Rev. Lett. **110**, 243601 (2013).

[88] A. Dodonov, Journal of Physics: Conference Series **161**, 012029 (2009).

[89] A. F. Kockum, V. Macrì, L. Garziano, S. Savasta, and F. Nori, Scientific reports **7**, 5313 (2017).

[90] F. Barachati, S. De Liberato, and S. Kéna-Cohen, Phys. Rev. A **92**, 033828 (2015).

[91] A. A. Anappara, S. De Liberato, A. Tredicucci, C. Ciuti, G. Biasiol, L. Sorba, and F. Beltram, Phys. Rev. B **79**, 201303 (2009).

[92] I. de Sousa and A. Dodonov, Journal of Physics A: Mathematical and Theoretical **48**, 245302 (2015).

[93] C. Ciuti, P. Schwendimann, and A. Quattropani, Semiconductor science and technology **18**, S279 (2003).

[94] W. Naylor, Phys. Rev. A **91**, 053804 (2015).

[95] V. Hizhnyakov, A. Loot, and S. Azizabadi, Applied Physics A **122**, 333 (2016).

[96] L. Caspani, R. P. M. Kaipurath, M. Clerici, M. Ferrera, T. Roger, J. Kim, N. Kinsey, M. Pietrzyk, A. Di Falco, V. M. Shalaev, A. Boltasseva, and D. Faccio, Phys. Rev. Lett. **116**, 233901 (2016).

[97] S. Vezzoli, A. Mussot, N. Westerberg, A. Kudlinski, H. D. Saleh, A. Prain, F. Biancalana, E. Lantz, and D. Faccio, Nat. Comm. Phys. **2**, (2019).

[98] C. Grosche and F. Steiner, *Handbook of Feynman Path Integrals* (Springer, 1998) Chap. 6.

[99] B. Pendleton, *Lecture notes on Quantum Theory* (The School of Physics and Astronomy, The University of Edinburgh, 2015).

[100] W. E. Boyce, R. C. DiPrima, and D. B. Meade, *Elementary differential equations and boundary value problems*, Vol. 9 (Wiley New York, 1992).

[101] F. Olness and R. Scalise, American Journal of Physics **79**, 306 (2011).

[102] I. M. Gel'fand and A. M. Yaglom, Journal of Mathematical Physics **1**, 48 (1960).

[103] H. Kleinert, *Path integral in quantum mechanics, statistics, polymer physics, and financial markets* (World scientific, 2009).

[104] S. Coleman, in *The whys of subnuclear physics* (Springer, 1979) pp. 805–941.

[105] C. Morette, Phys. Rev. **81**, 848 (1951).

[106] B. R. Holstein and A. R. Swift, American Journal of Physics **50**, 829 (1982).

[107] G. Agrawal, *Nonlinear Fiber Optics*, 5th ed. (Elsevier Inc. Academic Press, 2012).

[108] A. Smilga, International Journal of Modern Physics A **32**, 1730025 (2017).

[109] T. Kashiwa, T. Kashiwa, Y. Ohnuki, and M. Suzuki, *Path integral methods* (Oxford University Press on Demand, 1997).

[110] M. F. Linder, R. Schützhold, and W. G. Unruh, Phys. Rev. D **93**, 104010 (2016).

[111] C. Cohen-Tannoudji, J. Dupont-Roc, and G. Grynberg, *Photons and Atoms - Introduction to Quantum Electrodynamics* (Wiley-VCH, 1997).

[112] R. Y. Chiao, T. H. Hansson, J. M. Leinaas, and S. Viefers, Phys. Rev. A **69**, 063816 (2004).

[113] J. W. Goodman, *Introduction to Fourier optics* (Roberts and Company Publishers, 2005).

[114] G. F. Calvo, A. Picón, and E. Bagan, Phys. Rev. A **73**, 013805 (2006).

[115] C. Rovelli, *Quantum Gravity* (Cambridge University Press, 2007) Chap. 5.3.

[116] W. Heisenberg and H. Euler, Zeitschrift für Physik **98**, 714 (1936).

[117] H. Georgi, Annual Review of Nuclear and Particle science **43**, 209 (1993).

[118] B. Gripaios, arXiv preprint arXiv:1506.05039 (2015).

[119] J. C. P. Barros, M. Dalmonte, and A. Trombettoni, arXiv preprint arXiv:1708.06585 (2017).

[120] B. Grinstein, D. O'Connell, and M. B. Wise, Phys. Rev. D **77** (2008), 10.1103/PhysRevD.77.025012.

[121] R. K. Gainutdinov, Journal of Physics A: Mathematical and General **32**, 5657 (1999).

[122] A. Smilga, International Journal of Modern Physics A **32**, 1730025 (2017).

[123] M. Ismail and P. Simeonov, Proceedings of the American Mathematical Society **143**, 1397 (2015).

[124] A. Ghanmi, Integral Transforms and Special Functions **24**, 884 (2013).

[125] N. Cotfas, J. P. Gazeau, and K. Górska, Journal of Physics A: Mathematical and Theoretical **43**, 305304 (2010).

[126] A. Arbab, EPL (Europhysics Letters) **98**, 30008 (2012).

[127] J. V. Jelley, British Journal of Applied Physics **6**, 227 (1955).

[128] A. J. Macleod, A. Noble, and D. A. Jaroszynski, Phys. Rev. Lett. **122**, 161601 (2019).

[129] G. Chen, J. Tian, B. Bin-Mohsin, R. Nessler, A. Svidzinsky, and M. O. Scully, Physica Scripta **91**, 073004 (2016).

[130] A. Kempf and A. Prain, Journal of Mathematical Physics **58**, 082101 (2017).

[131] R. H. Hadfield, Nature photonics **3**, 696 (2009).

[132] M. Z. Alam, I. De Leon, and R. W. Boyd, Science , aae0330 (2016).

[133] P. Russell, Science **299**, 358 (2003).

[134] E. Bocquillon, C. Couteau, M. Razavi, R. Laflamme, and G. Weihs, Phys. Rev. A **79**, 035801 (2009).

[135] M. Petev, N. Westerberg, D. Moss, E. Rubino, C. Rimoldi, S. L. Cacciatori, F. Belgiorno, and D. Faccio, Phys. Rev. Lett. **111**, 043902 (2013).

[136] W. Gordon, Annalen der Physik **377**, 421 (1923).

[137] U. Leonhardt and T. G. Philbin, in *Progress in Optics*, Vol. 53 (Elsevier, 2009) pp. 69–152.

[138] N. Westerberg, S. Cacciatori, F. Belgiorno, F. Dalla Piazza, and D. Faccio, New Journal of Physics **16**, 075003 (2014).

[139] V. G. Dmitriev, G. G. Gurzadyan, and D. N. Nikogosyan, *Handbook of Nonlinear Optical Crystals*, Vol. 64 (Springer, 2013).

[140] N. Engheta, Science **340**, 286 (2013).

[141] I. Liberal and N. Engheta, Opt. Photon. News **27**, 26 (2016).

[142] I. Liberal and N. Engheta, Proceedings of the National Academy of Sciences **114**, 822 (2017).

[143] T. S. Luk, D. De Ceglia, S. Liu, G. A. Keeler, R. P. Prasankumar, M. A. Vincenti, M. Scalora, M. B. Sinclair, and S. Campione, Applied Physics Letters **106**, 151103 (2015).

[144] V. Fock, Zeitschrift für Physik A Hadrons and Nuclei **47**, 446 (1928).

[145] C. G. Darwin, in *Mathematical Proceedings of the Cambridge Philosophical Society*, Vol. 27 (Cambridge University Press, 1931) pp. 86–90.

[146] C. Kittel, *Introduction to solid state physics*, Vol. 8 (Wiley New York, 1976).

[147] I. M. Davies, Journal of Physics A: Mathematical and General **18**, 2737 (1985).

[148] C. Runge, Mathematical Annals **46**, 167 (1895).

[149] W. Kutta, Z. Math. Phys. **46**, 435 (1901).

[150] C. Cohen-Tannoudji, B. Diu, F. Laloe, and B. Dui, *Quantum Mechanics, Volume 1: Basic Concepts, Tools, and Applications*, 2nd ed. (Wiley-VCH, 2019) — Chapter 6, Complement E.

[151] L. D. Landau and E. M. Lifshitz, *Quantum mechanics: non-relativistic theory*, Vol. 3 (Elsevier, 2013).

[152] V. I. Arnol'd, *Mathematical methods of classical mechanics*, Vol. 60 (Springer Science & Business Media, 2013) Chap. 5.

[153] F. Zhang, *The Schur complement and its applications*, Vol. 4 (Springer Science & Business Media, 2006).

[154] G. W. Ford, J. T. Lewis, and R. F. O'Connell, Phys. Rev. A **37**, 4419 (1988).

[155] C. M. Savage and D. F. Walls, Phys. Rev. A **32**, 3487 (1985).

[156] C. Aslangul, N. Pottier, and D. Saint-James, Journal de Physique **48**, 1871 (1987).

[157] H. Dekker, Physics Reports **80**, 1 (1981).

[158] H. Grabert, U. Weiss, and P. Talkner, Zeitschrift für Physik B Condensed Matter **55**, 87 (1984).

[159] E. G. Harris, Phys. Rev. A **42**, 3685 (1990).

[160] T. G. Philbin, New Journal of Physics **14**, 083043 (2012).

[161] S. M. Barnett, J. D. Cresser, and S. Croke, arXiv preprint arXiv:1508.02442 (2015).

[162] G. S. Agarwal, in *Progress in optics*, Vol. 11 (Elsevier, 1973) pp. 1–76.

[163] F. Haake, in *Springer tracts in modern physics* (Springer, 1973) pp. 98–168.

[164] H. Carmichael, *An open systems approach to quantum optics: lectures presented at the Université Libre de Bruxelles, October 28 to November 4, 1991*, Vol. 18 (Springer Science & Business Media, 2009).

[165] L. M. Sieberer, M. Buchhold, and S. Diehl, Reports on Progress in Physics **79**, 096001 (2016).

[166] E. G. D. Torre, S. Diehl, M. D. Lukin, S. Sachdev, and P. Strack, Phys. Rev. A **87**, 023831 (2013).

[167] H. Seifoory and M. M. Dignam, Phys. Rev. A **97**, 023840 (2018).

[168] D. A. R. Dalvit, P. A. M. Neto, and F. D. Mazzitelli, *Casimir Physics*, edited by D. Dalvit, P. Milonni, D. Roberts, and F. da Rosa (Springer Berlin Heidelberg, Berlin, Heidelberg, 2011) pp. 419–457.

[169] T. Gruner and D.-G. Welsch, Phys. Rev. A **51**, 3246 (1995).

[170] W. G. Unruh and W. H. Zurek, Phys. Rev. D **40**, 1071 (1989).

[171] P. C. Martin, E. D. Siggia, and H. A. Rose, Phys. Rev. A **8**, 423 (1973).

[172] E. Abdalla, M. C. B. Abdalla, and K. D. Rothe, *Non-perturbative methods in 2 dimensional quantum field theory* (World Scientific, 1991) Chap. 4.

[173] O. Dippel, P. Schmelcher, and L. S. Cederbaum, Phys. Rev. A **49**, 4415 (1994).